Optimal Control of Self-Powered Systems Using Primal-Dual Techniques

by

Alyssa Kody

A dissertation submitted in partial fulfillment
of the requirements for the degree of
Doctor of Philosophy
(Electrical Engineering: Systems)
in the University of Michigan
2019

Doctoral Committee:

Associate Professor Jeffrey Scruggs, Co-Chair
Professor Heath Hofmann, Co-Chair
Professor James Freudenberg
Professor Ian Hiskens
Professor Ilya Kolmanovsky

Alyssa Kody
akody@umich.edu
ORCID iD: 0000-0002-4215-9197

Dedication

To my parents for their unconditional love and support

Acknowledgments

I greatly appreciate the financial support from the National Science Foundation Graduate Research Fellowship Program, and the Rackham Merit Fellowship Program. Thank you to the faculty and staff in both the Electrical Engineering and Computer Science, and the Civil and Environmental Engineering Departments at the University of Michigan.

I would like to acknowledge my committee, Professor Heath Hofmann, Professor Ian Hiskens, Professor Ilya Kolmanovsky, and Professor James Freudenberg, for taking the time to review my work and provide valuable feedback. I would also like to express my gratitude to Professor Jerome Lynch for his advice and encouragement. A special thanks to Nathan Tom for hosting me at the National Renewable Energy Laboratory and for the many useful discussions on wave energy conversion.

Thank you to my advisor, Professor Jeffrey Scruggs, for his guidance, patience, and kindness over the years. He has been been endlessly supportive of my classwork, research interests, and general well-being. I feel very fortunate to have an advisor who encouraged me to academically explore, and was willing to invest so much of his time and energy into my success. With Professor Scruggs' help, I was able to completely alter the direction of my career and I will be forever grateful to him for this. Also, I will greatly miss our post-research-meeting analyses of various television shows.

I want to thank my Ann Arbor friends for helping me through my Ph.D. with laughter, frisbee, and summer cookouts. To my brothers, Jason and Justin, who were also working towards their own degrees and careers, a special thanks for your unyielding support and comedic relief. I want express my sincere gratitude to my parents for their unconditional love, giving me the opportunity to pursue higher education, and providing a listening ear through many tough decisions. They have been the biggest supporters of my education, and have cheered me on when I needed it most. Finally, thank you to Phil for navigating graduate school with me, bringing me food during long nights in lab, and being my personal on-call mathematician. You provided encouragement and a steadying force through these stressful years, and I am excited to start our next adventure together.

Table of Contents

List of Figures

List of Acronyms

COCP Constrained Optimal Control Problem.

DARE Discrete-Time Algebraic Riccati Equation.

ECOCP Energy-Constrained Optimal Control Problem.

KKT Karush-Kuhn-Tucker.

LQR Linear Quadratic Regulator.

LTI Linear Time Invariant.

LTV Linear Time Varying.

MPC Model Predictive Control.

MQCQP Modification Quadratically Constrained Quadratic Program.

OCP Optimal Control Problem.

PR Positive Real.

PTO Power Take-Off.

QCQP Quadratically Constrained Quadratic Program.

QP Quadratic Program.

RDRDE Reverse Discrete-Time Riccati Difference Equation.

SDP Semi-Definite Program.

SDR Semi-Definite Relaxation.

SPR Strictly Positive Real.

SQP Sequential Quadratic Programming.

UOCP Unconstrained Optimal Control Problem.

WEC Wave Energy Converter.

ZOH Zero Order Hold.

List of Symbols

$\mathbb{R}$	the set of real numbers
$\mathbb{R}_{\geqslant 0}$, $\mathbb{R}_{>0}$	the set of real numbers on the interval $[0, \infty)$, and $(0, \infty)$
$\mathbb{C}$	the set of complex numbers
$\mathbb{Z}$	the set of integers
$\mathbb{R}^{n\times m}$, $\mathbb{R}^n$	the set of $n \times m$ real matrices, n-length real vectors
$\mathbb{S}^m$	the set of real, $m \times m$, symmetric matrices
$\mathbb{L}^2$	the Lebesgue space of square integrable functions
relint($\mathbb{X}$)	relative interior of set $\mathbb{X}$
int($\mathbb{X}$)	interior of set $\mathbb{X}$
$\partial\mathbb{X}$	boundary of set $\mathbb{X}$
$\boldsymbol{I}_n$	identity matrix of size $n \times n$
$\mathbf{0}_n$, $\mathbf{0}_{n\times m}$	matrix of zeros of size $n \times n$, matrix of zeros of size $n \times m$
$\boldsymbol{M}^T$	transpose of matrix $\boldsymbol{M}$

$\boldsymbol{M}^{-1}$	inverse of matrix $\boldsymbol{M}$
$\boldsymbol{M}^{\dagger}$	Moore-Penrose inverse of matrix $\boldsymbol{M}$
$\mathrm{Tr}(\boldsymbol{M})$	trace of matrix $\boldsymbol{M}$
$\mathcal{N}(\boldsymbol{M})$	nullspace of matrix $\boldsymbol{M}$
$\mathrm{dom}\, f(\cdot)$	domain of function $f(\cdot)$
$\bar{c}$	complex conjugate of $c \in \mathbb{C}$
$\mathrm{Re}(c)$	the real part of $c \in \mathbb{C}$
$\mathbf{1}(f(\cdot))$	indicator function of function $f(\cdot)$
δ	Kronecker delta
$\ln(x)$	natural log of $x \in \mathbb{R}$
$\boldsymbol{M} \succ 0$, $\boldsymbol{M} \succeq 0$	matrix $\boldsymbol{M}$ is positive definite, positive semi-definite
$\boldsymbol{M} \prec 0$, $\boldsymbol{M} \preceq 0$	matrix $\boldsymbol{M}$ is negative definite, negative semi-definite
$\boldsymbol{x} \geqslant 0$	element-by-element vector inequality
$\boldsymbol{x} \mapsto \boldsymbol{y}$	mapping between $\boldsymbol{x}$ and $\boldsymbol{y}$
$a \to b$	a approaches b

Abstract

Vibration-based *self-powered systems* are electromechanical technologies that are mechanically coupled to vibratory phenomena, and have the capability to convert this mechanical energy into electrical energy to power their operations. These systems are fully *energy-autonomous* because they derive all the energy needed for operation directly from the vibratory disturbances to which they are subjected. Examples include (i) a wireless sensor node that powers its sensing, computing, and transmission tasks by converting low-level structural vibrations into electrical energy, (ii) an ocean wave energy converter that transforms the oscillating motion of ocean waves into electrical energy and uses a portion of this converted energy to power its control operations, and (iii) a structural vibration suppression control system that powers its operation by storing and recycling the energy it extracts from the vibrating structure.

In this thesis, we consider the general problem of control design for vibration-based self-powered systems in the context of discrete-time optimal control theory, and realize the optimal control solution in real-time using Model Predictive Control (MPC). The functionality of a self-powered system is constrained due to the limited availability of the vibratory energy resource, and also due to the finite bounds of its on-board energy storage subsystem. In addition, there are parasitic losses associated with harvesting energy and running intelligence, as well as decay of stored energy. These effects further restrict the functionality of the system. Consequently, the main challenge associated with control design for these systems relates to carefully managing energy harvesting, usage, and storage.

First, we develop a general model for self-powered systems and provide conditions on the model parameters for stability and feasibility. We restrict our attention to linear, time-varying, discrete-time systems, and assume the exogenous disturbances are known exactly. We then formulate the discrete-time optimal control problem to minimize a quadratic performance measure subject to constraints on the on-board energy storage, which is, in general, a nonconvex quadratically constrained quadratic program. We formulate the dual relaxation

of the self-powered optimal control problem, which may be solved uniquely and efficiently. Its solution provides a lower bound on the optimal primal performance measure. The *duality gap* is the difference between the optimal primal and optimal dual objectives. We illustrate that if a certain easy-to-check condition holds for the obtained dual optimum, then there is no duality gap, and consequently the dual and primal optima are coincident. In this situation, it follows that this duality technique can be used as a convex means of solving the primal (nonconvex) optimal control problem exactly. If there is a nonzero duality gap, the resulting trajectory does not satisfy the constraints of the original optimal control problem. In this case, we introduce an algorithm to guarantee that the first time-step of the trajectory is feasible and can be implemented in real-time via MPC.

Chapter 1

Introduction

1.1 Motivation

The incorporation of embedded intelligence and actuation into the design and operation of electromechanical dynamical systems is increasing with the need for real-time sensing, control, and adaptation. It is often advantageous for these physical systems to operate in complete *energy-autonomy*, as they do not require access to an energy source, and instead have the capability to convert energy available in their environments into electricity to power their operations. In this thesis, we consider the general problem of control design for these energy-autonomous systems that are mechanically coupled to vibratory phenomena.

We assume the transducers used to implement the control have bi-directional power flow capability; that is, they can be controlled to inject power into a vibratory system (as actuators), and to remove power from this system (as generators). These transducers are electronically interfaced with localized energy storage subsystems so that they are capable of storing and reusing the energy they harvest. Crucially, we assume that the energy in these storage systems is the *only* energy that the transducers, sensors, and control intelligence can access to power their operation. This type of system is fully energy-autonomous since it derives all the energy needed for operation directly from the vibratory disturbances to which it is subjected. We refer to a vibratory network equipped with such control technologies as a *self-powered system*. To ground these concepts in technology, consider the following examples of self-powered systems excited by vibratory phenomena.

1. **Wireless Sensor Node:** Small-scale embedded sensing systems have applications across a wide range of fields including biomedical devices implanted within the human body, and structural monitoring systems in buildings and other civil infrastructure

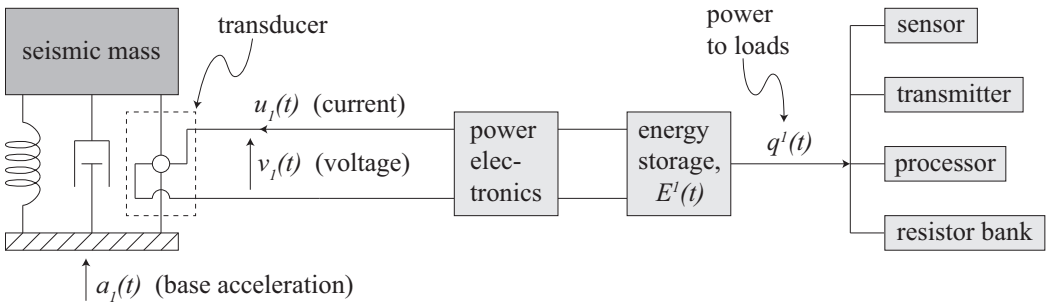

Figure 1.1: Vibration energy-harvesting wireless sensor node

[31]. In many cases, power availability is one of the most daunting challenges. In general, on-board batteries must be periodically replaced or recharged as their energy is depleted, and the service life of a sensing system can be several decades. This requires routine maintenance, which is undesirable for many reasons. For instance, it requires that the sensor (or at least the storage subsystem) be easily accessible. In infrastructure monitoring applications, this prohibits sensors from being embedded internally in structural components or joint connections during construction. In addition, required routine maintenance may prohibit the use of such sensors in hostile and remote environments [3, 67].

In infrastructure monitoring applications, low-level vibrations are a common form of available environmental energy, which can be exploited to power small-scale embedded sensing systems [45, 60]. Figure 1.1 shows a schematic of a vibration energy-harvesting wireless sensor node, where a base acceleration excites a mass-spring-damper system and this mechanical energy is converted into electrical energy via a transducer. Although many forms of transduction may be used to dynamically convert vibratory energy into electricity, at the μW-mW scale three modes of transduction – piezoelectric, electromagnetic, and electrostatic – are most prevalent. Harvested energy is stored in an energy storage system, which can either be used to power tasks like sensing or transmitting, or can be injected back into the mass-spring-damper system to aid in harvesting more energy.

2. **Active Vibration Suppression System:** There is a long history of research on the use of active control systems to suppress vibratory responses in civil structures (i.e., buildings and bridges) during seismic and wind events [34]. To implement active control requires the use of large-scale electromechanical actuators distributed throughout

the structure, which are controlled in real-time in response to sensor feedback. This technology can significantly outperform passive technologies (e.g., shock absorbers, tuned mass dampers, etc.). However, these control systems require enormous amounts of external power and energy in order to function properly. In many cases, especially in the case of seismic response protection, the external power grid cannot be relied upon. These reliability concerns have been one of the chief impediments to the adoption of active control technologies in structural engineering.

In many aerospace applications, structural vibration suppression is also a central concern. However, delivery of power to a wide array of actuators used for vibration suppression in an aerospace structure may be impractical or undesirable. Hence, many such applications make use of passive vibration suppression technologies; most notably, piezoelectric transducers [28, 61]. Although these passive technologies perform adequately in many circumstances, superior response suppression can theoretically be achieved via the use of active control.

Active vibration suppression systems that can simultaneously harvest energy (using, for example, piezoelectric [75] or electromagnetic devices [82, 83]) and suppress vibration without the need for an external power source, allow for the improved performance of active control without external power reliability concerns. Figure 1.2 depicts a self-powered active vibration suppression system for a civil structure subjected to a base acceleration. Each floor of the civil structure is equipped with a transducer, which is then connected to an energy storage system via power electronics.

3. **Wave Energy Converter:** WECs are devices that convert the oscillatory motion of ocean waves into electrical energy, and send this harvested energy back to shore to be incorporated into the power grid [20, 62]. There are many types of WECs, e.g., submerged flaps, attenuators of various geometries, and oscillating water columns; however, the most established technology is a point absorber buoy, which floats on the surface of the ocean and is connected to the seabed via moorings [17]. Various types of transducers (which are referred to as Power Take-Off (PTO) devices in the WEC industry) are used in point absorber buoys: hydraulic, direct drive mechanical, and linear generators, for instance. Actively controlled WEC buoys significantly outperform passively controlled buoys [59], but active controllers require an energy source to realize bi-directional power flow.

   Although a WEC could be designed to draw power for active control directly from

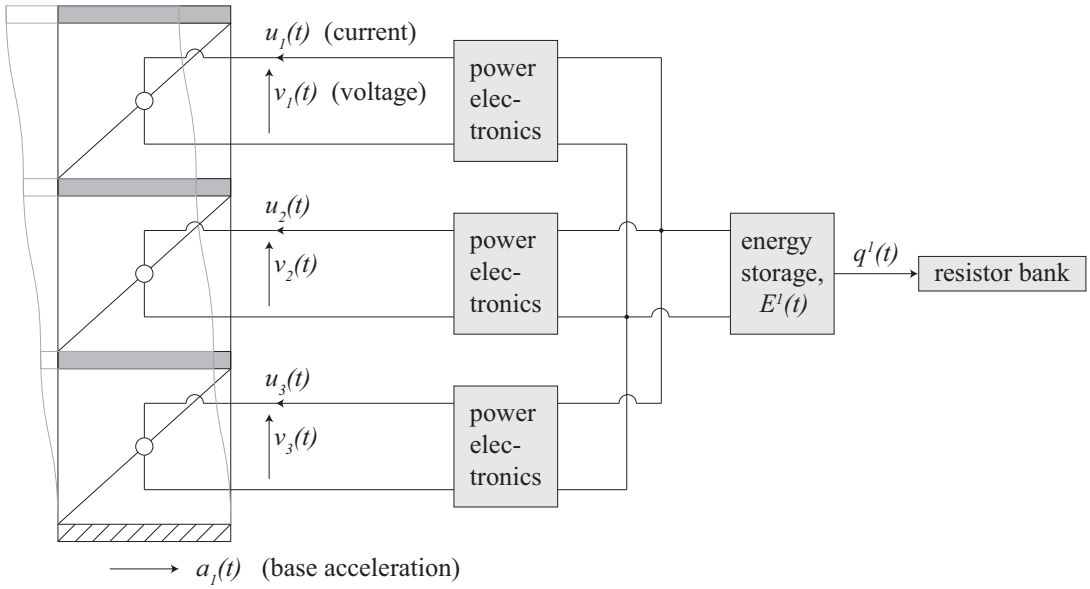

Figure 1.2: Self-powered active vibration suppression system for a civil structure

the grid, there are benefits to using a local, bottom-mounted energy storage device to provide this power. Figure 1.3 depicts a WEC farm consisting of four buoys, each connected to a common energy storage system. The system supports bi-directional power flow between the buoys and the energy storage system, but only single-directional power flow to the grid on shore. A benefit of this design is that the energy storage system can be used to smooth out the power sent to the grid. This is critical for WECs because, in general, these devices produce power with much higher variability than other renewable energy technologies, for instance, wind turbines [49]. From the perspective of a grid operator, single-directional power flow to shore simplifies the incorporation of these renewable energy devices into the larger grid and reduces reliability concerns. Furthermore, because WECs have access to a finite amount of stored energy, this method guarantees stability of the actively controlled buoy. Therefore, we classify this type of WECs with a bottom-mounted energy storage device as a self-powered system.

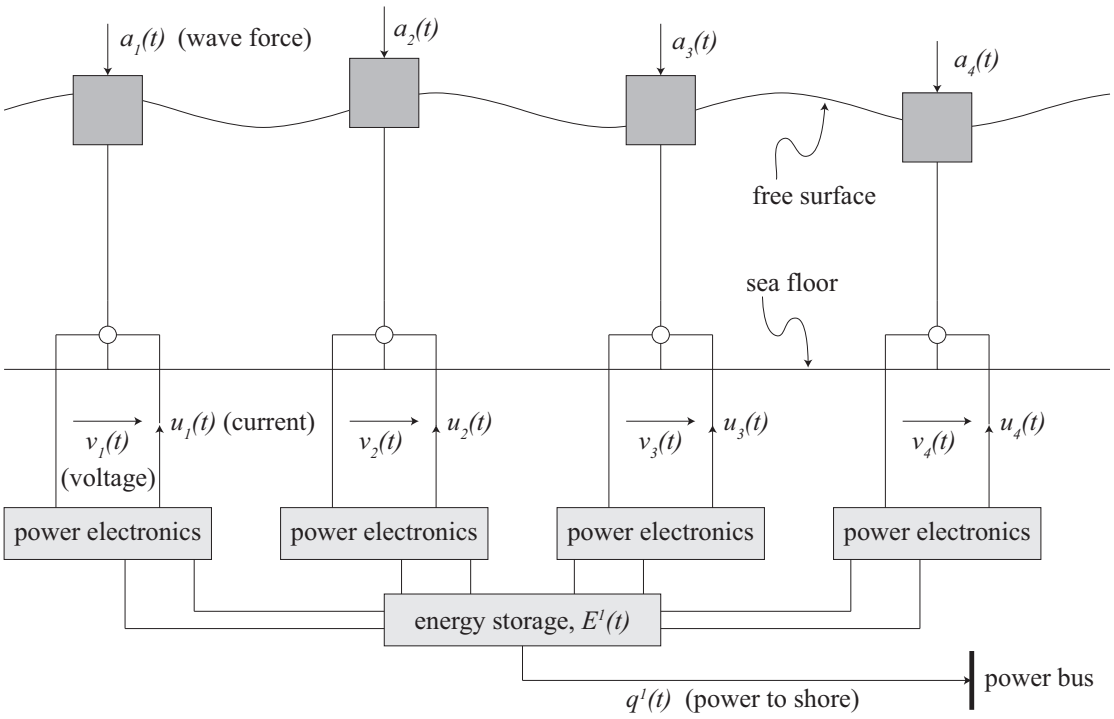

Figure 1.3: WEC farm with a common bottom-mounted energy storage system

1.2 Self-Powered System Model

Figure 1.4 shows a general model of a self-powered system. The plant is excited by d exogenous disturbances $\boldsymbol{a}(t) = \left[a^1(t) \cdots a^d(t)\right]^T$, and is actuated through m transducer ports. Transducer port j has an associated control input $u^j(t)$ and collocated potential variable $v^j(t)$. We collect control inputs and potential variables into vectors $\boldsymbol{u}(t)$ and $\boldsymbol{v}(t)$, respectively, i.e., $\boldsymbol{u}(t) = \left[u^1(t) \cdots u^m(t)\right]^T$ and $\boldsymbol{v}(t) = \left[v^1(t) \cdots v^m(t)\right]^T$. The ports are interfaced with p energy storage systems, where a single port can connect to a single storage system, but a storage system may connect to multiple ports. The energy in the i^{th} storage system is represented by $E^i(t)$, which, due to physical constraints on the storage device, is required to be within the bounds $E^i(t) \in [E^i_L, E^i_U]$, where $E^i_L, E^i_U \geqslant 0$ are the lower and upper energy constraints, respectively. Each energy storage system is connected to either a resistor bank or a power bus, which either burns off excess energy that cannot be stored or sends power to the bus. Let $q^i(t)$ be this power term for the i^{th} storage system, and collect all power terms in vector $\boldsymbol{q}(t) = \left[q^1(t) \cdots q^p(t)\right]^T$.

In addition to the restriction that they operate using only the energy they harvest, self-

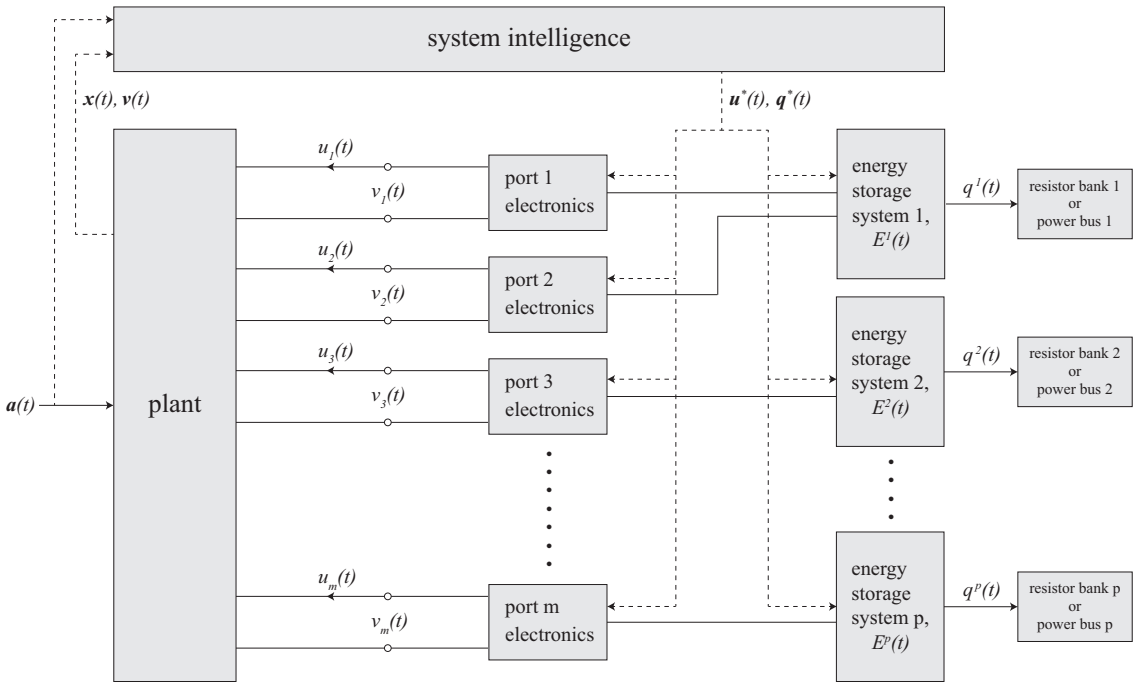

Figure 1.4: General schematic for a vibration-based self-powered system with d disturbances, p energy storage systems, and m ports

powered systems exhibit additional constraints as a consequence of the connectivity of their electronics. To illustrate this point, consider Figure 1.5 that shows a five degree-of-freedom mass-spring-damper system with three transducers for active vibration suppression. It also shows the connectivity of the transducers with the energy storage units through power-electronic interfaces. The three cases in the figure vary by the restrictions in the flow of energy. In Figure 1.5a, all transducers are connected to a single storage system, such that the energy extracted by one can be reused by any. In Figure 1.5b, two of the transducers share one storage system, while the third is isolated. In Figure 1.5c, each transducer's energy storage unit is isolated, implying that although they can each store and reuse energy, they cannot transmit energy between each other.

Figure 1.4 also illustrates a generic feedback loop that accepts the system state $\boldsymbol{x}(t)$ and disturbance $\boldsymbol{a}(t)$, and produces desired (i.e., commanded) values for the control inputs $\boldsymbol{u}^*(t)$, and the power dissipations $\boldsymbol{q}^*(t)$. These commands are then sent to the power electronic converters in the system, which facilitate high-bandwidth tracking between the desired and actual values. Designing the feedback law for self-powered systems is challenging for a few reasons:

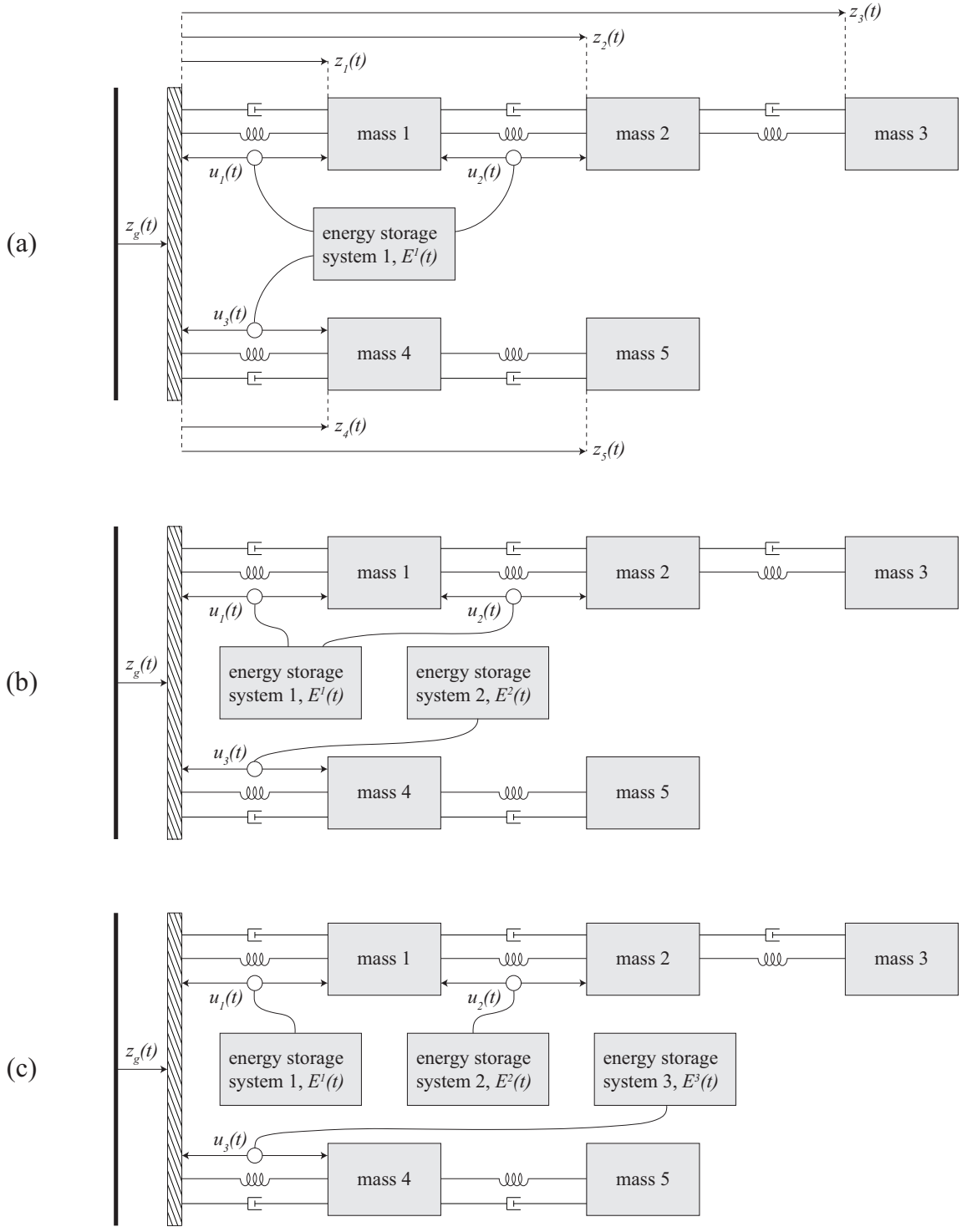

Figure 1.5: A five degree-of-freedom vibratory structure with three transducers, and various energy storage networks

1. **Exogenous disturbance forecasting:** Environmental energy sources are stochastic, and this randomness introduces uncertainty in the availability and magnitude of environmental energy. Therefore, supplemental to the control design, we require a predictor for the future stochastic process based on past and present disturbance measurements. In some situations, such as the WEC problem, the future disturbance can be known with a fair amount of accuracy ahead of time through the use of up-wave sensors.

2. **Finite energy resource and storage:** A self-powered system is constrained by the requirement that it not exceed its energy storage bounds at any time along its trajectory; i.e., it must be the case that $E^i(t) \in [E^i_L, E^i_U]$, $\forall t$, $i \in \{1...p\}$.

3. **Energy dissipation and decay:** We assume that the energy recovered by the system decays. Consequently, a self-powered system can operate at a higher efficiency if its control law reuses this energy more rapidly. In addition, because the presence of parasitic losses will in general depend on the control input $\boldsymbol{u}(t)$, these parasitics must be factored into the control design in order to properly account for the dissipation associated with a given control action.

4. **Divided control effort:** In some situations, harvesting energy and the primary performance objective require conflicting control actions. For instance, it is generally the case that optimal energy harvesting and optimal vibration suppression are conflicting control objectives. A control law that makes optimal effort to replenish the energy storage system may result in poor vibration suppression. On the other hand, a control law that disregards the replenishment of energy will likely result in violation of the energy constraints.

1.3 Scope

The objective of this thesis is to develop a general theory for the control design of self-powered systems that minimize a performance measure J while satisfying the physical constraints of the energy storage units. As discussed earlier, we are specifically interested in implementing these control algorithms on electromechanical systems subject to vibratory disturbances. For many of these types of devices, there are well-established linear dynamic models that characterize the plant in Figure 1.4. Due to the need to strictly enforce the physical constraints of the energy storage units, we develop a control design for these systems in the context of

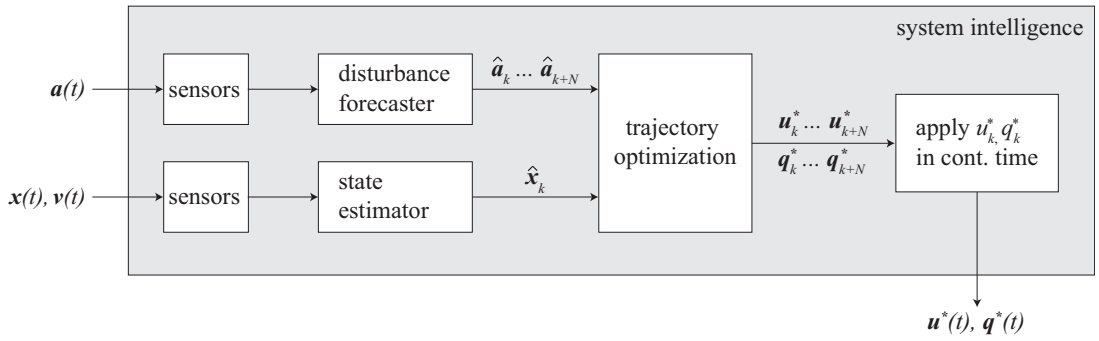

Figure 1.6: Components of the system intelligence block in Figure 1.4, where forecasted exogenous disturbances $\{\hat{\boldsymbol{a}}_k \dots \hat{\boldsymbol{a}}_{k+N}\}$ and the estimated current state $\hat{\boldsymbol{x}}_k$ are fed into a trajectory optimization algorithm, and then the first time-step of the optimized trajectory $\{\boldsymbol{u}_k^*, \boldsymbol{q}_k^*\}$ is implemented in ZOH.

discrete-time optimal control theory, and realize the optimal control solution in real-time using economic Model Predictive Control (MPC) techniques [9, 46].

Economic Model Predictive Control (MPC) is an iterative method in which the performance measure J is minimized over a finite-time horizon. Let k be the discrete-time step corresponding to the continuous-time interval $t \in [k\Delta t, (k+1)\Delta t)$, and let N be the number of time steps in the receding horizon. Figure 1.6 shows the components of the system intelligence block in Figure 1.4, which is used to implement the optimal control solution via MPC. For each time step k, the following steps are executed:

1. The exogenous disturbances are measured by a set of sensors, and then a disturbance forecaster uses these data to predict the next $N+1$ future disturbances $\{\hat{\boldsymbol{a}}_k \dots \hat{\boldsymbol{a}}_{k+N}\}$. Simultaneously, the states or outputs are also measured by sensors, and if not directly measured, the current state is estimated $\hat{\boldsymbol{x}}_k$.

2. Treating $\{\hat{\boldsymbol{a}}_k \dots \hat{\boldsymbol{a}}_{k+N}\}$ as deterministic, the trajectory optimization algorithm then calculates optimal control inputs $\{\boldsymbol{u}_k^* \dots \boldsymbol{u}_{k+N}^*\}$ and optimal energies flowing to the resistor banks or power buses $\{\boldsymbol{q}_k^* \dots \boldsymbol{q}_{k+N}^*\}$ to minimize a receding-horizon performance measure, J.

3. The first time-step of these trajectories, $\boldsymbol{u}_k^*$ and $\boldsymbol{q}_k^*$, are realized in Zero Order Hold (ZOH) over the duration $t \in [k\Delta t, (k+1)\Delta t)$.

To simplify the analysis, we assume that $\boldsymbol{u}^*(t)$ and $\boldsymbol{q}^*(t)$ can be tracked with infinite bandwidth by the power electronics, such that $\boldsymbol{u}^*(t) = \boldsymbol{u}(t)$ and $\boldsymbol{q}^*(t) = \boldsymbol{q}(t)$. Of these steps,

step 2 (i.e., trajectory optimization) is the computational bottleneck, and is the focus of the thesis.

1.3.1 Trajectory Optimization Techniques

In general, trajectory optimizations associated with self-powered systems are nonconvex. We show in Section 4.1.3 that the nonconvexity results from the physical constraints on the energy storage units, and that these constraints are *quadratic* functions in $\boldsymbol{u}$. If performance measure J is also a quadratic function, the trajectory optimization is a Quadratically Constrained Quadratic Program (QCQP). QCQPs have the following general form where $\boldsymbol{z} \in \mathbb{R}^m$ is the optimization variable and we enforce b quadratic constraints:

$$\text{QCQP} = \begin{cases} \textbf{Given:} & \boldsymbol{Q}_i, \boldsymbol{s}_i, \boldsymbol{r}_i, \quad \forall i \in \{0...b\} \\ \textbf{Minimize:} & \boldsymbol{z}^T \boldsymbol{Q}_0 \boldsymbol{z} + \boldsymbol{s}_0^T \boldsymbol{z} + r_0 \\ \textbf{Domain:} & \boldsymbol{z} \in \mathbb{R}^m \\ \textbf{Constraints:} & \boldsymbol{z}^T \boldsymbol{Q}_i \boldsymbol{z} + \boldsymbol{s}_i^T \boldsymbol{z} + r_i \leqslant 0, \quad \forall i \in \{1...b\}. \end{cases}$$

Specific QCQPs can be solved efficiently. For example, convex QCQPs can be solved in polynomial-time using well-known convex optimization techniques [10], and QCQPs with a single variable can be solved analytically. Nonconvex QCQPs with only one constraint have zero duality gap and hence can be solved in polynomial-time via its convex dual, which is known as the S-procedure or S-lemma [12]. However, these special cases do not encompass the trajectory optimizations for self-powered systems, which are nonconvex, and in general, MPC horizons extend beyond a single time-step. There are no specialized solution methods available for general nonconvex QCQPs, and these problems are NP-hard [55].

To solve the original nonconvex problem directly, it is common to use a generic nonlinear optimization algorithm, for instance, barrier methods or Sequential Quadratic Programming (SQP). When using barrier methods, we solve a sequence of equality-constrained minimizations, while in SQP, we solve a series of Quadratic Programs (QPs) [10]. There are many commercially available and open-source packages (e.g., Matlab's optimization toolbox, GAMS, AMPL, YALMIP) that implement these types of algorithms to solve generic nonlinear optimizations, and other available packages that calculate Nonlinear MPC control actions directly (e.g., Matlab's Model Predictive Control Toolbox, ACADO, PANOC). Although these techniques ensure local convergence, because a series of problems must be solved sequentially, the computational cost can be high. Furthermore, these techniques are

highly sensitive to the algorithm's starting point. As we plan to implement the optimal control actions via MPC, trajectory optimizations must be solved to an acceptable precision during a single time-step Δt, making computation time critical.

Instead of solving the original (primal) nonconvex problem, we can instead solve a convex relaxation to obtain bounds on the optimal performance measure. First, consider a Semi-Definite Relaxation (SDR) that lifts the original QCQP into a higher dimensional space through the introduction of the new variable $\boldsymbol{Z} \in \mathbb{S}^m$, where $\mathbb{S}^m$ is the set of all real $m \times m$ symmetric matrices:

$$\text{SDR} = \begin{cases} \textbf{Given:} & \boldsymbol{Q}_i, \boldsymbol{s}_i, \boldsymbol{r}_i, \quad \forall i \in \{0...b\} \\ \textbf{Minimize:} & \text{Tr}(\boldsymbol{Z}\boldsymbol{Q}_0) + \boldsymbol{s}_0^T \boldsymbol{z} + r_0 \\ \textbf{Domain:} & \boldsymbol{z} \in \mathbb{R}^m, \ \boldsymbol{Z} \in \mathbb{S}^m \\ \textbf{Constraints:} & \text{Tr}(\boldsymbol{Z}\boldsymbol{Q}_i) + \boldsymbol{s}_i^T \boldsymbol{z} + r_i \leqslant 0, \quad \forall i \in \{1..b\} \\ & \boldsymbol{Z} \succeq \boldsymbol{z}\boldsymbol{z}^T. \end{cases}$$

The optimal solution of the SDR is equivalent to the optimal solution of the original QCQP if $\boldsymbol{Z} = \boldsymbol{z}\boldsymbol{z}^T$ [11, 73]. SDRs are employed in various engineering problems: for example, in the context of the sensor network localization problem [44], and in the optimal power flow problem, where the relaxed solution is exact under special conditions [39].

Another type of convex relaxation is a dual (or Lagrangian) relaxation where we maximize over the Lagrange multipliers (as opposed to minimizing over the primal variables in the original problem). Let $L(\boldsymbol{z}, \boldsymbol{\lambda})$ be the Lagrangian, where $\boldsymbol{\lambda} \in \mathbb{R}^b_{\geqslant 0}$ are the Lagrange multipliers used to enforce the constraints:

$$L(\boldsymbol{z}, \boldsymbol{\lambda}) = \boldsymbol{z}^T \boldsymbol{Q}_0 \boldsymbol{z} + \boldsymbol{s}_0^T \boldsymbol{z} + r_0 + \sum_{i=1}^{b} \boldsymbol{\lambda}_i \left(\boldsymbol{z}^T \boldsymbol{Q}_i \boldsymbol{z} + \boldsymbol{s}_i^T \boldsymbol{z} + r_i \right).$$

Then, the dual relaxation is:

$$\text{Dual Relaxation} = \begin{cases} \textbf{Given:} & \boldsymbol{Q}_i, \boldsymbol{s}_i, \boldsymbol{r}_i, \quad \forall i \in \{0...b\} \\ \textbf{Maximize:} & G(\boldsymbol{\lambda}) = \inf_{\boldsymbol{z}} L(\boldsymbol{z}, \boldsymbol{\lambda}) \\ \textbf{Domain:} & \boldsymbol{\lambda} \\ \textbf{Constraints:} & \boldsymbol{\lambda} \geqslant 0, \end{cases}$$

where $G(\cdot)$ is the dual function (see Section 2.5 for an overview of Lagrangian duality). From the optimal Lagrange multipliers, we can recover the associated primal variable $\boldsymbol{z}$. The dual relaxation also provides a lower bound on the optimal solution of the primal problem, and can also be framed as a Semi-Definite Program (SDP) [10]. Dual relaxations are implemented in many engineering problems, for example, in the unit commitment problem [53, 74].

The dual relaxation and SDR are duals of each other, and consequently, they provide the *same* lower bound on the original nonconvex QCQP (assuming constraint qualifications are satisfied) [10, 11]. The original nonconvex trajectory optimization problem has $(m+p)(N+1)$ variables (at each time-step of the receding horizon, there is a control input u associated with each of the m transducer ports, and a power dissipation term q for each of the p energy storage units). For the SDR, in addition to the $(m+p)(N+1)$ original variables, there are $\frac{1}{2}((m+p)^2(N+1)^2+(m+p)(N+1))$ unique entries of symmetric matrix $\boldsymbol{Z}$. The dual relaxation has $2p(N+1)$ variables (see Chapter 5), significantly fewer than the SDR.

Both relaxations grow in dimensionality with the length of the MPC horizon (N) and the number of energy storage units (p). However, the SDR also grows with the number of transducer ports (m) and grows quadratically in all these variables. In this thesis, we only consider the dual relaxation. Furthermore, we exploit the specific structure of the self-powered optimal control problem in the formulation of the dual relaxation to increase efficiency.

1.3.2 Dual Relaxation Algorithm for Model Predictive Control

Dual relaxations provide lower bounds on the performance measure of the original nonconvex problem. However, if these bounds are not tight, the optimal trajectories produced by these relaxations are infeasible in the primal domain, i.e., they do not satisfy all the physical constraints of the energy storage units. Many researchers have explored stochastic SDRs, where the performance measure is minimized and constraints are satisfied in expectation [44]. Park and Boyd introduce the Suggest-and-Improve algorithm for obtaining approximate solutions to general QCQPs [56]. In this algorithm, a relaxation of the original problem is first solved (the suggest portion), and then a local optimization method is used to improve upon this initial solution (the improve portion). However, the Suggest-and-Improve algorithm also does not guarantee feasibility.

One way to guarantee feasibility is to verify that there is *zero duality gap*. The *duality gap* is the difference between the minimum performance measure of the nonconvex primal

trajectory optimization and the maximum dual function of the dual relaxation. Because the dual relaxation always produces a lower bound of the original primal problem, the duality gap is a nonnegative value. Under special circumstances, the duality gap is zero, meaning that the dual and primal optima are equal. When this is the case, the primal optimal solution can be found by solving the convex dual problem instead of the nonconvex primal problem, which always results in feasible trajectories. In Chapter 5, we introduce sufficient conditions for zero duality gap for the self-powered system trajectory optimization. For situations where there is a nonzero duality gap, we modify the trajectory resulting from the dual relaxation. Because we are implementing the trajectory optimization using MPC, we only need to guarantee feasibility of the first control action. In Chapter 6, we introduce an optimization algorithm to ensure feasibility of the first time-step.

1.4 Outline

The following is an overview of the content of each chapter of this thesis:

Chapter 2: We present a general overview of the foundational topics of the work presented in this thesis. We review linear matrix and system theory, input-output relations, discrete-time optimal control, and Lagrangian duality.

Chapter 3: We develop a general model for a self-powered system and provide conditions on the model parameters for stability and feasibility in continuous-time. The model for an energy storage subsystem is formulated to account for the decay of stored energy and transduction losses. We then discretize these models and provide discrete-time feasibility conditions.

Chapter 4: We formulate the trajectory optimization problem for self-powered systems, and derive conditions for convexity. Barrier methods are introduced to solve the original nonconvex problem, and then we demonstrate this method by maximizing the data transmission of an energy-harvesting wireless sensing node.

Chapter 5: We use the dual relaxation to solve the trajectory optimization presented in Chapter 4. A closed-form expression of the dual function is derived, as well as conditions to guarantee that it is finite. We present easy-to-check sufficient conditions for zero duality gap. Last, we demonstrate the techniques developed in this chapter on a piezoelectric vibration energy harvester.

Chapter 6: We first present an overview of MPC, and then introduce an algorithm to guarantee feasibility of the first time-step of the dual relaxation discussed in Chapter 5. We conclude this chapter by investigating two example problems: a spherical buoy-type WEC with the goal of maximizing energy generation, and an energy-harvesting active vibration suppression system.

Chapter 7: We first summarize the contributions of this thesis. Then, we discuss future work that builds on the ideas presented in this dissertation: (i) a method to forecast exogenous disturbances, (ii) a technique to smooth the power extracted from WECs, (iii) on-going work to derive necessary and sufficient conditions on the problem data to guarantee zero duality gap, and (iv) improvements to the loss model.

Chapter 2

Preliminaries

In this chapter, we first present the mathematical notation used throughout this thesis. We then provide a brief review of concepts from linear matrix and system theory, input-output theory, discrete-time optimal control, and Lagrangian duality that are relevant to this dissertation. Basic definitions and relations from linear algebra and linear system theory are not presented here; however, [33] can be used as a reference.

2.1 Notation

Let $\mathbb{R}$ be the set of real numbers, $\mathbb{C}$ be the set of complex numbers, and $\mathbb{Z}$ be the set of integers. Let $[a, b]$ be the set of real numbers on the interval from a to b, and $\{a...b\}$ be the set of integers from a to b. $\mathbb{R}^{n\times m}$ is the set of $n \times m$ real matrices, $\mathbb{R}^n$ is the set of $n \times 1$ real vectors, and $\mathbb{S}^n$ is the set of real $n \times n$ symmetric matrices. When applicable, these same notations are also used for the set of complex numbers $\mathbb{C}$. The complex conjugate of a complex number $c \in \mathbb{C}$ is designated as $\bar{c}$, and the real part of $c \in \mathbb{C}$ is $\mathrm{Re}\,(c)$. Let $\mathbb{L}^2$ be the Lebesgue space of functions that are square-integrable. All other sets are designated as uppercase letters in the blackboard (double-barred) font.

Matrices are bolded upper-case symbols (e.g., $\boldsymbol{M}$), and vectors are bolded lower-case symbols (e.g., $\boldsymbol{v}$). $\boldsymbol{I}_n$ is the $n \times n$ identity matrix, and $\boldsymbol{0}_{n\times m}$ is a $n \times m$ matrix of zeros. $\boldsymbol{M}(t)$ represents a continuous-time, time-varying matrix with $t \in \mathbb{R}$. In general, superscripts refer to parameters or variables related to the i^{th} energy storage system (e.g., $\boldsymbol{v}^i$). In general, the first subscript refers to discrete-time time-step, e.g., $\boldsymbol{v}_k$ is the discrete-time, time-varying matrix, where $k \in \mathbb{Z}$ is the counter. The j^{th} element of vector $\boldsymbol{v}_k$ is denoted as $v_{k,j}$. Let $\boldsymbol{M}_{k:m}$ be the sequence of discrete-time, time-varying matrices from time-step k to m, i.e.,

$\boldsymbol{M}_{k:m} = \{\boldsymbol{M}_k \dots \boldsymbol{M}_m\}$, and the same notation is used for vectors. Let $\boldsymbol{M} \leqslant 0$ ($\boldsymbol{M} = 0$) be refer to the element-by-element inequality (equality).

2.2 Linear Matrix and System Theory

Definition 2.1. *(Continuous-Time Linear Time Varying (LTV) System, Continuous-Time Linear Time Invariant (LTI) System) Let $\mathcal{S}_{c,LTV}$ be a* continuous-time LTV system*, which is represented by the following set of equations:*

$$\mathcal{S}_{c,LTV} : \begin{cases} \dot{\boldsymbol{x}}(t) = \boldsymbol{A}(t)\boldsymbol{x}(t) + \boldsymbol{B}(t)\boldsymbol{u}(t) \\ \boldsymbol{v}(t) = \boldsymbol{C}(t)\boldsymbol{x}(t) + \boldsymbol{D}(t)\boldsymbol{u}(t), \end{cases} \tag{2.1}$$

with initial condition $\boldsymbol{x}(0)$, and where $\boldsymbol{x}(t) \in \mathbb{R}^n$ is the state vector, $\boldsymbol{u}(t) \in \mathbb{R}^m$ is the input vector, $\boldsymbol{v}(t) \in \mathbb{R}^p$ is the output vector, $\boldsymbol{A}(t) \in \mathbb{R}^{n\times n}$, $\boldsymbol{B}(t) \in \mathbb{R}^{n\times m}$, $\boldsymbol{C}(t) \in \mathbb{R}^{p\times n}$, and $\boldsymbol{D}(t) \in \mathbb{R}^{p\times m}$ for all times $t \in \mathbb{R}$. If matrices $\boldsymbol{A}$, $\boldsymbol{B}$, $\boldsymbol{C}$, and $\boldsymbol{D}$ are time-invariant, then $\mathcal{S}_{c,LTV}$ becomes the continuous-time LTI system $\mathcal{S}_{c,LTI}$ *which is of the form:*

$$\mathcal{S}_{c,LTI} : \begin{cases} \boldsymbol{x}(t) = \boldsymbol{A}\boldsymbol{x}(t) + \boldsymbol{B}\boldsymbol{u}(t) \\ \boldsymbol{v}(t) = \boldsymbol{C}\boldsymbol{x}(t) + \boldsymbol{D}\boldsymbol{u}(t). \end{cases} \tag{2.2}$$

Definition 2.2. *(Discrete-Time LTV System, Discrete-Time LTI System) Let $\mathcal{S}_{d,LTV}$ be a* discrete-time LTV system*, which is represented by the following set of equations:*

$$\mathcal{S}_{d,LTV} : \begin{cases} \boldsymbol{x}_{k+1} = \boldsymbol{A}_k\boldsymbol{x}_k + \boldsymbol{B}_k\boldsymbol{u}_k \\ \boldsymbol{v}_k = \boldsymbol{C}_k\boldsymbol{x}_k + \boldsymbol{D}_k\boldsymbol{u}_k, \end{cases} \tag{2.3}$$

with initial condition $\boldsymbol{x}_0$, and where $\boldsymbol{x}_k \in \mathbb{R}^n$ is the state vector, $\boldsymbol{u}_k \in \mathbb{R}^m$ is the input vector, $\boldsymbol{v}_k \in \mathbb{R}^p$ is the output vector, $\boldsymbol{A}_k \in \mathbb{R}^{n\times n}$, $\boldsymbol{B}_k \in \mathbb{R}^{n\times m}$, $\boldsymbol{C}_k \in \mathbb{R}^{p\times n}$, and $\boldsymbol{D}_k \in \mathbb{R}^{p\times m}$ for all time indices $k \in \mathbb{Z}$. If matrices $\boldsymbol{A}$, $\boldsymbol{B}$, $\boldsymbol{C}$, and $\boldsymbol{D}$ are time-invariant, then $\mathcal{S}_{d,LTV}$ becomes the discrete-time LTI system $\mathcal{S}_{d,LTI}$ *which is of the form:*

$$\mathcal{S}_{d,LTI} : \begin{cases} \boldsymbol{x}_{k+1} = \boldsymbol{A}_k\boldsymbol{x}_k + \boldsymbol{B}_k\boldsymbol{u}_k \\ \boldsymbol{v}_k = \boldsymbol{C}_k\boldsymbol{x}_k + \boldsymbol{D}_k\boldsymbol{u}_k. \end{cases} \tag{2.4}$$

Definition 2.3. *(Matrix Definiteness) Let $\boldsymbol{M} \in \mathbb{S}^n$. If for all $\boldsymbol{x} \in \mathbb{R}^n \setminus \boldsymbol{0}$:*

1. $\boldsymbol{x}^T\boldsymbol{M}\boldsymbol{x} > 0$, $\boldsymbol{M}$ *is* positive definite, *denoted as* $\boldsymbol{M} \succ 0$

2. $\boldsymbol{x}^T\boldsymbol{M}\boldsymbol{x} \geqslant 0$, $\boldsymbol{M}$ *is* positive semi-definite, *denoted as* $\boldsymbol{M} \succeq 0$

3. $\boldsymbol{x}^T\boldsymbol{M}\boldsymbol{x} < 0$, $\boldsymbol{M}$ *is* negative definite, *denoted as* $\boldsymbol{M} \prec 0$

4. $\boldsymbol{x}^T\boldsymbol{M}\boldsymbol{x} \leqslant 0$, $\boldsymbol{M}$ *is* negative semi-definite, *denoted as* $\boldsymbol{M} \preceq 0$

Theorem 2.1. *(Matrix Inversion Lemma) [33]. Let* $\boldsymbol{B} = \boldsymbol{A}+\boldsymbol{X}\boldsymbol{R}\boldsymbol{Y}$*, where* $\boldsymbol{A} \in \mathbb{R}^n$ *is nonsingular,* $\boldsymbol{X} \in \mathbb{R}^{n\times m}$*,* $\boldsymbol{R} \in \mathbb{R}^{m\times m}$ *is nonsingular, and* $\boldsymbol{Y} \in \mathbb{R}^{m\times n}$*. Then, if* $(\boldsymbol{R}^{-1} + \boldsymbol{Y}\boldsymbol{A}^{-1}\boldsymbol{X})$ *and* $\boldsymbol{A}$ *are nonsingular, we can write the inverse of* $\boldsymbol{B}$ *as:*

$$\boldsymbol{B}^{-1} = \boldsymbol{A}^{-1} - \boldsymbol{A}^{-1}\boldsymbol{X}\left(\boldsymbol{R}^{-1} + \boldsymbol{Y}\boldsymbol{A}^{-1}\boldsymbol{X}\right)^{-1}\boldsymbol{Y}\boldsymbol{A}^{-1}.$$

Theorem 2.2. *(Derivative of Matrix Inverse) [33]. Let* $\boldsymbol{M}(x)$ *be a square matrix, which is a function of variable* x*, then the derivative of* $\boldsymbol{M}(x)$ *is:*

$$\frac{\partial \boldsymbol{M}(x)^{-1}}{\partial x} = -\boldsymbol{M}(x)^{-1}\frac{\partial \boldsymbol{M}(x)}{\partial x}\boldsymbol{M}(\boldsymbol{x})^{-1}.$$

Definition 2.4. *(Schur Complement) [33]. Let* $\boldsymbol{M} \in \mathbb{R}^{(n+m)\times(n+m)}$ *be a matrix of the form:*

$$\boldsymbol{M} = \begin{bmatrix} \boldsymbol{M}_{11} & \boldsymbol{M}_{12} \\ \boldsymbol{M}_{21} & \boldsymbol{M}_{22} \end{bmatrix},$$

where $\boldsymbol{M}_{11} \in \mathbb{R}^{n\times n}$*,* $\boldsymbol{M}_{12} \in \mathbb{R}^{n\times m}$*,* $\boldsymbol{M}_{21} \in \mathbb{R}^{m\times n}$ *and* $\boldsymbol{M}_{22} \in \mathbb{R}^{m\times m}$*. If block* $\boldsymbol{M}_{22}$ *is nonsingular, then the Schur complement of block* $\boldsymbol{M}_{22}$ *is:*

$$\boldsymbol{M}/\boldsymbol{M}_{22} = \boldsymbol{M}_{11} - \boldsymbol{M}_{12}\boldsymbol{M}_{22}^{-1}\boldsymbol{M}_{21}.$$

If block $\boldsymbol{M}_{11}$ *is nonsingular, then the Schur complement of block* $\boldsymbol{M}_{11}$ *is:*

$$\boldsymbol{M}/\boldsymbol{M}_{11} = \boldsymbol{M}_{22} - \boldsymbol{M}_{21}\boldsymbol{M}_{11}^{-1}\boldsymbol{M}_{12}.$$

Theorem 2.3. *(Schur Complement Condition for Positive Definiteness and Positive Semi-Definiteness) [33]. Let* $\boldsymbol{M} \in \mathbb{S}^{(n+m)}$ *be of the form:*

$$\boldsymbol{M} = \begin{bmatrix} \boldsymbol{M}_{11} & \boldsymbol{M}_{12} \\ \boldsymbol{M}_{12}^T & \boldsymbol{M}_{22} \end{bmatrix},$$

with $\boldsymbol{M}_{11} \in \mathbb{S}^n$, $\boldsymbol{M}_{12} \in \mathbb{R}^{n\times m}$, *and* $\boldsymbol{M}_{22} \in \mathbb{S}^m$. *Then, if* $\boldsymbol{M}_{11}$ *is nonsingular the following are true:*

1. $\boldsymbol{M} \succ 0$ *if and only if* $\boldsymbol{M}_{11} \succ 0$ *and* $\boldsymbol{M}/\boldsymbol{M}_{11} \succ 0$
2. $\boldsymbol{M} \succeq 0$ *if and only if* $\boldsymbol{M}_{11} \succ 0$ *and* $\boldsymbol{M}/\boldsymbol{M}_{11} \succeq 0$.

If $\boldsymbol{M}_{22}$ *is nonsingular, then the following are true:*

1. $\boldsymbol{M} \succ 0$ *if and only if* $\boldsymbol{M}_{22} \succ 0$ *and* $\boldsymbol{M}/\boldsymbol{M}_{22} \succ 0$
2. $\boldsymbol{M} \succeq 0$ *if and only if* $\boldsymbol{M}_{22} \succ 0$ *and* $\boldsymbol{M}/\boldsymbol{M}_{22} \succeq 0$.

Remark 2.1. *Let* $\boldsymbol{M}$ *be defined as in Theorem 2.3. If* $\boldsymbol{M}_{11}$ *is nonsingular, then:*

$$\begin{bmatrix} \boldsymbol{I} & -\boldsymbol{M}_{11}^{-1}\boldsymbol{M}_{12} \\ \boldsymbol{0} & \boldsymbol{I} \end{bmatrix}^T \begin{bmatrix} \boldsymbol{M}_{11} & \boldsymbol{M}_{12} \\ \boldsymbol{M}_{12}^T & \boldsymbol{M}_{22} \end{bmatrix} \begin{bmatrix} \boldsymbol{I} & -\boldsymbol{M}_{11}^{-1}\boldsymbol{M}_{12} \\ \boldsymbol{0} & \boldsymbol{I} \end{bmatrix} = \begin{bmatrix} \boldsymbol{M}_{11} & \boldsymbol{0} \\ \boldsymbol{0} & \boldsymbol{M}/\boldsymbol{M}_{11} \end{bmatrix}.$$

If $\boldsymbol{M}_{22}$ *is nonsingular, then:*

$$\begin{bmatrix} \boldsymbol{I} & -\boldsymbol{M}_{22}^{-1}\boldsymbol{M}_{12} \\ \boldsymbol{0} & \boldsymbol{I} \end{bmatrix} \begin{bmatrix} \boldsymbol{M}_{11} & \boldsymbol{M}_{12} \\ \boldsymbol{M}_{12}^T & \boldsymbol{M}_{22} \end{bmatrix} \begin{bmatrix} \boldsymbol{I} & -\boldsymbol{M}_{22}^{-1}\boldsymbol{M}_{12} \\ \boldsymbol{0} & \boldsymbol{I} \end{bmatrix}^T = \begin{bmatrix} \boldsymbol{M}/\boldsymbol{M}_{22} & \boldsymbol{0} \\ \boldsymbol{0} & \boldsymbol{M}_{22} \end{bmatrix}.$$

Definition 2.5. *(Reverse Discrete-Time Riccati Difference Equation (RDRDE), Discrete-Time Algebraic Riccati Equation (DARE)) [2]. Let* $\boldsymbol{P}_k \in \mathbb{S}^n$, $\boldsymbol{A}_k \in \mathbb{R}^{n\times n}$, $\boldsymbol{B}_k \in \mathbb{R}^{n\times m}$, $\boldsymbol{R}_k \in \mathbb{R}^{m\times m}$, *and* $\boldsymbol{Q}_k \in \mathbb{R}^{n\times n}$ *for all* $k \in \mathbb{Z}_{\geqslant 0}$. *The* RDRDE *is of the form:*

$$\boldsymbol{P}_{k-1} = \boldsymbol{A}_k^T\boldsymbol{P}_k\boldsymbol{A}_k - \left(\boldsymbol{B}_k^T\boldsymbol{P}_k\boldsymbol{A}_k\right)^T \left(\boldsymbol{R}_k + \boldsymbol{B}_k^T\boldsymbol{P}_k\boldsymbol{B}_k\right)^{-1} \left(\boldsymbol{B}_k^T\boldsymbol{P}_k\boldsymbol{A}_k\right) + \boldsymbol{Q}_k.$$

If matrices $\boldsymbol{A}$, $\boldsymbol{B}$, $\boldsymbol{R}$, $\boldsymbol{Q}$, *and* $\boldsymbol{P}$ *are time-invarient, the RDRDE reduces to the* DARE *as:*

$$\boldsymbol{P} = \boldsymbol{A}^T\boldsymbol{P}\boldsymbol{A} - \left(\boldsymbol{B}^T\boldsymbol{P}\boldsymbol{A}\right)^T \left(\boldsymbol{R} + \boldsymbol{B}^T\boldsymbol{P}\boldsymbol{B}\right)^{-1} \left(\boldsymbol{B}^T\boldsymbol{P}\boldsymbol{A}\right) + \boldsymbol{Q}.$$

Definition 2.6. *(Markov Parameters) Consider the discrete-time, LTV system* $\mathcal{S}_{d,LTV}$ *in* (2.3). *The matrix impulse response with initial condition* $\boldsymbol{x}_0 = 0$ *is:*

$$\boldsymbol{H}_k = \begin{cases} \boldsymbol{D}_k, & k = 0 \\ \boldsymbol{C}_k \prod_{i=1}^{k-1} \boldsymbol{A}_i\boldsymbol{B}_0, & k > 0, \end{cases} \tag{2.5}$$

where the terms $\boldsymbol{H}_k$ *are the* Markov parameters *of system* (2.3).

Definition 2.7. *(Continuous-Time State Transition Matrix) Consider the continuous-time LTV, unforced system of the form* $\dot{\boldsymbol{x}}(t) = \boldsymbol{A}(t)\boldsymbol{x}(t)$ *with initial condition* $\boldsymbol{x}(0)$*. Let* $t_1, t_2 \in \mathbb{R}$ *and* $t_1 \leqslant t_2$*. Then,* $\boldsymbol{\Phi}(t_2, t_1)$ *is the* continuous-time state transition matrix*, and is the unique solution to:*

$$\tfrac{\partial}{\partial t_2}\boldsymbol{\Phi}(t_2, t_1) = \boldsymbol{A}(t_2)\boldsymbol{\Phi}(t_2, t_1), \tag{2.6}$$

with the initial condition $\boldsymbol{\Phi}(t_1, t_1) = \boldsymbol{I}$*.*

Definition 2.8. *(Discrete-Time State Transition Matrix) Consider the discrete-time LTV, unforced system of the form* $\boldsymbol{x}_{k+1} = \boldsymbol{A}_k\boldsymbol{x}_k$ *with initial condition* $\boldsymbol{x}_0$*. Let* $k, i \in \mathbb{Z}$*, and* $k \geqslant i$*.* $\boldsymbol{\Psi}(k, i)$ *is the* discrete-time state transition matrix *and is the unique solution to:*

$$\boldsymbol{\Psi}(k+1, i) = \boldsymbol{A}_k\boldsymbol{\Psi}(k, i), \tag{2.7}$$

with the initial condition $\boldsymbol{\Psi}(i, i) = \boldsymbol{I}$*.*

2.3 Input-Output Theory

2.3.1 Continuous Time

Definition 2.9. *(Bounded-Input-Bounded-State Stable) Consider the continuous-time system represented by the following differential equation with initial condition* $\boldsymbol{x}(0) = 0$*:*

$$\dot{\boldsymbol{x}}(t) = \boldsymbol{f}(t, \boldsymbol{u}(t), \boldsymbol{x}(t)), \tag{2.8}$$

where $\boldsymbol{f} : \mathbb{R} \times \mathbb{R}^m \times \mathbb{R}^n \to \mathbb{R}^n$*. If there exist a constant* $\alpha \in \mathbb{R}$ *such that for all* $\boldsymbol{u} \in (\mathbb{L}^2)^m$ *and* $t \geqslant 0$*:*

$$\int_0^t \boldsymbol{x}^T(\tau)\boldsymbol{x}(\tau)d\tau \leqslant \alpha \int_0^t \boldsymbol{u}^T(\tau)\boldsymbol{u}(\tau)d\tau, \tag{2.9}$$

then (2.8) *is* bounded-input-bounded-state stable*.*

Definition 2.10. *(Continuous-Time Passive System) [14]. Let* $\mathcal{S}_c$ *be a continuous-time system represented by the following set of equations:*

$$\mathcal{S}_c : \begin{cases} \dot{\boldsymbol{x}}(t) = \boldsymbol{f}(t, \boldsymbol{u}(t), \boldsymbol{x}(t)) \\ \boldsymbol{v}(t) = \boldsymbol{g}(t, \boldsymbol{u}(t), \boldsymbol{x}(t), \end{cases} \tag{2.10}$$

where $\boldsymbol{f} : \mathbb{R} \times \mathbb{R}^m \times \mathbb{R}^n \to \mathbb{R}^n$ *and* $\boldsymbol{g} : \mathbb{R} \times \mathbb{R}^m \times \mathbb{R}^n \to \mathbb{R}^m$ *. If for each initial condition* $\boldsymbol{x}(0) \in \mathbb{R}^n$*, there exists a* $\beta \geqslant 0$ *such that for all* $\boldsymbol{u} \in (\mathbb{L}^2)^m$ *and* $t \geqslant 0$*:*

$$\int_0^t \boldsymbol{u}^T(\tau)\boldsymbol{v}(\tau)d\tau \geqslant -\beta,$$

then $\mathcal{S}_c$ *is* continuous-time passive.

Definition 2.11. *(Continuous-Time Positive Real (PR) and Strictly Positive Real (SPR) Transfer Functions) [38]. Consider a* $m \times m$ *continuous-time transfer function* $\boldsymbol{T}(s) : \mathbb{C} \to \mathbb{C}^{m \times m}$ *of real, rational functions, where* $s \in \mathbb{C}$*.* $\boldsymbol{T}(s)$ *is* PR *if:*

1. *all elements of* $\boldsymbol{T}(s)$ *are analytic for all* $s \in \mathbb{C}$ *such that* $\mathrm{Re}(s) > 0$
2. $\boldsymbol{T}(s)$ *is real for all real, positive values of* s
3. $\boldsymbol{T}(s) + \boldsymbol{T}^T(\bar{s}) \succeq 0$*, for all* $s \in \mathbb{C}$ *such that* $\mathrm{Re}(s) > 0$*.*

$\boldsymbol{T}(s)$ *is* SPR *if there exists an* $\alpha > 0$ *such that* $\boldsymbol{T}(s - \alpha)$ *is PR.*

Theorem 2.4. *(Continuous-Time, Time-Invariant Positive Real Lemma) [38]. Let* $\{\boldsymbol{A}, \boldsymbol{B}, \boldsymbol{C}, \boldsymbol{D}\}$ *be a minimal realization of the continuous-time, LTI system* $\mathcal{S}_{c,LTI}$ *in* (2.2)*. Then, let the continuous-time, real, proper, and rational transfer function of* $\boldsymbol{u} \mapsto \boldsymbol{v}$ *be:*

$$\boldsymbol{T}(s) = \boldsymbol{C}\left[s\boldsymbol{I} - \boldsymbol{A}\right]^{-1}\boldsymbol{B} + \boldsymbol{D}. \tag{2.11}$$

$\boldsymbol{T}(s)$ *is PR if and only if there exists* $\boldsymbol{P} = \boldsymbol{P}^T \succ 0$ *such that:*

$$\begin{bmatrix} \boldsymbol{A}^T\boldsymbol{P} + \boldsymbol{P}\boldsymbol{A} & \boldsymbol{P}\boldsymbol{B} - \boldsymbol{C}^T \\ (\boldsymbol{P}\boldsymbol{B} - \boldsymbol{C}^T)^T & -(\boldsymbol{D} + \boldsymbol{D}^T) \end{bmatrix} \preceq 0.$$

Theorem 2.5. *(Passivity of Continuous-Time LTI Systems) [38]. Let* $\{\boldsymbol{A}, \boldsymbol{B}, \boldsymbol{C}, \boldsymbol{D}\}$ *be a minimal realization of the continuous-time, LTI system system* $\mathcal{S}_{c,LTI}$ *in* (2.2)*. Let* $\boldsymbol{T}(s)$ *be the continuous-time, real, proper, and rational transfer function of* $\boldsymbol{u} \mapsto \boldsymbol{v}$ *in* (2.11)*. Then,* $\boldsymbol{T}(s)$ *is PR if and only if system* (2.3) *is a continuous-time, passive system.*

2.3.2 Discrete Time

Definition 2.12. *(Discrete-Time Passive System) [38]. Let* $\mathcal{S}_d$ *be a system represented by*

the following set of equations:

$$\mathcal{S}_d : \begin{cases} \boldsymbol{x}_{k+1} = \boldsymbol{f}_k(\boldsymbol{u}_k, \boldsymbol{x}_k) \\ \boldsymbol{v}_k = \boldsymbol{g}_k(\boldsymbol{u}_k, \boldsymbol{x}_k), \end{cases} \tag{2.12}$$

where $\boldsymbol{f} : \mathbb{R}^m \times \mathbb{R}^n \to \mathbb{R}^n$ *and* $\boldsymbol{g} : \mathbb{R}^m \times \mathbb{R}^n \to \mathbb{R}^m$*. If for each initial condition* $\boldsymbol{x}_0 \in \mathbb{R}^n$*, there exists a* $\beta \geqslant 0$ *such that for all* $\boldsymbol{u}_{0:k} \in (\mathbb{R}^m)^{k+1}$ *and* $k \in \mathbb{Z}_{\geqslant 0}$*:*

$$\sum_{i=0}^{k} \boldsymbol{u}_i^T \boldsymbol{y}_i \geqslant -\beta,$$

then S_d *is* discrete-time passive*.*

Definition 2.13. *(Discrete-time PR and SPR Transfer Functions) [38]. Consider a* $m \times m$*, rational, and proper discrete-time transfer function* $\boldsymbol{T}(z) : \mathbb{C} \to \mathbb{C}^{m \times m}$*, where* $z \in \mathbb{C}$*.* $\boldsymbol{T}(z)$ *is* PR *if:*

1. *all elements of* $\boldsymbol{T}(z)$ *are analytic for* $|z| > 1$
2. $\boldsymbol{T}(z) + \boldsymbol{T}^T(\bar{z}) \succeq 0$*,* $\forall |z| > 1$*.*

$\boldsymbol{T}(z)$ *is* SPR *if there exists an* $\alpha \in (0, 1)$ *such that* $\boldsymbol{T}(\alpha z)$ *is PR.*

Theorem 2.6. *(Discrete-Time Time-Invariant Positive Real Lemma) [38]. Let* $\{\boldsymbol{A}, \boldsymbol{B}, \boldsymbol{C}, \boldsymbol{D}\}$ *be a minimal realization of discrete-time LTI system* $\mathcal{S}_{d,LTI}$ *in* (2.4)*. Then, let the discrete-time, real, proper, and rational transfer function of* $\boldsymbol{u} \mapsto \boldsymbol{v}$ *be:*

$$\boldsymbol{T}(z) = \boldsymbol{C}\left[z\boldsymbol{I} - \boldsymbol{A}\right]^{-1}\boldsymbol{B} + \boldsymbol{D}. \tag{2.13}$$

$\boldsymbol{T}(z)$ *is PR if and only if there exists* $\boldsymbol{P} = \boldsymbol{P}^T \succ 0$ *such that:*

$$\begin{bmatrix} \boldsymbol{A}^T\boldsymbol{P}\boldsymbol{A} - \boldsymbol{P} & \boldsymbol{A}^T\boldsymbol{P}\boldsymbol{B} - \boldsymbol{C}^T \\ (\boldsymbol{A}^T\boldsymbol{P}\boldsymbol{B} - \boldsymbol{C}^T)^T & -(\boldsymbol{D} + \boldsymbol{D}^T) + \boldsymbol{B}^T\boldsymbol{P}\boldsymbol{B} \end{bmatrix} \preceq 0.$$

and $\boldsymbol{T}(z)$ *is SPR if and only if the above matrix is negative definite.*

Theorem 2.7. *(Passivity of Discrete-Time LTI Systems) [38]. Let* $\{\boldsymbol{A}, \boldsymbol{B}, \boldsymbol{C}, \boldsymbol{D}\}$ *be a minimal realization of discrete-time LTI system* $\mathcal{S}_{d,LTI}$ *in* (2.4)*. Consider* $\boldsymbol{T}(z)$*, the discrete-time, real, proper, and rational transfer function of* $\boldsymbol{u} \mapsto \boldsymbol{v}$ *in* (2.13)*. Then,* $\boldsymbol{T}(z)$ *is PR if and only if system* (2.4) *is a discrete-time, passive system.*

2.4 Discrete-Time Optimal Control

Definition 2.14. *(Discrete-Time Performance Measure, Lagrangian, Optimal Control Problem (OCP), Constrained Optimal Control Problem (COCP), Unconstrained Optimal Control Problem (UOCP)) Consider the following discrete-time difference equation for the evolution of* $\boldsymbol{x}$ *with initial condition* $\boldsymbol{x}_0 \in \mathbb{R}^n$*:*

$$\boldsymbol{x}_{k+1} = \boldsymbol{f}_k(\boldsymbol{u}_k, \boldsymbol{x}_k), \tag{2.14}$$

where $k \in \mathbb{Z}_{\geqslant 0}$ *is the discrete-time counter,* $\boldsymbol{u}_k \in \mathbb{R}^m$ *is the control input, and* $\boldsymbol{x}_k \in \mathbb{R}^n$ *is the state vector.*

Let the discrete-time performance measure *(also referred to as the* objective function *or* cost function*) be* $J(\boldsymbol{u}_{0:N}, \boldsymbol{x}_{0:N+1}) : (\mathbb{R}^m)^{N+1} \times (\mathbb{R}^n)^{N+2} \to \mathbb{R}$*, which is:*

$$J(\boldsymbol{u}_{0:N}, \boldsymbol{x}_{0:N+1}) = \Phi(\boldsymbol{x}_{N+1}) + \sum_{k=0}^{N} L_k(\boldsymbol{u}_k, \boldsymbol{x}_k), \tag{2.15}$$

where $N \in \mathbb{Z}_{\geqslant 0}$ *is the length of the MPC horizon,* $\Phi(\boldsymbol{x}_{N+1}) : \mathbb{R}^n \to \mathbb{R}$ *is a final-time penalty function, and* $L_k(\boldsymbol{u}_k, \boldsymbol{x}_k) : \mathbb{R}^m \times \mathbb{R}^n \to \mathbb{R}$ *is the* Lagrangian*.*

Let $\boldsymbol{c}_k(\boldsymbol{u}_k, \boldsymbol{x}_k) : \mathbb{R}^m \times \mathbb{R}^n \to \mathbb{R}^i$ *be the* i *inequality constraint functions, and* $\boldsymbol{h}_k(\boldsymbol{u}_k, \boldsymbol{x}_k) : \mathbb{R}^m \times \mathbb{R}^n \to \mathbb{R}^j$ *be the* j *equality constraint functions. Now, let a* COCP *have the following form:*

$$COCP = \begin{cases} \textbf{\textit{Given:}} & \boldsymbol{f}_k(\cdot,\cdot),\ \boldsymbol{c}_k(\cdot,\cdot),\ \boldsymbol{h}_k(\cdot,\cdot),\ L_k(\cdot,\cdot),\ \forall k \in \{0...N\} \\ & \Phi(\cdot),\ \boldsymbol{x}_0 \in \mathbb{R}^n \\ \textbf{\textit{Minimize:}} & J(\boldsymbol{u}_{0:N}, \boldsymbol{x}_{0:N+1}) \\ \textbf{\textit{Domain:}} & \boldsymbol{u}_{0:N},\ \boldsymbol{x}_{0:N+1} \\ \textbf{\textit{Constraints:}} & \boldsymbol{x}_{k+1} = \boldsymbol{f}_k(\boldsymbol{u}_k, \boldsymbol{x}_k), \\ & \boldsymbol{c}_k(\boldsymbol{u}_k, \boldsymbol{x}_k) \leqslant 0, \\ & \boldsymbol{h}_k(\boldsymbol{u}_k, \boldsymbol{x}_k) = 0, \\ & \forall k \in \{0...N\}, \end{cases} \tag{2.16}$$

where we optimize over control inputs $\boldsymbol{u}_{0:N}$ *and states* $\boldsymbol{x}_{0:N+1}$ *to minimize the performance objective* $J(\boldsymbol{u}_{0:N}, \boldsymbol{x}_{0:N+1})$ *while satisfying the* $i(N+1)$ *inequality constraints (*$\boldsymbol{c}_k(\boldsymbol{u}_k, \boldsymbol{x}_k) \leqslant 0$*) and* $j(N+1)$ *equality constraints (*$\boldsymbol{h}_k(\boldsymbol{u}_k, \boldsymbol{x}_k) = 0$*).*

Let a UOCP *have the following form:*

$$UOCP = \begin{cases} \textbf{\textit{Given:}} & \boldsymbol{f}_k(\cdot,\cdot),\ L_k(\cdot,\cdot),\ \forall k \in \{0...N\} \\ & \Phi(\cdot),\ \boldsymbol{x}_0 \in \mathbb{R}^n \\ \textbf{\textit{Minimize:}} & J(\boldsymbol{u}_{0:N}, \boldsymbol{x}_{0:N+1}) \\ \textbf{\textit{Domain:}} & \boldsymbol{u}_{0:N},\ \boldsymbol{x}_{0:N+1} \\ \textbf{\textit{Constraints:}} & \boldsymbol{x}_{k+1} = \boldsymbol{f}_k(\boldsymbol{u}_k, \boldsymbol{x}_k), \\ & \forall k \in \{0...N\}, \end{cases} \tag{2.17}$$

i.e., there are no inequality or equality constraints. We refer to both COCPs and UOCPs as OCPs.

Definition 2.15. *(Primal Domain, Feasible and Infeasible Primal Domains, Feasible and Infeasible Primal Trajectories, Feasible and Infeasible OCPs) [10]. Let* $\mathbb{D}^p \subseteq ((\mathbb{R}^m)^{N+1} \times (\mathbb{R}^n)^{N+1})$ *be the* primal domain *of an OCP in Definition 2.14, which is defined as:*

$$\mathbb{D}^p = \operatorname{dom} J(\boldsymbol{u}_{0:N}, \boldsymbol{x}_{0:N+1}) \bigcap_{k=0}^{N} \operatorname{dom} \boldsymbol{f}_k(\boldsymbol{u}_k, \boldsymbol{x}_k) \bigcap_{k=0}^{N} \operatorname{dom} \boldsymbol{c}_k(\boldsymbol{u}_k, \boldsymbol{x}_k) \bigcap_{k=0}^{N} \operatorname{dom} \boldsymbol{h}_k(\boldsymbol{u}_k, \boldsymbol{x}_k).$$

Now, let $\mathbb{F}^p \subseteq \mathbb{D}^p$ *be the* feasible primal domain*, which is defined as the set of control inputs and states* $\{\boldsymbol{u}_{0:N}, \boldsymbol{x}_{0:N+1}\}$ *that satisfy the constraints, i.e.:*

$$\mathbb{F}^p = \left\{ \{\boldsymbol{u}_{0:N}, \boldsymbol{x}_{0:N+1}\} \;\middle|\; \begin{array}{l} \boldsymbol{x}_{k+1} = \boldsymbol{f}_k(\boldsymbol{u}_k, \boldsymbol{x}_k),\ \ \boldsymbol{c}_k(\boldsymbol{u}_k, \boldsymbol{x}_k) \leqslant 0 \\ \boldsymbol{h}_k(\boldsymbol{u}_k, \boldsymbol{x}_k) = 0,\ \ \forall k \in \{0...N\} \end{array} \right\}.$$

Then, the infeasible primal domain *is* $((\mathbb{R}^m)^{N+1} \times (\mathbb{R}^n)^{N+2}) \setminus \mathbb{F}^p$*. A primal trajectory* $\{\boldsymbol{u}_{0:N}, \boldsymbol{x}_{0:N+1}\}$ *is* feasible *if* $\{\boldsymbol{u}_{0:N}, \boldsymbol{x}_{0:N+1}\} \in \mathbb{F}^p$*, and* infeasible *otherwise. An OCP is* infeasible *if* $\mathbb{F}^p = \emptyset$*, and* feasible *otherwise.*

Definition 2.16. *(Minimal Performance Measure, Unbounded Optimal Control Problem, Optimal Trajectory) [10]. Consider the definition of an OCP in Definition 2.14, and let* $\mathbb{F}^p$ *be the primal feasible domain in Definition 2.15. Now, let* J^* *be the* minimal performance

measure*, which is defined as:*

$$J^* = \begin{cases} \infty, & \mathbb{F}^p = \emptyset \\ \inf \left\{ J(\boldsymbol{u}_{0:N}, \boldsymbol{x}_{0:N+1}) \;\middle|\; \begin{array}{l} \boldsymbol{x}_{k+1} = \boldsymbol{f}_k(\boldsymbol{u}_k, \boldsymbol{x}_k),\ \boldsymbol{c}_k(\boldsymbol{u}_k, \boldsymbol{x}_k) \leqslant 0, \\ \boldsymbol{h}_k(\boldsymbol{u}_k, \boldsymbol{x}_k) = 0,\ \forall k \in \{0..N\} \end{array} \right\}, & \mathbb{F}^p \neq \emptyset. \end{cases} \tag{2.18}$$

An OCP is unbounded *if* $J^* = -\infty$*. Let* $\{\boldsymbol{u}^*_{0:N}, \boldsymbol{x}^*_{0:N+1}\} \in \mathbb{F}^p$ *be an* optimal trajectory *if* $J(\boldsymbol{u}^*_{0:N}, \boldsymbol{x}^*_{0:N+1}) = J^*$*.*

Definition 2.17. *(Hamiltonian, Lagrange Multipliers, Costates, Dual Variables, Augmented Performance Measure) [15]. Consider an OCP from Definition 2.14. Then, the* Hamiltonian *for the* k^{th} *time step is* $\mathcal{H}_k(\boldsymbol{u}_k, \boldsymbol{x}_k, \boldsymbol{\lambda}_k, \boldsymbol{\sigma}_k, \boldsymbol{\rho}_k) : \mathbb{R}^m \times \mathbb{R}^n \times \mathbb{R}^i \times \mathbb{R}^j \times \mathbb{R}^n \to \mathbb{R}$*, which is defined as:*

$$\begin{aligned} \mathcal{H}_k\left(\boldsymbol{u}_k, \boldsymbol{x}_k, \boldsymbol{\lambda}_k, \boldsymbol{\sigma}_k, \boldsymbol{\rho}_k\right) =& L_k(\boldsymbol{u}_k, \boldsymbol{x}_k) + \boldsymbol{\lambda}_k^T \boldsymbol{c}_k(\boldsymbol{u}_k, \boldsymbol{x}_k) \\ &+ \boldsymbol{\sigma}_k^T \boldsymbol{h}_k(\boldsymbol{u}_k, \boldsymbol{x}_k) + \boldsymbol{\rho}_{k+1}^T \boldsymbol{f}_k(\boldsymbol{u}_k, \boldsymbol{x}_k), \end{aligned} \tag{2.19}$$

where $L_k(\boldsymbol{u}_k, \boldsymbol{x}_k)$ *is the Lagrangian from Definition 2.14,* $\boldsymbol{\lambda}_k \in \mathbb{R}^i_{\geqslant 0}$ *are the* Lagrange multipliers *that enforce the* i *inequality constraints (*$\boldsymbol{c}_k(\boldsymbol{u}_k, \boldsymbol{x}_k) \leqslant \boldsymbol{0}$*) at the* k^{th} *time step,* $\boldsymbol{\sigma}_k \in \mathbb{R}^j$ *are the* Lagrange multipliers *that enforce the* j *equality constraints (*$\boldsymbol{h}_k(\boldsymbol{u}_k, \boldsymbol{x}_k) = \boldsymbol{0}$*) at the* k^{th} *time step, and* $\boldsymbol{\rho}_{k+1} \in \mathbb{R}^n$ *are the* costates *that enforce the evolution of the state dynamics (*$\boldsymbol{x}_{k+1} = \boldsymbol{f}_k(\boldsymbol{u}_k, \boldsymbol{x}_k)$*) at the* k^{th} *time step.*

The Lagrange multipliers *and* costates *are also referred to as* dual variables*. Now, reference the performance measure in Definition 2.14, and let the* augmented performance measure $\bar{J}(\boldsymbol{u}_{0:N}, \boldsymbol{x}_{0:N+1}, \boldsymbol{\lambda}_{0:N}, \boldsymbol{\sigma}_{0:N}, \boldsymbol{\rho}_{1:N+1}) : (\mathbb{R}^m)^{N+1} \times (\mathbb{R}^n)^{N+2} \times (\mathbb{R}^i)^{N+1} \times (\mathbb{R}^j)^{N+1} \times (\mathbb{R}^n)^{N+2} \to \mathbb{R}$ *be:*

$$\bar{J}(\boldsymbol{u}_{0:N}, \boldsymbol{x}_{0:N+1}, \boldsymbol{\lambda}_{0:N}, \boldsymbol{\sigma}_{0:N}, \boldsymbol{\rho}_{1:N+1}) = \Phi(\boldsymbol{x}_{N+1}) + \sum_{k=0}^{N} \mathcal{H}_k(\boldsymbol{u}_k, \boldsymbol{x}_k, \boldsymbol{\lambda}_k, \boldsymbol{\sigma}_k, \boldsymbol{\rho}_k). \tag{2.20}$$

Definition 2.18. *(Primal Minimax Problem) Consider an OCP from Definition 2.14, which can be written in the following* primal minimax form*:*

$$J^* = \inf_{\{\boldsymbol{u}_{0:N},\, \boldsymbol{x}_{0:N+1}\}} \sup_{\{\boldsymbol{\lambda}_{0:N} \geqslant 0, \boldsymbol{\sigma}_{0:N}, \boldsymbol{\rho}_{1:N+1}\}} \bar{J}(\boldsymbol{u}_{0:N}, \boldsymbol{x}_{0:N+1}, \boldsymbol{\lambda}_{0:N}, \boldsymbol{\sigma}_{0:N}, \boldsymbol{\rho}_{1:N+1}), \tag{2.21}$$

where $\bar{J}$ *is the augmented performance objective in* (2.20)*, and* J^* *is the minimal performance*

objective in (2.18)*. The associated optimal trajectory is then:*

$$\{\boldsymbol{u}^*_{0:N}, \boldsymbol{x}^*_{0:N+1}\} = \underset{\{\boldsymbol{u}_{0:N},\, \boldsymbol{x}_{0:N+1}\}}{\operatorname{arginf}} \; \sup_{\{\boldsymbol{\lambda}_{0:N} \geqslant 0, \boldsymbol{\sigma}_{0:N}, \boldsymbol{\rho}_{1:N+1}\}} \bar{J}(\boldsymbol{u}_{0:N}, \boldsymbol{x}_{0:N+1}, \boldsymbol{\lambda}_{0:N}, \boldsymbol{\sigma}_{0:N}, \boldsymbol{\rho}_{1:N+1}).$$

Theorem 2.8. *(Finite-horizon, discrete-time Linear Quadratic Regulator (LQR)) [41]. The* finite-horizon, discrete-time LQR problem *is an UOCP where the state dynamics are represented by the discrete-time LTV system* (2.3)*, and the performance measure is of the form:*

$$J(\boldsymbol{u}_{0:N}, \boldsymbol{x}_{0:N+1}) = \frac{1}{2}\boldsymbol{x}^T_{N+1}\boldsymbol{P}_{N+1}\boldsymbol{x}_{N+1} + \frac{1}{2}\sum_{k=0}^{N} \boldsymbol{x}^T_k \boldsymbol{Q}_k \boldsymbol{x}_k + \boldsymbol{u}^T_k \boldsymbol{R}_k \boldsymbol{u}_k + 2\boldsymbol{u}^T_k \boldsymbol{S}_k \boldsymbol{x}_k,$$

where $\boldsymbol{P}^T_{N+1} = \boldsymbol{P}_{N+1} \succeq 0$, $\boldsymbol{R}^T_k = \boldsymbol{R}_k \succ 0$*. Then, the optimal control input trajectory* $\forall k \in \{0...N\}$ *is* $\boldsymbol{u}^*_k = -\boldsymbol{K}_k \boldsymbol{x}_k$ *where:*

$$\boldsymbol{K}_k = \left(\boldsymbol{R}_k + \boldsymbol{B}^T_k \boldsymbol{P}_k \boldsymbol{B}_k\right)^{-1} \boldsymbol{B}^T_k \boldsymbol{P}_k \tilde{\boldsymbol{A}}_k + \boldsymbol{R}^{-1}_k \boldsymbol{S}^T_k.$$

Let $\tilde{\boldsymbol{A}}_k = \boldsymbol{A}_k - \boldsymbol{B}_k \boldsymbol{R}^{-1}_k \boldsymbol{S}^T_k$*, and the* $\boldsymbol{P}_k$ *is the solution to the following RDRDE:*

$$\boldsymbol{P}_{k-1} = \tilde{\boldsymbol{Q}}_k + \tilde{\boldsymbol{A}}^T_k \boldsymbol{P}_k \tilde{\boldsymbol{A}}_k - \tilde{\boldsymbol{A}}^T_k \boldsymbol{P}_k \boldsymbol{B}_k \left(\boldsymbol{R}_k + \boldsymbol{B}^T_k \boldsymbol{P}_k \boldsymbol{B}_k\right)^{-1} \boldsymbol{B}_k \boldsymbol{P}_k \tilde{\boldsymbol{A}}_k,$$

with final condition $\boldsymbol{P}_{N+1}$*.*

2.4.1 Convexity

Definition 2.19. *(Convex Set, Nonconvex Set) [10]. A set* $\mathbb{A}$ *is* convex *if* $\forall \boldsymbol{x}, \boldsymbol{y} \in \mathbb{A}$ *and* $\forall \alpha \in [0, 1]$*:*

$$\alpha \boldsymbol{x} + (1 - \alpha)\boldsymbol{y} \in \mathbb{A},$$

and set $\mathbb{A}$ *is* nonconvex *otherwise.*

Definition 2.20. *(Convex Function, Strictly Convex Function, Concave Function, Strictly Concave Function) A function* $g(\boldsymbol{x}) : \mathbb{R}^n \to \mathbb{R}$ *is* convex *in* $\boldsymbol{x}$ *if the following are true:*

1. $\operatorname{dom} g(\boldsymbol{x})$ *is a convex set*
2. $\forall \boldsymbol{x}, \boldsymbol{y} \in \operatorname{dom} g(\boldsymbol{x})$ *and* $\forall \alpha \in [0, 1]$, $g(\alpha \boldsymbol{x} + (1 - \alpha)\boldsymbol{y}) \leqslant \alpha g(\boldsymbol{x}) + (1 - \alpha) g(\boldsymbol{y})$.

Function $g(\boldsymbol{x})$ is strictly convex *if the inequality in the second requirement is strict. Function $g(\boldsymbol{x})$ is* concave *if $-g(\boldsymbol{x})$ is convex, and* strictly concave *if $-g(\boldsymbol{x})$ satisfies the second requirement with strict inequality.*

Definition 2.21. *(Convex OCP, Nonconvex OCP) [10]. Let $\boldsymbol{x}^{\circ}_{0:N}(\boldsymbol{u}_{0:N}, \boldsymbol{x}_0)$ be the solution to* (2.14) *over the interval $k \in \{0...N\}$; i.e.,*

$$\boldsymbol{x}^{\circ}_{k+1}(\boldsymbol{u}_{0:N}, \boldsymbol{x}_0) = \boldsymbol{f}_k(\boldsymbol{u}_k, \boldsymbol{x}^{\circ}_k(\boldsymbol{u}_{0:N}, \boldsymbol{x}_0)).$$

An OCP from Definition 2.14 is convex *if the following are true:*

1. *Performance measure $J(\boldsymbol{u}_{0:N}, \boldsymbol{x}^{\circ}_{0:N+1}(\boldsymbol{u}_{0:N}, \boldsymbol{x}_0))$ is convex in $\boldsymbol{u}_{0:N}$*
2. *Inequality constraint functions $\boldsymbol{c}_k(\boldsymbol{u}_k, \boldsymbol{x}^{\circ}_k(\boldsymbol{u}_{0:N}, \boldsymbol{x}_0)) \leqslant 0$ are convex in $\boldsymbol{u}_{0:N}$, $\forall k \in \{0...N\}$*
3. *Equality constraint functions, $\boldsymbol{h}_k(\boldsymbol{u}_k, \boldsymbol{x}^{\circ}_k(\boldsymbol{u}_{0:N}, \boldsymbol{x}_0)) = 0$ are affine in $\boldsymbol{u}_{0:N}$, $\forall k \in \{0...N\}$.*

It follows that the feasible primal domain of a convex OCP, $\mathbb{F}^p$, is a convex set. An OCP is nonconvex *if it is not convex.*

2.4.2 Special Optimization Problem Forms

Definition 2.22. *(QP) [10]. A* QP *is a optimization problem with a quadratic performance measure that has the form:*

$$QP = \begin{cases} \textbf{\textit{Given:}} & \boldsymbol{Q} \in \mathbb{S}^n, \boldsymbol{s} \in \mathbb{R}^n, r, \\ & \boldsymbol{M} \in \mathbb{R}^{m \times n}, \boldsymbol{p} \in \mathbb{R}^m, \boldsymbol{A} \in \mathbb{R}^{p \times n}, \boldsymbol{b} \in \mathbb{R}^p \\ \textbf{\textit{Minimize:}} & \boldsymbol{x}^T \boldsymbol{Q} \boldsymbol{x} + \boldsymbol{s}^T \boldsymbol{x} + r \\ \textbf{\textit{Domain:}} & \boldsymbol{x} \in \mathbb{R}^n \\ \textbf{\textit{Constraints:}} & \boldsymbol{M}\boldsymbol{x} \leqslant \boldsymbol{p}, \\ & \boldsymbol{A}\boldsymbol{x} = \boldsymbol{b}. \end{cases}$$

The QP is convex if $\boldsymbol{Q} \succ 0$.

Definition 2.23. *(QCQP) [10]. A* QCQP *is an optimization problem with a quadratic*

performance measure and quadratic inequality constraints that has the form:

$$QCQP = \begin{cases} \textbf{\textit{Given:}} & \boldsymbol{Q}_i \in \mathbb{S}^n, \boldsymbol{s}_i \in \mathbb{R}^n, r_i, \ \forall i \in \{0...m\} \\ & \boldsymbol{A} \in \mathbb{R}^{p \times n}, \boldsymbol{b} \in \mathbb{R}^p \\ \textbf{\textit{Minimize:}} & \boldsymbol{x}^T \boldsymbol{Q}_0 \boldsymbol{x} + \boldsymbol{s}_0^T \boldsymbol{x} + r_0 \\ \textbf{\textit{Domain:}} & \boldsymbol{x} \in \mathbb{R}^n \\ \textbf{\textit{Constraints:}} & \boldsymbol{x}^T \boldsymbol{Q}_i \boldsymbol{x} + \boldsymbol{s}_i^T \boldsymbol{x} + r_i \leqslant 0, \quad \forall i \in \{1...m\} \\ & \boldsymbol{A}\boldsymbol{x} = \boldsymbol{b}, \end{cases}$$

If $\boldsymbol{Q}_i = \boldsymbol{0}$ for all $i \in \{1...m\}$, then the constraints are linear and the problem is a QP. The QCQP is convex if $\boldsymbol{Q}_i \succeq 0$, for all $i \in \{0...m\}$, and nonconvex if there exists an $i \in \{0...m\}$ such that $\boldsymbol{Q}_i$ is not positive semi-definite.

Definition 2.24. *(SDP) [10]. A* SDP *is an optimization problem that has the form:*

$$SDP = \begin{cases} \textbf{\textit{Given:}} & \boldsymbol{C} \in \mathbb{S}^n, \boldsymbol{b} \in \mathbb{R}^m, \boldsymbol{A}_k \in \mathbb{S}^n, \forall k \in \{1...m\} \\ \textbf{\textit{Minimize:}} & \displaystyle\sum_{i=1}^{n} \sum_{j=1}^{n} C_{ij} X_{ij} \\ \textbf{\textit{Domain:}} & \boldsymbol{X} \in \mathbb{S}^n \\ \textbf{\textit{Constraints:}} & \displaystyle\sum_{i=1}^{n} \sum_{j=1}^{n} A_{k,ij} X_{ij} = b_k, \ \forall k \in \{1...m\} \\ & \boldsymbol{X} \succeq 0. \end{cases}$$

2.5 Lagrangian Duality

Definition 2.25. *(Dual Function, Dual Problem, Dual Minimax Problem, Dual Feasible, Optimal Dual Solution) Consider the COCP from Definition 2.14, and let the* dual function *$G : (\mathbb{R}^i_{\geqslant 0})^{N+1} \times (\mathbb{R}^j)^{N+1} \to \mathbb{R}$ be defined as:*

$$G(\boldsymbol{\lambda}_{0:N}, \boldsymbol{\sigma}_{0:N}) = \sup_{\boldsymbol{\rho}_{1:N+1}} \inf_{\{\boldsymbol{u}_{0:N}, \boldsymbol{x}_{0:N+1}\}} \bar{J}(\boldsymbol{u}_{0:N}, \boldsymbol{x}_{0:N+1}, \boldsymbol{\lambda}_{0:N}, \boldsymbol{\sigma}_{0:N}, \boldsymbol{\rho}_{1:N+1}),$$

where $\bar{J}$ is the augmented performance objective in (2.20)*. The dual function $G(\boldsymbol{\lambda}_{0:N}, \boldsymbol{\sigma}_{0:N})$*

is always a lower bound on the minimal primal performance measure, i.e.,

$$G(\boldsymbol{\lambda}_{0:N}, \boldsymbol{\sigma}_{0:N}) \leqslant J^*, \quad \forall \{\boldsymbol{\lambda}_{0:N}, \boldsymbol{\sigma}_{0:N}\} \in ((\mathbb{R}^i_{\geqslant 0})^{N+1} \times (\mathbb{R}^j)^{N+1}).$$

Then, the problem of finding the greatest lower bound on J^*, which is the maximal dual function G^*, is the dual problem*, i.e.:*

$$\textit{Dual COCP} = \begin{cases} \textbf{\textit{Given:}} & G(\cdot, \cdot) \\ \textbf{\textit{Maximize:}} & G(\boldsymbol{\lambda}_{0:N}, \boldsymbol{\sigma}_{0:N}) \\ \textbf{\textit{Domain:}} & \boldsymbol{\lambda}_{0:N}, \boldsymbol{\sigma}_{0:N} \\ \textbf{\textit{Constraints:}} & \boldsymbol{\lambda}_{0:N} \geqslant 0. \end{cases}$$

Note that the dual function is concave, regardless of the convexity of the primal problem which can be written in the following dual minimax form*:*

$$G^* = \sup_{\{\boldsymbol{\lambda}_{0:N} \geqslant 0, \boldsymbol{\sigma}_{0:N}, \boldsymbol{\rho}_{1:N+1}\}} \inf_{\{\boldsymbol{u}_{0:N},\, \boldsymbol{x}_{0:N+1}\}} \bar{J}(\boldsymbol{u}_{0:N}, \boldsymbol{x}_{0:N+1}, \boldsymbol{\lambda}_{0:N}, \boldsymbol{\sigma}_{0:N}, \boldsymbol{\rho}_{1:N+1}). \tag{2.22}$$

Let $\{\boldsymbol{\lambda}_{0:N}, \boldsymbol{\sigma}_{0:N}\}$ be dual feasible *if $\boldsymbol{\lambda}_{0:N} \geqslant 0$. Let $\{\boldsymbol{\lambda}^*_{0:N}, \boldsymbol{\sigma}^*_{0:N}\}$ be an* optimal dual point *if $G(\boldsymbol{\lambda}^*_{0:N}, \boldsymbol{\sigma}^*_{0:N}) = G^*$.*

Definition 2.26. *(Duality Gap, Strong Duality) [10]. The difference between the minimum performance measure, J^*, and the maximum dual function, G^*, is the* duality gap*, i.e., $J^* - G^*$, which is always a nonnegative value. An optimization problem has zero duality gap if $J^* = G^*$, then we say that* strong duality holds*.*

Definition 2.27. *(Karush-Kuhn-Tucker (KKT) Conditions, Constraint Qualification) [10]. Consider the COCP from Definition 2.14. Let the performance measure $J(\cdot, \cdot)$, inequality constraints $\boldsymbol{c}_k(\cdot, \cdot)$, and equality constraints $\boldsymbol{h}_k(\cdot, \cdot)$ be differentiable functions in $\boldsymbol{u}_{0:N}$ and $\boldsymbol{x}_{0:N+1}$. The KKT conditions are the first-order necessary conditions for the primal solution:*

$$\{\boldsymbol{u}^*_{0:N}, \boldsymbol{x}^*_{0:N+1}, \boldsymbol{\lambda}^*_{0:N}, \boldsymbol{\sigma}^*_{0:N}, \boldsymbol{\rho}^*_{1:N+1}\}$$

to be optimal, given that a constraint qualification *(also known as a* regularity condition*) is satisfied. The KKT conditions are:*

1. $\boldsymbol{c}_k(\boldsymbol{u}^*_{0:N}, \boldsymbol{x}^*_{0:N+1}) \leqslant \mathbf{0}$ *and* $\boldsymbol{h}_k(\boldsymbol{u}^*_{0:N}, \boldsymbol{x}^*_{0:N+1}) = \mathbf{0}$, $\forall k \in \{0...N\}$ *(primal feasibility)*

2. $\boldsymbol{\lambda}_k^* \geqslant \mathbf{0}$, $\forall k \in \{0...N\}$ *(dual feasibility)*

3. $(\boldsymbol{\lambda}_k^*)^T \boldsymbol{c}_k(\boldsymbol{u}_{0:N}^*, \boldsymbol{x}_{0:N+1}^*) = 0$, $\forall k \in \{0...N\}$ *(complementary slackness)*

4. $\nabla J(\boldsymbol{u}_{0:N}^*, \boldsymbol{x}_{0:N+1}^*) + \sum_{k=0}^{N} (\boldsymbol{\lambda}_k^*)^T \nabla \boldsymbol{c}_k(\boldsymbol{u}_{0:N}^*, \boldsymbol{x}_{0:N+1}^*) + (\boldsymbol{\sigma}_k^*)^T \nabla \boldsymbol{h}_k(\boldsymbol{u}_{0:N}^*, \boldsymbol{x}_{0:N+1}^*)$
$+ (\boldsymbol{\rho}_{k+1}^*)^T \nabla \boldsymbol{f}_k(\boldsymbol{u}_k^*, \boldsymbol{x}_k^*) = \mathbf{0}$ *(zero gradient).*

Theorem 2.9. *(Slater's Constraint Qualification) [8, 10]. Consider a convex COCP from Definition 2.14, and let $\mathbb{F}^p$ be its feasible domain. Then, if there exists $\{\boldsymbol{u}_{0:N}, \boldsymbol{x}_{0:N}\} \in$ relint$(\mathbb{F}^p)$ such that $\boldsymbol{c}_k(\boldsymbol{u}_{0:N}, \boldsymbol{x}_{0:N+1}) < 0$, $\boldsymbol{x}_{k+1} = \boldsymbol{f}_k(\boldsymbol{u}_k, \boldsymbol{x}_k)$, and $\boldsymbol{h}_k(\boldsymbol{u}_{0:N}, \boldsymbol{x}_{0:N+1}) = 0$, $\forall k \in \{0...N\}$ (i.e., the inequality constraints hold with strict inequality), then strong duality holds.*

Chapter 3

Self-Powered System Modeling

In this chapter, we introduce continuous-time dynamical models for the plant and energy storage blocks in Figure 1.4. We characterize each of the components of these models. Then, we show that for plant models satisfying certain properties, a self-powered system cannot be destabilized by any feasible control input. Last, we discretize the dynamics of the plant energy storage system models, and then discuss properties of the discrete-time models that guarantee a nonempty feasible domain.

3.1 Continuous-Time Model for Self-Powered Systems

3.1.1 Continuous-Time Plant Model

We begin by modeling the linear, time-varying dynamics of the plant in Figure 1.4 in continuous time with n states, m control inputs, and d exogenous disturbances as:

$$\mathcal{P}: \begin{cases} \dot{\boldsymbol{x}}(t) = \bar{\boldsymbol{A}}(t)\boldsymbol{x}(t) + \bar{\boldsymbol{B}}(t)\boldsymbol{u}(t) + \bar{\boldsymbol{G}}(t)\boldsymbol{a}(t) \\ \boldsymbol{v}(t) = \bar{\boldsymbol{C}}(t)\boldsymbol{x}(t) + \bar{\boldsymbol{D}}(t)\boldsymbol{u}(t), \end{cases} \tag{3.1}$$

where the overbar later distinguishes the continuous-time system matrices from the discretized matrices.

Definition 3.1. *For continuous-time plant models of the form* (3.1)*, we define* $\mathbb{P}$ *to be the set of all models satisfying the following properties:*

1. *The mapping* $\boldsymbol{u} \mapsto \boldsymbol{v}$ *is* continuous-time passive *(see Definition 2.10)*

2. *The plant is* bounded-input-bounded-state stable *(see Definition 2.9), i.e., there exist constants g_u and g_a such that for $\boldsymbol{x}(0) = 0$, $\boldsymbol{a}(t) \in (\mathbb{L}^2)^d$, $\boldsymbol{u} \in (\mathbb{L}^2)^m$, and $t \geqslant 0$:*

$$\int_0^t \boldsymbol{x}^T(\tau)\boldsymbol{x}(\tau)d\tau \leqslant g_u \int_0^t \boldsymbol{u}^T(\tau)\boldsymbol{u}(\tau)d\tau + g_a \int_0^t \boldsymbol{a}^T(\tau)\boldsymbol{a}(\tau)d\tau.$$

Assumption 1. *We assume $\mathcal{P} \in \mathbb{P}$ for the entirety of this thesis.*

The passivity of $\boldsymbol{u} \mapsto \boldsymbol{v}$ is a consequence of thermodynamic constraints on the plant. Physically, the plant is a passive vibratory network, implying that it contains no internal energy sources. Equivalently, as seen from the terminals of the transducer ports, the equivalent circuit for the driving point impedance of the plant can be realized via a network of ideal, time-varying resistors, capacitors, inductors, transformers and gyrators.

Both the passivity property and the bounded-input-bounded-state property is important in proving the guaranteed stability of self-powered systems (see Section 3.1.5). If either of these conditions are violated it may still be the case that the MPC algorithm to be presented here could be applied in this situation. However, in that case closed-loop stability would need to be guaranteed explicitly for the MPC algorithm.

3.1.2 Continuous-Time Energy Storage Model

Reference Figure 1.4, where m transducer ports are interfaced with p energy storage systems. The energy in the i^{th} storage system is represented by $E^i(t)$, which, due to physical constraints on the storage device, is required to be within the bounds $E_L^i \leqslant E^i(t) \leqslant E_U^i$, where $E_L^i, E_U^i \geqslant 0$ are the lower and upper energy constraints, respectively. Each energy storage system is connected to a resistor bank or power bus. The evolution of stored energy in the i^{th} energy storage system is:

$$\tfrac{d}{dt}E^i(t) = -\tfrac{1}{T_S^i}E^i(t) - \boldsymbol{u}^T(t)\boldsymbol{K}^i\boldsymbol{v}(t) - \mu^i(t) - q^i(t), \tag{3.2}$$

where:

- $T_S^i > 0$ is a time constant derived from the physical parameters of the i^{th} storage system that accounts for the loss of energy due to decay in the storage system. For $T_S^i \to \infty$, there is no decay of energy in the storage system, and for $T_S^i = 0$, no energy can be stored in the storage system.

- $\boldsymbol{K}^i$ is an $m \times m$ diagonal matrix with entries of $\{1, 0\}$ that describe the connectivity between the m ports and the i^{th} energy storage system. Each port can only connect to a single energy storage system, however, each energy storage system may have multiple ports connected to it. Therefore, we require $\sum_{i=1}^{p} \boldsymbol{K}^i = \boldsymbol{I}_m$. Let $\mathbb{K}^i$ be the set of all ports connected to the i^{th} energy storage unit, e.g., in Figure 1.5b $\mathbb{K}^1 = \{1, 2\}$ and $\mathbb{K}^2 = \{3\}$.

- $\mu^i(t)$ accounts for transmission power dissipation, e.g., due to losses within the power electronics, which we discuss in detail in Section 3.1.3.

- $q^i(t) \geqslant 0$ is the power sent from energy storage system i to its resistor bank or power bus.

3.1.3 Continuous-Time Transmission Loss Model

In equation (3.2), $\mu^i(t)$ represents the transmission losses associated with the facilitation of power flow from the transducer ports to storage system i. In this work, we assume $\mu^i(t)$ to be a quadratic function of $\boldsymbol{u}(t)$ and $\boldsymbol{v}(t)$; i.e.,

$$\mu^i(t, \boldsymbol{u}(t), \boldsymbol{v}(t)) = \begin{bmatrix} \boldsymbol{u}(t) \\ \boldsymbol{v}(t) \end{bmatrix} \boldsymbol{M}^i(t) \begin{bmatrix} \boldsymbol{u}(t) \\ \boldsymbol{v}(t) \end{bmatrix}. \tag{3.3}$$

Assumption 2. *We make the following assumptions regarding $\mu^i(\cdot, \cdot, \cdot)$, $i \in \{1...p\}$.*

1. *For all $t \geqslant 0$, $\boldsymbol{M}^i(t, \boldsymbol{u}(t), \boldsymbol{v}(t)) \succeq 0$.*

2. *There exists a matrix $\boldsymbol{R}_L \succ 0$ such that $\forall \{\boldsymbol{u}(t), \boldsymbol{v}(t)\} \in (\mathbb{R}^m \times \mathbb{R}^m)$ and $\forall t \geqslant 0$:*

$$\sum_{i=1}^{p} \mu^i(t, \boldsymbol{u}(t), \boldsymbol{v}(t)) \succeq \boldsymbol{u}^T(t) \boldsymbol{R}_L \boldsymbol{u}(t).$$

3. *For each $\boldsymbol{v}(t) \in \mathbb{R}^m$ and $t \geqslant 0$, there exists a $\boldsymbol{u}(t) \in \mathbb{R}^m$ such that:*

$$\boldsymbol{u}^T(t)\boldsymbol{v}(t) + \mu^i(t, \boldsymbol{u}(t), \boldsymbol{v}(t)) \leqslant 0, \quad \forall i \in \{1...p\}. \tag{3.4}$$

Assumption 2.1 ensures that the power dissipated upon transmission from the transducer ports to storage system i is uniformly nonnegative. This is a consequence of physical constraints on the network. Assumption 2.2 is only of importance for proving the unconditional

stability of the self-powered system, to be discussed later in Section 3.1.5. Assumption 2.3 stipulates that for each potential variable, there exists a control input such that the power extracted at the transducer ports exceeds the transmission losses incurred in the electronics. This assumption is important for the feasibility analysis to be discussed next.

3.1.4 Valid Continuous-Time Models and Control Feasibility

Definition 3.2. *We refer to a self-powered system model $\mathcal{M}$ as the collection of the following:*

1. *A continuous-time plant model $\mathcal{P}$ as in* (3.1)
2. *A set of p continuous-time energy storage models as in* (3.2)*, together with physical storage bounds $\{E_L^1 \dots E_L^p\}$ and $\{E_U^1 \dots E_U^p\}$*
3. *A set of p continuous-time transmission loss models $\{\mu^1(\cdot,\cdot,\cdot) \dots \mu^p(\cdot,\cdot,\cdot)\}$ as in* (3.3)*.*

Definition 3.3. *We define a model $\mathcal{M}$ to be* valid *if:*

1. $\mathcal{P} \in \mathbb{P}$
2. $T_S^i \in (0,\infty]$*, and* $0 \leqslant E_L^i \leqslant E_U^i$*,* $\forall i \in \{1 \dots p\}$
3. *Assumption 2 holds for the transmission loss models $\{\mu^1(\cdot,\cdot,\cdot) \dots \mu^p(\cdot,\cdot,\cdot)\}$.*

Definition 3.4. *We refer to the set of all valid models as $\mathbb{M}$.*

For a given $\mathcal{M} \in \mathbb{M}$, we collect all energy storage values in vector $\boldsymbol{E}(t)$ as:

$$\boldsymbol{E}(t) = \begin{bmatrix} E^1(t) & \cdots & E^p(t) \end{bmatrix}^T,$$

and then we define the feasibility domain of $\boldsymbol{E}(t)$ as:

$$\mathbb{R}_E = [E_L^1, E_U^1] \times \cdots \times [E_L^p, E_U^p].$$

Definition 3.5. *Given model $\mathcal{M} \in \mathbb{M}$, disturbance $\boldsymbol{a} \in (\mathbb{L}^2)^d$, state initial condition $\boldsymbol{x}(0) \in \mathbb{R}^n$, and energy initial condition $\boldsymbol{E}(0) \in \mathbb{R}_E$:*

1. *Control inputs $\{\boldsymbol{u}, \boldsymbol{q}\} \in (\mathbb{L}^2)^m \times (\mathbb{L}^2)^p$ are called* feasible *if they result in $\boldsymbol{E}(t) \in \mathbb{R}_E$ and $\boldsymbol{q}(t) \geqslant 0$, for all $t \geqslant 0$.*
2. *The set of all feasible control inputs is denoted $\mathbb{F}_{\mathcal{M}}(\boldsymbol{a}, \boldsymbol{x}(0), \boldsymbol{E}(0))$.*

Lemma 3.1. *Let $\mathcal{M} \in \mathbb{M}$, and for each $i \in \{1...p\}$ either $E_L^i = 0$ or $T_S^i \to \infty$. Then, $\mathbb{F}_{\mathcal{M}}(\boldsymbol{a}, \boldsymbol{x}(0), \boldsymbol{E}(0))$ is nonempty for all $\{\boldsymbol{a}, \boldsymbol{x}(0), \boldsymbol{E}(0)\} \in (\mathbb{L}^2)^d \times \mathbb{R}^n \times \mathbb{R}_E$.*

Proof. $\mathcal{M} \in \mathbb{M}$ implies that Assumption 2.3 holds. Then, there exists a feedback law $\boldsymbol{\kappa}$ which maps $\{\boldsymbol{x}(t), t\} \mapsto \boldsymbol{u}(t)$ such that (3.4) holds uniformly for $t \geqslant 0$. Let $\boldsymbol{x}(t)$ be the response of plant $\mathcal{P}$ with this feedback law imposed under exogenous disturbance $\boldsymbol{a}$, and let:

$$p_\mu^i(t) = \boldsymbol{v}^T(t)\boldsymbol{\kappa}(\boldsymbol{x}(t), t) + \mu^i(t, \boldsymbol{\kappa}(\boldsymbol{x}(t), t), \boldsymbol{v}(t)) \leqslant 0,$$

be evaluated along this response trajectory. First, consider the case where $E_L^i = 0$. Then:

$$\tfrac{d}{dt}E^i(t) = -\tfrac{1}{T_S^i}E^i(t) - p_\mu^i(t) - q^i(t).$$

Now let:

$$q^i(t) = \begin{cases} \max\left\{0, -\tfrac{1}{T_S^i}E^i(t) - p_\mu^i(t)\right\}, & E^i(t) = E_U^i \\ 0, & E^i(t) \neq E_U^i. \end{cases}$$

Clearly, $q^i(t) \geqslant 0$, $\forall t \geqslant 0$. Then, because $p_\mu^i(t) \leqslant 0$ and $q^i(t) = 0$ when $E^i(t) = 0$, it follows that $E^i(t) \geqslant 0$, $\forall t \geqslant 0$. Furthermore, for $q^i(t)$ as above, $E^i(t)$ cannot exceed E_U^i for any $t \geqslant 0$ if $E^i(0) \leqslant E_U^i$. For the case where $T_S^i \to \infty$, the proof follows analogously, but the above differential equation reduces to:

$$\tfrac{d}{dt}E^i(t) = -p_U^i(t) - q^i(t),$$

and then because $E^i(0) \in [E_L^i, E_U^i]$, it follows that $E^i(t) \geqslant E_L^i$, $\forall t \geqslant 0$. □

3.1.5 Stability

Theorem 3.1. *Let $\mathcal{M} \in \mathbb{M}$ be subject to exogenous disturbance $\boldsymbol{a} \in (\mathbb{L}^2)^d$, and initial conditions $\boldsymbol{x}(0) \in \mathbb{R}^n$, and $\boldsymbol{E}(0) \in \mathbb{R}_E$. Then there exists a function $f_{\mathcal{M}}(\boldsymbol{a}, \boldsymbol{x}(0), \boldsymbol{E}(0)) < \infty$, such that:*

$$\int_0^\infty \boldsymbol{x}^T(t)\boldsymbol{x}(t)dt \leqslant f_{\mathcal{M}}(\boldsymbol{a}, \boldsymbol{x}(0), \boldsymbol{E}(0)), \tag{3.5}$$

for all $\{\boldsymbol{u}, \boldsymbol{q}\} \in \mathbb{F}_{\mathcal{M}}(\boldsymbol{a}, \boldsymbol{x}(0), \boldsymbol{E}(0))$.

Proof. First, we define:

$$V(t) = \sum_{i=1}^{p} E^i(0) + \int_0^t \left(-\boldsymbol{u}^T(\tau)\boldsymbol{v}(\tau) - \boldsymbol{u}^T(\tau)\boldsymbol{R}_L\boldsymbol{u}(\tau)\right) d\tau.$$

Then it follows that $V(t) \geqslant \sum_{i=1}^{p} E^i(t)$, for all $t \geqslant 0$. To see this, consider that:

$$\frac{d}{dt}\left(\sum_{i=1}^{p} E^i(t) - V(t)\right) = -\sum_{i=1}^{p}\left(\frac{1}{T_S^i}E^i(t) + q^i(t) + \mu^i(t, \boldsymbol{u}(t), \boldsymbol{v}(t)) - \boldsymbol{u}^T(t)\boldsymbol{R}_L^i\boldsymbol{u}(t)\right).$$

If $\mathcal{M}$ is a valid model then by Assumption 2.2, the second term on the right-hand side is negative. If $\{\boldsymbol{u}, \boldsymbol{q}\}$ is feasible then the first term must be negative, and consequently we have that $\sum_{i=1}^{p} E^i(t) - V(t)$ is a non-increasing function, which, with an initial condition of 0, must therefore be nonpositive for all $t \geqslant 0$. Consequently, we have that:

$$V(t) \geqslant \sum_{i=1}^{p} E^i(t).$$

But if $\{\boldsymbol{u}, \boldsymbol{q}\}$ is feasible then $E^i(t) \geqslant 0$, $\forall i \in \{1...p\}$ and then we conclude that $V(t) \geqslant 0$, $\forall t \geqslant 0$. This is equivalent to stating that:

$$\sum_{i=1}^{p} E^i(0) - \int_0^t \boldsymbol{u}^T(\tau)\boldsymbol{v}(\tau)d\tau \geqslant \int_0^t \boldsymbol{u}^T(\tau)\boldsymbol{R}_L\boldsymbol{u}(\tau)d\tau. \tag{3.6}$$

But if $\mathcal{M} \in \mathbb{M}$ this implies that $\mathcal{P} \in \mathbb{P}$, which, by Definition 3.1, implies the existence of a $\beta(\boldsymbol{x}_0, \boldsymbol{a}) \geqslant 0$ such that:

$$\int_0^t \boldsymbol{u}^T(\tau)\boldsymbol{v}(\tau)d\tau \geqslant -\beta(\boldsymbol{x}_0, \boldsymbol{a}) \quad , \quad \forall t \in \mathbb{R}_{>0}. \tag{3.7}$$

Adding (3.6) and (3.7) we have that:

$$\sum_{i=1}^{p} E^i(0) + \beta(\boldsymbol{x}_0, \boldsymbol{a}) \geqslant \int_0^t \boldsymbol{u}^T(\tau)\boldsymbol{R}_L\boldsymbol{u}(\tau)d\tau.$$

By Assumption 2.2, $\boldsymbol{R}_L \succ 0$. As such, let $\underline{\lambda}(\boldsymbol{R}_L) > 0$ be the minimum eigenvalue of $\boldsymbol{R}_L$ and

we have the further bound:

$$\frac{\sum_{i=1}^{p} E^i(0) + \beta(\boldsymbol{x}_0, \boldsymbol{a})}{\underline{\lambda}(\boldsymbol{R}_L)} \geqslant \int_0^t \boldsymbol{u}^T(\tau)\boldsymbol{u}(\tau)d\tau.$$

Because $\mathcal{P} \in \mathbb{P}$, it follows that (2.9) holds independently of $\boldsymbol{a}$ and $\boldsymbol{u}$ and consequently:

$$\int_0^t \boldsymbol{x}^T(\tau)\boldsymbol{x}(\tau)d\tau \leqslant \alpha_u \frac{\sum_{i=1}^{p} E^i(0) + \beta(\boldsymbol{x}_0, \boldsymbol{a})}{\underline{\lambda}(\boldsymbol{R}_L)} + \alpha_a \int_0^t \boldsymbol{a}^T(\tau)\boldsymbol{a}(\tau)d\tau.$$

However, $\boldsymbol{a} \in (\mathbb{L}^2)^d$ so the integral on the right-hand side has finite value as $t \to \infty$ and consequently there exists a $\alpha_u, \alpha_a \in \mathbb{R}$ such that (3.5) holds. □

Theorem 3.1 states that a valid plant for a self-powered system cannot be destabilized by any control input that is physically realizable (i.e., feasible). As such, it is physically impossible for a self-powered system to destabilize.

3.1.6 Alternative Modeling Methods

In the previous subsection, we define self-powered system model $\mathcal{M}$ in Definition 3.2, and as mentioned earlier, $\{\boldsymbol{u}(t), \boldsymbol{q}(t)\}$ are the control variables over which we optimize. The challenging aspect of this modeling method is that the differential equation for the energy in the storage system (3.2) is nonlinear (specifically, quadratic in $\boldsymbol{u}(t)$), and because $E^i(t)$ is not guaranteed to be in the range $[E_L^i, E_U^i]$, we must enforce constraints to ensure the physical bounds of the storage units are satisfied. However, there are alternative methods of formulating the self-powered system problem, which introduce different challenges. Consider the following alternative methods.

1. **Directly Controlling Transducer Power Flow:** To explain this approach, we consider the case with one port ($m = 1$) and one energy storage system ($p = 1$). It is common in power systems engineering to control power flow $p_T(t) = u(t)v(t)$ explicity, as opposed $u(t)$. Then, the differential equation for the evolution of energy in the storage system is linear in $p_T(t)$:

$$\tfrac{d}{dt}E(t) = -\tfrac{1}{T_S}E(t) - p_T(t) - \mu(t) - q(t).$$

However, depending on how the transmission losses $\mu(\cdot,\cdot,\cdot)$ are modeled, this linearity may be lost. Commonly, transmission losses are modeled assuming a fixed efficiency $\eta \in (0,1)$ as:

$$\mu(p_T(t)) = \begin{cases} (1-\eta)p_T(t), & p_T(t) \geqslant 0 \\ (1-\frac{1}{\eta})p_T(t), & p_T(t) < 0. \end{cases}$$

If this is the case, then $\frac{d}{dt}E(t)$ is no longer linear in $p_T(t)$, and the benefits of instead controlling transducer power $p_T(t)$ are unclear. Furthermore, the plant $\mathcal{P}$ in (3.1) also becomes nonlinear:

$$\mathcal{P}: \begin{cases} \dot{\boldsymbol{x}}(t) = \bar{\boldsymbol{A}}(t)\boldsymbol{x}(t) + \bar{\boldsymbol{B}}(t)\dfrac{p_T(t)}{v(t)} + \bar{\boldsymbol{G}}(t)\boldsymbol{a}(t) \\ v(t) = -\dfrac{\bar{\boldsymbol{C}}(t)\boldsymbol{x}(t)}{2} \pm \sqrt{\left(\dfrac{\bar{\boldsymbol{C}}(t)\boldsymbol{x}(t)}{2}\right)^2 - \bar{\boldsymbol{D}}(t)p_T(t)}. \end{cases}$$

2. **Modeling Energy Storage Units as Capacitors:** For the special case where the energy storage units are modeled as capacitors (or flywheels, which are the mechanical analogy of capacitors), let $i_c^i(t)$ be the current, $w_c^i(t)$ be the voltage, and C^i be the capacitance of the i^{th} capacitor. Then, $i_c^i(t) = C^i\frac{dw_c^i(t)}{dt}$, and the energy in the capacitor is:

$$E^i(t) = \frac{1}{2}C^i(w_c^i(t))^2,$$

which is nonnegative for all $w_c^i(t) \in \mathbb{L}^2$. Therefore, for this modeling method, there is no need to enforce the energy storage constraints when $E_L^i = 0$ because $E^i(t)$ is always nonnegative. However, we do need to enforce a maximum allowable voltage: $|w_c^i(t)| \leqslant w_{max}$. Then, the power delivered to the capacitor is:

$$i_c^i(t)w_c^i(t) = -\boldsymbol{u}^T(t)\boldsymbol{K}^i\boldsymbol{v}(t) - \mu^i(t).$$

Let the evolution of the capacitor voltage be modeled via the following nonlinear differential equation for $w_c^i(t) \neq 0$:

$$\frac{dw_c^i(t)}{dt} = -\frac{1}{C}\left(\frac{\boldsymbol{u}^T(t)\boldsymbol{K}^i\boldsymbol{v}(t) + \mu^i(t)}{w_c^i(t)}\right). \tag{3.8}$$

Although this modeling method does not require the use of energy storage constraints, it introduces the nonlinear differential equation for $w_c^i(t)$ in (3.8). This nonlinear

differential equation does not linearize well, which can make control strategies difficult to implement.

All three modeling approaches include nonlinearities somewhere in the their formulation, but the quadratic nonlinearity in $\boldsymbol{u}(t)$ in (3.2) may be the easiest to implement numerically. In the method used in this thesis, we are also able to model the plant via linear differential equations, which is exploited in later sections to simplify the analysis. The downside of this method is that it necessitates the use of constraint functions, which, as we discuss in Section 4.1.3, introduces nonconvexity into the optimal control problem. Although Methods 1 and 2 discussed above are also viable approaches, we use the model presented in Sections 3.1.1 and 3.1.2 because of the linear plant dynamics and quadratic energy storage model.

3.2 Discrete-Time Model for Self-powered Systems

3.2.1 Discrete-Time Plant Model

The ultimate purpose of the continuous-time physical model developed in the previous section is for use in a MPC trajectory optimization algorithm. Hence, the continuous-time model $\mathcal{M}$ must be converted to a discrete-time model. Inputs $\boldsymbol{u}$ are mapped from discrete to continuous time via ZOH, i.e.:

$$\boldsymbol{u}(t) = \boldsymbol{u}_k \quad , \quad t \in [k\Delta t, (k+1)\Delta t) \tag{3.9}$$

where $k \in \mathbb{Z}_{\geqslant 0}$ denotes the discrete-time counter, and Δt is the discrete time-step.

The dynamics of plant $\mathcal{P}$ in (3.1) can be modeled in discrete time using the following linear, time-varying state space:

$$\boldsymbol{x}_{k+1} = \boldsymbol{A}_k \boldsymbol{x}_k + \boldsymbol{B}_k \boldsymbol{u}_k + \boldsymbol{a}_k \tag{3.10}$$

$$\boldsymbol{v}_k = \boldsymbol{C}_k \boldsymbol{x}_k + \boldsymbol{D}_k \boldsymbol{u}_k, \tag{3.11}$$

where the discrete-time disturbance is:

$$\boldsymbol{a}_k = \int_{k\Delta t}^{(k+1)\Delta t} \boldsymbol{\Phi}((k+1)\Delta t, \tau) \bar{\boldsymbol{G}}(\tau) \boldsymbol{a}(\tau) d\tau, \tag{3.12}$$

the discrete-time matrices are:

$$\begin{aligned} \boldsymbol{A}_k =& \boldsymbol{\Phi}((k+1)\Delta t, k\Delta t), \quad \boldsymbol{B}_k = \int_{k\Delta t}^{(k+1)\Delta t} \boldsymbol{\Phi}((k+1)\Delta t, \tau)\bar{\boldsymbol{B}}(\tau)d\tau \\ \boldsymbol{C}_k =& \bar{\boldsymbol{C}}(k\Delta t), \qquad\qquad\qquad \boldsymbol{D}_k = \bar{\boldsymbol{D}}(k\Delta t), \end{aligned} \tag{3.13}$$

and where $\boldsymbol{\Phi}(t_2, t_1)$ is the continuous-time state transition matrix (see Definition 2.7).

3.2.2 Discrete-Time Energy Storage Model

Let the stored energies at the discrete-time points be:

$$E_k^i = E^i(k\Delta t), \quad \forall k \in \mathbb{Z}_{\geqslant 0}, \quad \forall i \in \{1...p\}. \tag{3.14}$$

We collect all the discrete-time energies at time-step k in vector $\boldsymbol{E}_k$ as:

$$\boldsymbol{E}_k = \begin{bmatrix} E_k^1 & \cdots & E_k^p \end{bmatrix}^T.$$

We want to develop a discrete-time evolution equation for E_k^i such that (3.14) is satisfied exactly. We define this type of discrete-time model as *energy-preserving*. To create energy-preserving storage models, we first define $\boldsymbol{y}_k^i$ as:

$$\begin{aligned} \boldsymbol{y}_k^i =& \boldsymbol{K}^i \int_{k\Delta t}^{(k+1)\Delta t} e^{\frac{-(k+1)\Delta t + t}{T_s^i}} \boldsymbol{v}(t)dt \\ =& \boldsymbol{C}_{E,k}^i \boldsymbol{x}_k + \boldsymbol{D}_{E,k}^i \boldsymbol{u}_k + \boldsymbol{a}_{E,k}^i, \end{aligned} \tag{3.15}$$

where:

$$\boldsymbol{C}_{E,k}^i = \boldsymbol{K}^i \int_{k\Delta t}^{(k+1)\Delta t} e^{\frac{-(k+1)\Delta t + \tau}{T_s^i}} \bar{\boldsymbol{C}}(\tau)\boldsymbol{\Phi}(\tau, k\Delta t)d\tau \tag{3.16}$$

$$\boldsymbol{D}_{E,k}^i = \boldsymbol{K}^i \int_{k\Delta t}^{(k+1)\Delta t} e^{\frac{-(k+1)\Delta t + \tau}{T_s^i}} \left(\bar{\boldsymbol{D}}(\tau) + \bar{\boldsymbol{C}}(\tau) \int_{k\Delta t}^{\tau} \boldsymbol{\Phi}(\alpha, k\Delta t)\bar{\boldsymbol{B}}(\alpha)d\alpha \right) d\tau \tag{3.17}$$

$$\boldsymbol{a}_{E,k}^i = \boldsymbol{K}^i \int_{k\Delta t}^{(k+1)\Delta t} e^{\frac{-(k+1)\Delta t + \tau}{T_s^i}} \bar{\boldsymbol{C}}(\tau) \int_{k\Delta t}^{\tau} \boldsymbol{\Phi}(\alpha, k\Delta t)\bar{\boldsymbol{G}}(\alpha)\boldsymbol{a}(\alpha)d\alpha d\tau. \tag{3.18}$$

In terms of these quantities, E_k^i evolves in discrete time according to:

$$E_{k+1}^i = \gamma^i E_k^i - \boldsymbol{u}_k^T \boldsymbol{y}_k^i - \mu_k^i - q_k^i, \tag{3.19}$$

where $E_0^i \in [E_L^i, E_U^i]$ is the initial energy in storage system i, and where γ^i, μ_k^i, and q_k^i are defined as follows.

The unitless variable γ^i represents the decay of energy in the i^{th} storage system, and is calculated as:

$$\gamma^i = e^{\frac{-\Delta t}{T_S^i}}, \tag{3.20}$$

which exists in the range $[0, 1]$. An ideal storage system with no decay has $\gamma^i = 1$, and a system with no ability to store energy has $\gamma^i = 0$.

The power sent to the i^{th} resistor bank or power bus, $q^i(t)$, is mapped from discrete to continuous time via ZOH. However, for simplicity, in discrete time we instead control the *energy* sent during time step k. Let q_k^i be the ZOH discrete-time energy sent to the i^{th} resistor bank or power bus:

$$q_k^i = \chi^i q^i(k\Delta t) \quad , \quad t \in [k\Delta t, (k+1)\Delta t), \tag{3.21}$$

where the scalar χ^i, which has units of time, is a function of T_S^i, Δt and γ^i:

$$\chi^i = \begin{cases} \Delta t, & \gamma^i = 1 \\ T_S^i(1-\gamma^i), & 0 < \gamma^i < 1 \\ 0, & \gamma^i = 0. \end{cases}$$

Now, we collect all energies sent to the resistor banks or power buses at time-step k in vector $\boldsymbol{q}_k$:

$$\boldsymbol{q}_k = \begin{bmatrix} q_k^1 & \cdots & q_k^p \end{bmatrix}^T.$$

3.2.3 Discrete-Time Transmission Loss Model

The term μ_k^i captures the transmission losses in discrete time. Technically, this should be evaluated as:

$$\mu_k^i = \int_{k\Delta t}^{(k+1)\Delta t} e^{\frac{\tau-(k+1)\Delta t}{T_S^i}} \mu^i(t, \boldsymbol{u}(t), \boldsymbol{v}(t)) dt.$$

However, for the purposes of MPC trajectory optimization we assume this discrete-time transmission loss can be approximated (or, at least, conservatively over-bounded) by a quadratic loss model, which is described in the next.

Quadratic Loss Models

For the purposes of MPC trajectory optimization we assume that the transmission loss μ_k^i is a quadratic function of $\{\boldsymbol{u}_k, \boldsymbol{y}_k^i\}$; i.e.,

$$\mu_k^i(\boldsymbol{u}_k, \boldsymbol{y}_k^i) = \begin{bmatrix} \boldsymbol{u}_k \\ \boldsymbol{y}_k^i \end{bmatrix}^T \begin{bmatrix} \boldsymbol{M}_{uu,k}^i & \boldsymbol{M}_{uy,k}^i \\ (\boldsymbol{M}_{uy,k}^i)^T & \boldsymbol{M}_{yy,k}^i \end{bmatrix} \begin{bmatrix} \boldsymbol{u}_k \\ \boldsymbol{y}_k^i \end{bmatrix}, \tag{3.22}$$

where $\boldsymbol{M}_k^i \succeq 0$. The simplest transmission loss model is the case in which $\boldsymbol{M}_{uy,k}^i = 0$, $\boldsymbol{M}_{yy,k}^i = 0$, and $\boldsymbol{M}_{uu,k}^i \succ 0$. In this case, the losses are modeled as a quadratic penalty on the control inputs $\boldsymbol{u}$. Physically, if these inputs $\boldsymbol{u}$ correspond to transducer currents or voltages, then this simple loss model captures the "i^2R" losses associated with the control, with $\boldsymbol{M}_{uu}^i$ taking the form of a resistance or admittance matrix, respectively.

In many cases, the system's energy dissipation may be best modeled via a non-quadratic loss function. Let $\hat{\mu}_k^i(\boldsymbol{u}_k, \boldsymbol{y}_k^i)$ be the true, non-quadratic loss model. Then, in some cases it is possible to find a quadratic overbound of $\hat{\mu}_k^i(\boldsymbol{u}_k, \boldsymbol{y}_k^i)$, which has the form (3.22) and where:

$$\mu_k^i\left(\boldsymbol{u}_k, \boldsymbol{y}_k^i\right) \geqslant \hat{\mu}_k^i\left(\boldsymbol{u}_k, \boldsymbol{y}_k^i\right), \quad \forall \{\boldsymbol{u}_k, \boldsymbol{y}_k^i\} \in (\mathbb{R}^m \times \mathbb{R}^m).$$

For example, in many studies, the efficiency of a self-powered system is assumed to be a static value. Consider port j, and let $\eta_j \in (0, 1)$ be the efficiency between port j and the storage system to which it is connected. Then, at time-step k, let $u_{k,j}$ be the control input for this port and $y_{k,j}^i$ be its colocated energy-preserving output for the i^{th} storage unit. We model the energy dissipation over one time sample via a static efficiency as:

$$\hat{\mu}_{k,j}^i(u_{k,j}, y_{k,j}^i) = \begin{cases} (1-\eta_j) u_{k,j} y_{k,j}^i, & u_{k,j} y_{k,j}^i \geqslant 0 \\ \left(1 - \frac{1}{\eta_j}\right) u_{k,j} y_{k,j}^i, & u_{k,j} y_{k,j}^i < 0. \end{cases}$$

Then, the true non-quadratic loss model for the i^{th} energy storage unit is the summation of the losses of its connected ports:

$$\hat{\mu}_k^i\left(\boldsymbol{u}_k, \boldsymbol{y}_k^i\right) = \sum_{j \in \mathbb{K}^i} \hat{\mu}_{k,j}^i(u_{k,j}, y_{k,j}^i),$$

where $\mathbb{K}^i$ is the set of all ports connected to storage system i (see Section 3.1.2). We now show that it is possible to find a quadratic overbound function for $\hat{\mu}_k^i(\cdot, \cdot)$ of the form (3.22)

with the following matrices:

$$\boldsymbol{M}^i_{uu,k} = \begin{bmatrix} M_{uu,k,1} & & \\ & \ddots & \\ & & M_{uu,k,m} \end{bmatrix} \boldsymbol{M}^i_{yy,k} = \begin{bmatrix} M_{yy,k,1} & & \\ & \ddots & \\ & & M_{yy,k,m} \end{bmatrix} \boldsymbol{M}^i_{uy,k} = \begin{bmatrix} M_{uy,k,1} & & \\ & \ddots & \\ & & M_{uy,k,m} \end{bmatrix}.$$

From the definition of $\boldsymbol{y}^i_k$ in (3.15) and because the above matrices are diagonal, we can rewrite the quadratic overbound as:

$$\mu^i_k\left(\boldsymbol{u}_k, \boldsymbol{y}^i_k\right) = \sum_{j\in\mathbb{K}^i} \mu^i_{k,j}(u_{k,j}, y^i_{k,j}) = \sum_{j\in\mathbb{K}^i} \begin{bmatrix} u_{k,j} \\ y^i_{k,j} \end{bmatrix}^T \begin{bmatrix} M_{uu,k,j} & M_{uy,k} \\ (M_{uy,k,j})^T & M_{yy,k,j} \end{bmatrix} \begin{bmatrix} u_{k,j} \\ y^i_{k,j} \end{bmatrix}. \tag{3.23}$$

For each port $j \in \{1...m\}$, let $h_{k,j} > 0$ be a design parameter. The overbound then satisfies:

$$\mu^i_{k,j}(u_{k,j}, y^i_{k,j}) \geqslant \hat{\mu}^i_{k,j}(u_{k,j}, y^i_{k,j}), \quad \forall\{u_{k,j}, y^i_{k,j}\} \in (\mathbb{R}\times\mathbb{R}), \tag{3.24}$$

and the equality holds if $u_{k,j} = -h_{k,j}y^i_{k,j}$; i.e.,

$$\mu^i_{k,j}(-h_{k,j}y^i_{k,j}, y^i_{k,j}) = \hat{\mu}^i_{k,j}(h_{k,j}y^i_{k,j}, y^i_{k,j}) \tag{3.25}$$

$$= (1-\eta_j)h_{k,j}(y^i_{k,j})^2. \tag{3.26}$$

In order for conditions (3.2.3) and (3.23) to satisfy (3.24) for all $\{u_{k,j}, y^i_{k,j}\} \in (\mathbb{R}\times\mathbb{R})$, both of the following equations must hold:

$$(2M_{uy,k,j} - 1 + \eta_j)^2 \leqslant 4M_{uu,k,j}M_{yy,k,j} \quad \text{or} \quad 2M_{uy,k,j} - 1 + \eta_j > 0 \tag{3.27}$$

$$\left(2M_{uy,k,j} - 1 + \frac{1}{\eta_j}\right)^2 \leqslant 4M_{uu,k,j}M_{yy,k,j} \quad \text{or} \quad 2M_{uy,k,j} - 1 + \frac{1}{\eta_j} < 0. \tag{3.28}$$

Condition (3.26) requires that:

$$2M_{uy,k,j} - 1 + \eta_j = -\frac{M_{yy,k,j}}{h_{k,j}} - M_{uu,k,j}h_{k,j}.$$

Noting that the right-hand side is always negative, (3.27) and (3.28) become:

$$\left(\frac{M_{yy,k,j}}{h_{k,j}} - M_{uu,k,j}h_{k,j}\right)^2 \leqslant 0 \tag{3.29}$$

$$-\frac{M_{yy,k,j}}{h_{k,j}} - M^j_{uu,k}h_{k,j} - \eta_j + \frac{1}{\eta_j} \leqslant 2\sqrt{M_{uu,k,j}M_{yy,k,j}}. \tag{3.30}$$

The only way (3.29) can be satisfied is to set:

$$M_{yy,k,j} = M_{uu,k,j}(h_{k,j})^2.$$

Then (3.30) becomes:

$$-\eta_j + \frac{1}{\eta_j} \leqslant 2M_{uu,k,j}h_{k,j}.$$

The least-conservative value of $M_{uu,k,j}$ satisfying this is:

$$M_{uu,k,j} = \frac{1-(\eta_j)^2}{2\eta_j h_{k,j}}.$$

Then, the values of $M_{yy,k,j}$, and $M_{uy,k,j}$ that are the least conservative over-bound are:

$$\begin{aligned} M_{yy,k,j} =& \frac{1-(\eta_j)^2}{2\eta_j}h_{k,j} \\ M_{uy,k,j} =& \frac{1-\eta_j}{2} - \frac{1-(\eta_j)^2}{2\eta_j}. \end{aligned}$$

3.2.4 Valid Discrete-Time Models and Control Feasibility

Definition 3.6. *For a valid self-powered system model $\mathcal{M}$, discrete time step Δt, and exogenous disturbance $\boldsymbol{a} \in (\mathbb{L}^2)^d$, the associated discrete-time model $\mathcal{D}(\mathcal{M}, \Delta t, \boldsymbol{a})$ is comprised of:*

1. *Discrete-time state evolution equation* (3.10) *with energy-preserving outputs $\boldsymbol{y}^i$ as in* (3.15) *for $i \in \{1...p\}$*
2. *Discrete-time energy evolution equations* (3.19) *for $i \in \{1...p\}$*
3. *Discrete-time loss modeling equation* (3.22) *for $i \in \{1...p\}$.*

Note that for a discrete-time model, the continuous-time exogenous disturbance $\boldsymbol{a}$ generates time-varying parameters that affect the discrete-time state evolution, energy evolution,

and loss model equations in different ways. In the state evolution equation the consequence of $\boldsymbol{a}$ is the presence of discrete-time exogenous input $\boldsymbol{a}_k$, as evaluated from (3.12). In the energy evolution equations, the consequence of $\boldsymbol{a}$ is the presence of output disturbances $\boldsymbol{a}_{E,k}$, as evaluated from (3.18).

When implementing trajectory optimizations via MPC, it is necessary to constrain the discrete-time control inputs $\boldsymbol{u}_k$ and $\boldsymbol{q}_k$ such that, when mapped back to continuous-time via (3.9) and (3.21), they result in feasibility; i.e., they render $\boldsymbol{E}(t) \in \mathbb{R}_E$, for all $t \geqslant 0$ within the optimization horizon. However, imposing this constraint over a continuous time interval is computationally problematic. Therefore, we define a relaxation of feasibility for use in discrete-time optimization, as described below.

Definition 3.7. *Let $\mathcal{M}_d = \mathcal{D}(\mathcal{M}, \Delta t, \boldsymbol{a})$ be a discrete-time model, in which $\mathcal{M} \in \mathbb{M}$. At discrete time k, let $\boldsymbol{x}_k \in \mathbb{R}^n$ and $\boldsymbol{E}_k \in \mathbb{R}_E$. Let inputs $\{\boldsymbol{u}_\ell, \boldsymbol{q}_\ell\}$ be defined over the interval $\ell = \{k...k+N\}$. Then:*

1. *We say that these inputs are* finite-horizon discrete-time feasible *if they result in $\boldsymbol{E}_{\ell+1} \in \mathbb{R}_E$ for $\ell \in \{k...k+N\}$.*

2. *Denote the set of all finite-horizon discrete-time feasible inputs as $\mathbb{F}_{\mathcal{M}_d}(\boldsymbol{x}_k, \boldsymbol{E}_k, N)$.*

Finite-horizon discrete-time feasibility does not imply continuous-time feasibility, because the constraint $E^i(t) \in [E^i_L, E^i_U]$ is only enforced at discrete times $t = k\Delta t$. It is therefore possible that for some $i \in \{1...p\}$, $E^i(t)$ could satisfy the feasibility condition at two consecutive discrete time points but violate it in between. This is illustrated in Figure 3.1 for the case with $E^i_L = 0$. For a physical self-powered system with $E^i_L = 0$, if such a control input is commanded, the result is that the continuous-time control inputs $\{\boldsymbol{u}(t), \boldsymbol{q}(t)\}$ would fail to track their zero-order-hold commands, $\{\boldsymbol{u}^*, \boldsymbol{q}^*\}$. Consequently there would be distortion in the ZOH inputs, to the degree necessary to maintain $E^i(t) \geqslant 0$. This distortion is shown in red in Figure 3.1. For the purposes of MPC trajectory optimization, we do not model these distortion effects.

Discrete-time feasibility *does* imply continuous-time feasibility if one assumes that the continuous-time function $\boldsymbol{E}(t)$ can be recovered from discrete-time samples $\boldsymbol{E}_k$ via linear interpolation. As Δt is made smaller, this assumption becomes more justified. In the case with $\Delta t \to 0$, the assumption may be viewed as being asymptotically exact.

The following Lemma gives conditions for a nonempty set of feasible inputs $\mathbb{F}_{\mathcal{M}_d}(\boldsymbol{x}_k, \boldsymbol{E}_k, N)$. First, we introduce $\check{\boldsymbol{y}}^i_k$, which is the portion of $\boldsymbol{y}^i_k$ that does not depend on the k^{th} input $\boldsymbol{u}_k$, i.e., $\boldsymbol{y}^i_k = \check{\boldsymbol{y}}^i_k + \boldsymbol{D}^i_{E,k}\boldsymbol{u}_k$.

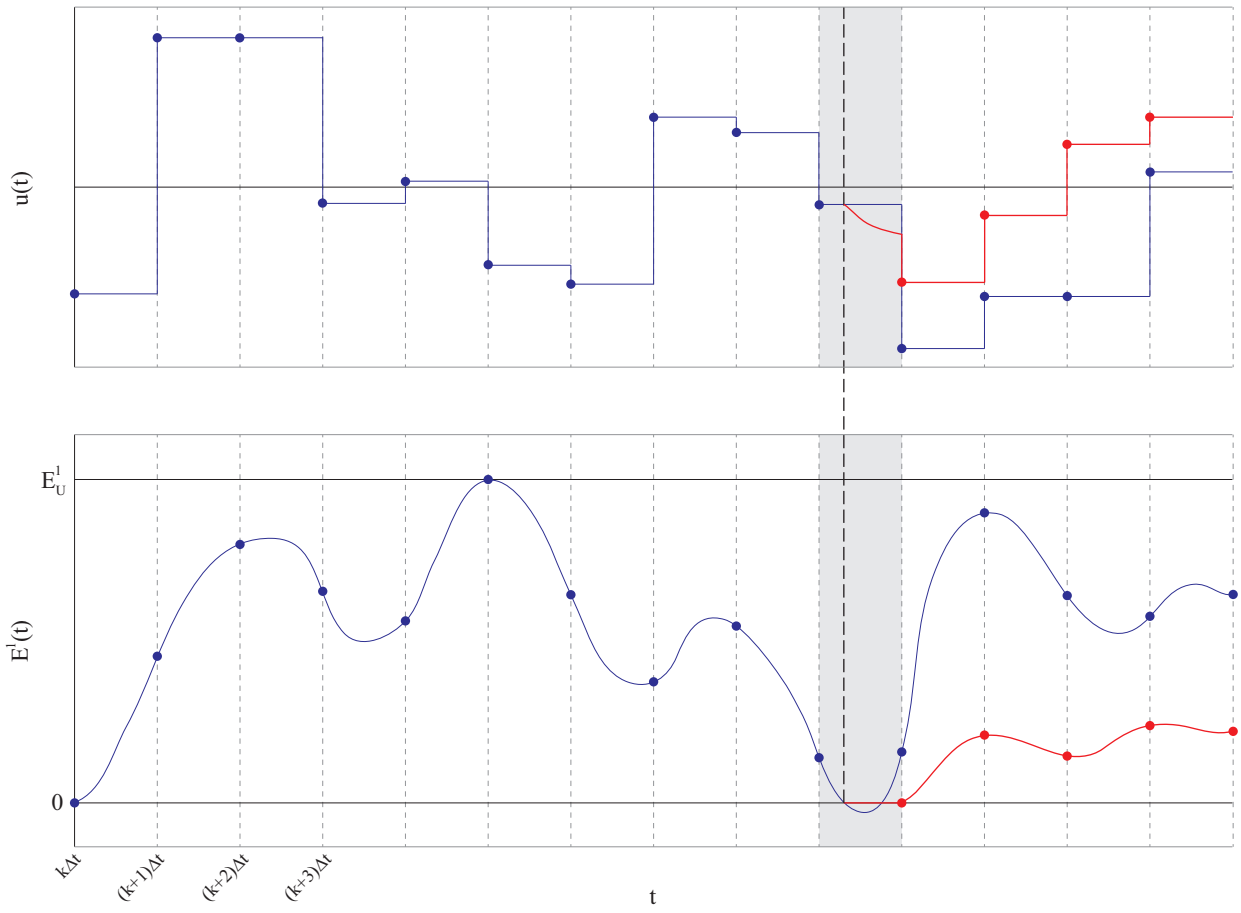

Figure 3.1: Trajectory violating the lower energy storage bound is shown in blue, and the ZOH input distortion is shown in red as a consequence of inter-sample loss of feasibility

Lemma 3.2. *Let $\mathcal{M}_d = \mathcal{D}(\mathcal{M}, \Delta t, \boldsymbol{a})$ be a discrete-time model in which $\mathcal{M} \in \mathbb{M}$, and for each $i \in \{1...p\}$ let either $E_L^i = 0$ or $\gamma^i = 1$. For all $i \in \{1...p\}$, $\ell \in \{k...k+N\}$, and each $\check{\boldsymbol{y}}_\ell^i \in \mathbb{R}^m$, let there exists a $\boldsymbol{u}_\ell \in \mathbb{R}^m$ such that:*

$$\begin{bmatrix} \boldsymbol{u}_\ell \\ \boldsymbol{y}_\ell^i \end{bmatrix}^T \begin{bmatrix} \boldsymbol{M}_{uu,\ell}^i & \boldsymbol{M}_{uy,\ell}^i + \frac{1}{2}\boldsymbol{I} \\ (\boldsymbol{M}_{uy,\ell}^i)^T + \frac{1}{2}\boldsymbol{I} & \boldsymbol{M}_{yy,\ell}^i \end{bmatrix} \begin{bmatrix} \boldsymbol{u}_\ell \\ \boldsymbol{y}_\ell^i \end{bmatrix} \leqslant 0. \tag{3.31}$$

At discrete time ℓ, let $\boldsymbol{x}_\ell \in \mathbb{R}^n$ and $\boldsymbol{E}_\ell \in \mathbb{R}_E$. Then, $\mathbb{F}_{\mathcal{M}_d}(\boldsymbol{x}_k, \boldsymbol{E}_k, N)$ is nonempty.

Proof. The proof is directly analogous to the that of Lemma 3.1 for the continuous-time case, and is omitted in the interest of brevity. □

Note that it is trivial to verify that if $\boldsymbol{M}_{uy,\ell}^i = 0$ and $\boldsymbol{M}_{yy,\ell}^i = 0$ for all $i \in \{1...p\}$, then (3.31) is satisfied with $\boldsymbol{u}_k = 0$. It is also straight-forward to verify that the inequality can also be satisfied for the static efficiency loss model example discussed in Section 3.2.3, by setting $u_{k,j} = -h_{k,j} y_{k,j}^i$ for all $i \in \{1...p\}$ and all $j \in \mathbb{K}^i$.

Assumption 3. *We assume that for the discrete time models $\mathcal{M}_d$ considered, for all $i \in \{1...p\}$, $\ell \in \{k...k+N\}$, and each $\check{\boldsymbol{y}}_\ell^i \in \mathbb{R}^m$, there exists a $\boldsymbol{u}_\ell \in \mathbb{R}^m$ such that (3.31) holds.*

Chapter 4

Trajectory Optimization

In this chapter, we first formulate the trajectory optimization problem associated with the self-powered system in Figure 1.4. We then show that this trajectory optimization is nonconvex in general, and determine specific conditions for which the problem regains convexity. Next, we discuss special cases of this optimization: the LTI version, passivity-constrained problem, energy harvesting problem, and zero energy storage problem. Last, we introduce the barrier method to solve the original nonconvex trajectory optimization in the primal domain, and present an example using an energy-harvesting piezoelectric wireless sensor node with the goal of maximizing data transmission.

4.1 Formulating the Trajectory Optimization Problem

Referring back to Figure 1.6, the core of the MPC feedback law is the trajectory optimization that maps the state estimation $\hat{\boldsymbol{x}}_k$ and the exogenous disturbance trajectory forecast $\hat{\boldsymbol{a}}(t)$, $t \in (k\Delta t, (k+N)\Delta t]$ into an input command $\{\boldsymbol{u}_k^*, \boldsymbol{q}_k^*\}$. As discussed in the introduction, this problem is made tractable by two key assumptions:

1. $\{\boldsymbol{u}, \boldsymbol{q}\}$ track their commanded values $\{\boldsymbol{u}^*, \boldsymbol{q}^*\}$ with high bandwidth, and consequently the algorithm can be viewed as optimizing $\{\boldsymbol{u}_{k:k+N}, \boldsymbol{q}_{k:k+N}\}$ directly.

2. For the purposes of trajectory optimization, $\hat{\boldsymbol{a}}(t) = \boldsymbol{a}(t)$, for $t \in (k\Delta t, (k+N)\Delta t]$, and $\hat{\boldsymbol{x}}_k = \boldsymbol{x}_k$. That is, we assume perfect knowledge of the exogenous disturbances and that we can measure all states at time-step k.

In the interest of reducing the notation, we present the results for the specific case in which $k = 0$.

4.1.1 Performance Measure

Let $J(\boldsymbol{u}_{0:N}, \boldsymbol{q}_{0:N}, \boldsymbol{x}_{0:N+1}) : (\mathbb{R}^m)^{N+1} \times (\mathbb{R}^p)^{N+1} \times (\mathbb{R}^n)^{N+2} \to \mathbb{R}$ be the performance measure function to be minimized by the trajectory optimization algorithm. Then, $J(\cdot,\cdot,\cdot)$ has the form:

$$J(\boldsymbol{u}_{0:N}, \boldsymbol{q}_{0:N}, \boldsymbol{x}_{0:N+1}) = \phi(\boldsymbol{x}_{N+1}) + \sum_{k=0}^{N} L_k(\boldsymbol{u}_k, \boldsymbol{q}_k, \boldsymbol{x}_k), \tag{4.1}$$

where $\phi(\cdot)$ is the final state penalty term, and $L_k(\cdot,\cdot,\cdot)$ is the Lagrangian (see Definition 2.14).

Quadratic Performance Measure

Consider the special case where the performance measure is a function of, and quadratic in $\{\boldsymbol{u}_{0:N}, \boldsymbol{x}_{0:N+1}\}$, i.e.,

$$J(\boldsymbol{u}_{0:N}, \boldsymbol{x}_{0:N+1}) = \boldsymbol{x}_{N+1}^T \boldsymbol{P}_{N+1} \boldsymbol{x}_{N+1} + \sum_{k=0}^{N} \begin{bmatrix} \boldsymbol{x}_k \\ \boldsymbol{u}_k \\ \boldsymbol{a}_k \end{bmatrix}^T \begin{bmatrix} \boldsymbol{Q}_k & \boldsymbol{S}_k & \boldsymbol{T}_k \\ \boldsymbol{S}_k^T & \boldsymbol{R}_k & \boldsymbol{U}_k \\ \boldsymbol{T}_k^T & \boldsymbol{U}_k^T & \boldsymbol{V}_k \end{bmatrix} \begin{bmatrix} \boldsymbol{x}_k \\ \boldsymbol{u}_k \\ \boldsymbol{a}_k \end{bmatrix}, \tag{4.2}$$

where for the purposes of our analysis we assume $\boldsymbol{R}_k \succ 0$ and $\boldsymbol{P}_{N+1} \succeq 0$.

This quadratic form encompasses many performance measures of interest, for example, the energy harvesting problem (see Section 4.2.2), and the vibration suppression problem (see Section 6.4). Therefore, we focus to this specific quadratic form in later chapters.

In most optimal control applications, it is also customary to make the assumption that $\boldsymbol{Q}_k - \boldsymbol{S}_k \boldsymbol{R}_k^{-1} \boldsymbol{S}_k^T \succeq 0$, $\forall k \in \{0...N\}$, which renders the Lagrangian positive-semidefinite, therefore guaranteeing the existence of a finite minimum of the optimization. However, for the analyses to be conducted, this condition is conservative, and may be relaxed while still guaranteeing that $J(\cdot,\cdot)$ has a finite global minimum. This is shown in Theorem 4.1 below. However, prior to presenting this theorem we first introduce the notation $\boldsymbol{x}^\circ_{0:N}(\boldsymbol{u}_{0:N}, \boldsymbol{x}_0)$ as the solution to (3.10) over the interval $k \in \{0...N\}$; i.e.,

$$\boldsymbol{x}^\circ_k(\boldsymbol{u}_{0:N}, \boldsymbol{x}_0) = \bar{\boldsymbol{x}}_k(\boldsymbol{x}_0) + \sum_{j=0}^{N} \boldsymbol{\Psi}(k,j) \boldsymbol{B}_j \boldsymbol{u}_j,$$

where $\boldsymbol{\Psi}(k,j)$ is the discrete-time state transition matrix (see Definition 2.8):

$$\boldsymbol{\Psi}(k,j) = \begin{cases} \mathbf{0}, & k \leqslant j \\ \boldsymbol{I}, & k = j+1 \\ \boldsymbol{A}_{k-1} \dots \boldsymbol{A}_{j+1}, & k \geqslant j+2, \end{cases} \tag{4.3}$$

and where $\bar{\boldsymbol{x}}_k$ isolates the terms related to the initial condition $\boldsymbol{x}_0$ and disturbance $\boldsymbol{a}$:

$$\bar{\boldsymbol{x}}_k(\boldsymbol{x}_0) = \boldsymbol{\Psi}(k,0)\boldsymbol{x}_0 + \sum_{j=0}^{N} \boldsymbol{\Psi}(k,j)\boldsymbol{a}_j. \tag{4.4}$$

Theorem 4.1. *Let $J(\cdot,\cdot)$ be the quadratic performance measure in (4.2). Let $\boldsymbol{x}_k$ evolve according to (3.10), with initial condition $\boldsymbol{x}_0 \in \mathbb{R}^n$, and with disturbance $\boldsymbol{a}_{0:N} \in \mathbb{R}^{d\times(N+1)}$. Let $\boldsymbol{R}_k \succ 0$, $\forall k \in \{0...N\}$, and $\boldsymbol{P}_{N+1} \succeq 0$. Then, $J(\boldsymbol{u}_{0:N}, \boldsymbol{x}^{\circ}_{0:N+1}(\boldsymbol{u}_{0:N}, \boldsymbol{x}_0))$ has a unique, finite minimum over $\boldsymbol{u}_{0:N}$ if and only if $\boldsymbol{\Upsilon}_k = (\boldsymbol{R}_k + \boldsymbol{B}_k^T \boldsymbol{P}_k \boldsymbol{B}_k) \succ 0$, $\forall k \in \{0 \dots N\}$, where $\boldsymbol{P}_k$ is solution to the following RDRDE:*

$$\boldsymbol{P}_{k-1} = \boldsymbol{Q}_k + \boldsymbol{A}_k^T \boldsymbol{P}_k \boldsymbol{A}_k - \left(\boldsymbol{S}_k + \boldsymbol{B}_k^T \boldsymbol{P}_k \boldsymbol{A}_k\right)^T \left(\boldsymbol{R}_k + \boldsymbol{B}_k^T \boldsymbol{P}_k \boldsymbol{B}_k\right)^{-1} \left(\boldsymbol{S}_k + \boldsymbol{B}_k^T \boldsymbol{P}_k \boldsymbol{A}_k\right), \tag{4.5}$$

with terminal constraint $\boldsymbol{P}_{N+1}$.complement

Proof. ($\Leftarrow$ Sufficient) Assume that $(\boldsymbol{R}_k + \boldsymbol{B}_k^T \boldsymbol{P}_k \boldsymbol{B}_k) \succ 0$, $\forall k \in \{0...N\}$. Let $\boldsymbol{H}$ be the Hessian of $J(\cdot,\cdot)$ with respect to the input $\boldsymbol{u}$, i.e., $\boldsymbol{H} = \frac{\partial^2 J}{\partial \boldsymbol{u} \partial \boldsymbol{u}^T}$. $J(\cdot,\cdot)$ has a unique, finite minimum if and only if $\boldsymbol{H} \succ 0$. Let $\hat{\boldsymbol{H}}$ be the block diagonal matrix:

$$\hat{\boldsymbol{H}} = \begin{bmatrix} \boldsymbol{\Upsilon}_0 & & & \\ & \boldsymbol{\Upsilon}_1 & & \\ & & \ddots & \\ & & & \boldsymbol{\Upsilon}_N \end{bmatrix}.$$

We construct the transformation matrix $\boldsymbol{T}$ such that $\boldsymbol{H} = \boldsymbol{T}\hat{\boldsymbol{H}}\boldsymbol{T}^T$. Let $\boldsymbol{\Psi}(k,i)$ be the discrete-time state transition matrix in (4.3), where $i,k \in \{0...N\}$ and $\boldsymbol{x}_{k+1} = \boldsymbol{\Psi}(k,0)\boldsymbol{x}_0 +$

$\sum_{i=0}^{k-1} \boldsymbol{\Psi}(k,i)(\boldsymbol{B}_i\boldsymbol{u}_i + \boldsymbol{G}_i\boldsymbol{a}_i)$. Let $\boldsymbol{H}_{i,j} = \frac{\partial^2 J}{\partial \boldsymbol{u}_i \partial \boldsymbol{u}_j^T}$ be the $m \times m$ submatrix of $\boldsymbol{H}$, where:

$$\boldsymbol{H}_{i,j} = \boldsymbol{B}_i^T \boldsymbol{\Psi}(N+1,i)^T \boldsymbol{P}_N \boldsymbol{\Psi}(N+1,j)\boldsymbol{B}_j + \sum_{k=0}^{N} \boldsymbol{B}_i^T \boldsymbol{\Psi}(k,i)^T \boldsymbol{Q}_k \boldsymbol{\Psi}(k,j)\boldsymbol{B}_j + \delta_{i,j}\boldsymbol{R}_i + \boldsymbol{B}_i^T \boldsymbol{\Psi}(j,i)^T \boldsymbol{S}_j + \boldsymbol{S}_i^T \boldsymbol{\Psi}(i,j)\boldsymbol{B}_j.$$

Assume that the transformation matrix $\boldsymbol{T}$ is the product of N matrices as $\boldsymbol{T} = \boldsymbol{T}_N \dots \boldsymbol{T}_2\boldsymbol{T}_1$. Now, let $\hat{\boldsymbol{H}}_k = (\boldsymbol{T}_k \dots \boldsymbol{T}_2\boldsymbol{T}_1)\, \hat{\boldsymbol{H}}\, \left(\boldsymbol{T}_1^T\boldsymbol{T}_2^T \dots \boldsymbol{T}_k^T\right)$. We then define:

$$\boldsymbol{H}_{i,j}^{\ell} = \boldsymbol{B}_i^T \Psi(\ell+1,i)^T \boldsymbol{P}_\ell \boldsymbol{\Psi}(\ell+1,j)\boldsymbol{B}_j + \tilde{\boldsymbol{H}}_{i,j}^{\ell},$$

where $\ell \in \{0 \dots N\}$ and:

$$\tilde{\boldsymbol{H}}_{i,j}^{\ell} = \sum_{k=0}^{\ell} \boldsymbol{B}_i^T \boldsymbol{\Psi}(k,i)^T \boldsymbol{Q}_k \boldsymbol{\Psi}(k,j)\boldsymbol{B}_j + \delta_{i,j}\boldsymbol{R}_i + \boldsymbol{B}_i^T \boldsymbol{\Psi}(j,i)^T \boldsymbol{S}_j + \boldsymbol{S}_i^T \boldsymbol{\Psi}(i,j)\boldsymbol{B}_j.$$

Then, note that $\boldsymbol{H}_{i,j}^{N} = \boldsymbol{H}_{i,j}$. We begin to construct $\boldsymbol{T}_1$ by first expanding $\boldsymbol{P}_0$ according to Riccati equation (4.5) in $\boldsymbol{\Upsilon}_0 = \boldsymbol{R}_0 + \boldsymbol{B}_0^T\boldsymbol{P}_0\boldsymbol{B}_0$ as:

$$\boldsymbol{\Upsilon}_0 \;=\; \boldsymbol{R}_0 + \boldsymbol{B}_0^T \left(\boldsymbol{Q}_1 + \boldsymbol{A}_1^T\boldsymbol{P}_1\boldsymbol{A}_1\right)\boldsymbol{B}_0 \;-\; \boldsymbol{B}_0^T \left(\boldsymbol{S}_1 + \boldsymbol{B}_1^T\boldsymbol{P}_1\boldsymbol{A}_1\right)^T \boldsymbol{\Upsilon}_1^{-1} \left(\boldsymbol{S}_1 + \boldsymbol{B}_1^T\boldsymbol{P}_1\boldsymbol{A}_1\right)\boldsymbol{B}_0. \tag{4.6}$$

Noting that (4.6) is the Schur complement of the matrix:

$$\begin{bmatrix} \boldsymbol{R}_0 + \boldsymbol{B}_0^T \left(\boldsymbol{Q}_1 + \boldsymbol{A}_1^T\boldsymbol{P}_1\boldsymbol{A}_1\right)\boldsymbol{B}_0 & \boldsymbol{B}_0^T \left(\boldsymbol{S}_1 + \boldsymbol{B}_1^T\boldsymbol{P}_1\boldsymbol{A}_1\right)^T \\ \left(\boldsymbol{S}_1 + \boldsymbol{B}_1^T\boldsymbol{P}_1\boldsymbol{A}_1\right)\boldsymbol{B}_0 & \boldsymbol{\Upsilon}_1 \end{bmatrix},$$

we let $\boldsymbol{T}_1$ be:

$$\boldsymbol{T}_1 = \begin{bmatrix} \boldsymbol{I}_m & \boldsymbol{B}_0^T \left(\boldsymbol{S}_1 + \boldsymbol{B}_1^T\boldsymbol{P}_1\boldsymbol{A}_1\right)^T \boldsymbol{\Upsilon}_1^{-1} & & \\ \boldsymbol{0}_m & \boldsymbol{I}_m & & \\ & & \ddots & \\ & & & \boldsymbol{I}_m \end{bmatrix}.$$

Then $\hat{\boldsymbol{H}}_1 = \boldsymbol{T}_1^T \hat{\boldsymbol{H}} \boldsymbol{T}_1$, and:

$$\hat{\boldsymbol{H}}_1 = \begin{bmatrix} \tilde{\boldsymbol{H}}_{0,0}^1 & \tilde{\boldsymbol{H}}_{0,1}^1 & & & \\ \tilde{\boldsymbol{H}}_{1,0}^1 & \tilde{\boldsymbol{H}}_{1,1}^1 & & & \\ & & \boldsymbol{\Upsilon}_2 & & \\ & & & \ddots & \\ & & & & \boldsymbol{\Upsilon}_N \end{bmatrix} + \begin{bmatrix} \boldsymbol{B}_0^T \boldsymbol{A}_1^T \\ \boldsymbol{B}_1^T \\ \boldsymbol{0} \\ \vdots \\ \boldsymbol{0} \end{bmatrix} \boldsymbol{P}_1 \begin{bmatrix} \boldsymbol{B}_0^T \boldsymbol{A}_1^T \\ \boldsymbol{B}_1^T \\ \boldsymbol{0} \\ \vdots \\ \boldsymbol{0} \end{bmatrix}^T .$$

We repeat this process by expanding $\boldsymbol{P}_1$ according to Riccati equation (4.5). The k^{th} transformation matrix $\boldsymbol{T}_k$ is:

$$\boldsymbol{T_k} = \begin{bmatrix} \boldsymbol{I}_{km} & \boldsymbol{\Pi}_k \boldsymbol{\Upsilon}_k^{-1} & & \\ \boldsymbol{0}_{m \times km} & \boldsymbol{I}_m & & \\ & & \ddots & \\ & & & \boldsymbol{I}_m \end{bmatrix}$$

where:

$$\boldsymbol{\Pi}_k = \begin{bmatrix} (\boldsymbol{B}_0^T \boldsymbol{A}_1^T \cdots \boldsymbol{A}_{k-1}^T) \\ \vdots \\ \boldsymbol{B}_{k-1}^T \end{bmatrix} \left(\boldsymbol{S}_k + \boldsymbol{B}_k^T \boldsymbol{P}_k \boldsymbol{A}_k \right)^T ,$$

and $\hat{\boldsymbol{H}}_k$ is:

$$\hat{\boldsymbol{H}}_k = \begin{bmatrix} \tilde{\boldsymbol{H}}_{0,0}^k & \cdots & \tilde{\boldsymbol{H}}_{0,k}^k & & & \\ \vdots & \ddots & \vdots & & & \\ \tilde{\boldsymbol{H}}_{k,0}^k & \cdots & \tilde{\boldsymbol{H}}_{k,k}^k & & & \\ & & & \boldsymbol{\Upsilon}_{k+1} & & \\ & & & & \ddots & \\ & & & & & \boldsymbol{\Upsilon}_N \end{bmatrix} + \begin{bmatrix} \boldsymbol{B}_0^T \boldsymbol{A}_1^T \cdots \boldsymbol{A}_k^T \\ \vdots \\ \boldsymbol{B}_k^T \\ \boldsymbol{0} \\ \vdots \\ \boldsymbol{0} \end{bmatrix} \boldsymbol{P}_k \begin{bmatrix} \boldsymbol{B}_0^T \boldsymbol{A}_1^T \cdots \boldsymbol{A}_k^T \\ \vdots \\ \boldsymbol{B}_k^T \\ \boldsymbol{0} \\ \vdots \\ \boldsymbol{0} \end{bmatrix}^T .$$

Then we have that $\hat{\boldsymbol{H}}_N = \boldsymbol{H}$, i.e.,

$$\begin{aligned}
\hat{\boldsymbol{H}}_N &= \begin{bmatrix} \tilde{\boldsymbol{H}}^N_{0,0} & \cdots & \tilde{\boldsymbol{H}}^N_{0,N} \\ \vdots & \ddots & \vdots \\ \tilde{\boldsymbol{H}}^N_{N,0} & \cdots & \tilde{\boldsymbol{H}}^N_{N,N} \end{bmatrix} + \begin{bmatrix} \boldsymbol{B}_0^T \boldsymbol{A}_1^T \cdots \boldsymbol{A}_N^T \\ \vdots \\ \boldsymbol{B}_N^T \end{bmatrix} \boldsymbol{P}_N \begin{bmatrix} \boldsymbol{B}_0^T \boldsymbol{A}_1^T \cdots \boldsymbol{A}_N^T \\ \vdots \\ \boldsymbol{B}_N^T \end{bmatrix}^T \\
&= \begin{bmatrix} \boldsymbol{H}_{0,0} & \cdots & \boldsymbol{H}_{0,N} \\ \vdots & \ddots & \vdots \\ \boldsymbol{H}_{N,0} & \cdots & \boldsymbol{H}_{N,N} \end{bmatrix} \\
&= \boldsymbol{H}.
\end{aligned}$$

($\Rightarrow$ Necessary) Transformation matrix $\boldsymbol{T}_k$ is upper triangular with identity matrices along the diagonal, therefore $\boldsymbol{T}_k$, $k \in \{0...N\}$, is invertible. And we have that $\boldsymbol{T}^{-1}\boldsymbol{H}\boldsymbol{T}^{-T} = \hat{\boldsymbol{H}}$. □

Corollary 4.1. *For the conditions in Theorem 4.1, if $J(\boldsymbol{u}_{0:N}, \boldsymbol{x}^\circ_{0:N+1}(\boldsymbol{u}_{0:N}, \boldsymbol{x}_0))$ has a finite and unique minimum in $\boldsymbol{u}_{0:N}$, then $J(\boldsymbol{u}_{0:N}, \boldsymbol{x}^\circ_{0:N+1}(\boldsymbol{u}_{0:N}, \boldsymbol{x}_0))$ is a convex function of $\boldsymbol{u}_{0:N}$.*

Proof. The proof follows directly from the fact that $J(\boldsymbol{u}_{0:N}, \boldsymbol{x}^\circ_{0:N+1}(\boldsymbol{u}_{0:N}, \boldsymbol{x}_0))$ is quadratic in $\boldsymbol{u}_{0:N}$. □

Theorem 4.1 has a close connection to (Q, S, R) dissipativity, as defined in [38]. Indeed, it may be viewed as providing necessary and sufficient conditions for discrete-time, time-varying, finite-horizon (Q, S, R) dissipativity. In special cases for choices of $\{\boldsymbol{Q}_k, \boldsymbol{S}_k, \boldsymbol{R}_k\}$ it distills to conditions for various versions of the finite-horizon Kalman-Yakubovich-Popov (KYP) Lemma, including the positive-real and bounded-real lemmas. Anderson and Vongpanitlerd in [5] provide an optimal-control-based proof of the finite-horizon positive-real lemma in continuous-time, before taking the asymptotic limit as the time horizon approaches infinity, and showing that for time-invariant plant parameters one arrives at the matrix inequality condition for positive-realness of time-invariant plants. Green and Limebeer, in [26], show the analogous continuous-time, optimal-control-based proof to Theorem 4.1 for the bounded real lemma.

However, there does not appear to be analogous finite-horizon proofs in the open literature in the discrete-time case. Rather, the discrete-time version of the KYP lemma (whether in its general form, or specifically for positive-real or bounded-real cases) is usually only proved in the time-invariant, infinite-horizon case, with the usual approach being to relate it to the continuous-time KYP lemma using a bilinear transformation (e.g., [14, 25, 32]). The

discrete-time finite-horizon time-varying positive real lemma follows directly from Theorem 4.1.

Corollary 4.2. *(Discrete-Time Finite-Horizon Time-Varying Positive Real Lemma) Let* $\boldsymbol{x}_k$ *evolve according to the LTV difference equation* (3.10) *with initial condition* $\boldsymbol{x}_0 \in \mathbb{R}^n$*, and exogenous disturbance* $\boldsymbol{a}_{0:N} \in \mathbb{R}^{d\times(N+1)}$*. Now, let* $p = 1$ *and* $\boldsymbol{y}_k^1$ *be defined according to* (3.15)*, and let performance measure* $J(\cdot,\cdot)$ *be:*

$$J(\boldsymbol{u}_{0:N}, \boldsymbol{x}^\circ_{0:N+1}(\boldsymbol{u}_{0:N}, \boldsymbol{x}_0)) = \sum_{k=0}^{N} \boldsymbol{u}_k^T \boldsymbol{y}_k^1,$$

which can be written in the form (4.2) *with* $\boldsymbol{P}_{N+1} = \boldsymbol{0}$ *and with matrix parameters:*

$$\begin{aligned} \boldsymbol{S}_k =& \frac{1}{2}(\boldsymbol{C}^1_{E,k})^T, \quad \boldsymbol{R}_k = \frac{1}{2}(\boldsymbol{D}^1_{E,k} + (\boldsymbol{D}^1_{E,k})^T) \\ \boldsymbol{U}_k =& \boldsymbol{I}, \qquad\qquad \boldsymbol{Q}_k = \boldsymbol{T}_k = \boldsymbol{V}_k = \boldsymbol{0}, \end{aligned}$$

where $\boldsymbol{C}^1_{E,k}$*, and* $\boldsymbol{D}^1_{E,k}$ *are defined in* (3.16)*, and* (3.17)*, respectively. Then, the discrete-time mapping* $\boldsymbol{u} \mapsto \boldsymbol{y}^1$ *is passive if and only if the RDRDE:*

$$\tilde{\boldsymbol{P}}_{k-1} = \boldsymbol{A}_k^T \tilde{\boldsymbol{P}}_k \boldsymbol{A}_k + \left(\boldsymbol{C}^1_{E,k} - \boldsymbol{B}_k^T \tilde{\boldsymbol{P}}_k \boldsymbol{A}_k\right)^T \left(\boldsymbol{D}^1_{E,k} + (\boldsymbol{D}^1_{E,k})^T - \boldsymbol{B}_k^T \tilde{\boldsymbol{P}}_k \boldsymbol{B}_k\right)^{-1} \left(\boldsymbol{C}^1_{E,k} - \boldsymbol{B}_k^T \tilde{\boldsymbol{P}}_k \boldsymbol{A}_k\right),$$

with final condition $\tilde{\boldsymbol{P}}_{N+1} = \boldsymbol{0}$*, has a solution where* $(\boldsymbol{D}^1_{E,k} + (\boldsymbol{D}^1_{E,k})^T - \boldsymbol{B}_k^T \tilde{\boldsymbol{P}}_k \boldsymbol{B}_k) \succ 0$*. If the solution to* $\tilde{\boldsymbol{P}}_k$ *exists, then* $\tilde{\boldsymbol{P}}_k \succeq 0$*,* $\forall k \in \{0...N+1\}$*.*

Proof. The proof follows analogously from Theorem 4.1, where $\tilde{\boldsymbol{P}}_k = -\boldsymbol{P}_k$ in Equation (4.5). Because $\boldsymbol{Q}_k = \boldsymbol{0}$, $\tilde{\boldsymbol{P}}_{N+1} = \boldsymbol{0}$, and $\left(\boldsymbol{D}^1_{E,k} + (\boldsymbol{D}^1_{E,k})^T - \boldsymbol{B}_k^T \tilde{\boldsymbol{P}}_k \boldsymbol{B}_k\right) \succ 0$, we can conclude that $\tilde{\boldsymbol{P}}_k \succeq 0$, $\forall k \in \{0...N+1\}$. □

Assumption 4. *Let* $\mathcal{M}_d = \mathcal{D}(\mathcal{M}, \Delta t, \boldsymbol{a})$ *be the discrete-time model under consideration, and let* $\boldsymbol{x}$ *evolve according to* (3.10)*. Then, we assume that if the performance measure is of form* (4.1)*, then* $J(\boldsymbol{u}_{0:N}, \boldsymbol{q}_{0:N}, \boldsymbol{x}^\circ_{0:N}(\boldsymbol{u}_{0:N}, \boldsymbol{x}_0))$ *is convex in* $\{\boldsymbol{u}_{0:N}, \boldsymbol{q}_{0:N}\}$*. If the performance measure is of form* (4.2)*, then* $J(\boldsymbol{u}_{0:N}, \boldsymbol{x}^\circ_{0:N}(\boldsymbol{u}_{0:N}, \boldsymbol{0}))$ *is convex in* $\boldsymbol{u}_{0:N}$*.*

4.1.2 Energy-Constrained Optimal Control Problem

The energy stored in the i^{th} unit E^i_{k+1} can be written explicitly in terms of $\{\boldsymbol{u}_{0:N}, \boldsymbol{q}_{0:N}, \boldsymbol{x}_{0:N}\}$ as:

$$E^i_{k+1}(\boldsymbol{u}_{0:N}, \boldsymbol{q}_{0:N}, \boldsymbol{x}_{0:N}) = (\gamma^i)^{k+1} E^i_0 - \sum_{\ell=0}^{k} (\gamma^i)^{k-\ell} (\boldsymbol{u}_\ell^T \boldsymbol{y}^i_\ell + \mu^i_\ell(\boldsymbol{u}_\ell, \boldsymbol{y}^i_\ell) + q^i_\ell),$$

where $\boldsymbol{y}^i_\ell$ is related to $\{\boldsymbol{u}_{0:N}, \boldsymbol{q}_{0:N}, \boldsymbol{x}_{0:N}\}$ via (3.15). Let $\boldsymbol{c}^L_k(\cdot,\cdot,\cdot)$ and $\boldsymbol{c}^U_k(\cdot,\cdot,\cdot)$ be the set of p lower and p upper energy constraint functions, respectively:

$$\begin{aligned}\boldsymbol{c}^L_k(\boldsymbol{u}_{0:N}, \boldsymbol{q}_{0:N}, \boldsymbol{x}_{0:N}) =& \boldsymbol{E}_L - \boldsymbol{E}_{k+1} \\ \boldsymbol{c}^U_k(\boldsymbol{u}_{0:N}, \boldsymbol{q}_{0:N}, \boldsymbol{x}_{0:N}) =& \boldsymbol{E}_{k+1} - \boldsymbol{E}_U,\end{aligned}$$

where $\boldsymbol{E}_L = \begin{bmatrix} E^1_L \cdots E^p_L \end{bmatrix}^T$ and $\boldsymbol{E}_U = \begin{bmatrix} E^1_U \cdots E^p_U \end{bmatrix}^T$. Then clearly:

$$\boldsymbol{E}_{k+1} \in \mathbb{R}_E \iff \boldsymbol{c}^L_k(\boldsymbol{u}_{0:N}, \boldsymbol{q}_{0:N}, \boldsymbol{x}_{0:N}) \leqslant 0, \quad \boldsymbol{c}^U_k(\boldsymbol{u}_{0:N}, \boldsymbol{q}_{0:N}, \boldsymbol{x}_{0:N}) \leqslant 0,$$

with the inequalities taken element-by-element. Let the trajectory optimization, where we enforce that the discrete-time states evolve according to (3.10), be the Energy-Constrained Optimal Control Problem (ECOCP), which has the following form:

$$\text{ECOCP} = \begin{cases} \textbf{Given:} & \boldsymbol{x}_0,\ \boldsymbol{E}_0, \boldsymbol{a}_k, \boldsymbol{a}^i_{E,k}, \\ & \boldsymbol{A}_k, \boldsymbol{B}_k, \boldsymbol{C}^i_{E,k}, \boldsymbol{D}^i_{E,k}, \gamma^i, \boldsymbol{M}^i_k \\ & \forall k \in \{0...N\},\ \forall i \in \{1...p\} \\ \textbf{Minimize:} & J(\boldsymbol{u}_{0:N}, \boldsymbol{q}_{0:N}, \boldsymbol{x}^\circ_{0:N+1}(\boldsymbol{u}_{0:N}, \boldsymbol{x}_0)) \\ \textbf{Domain:} & \boldsymbol{u}_{0:N},\ \boldsymbol{q}_{0:N} \\ \textbf{Constraints:} & \boldsymbol{c}^L_k(\boldsymbol{u}_{0:N}, \boldsymbol{q}_{0:N}, \boldsymbol{x}^\circ_{0:N}(\boldsymbol{u}_{0:N}, \boldsymbol{x}_0)) \leqslant 0, \\ & \boldsymbol{c}^U_k(\boldsymbol{u}_{0:N}, \boldsymbol{q}_{0:N}, \boldsymbol{x}^\circ_{0:N}(\boldsymbol{u}_{0:N}, \boldsymbol{x}_0)) \leqslant 0, \\ & \boldsymbol{q}_k \geqslant 0, \\ & \forall k \in \{0...N\}. \end{cases} \tag{4.7}$$

Define the Lagrange multipliers that enforce the k^{th} lower energy constraint, and k^{th} upper energy constraint of the i^{th} energy storage system as $\lambda^{L,i}_k$ and $\lambda^{U,i}_k$, respectively. Let $\boldsymbol{\lambda}^L_k$ and $\boldsymbol{\lambda}^L_k$ be vectors of length p containing these Lagrange multipliers for each energy storage

system:

$$\boldsymbol{\lambda}_k^L = \begin{bmatrix} \lambda_k^{L,1} & \cdots & \lambda_k^{L,p} \end{bmatrix}^T, \qquad \boldsymbol{\lambda}_k^U = \begin{bmatrix} \lambda_k^{U,1} & \cdots & \lambda_k^{U,p} \end{bmatrix}^T.$$

Now, let $\boldsymbol{\lambda}_k$ be a vector of length $2p$ of all these Lagrange multipliers at the k^{th} time step:

$$\begin{aligned} \boldsymbol{\lambda}_k &= \begin{bmatrix} (\boldsymbol{\lambda}_k^L)^T & (\boldsymbol{\lambda}_k^U)^T \end{bmatrix}^T \\ &= \begin{bmatrix} \lambda_k^{L,1} & \cdots & \lambda_k^{L,p} & \lambda_k^{U,1} & \cdots & \lambda_k^{U,p} \end{bmatrix}^T. \end{aligned}$$

The KKT conditions require these Lagrange multipliers to be non-negative at the optimum, i.e., $\boldsymbol{\lambda}_k^L, \boldsymbol{\lambda}_k^U \geqslant 0$, $\forall k \in \{0...N\}$. We explicitly enforce the energy constraints and state dynamics in the augmented performance measure function $\bar{J}(\cdot,\cdot,\cdot,\cdot)$ as:

$$\begin{aligned} \bar{J}(\boldsymbol{u}_{0:N}, \boldsymbol{q}_{0:N}, \boldsymbol{x}^\circ_{0:N+1}(\boldsymbol{u}_{0:N}, \boldsymbol{x}_0), \boldsymbol{\lambda}_{0:N}) &= \boldsymbol{x}^\circ_{N+1}(\boldsymbol{u}_N, \boldsymbol{x}_0)^T \boldsymbol{P}_{N+1} \boldsymbol{x}^\circ_{N+1}(\boldsymbol{u}_{0:N}, \boldsymbol{x}_0) \\ &+ \sum_{k=0}^{N} L_k(\boldsymbol{u}_k, \boldsymbol{x}^\circ_k(\boldsymbol{u}_{0:N}, \boldsymbol{x}_0)) + \sum_{k=0}^{N} (\boldsymbol{\lambda}_k^L)^T \boldsymbol{c}_k^L(\boldsymbol{u}_{0:N}, \boldsymbol{q}_{0:N}, \boldsymbol{x}^\circ_{0:N}(\boldsymbol{u}_{0:N}, \boldsymbol{x}_0)) \\ &+ \sum_{k=0}^{N} (\boldsymbol{\lambda}_k^U)^T \boldsymbol{c}_k^U(\boldsymbol{u}_{0:N}, \boldsymbol{q}_{0:N}, \boldsymbol{x}^\circ_{0:N}(\boldsymbol{u}_{0:N}, \boldsymbol{x}_0)). \end{aligned} \tag{4.8}$$

Then, the ECOCP is equivalent to the following *primal minimax problem*:

$$J^*(\boldsymbol{x}_0) = \inf_{\boldsymbol{u}_{0:N},\, \boldsymbol{q}_{0:N} \geqslant 0} \left\{ \sup_{\boldsymbol{\lambda}_{0:N} \geqslant 0} \bar{J}(\boldsymbol{u}_{0:N}, \boldsymbol{q}_{0:N}, \boldsymbol{x}^\circ_{0:N+1}(\boldsymbol{u}_{0:N}, \boldsymbol{x}_0), \boldsymbol{\lambda}_{0:N}) \right\}. \tag{4.9}$$

4.1.3 Convexity

The ECOCP is convex if performance measure $J(\boldsymbol{u}_{0:N}, \boldsymbol{q}_{0:N}, \boldsymbol{x}^\circ_{0:N+1}(\boldsymbol{u}_{0:N}, \boldsymbol{x}_0))$ in (4.1) is a convex function of $\{\boldsymbol{u}_{0:N}, \boldsymbol{q}_{0:N}\}$, and if the inequality constraint functions:

$$\boldsymbol{c}_k^L(\boldsymbol{u}_{0:N}, \boldsymbol{q}_{0:N}, \boldsymbol{x}^\circ_{0:N}(\boldsymbol{u}_{0:N}, \boldsymbol{x}_0)) \leqslant 0 \quad \text{and} \quad \boldsymbol{c}_k^L(\boldsymbol{u}_{0:N}, \boldsymbol{q}_{0:N}, \boldsymbol{x}^\circ_{0:N}(\boldsymbol{u}_{0:N}, \boldsymbol{x}_0)) \leqslant 0$$

are convex in $\{\boldsymbol{u}_{0:N}, \boldsymbol{q}_{0:N}\}$, for all $k \in \{0...N\}$ (see Definition 2.21). If the ECOCP is convex, then its feasibility domain $\mathbb{F}_{\mathcal{M}_d}(\boldsymbol{x}_k, \boldsymbol{E}_k, N)$ is a convex set. Assumption 4 ensures that $J(\boldsymbol{u}_{0:N}, \boldsymbol{q}_{0:N}, \boldsymbol{x}^\circ_{0:N+1}(\boldsymbol{u}_{0:N}, \boldsymbol{x}_0))$ is a convex function of $\{\boldsymbol{u}_{0:N}, \boldsymbol{q}_{0:N}\}$. Hence, we focus on the

convexity of the storage constraint functions, but first, we introduce some notation. Let:

$$\tilde{\boldsymbol{u}}_k^i = (\gamma^i)^{-k/2}\boldsymbol{u}_k, \qquad \tilde{\boldsymbol{x}}_k^i = (\gamma^i)^{-k/2}\boldsymbol{x}_k, \qquad \tilde{\boldsymbol{y}}_k^i = (\gamma^i)^{-k/2}\boldsymbol{y}_k^i, \tag{4.10}$$

and then we define the i^{th} modified system as:

$$\begin{aligned} \left(\gamma^i\right)^{1/2}\tilde{\boldsymbol{x}}_{k+1}^i &= \boldsymbol{A}_k\tilde{\boldsymbol{x}}_k^i + \boldsymbol{B}_k\tilde{\boldsymbol{u}}_k^i \\ \tilde{\boldsymbol{y}}_k^i &= \boldsymbol{C}_{E,k}^i\tilde{\boldsymbol{x}}_k^i + \boldsymbol{D}_{E,k}^i\tilde{\boldsymbol{u}}_k^i, \end{aligned} \tag{4.11}$$

with initial condition $\tilde{\boldsymbol{x}}_0^i = \boldsymbol{x}_0 \in \mathbb{R}^n$. Recall that $\gamma^i \in (0,1]$ is a unitless scalar that quantifies the decay of energy within the i^{th} storage system as defined in (3.20).

Theorem 4.2. *For all $i \in \{1...p\}$, let the mapping $\tilde{\boldsymbol{u}}^i \mapsto \tilde{\boldsymbol{y}}^i$ be discrete-time passive (see Definition 2.12). Then, the following are true $\forall k \in \{0...N\}$:*

1. *$\boldsymbol{c}_k^L(\boldsymbol{u}_{0:N}, \boldsymbol{q}_{0:N}, \boldsymbol{x}_{0:N}^\circ(\boldsymbol{u}_{0:N}, \boldsymbol{x}_0))$ is a vector of convex functions in $\{\boldsymbol{u}_{0:N}, \boldsymbol{q}_{0:N}\}$*
2. *$\boldsymbol{c}_k^U(\boldsymbol{u}_{0:N}, \boldsymbol{q}_{0:N}, \boldsymbol{x}_{0:N}^\circ(\boldsymbol{u}_{0:N}, \boldsymbol{x}_0))$ is a vector of concave functions in $\{\boldsymbol{u}_{0:N}, \boldsymbol{q}_{0:N}\}$.*

Proof. First, we show statement 1. Let $\{\boldsymbol{u}_{0:N}^a, \boldsymbol{q}_{0:N}^{i,a}\}$ and $\{\boldsymbol{u}_{0:N}^b, \boldsymbol{q}_{0:N}^{i,b}\}$ each satisfy the lower energy constraint for the i^{th} energy storage unit, $c_k^{L,i}(\cdot,\cdot,\cdot) \leqslant 0$ for $k \in \{0...N\}$, i.e., they are feasible trajectories for these constraints. Let $E_{0:N+1}^{i,a}$ and $E_{0:N+1}^{i,b}$ be the resulting energies from implementing these feasible inputs. Let $\alpha \in [0,1]$, and define the linear interpolation between these two feasible trajectories as:

$$\begin{aligned} \boldsymbol{u}_{0:N}^{ab} &= \alpha\boldsymbol{u}_{0:N}^a + (1-\alpha)\boldsymbol{u}_{0:N}^b, \\ q_{0:N}^{i,ab} &= \alpha q_{0:N}^{i,a} + (1-\alpha)q_{0:N}^{i,b}, \end{aligned} \tag{4.12}$$

and let $E_{0:N+1}^{i,ab}$ be the resulting energy from implementing these interpolated inputs. Due to linearity, the corresponding responses for $\boldsymbol{y}_{0:N}^i$ and $\boldsymbol{x}_{0:N}$ are also interpolations; i.e.,

$$\begin{aligned} \boldsymbol{y}_{0:N}^{i,ab} &= \alpha\boldsymbol{y}_{0:N}^{i,a} + (1-\alpha)\boldsymbol{y}_{0:N}^{i,b}, \\ \boldsymbol{x}_{0:N}^{ab} &= \alpha\boldsymbol{x}_{0:N}^a + (1-\alpha)\boldsymbol{x}_{0:N}^b. \end{aligned}$$

Function $c_k^{L,i}(\cdot,\cdot,\cdot)$ is convex if:

$$F_k = c_k^{L,i}(\boldsymbol{u}_{0:N}^{ab}, \boldsymbol{q}_{0:N}^{ab}, \boldsymbol{x}_{0:N}^{ab}) - \alpha c_k^{L,i}(\boldsymbol{u}_{0:N}^a, \boldsymbol{q}_{0:N}^a, \boldsymbol{x}_{0:N}^a) - (1-\alpha)c_k^{L,i}(\boldsymbol{u}_{0:N}^b, \boldsymbol{q}_{0:N}^b, \boldsymbol{x}_{0:N}^b) \leqslant 0.$$

Then, simplifying we have that:

$$\begin{aligned}
F_k =& -E_{k+1}^{i,ab} + \alpha E_{k+1}^{i,a} + (1-\alpha)E_{k+1}^{i,b} \\
=& \sum_{\ell=0}^{k} (\gamma^i)^{k-\ell}((\boldsymbol{u}_\ell^{ab})^T \boldsymbol{y}_\ell^{i,ab} + \mu_\ell^i(\boldsymbol{u}_\ell^{ab}, \boldsymbol{y}_\ell^{i,ab}) + q_\ell^{i,ab}) \\
& - \alpha \sum_{\ell=0}^{k} (\gamma^i)^{k-\ell}((\boldsymbol{u}_\ell^{a})^T \boldsymbol{y}_\ell^{i,a} + \mu_\ell^i(\boldsymbol{u}_\ell^{a}, \boldsymbol{y}_\ell^{i,a}) + q_\ell^{i,a}) \\
& - (1-\alpha) \sum_{\ell=0}^{k} (\gamma^i)^{k-\ell}((\boldsymbol{u}_\ell^{b})^T \boldsymbol{y}_\ell^{i,b} + \mu_\ell^i(\boldsymbol{u}_\ell^{b}, \boldsymbol{y}_\ell^{i,b}) + q_\ell^{i,b}).
\end{aligned}$$

Because $\mu_\ell(\cdot,\cdot)$ is quadratic, this simplifies to:

$$F_k = -(\alpha - \alpha^2)\left(\sum_{\ell=0}^{k} (\gamma^i)^{k-\ell}(\boldsymbol{u}_\ell^a - \boldsymbol{u}_\ell^b)^T(\boldsymbol{y}_\ell^{i,a} - \boldsymbol{y}_\ell^{i,b}) + \sum_{\ell=0}^{k} (\gamma^i)^{k-\ell}\mu_\ell^i(\boldsymbol{u}_\ell^a - \boldsymbol{u}_\ell^b, \boldsymbol{y}_\ell^{i,a} - \boldsymbol{y}_\ell^{i,b})\right)$$

The second term in the parentheses is positive because $\mu_\ell(\cdot,\cdot)$ is positive-semidefinite. Then, we have that:

$$F_k \leqslant -(\alpha - \alpha^2)\gamma^k \sum_{\ell=0}^{k} (\tilde{\boldsymbol{u}}_\ell^i)^T \tilde{\boldsymbol{y}}_\ell^i,$$

where $\tilde{\boldsymbol{u}}_\ell^i = (\gamma^i)^{-\ell/2}(\boldsymbol{u}_\ell^a - \boldsymbol{u}_\ell^b)$ and $\tilde{\boldsymbol{y}}_\ell^i = (\gamma^i)^{-\ell/2}(\boldsymbol{y}_\ell^{i,a} - \boldsymbol{y}_\ell^{i,b})$. Note that $\tilde{\boldsymbol{y}}_\ell^i$ depends only on $\tilde{\boldsymbol{u}}_{0:N}^i$ (but not $\boldsymbol{a}$ and $\boldsymbol{x}_0$). Recall that the mapping $\tilde{\boldsymbol{u}}^i \mapsto \tilde{\boldsymbol{y}}^i$ is discrete-time passive, and this requires that with $\boldsymbol{x}_0 = 0$ and $\boldsymbol{a}_{0:N} = 0$:

$$\sum_{\ell=0}^{k} \left(\tilde{\boldsymbol{u}}_\ell^i\right)^T \tilde{\boldsymbol{y}}_\ell^i \geqslant 0, \quad \forall \tilde{\boldsymbol{u}}_{0:N}^i \in \mathbb{R}^{m\times(N+1)}, \quad \forall k \in \mathbb{Z}_{\geqslant 0}.$$

Then, it follows that $F_k \leqslant 0$, $\forall k \in \{0...N\}$. Thus, completing the proof for statement 1.

To show statement 2, we repeat the same process, but instead show that $F_k \geqslant 0$ $\forall k \in \{0...N\}$, and therefore $c_k^{U,i}(\boldsymbol{u}_{0:N}, \boldsymbol{q}_{0:N}, \boldsymbol{x}_{0:N}^\circ(\boldsymbol{u}_{0:N}, \boldsymbol{x}_0))$ is a concave constraint in $\{\boldsymbol{u}_{0:N}, \boldsymbol{q}_{0:N}\}$. □

In the above proof, we show that the energy storage constraints are quadratic in $\boldsymbol{u}_{0:N}$, and therefore if the performance measure is also quadratic in $\boldsymbol{u}_{0:N}$, the ECOCP is a nonconvex QCQP in general. However, under special conditions on the model parameters, the ECOCP

is convex.

Let E^i_{max} be the maximum possible energy that the i^{th} storage system can extract at time-step $N+1$ from disturbance $\boldsymbol{a}_{0:N} \in (\mathbb{R}^d)^{(N+1)}$ with initial condition $\boldsymbol{x}_0 \in \mathbb{R}^n$, no decay in the storage system ($\gamma^i = 1$), and ignoring lower storage bounds. That is:

$$E^i_{max} = \max_{\boldsymbol{u}_{0:N}} \Big\{ E^i_{N+1}(\boldsymbol{u}_{0:N}, q^i_{0:N} = 0, \boldsymbol{x}^\circ_{0:N}(\boldsymbol{u}_{0:N}, \boldsymbol{x}_0)) \Big\}. \tag{4.13}$$

Therefore, E^i_{max} is an upper bound on the amount of energy in storage system i.

Corollary 4.3. *For a given set of initial conditions and exogenous disturbances, there exists bounds $\{\hat{E}^1_U \cdots \hat{E}^p_U\}$ such that the ECOCP is convex if for all $i \in \{1...p\}$:*

1. *$E^i_U \geqslant \hat{E}^i_U$*
2. *The mapping $\tilde{\boldsymbol{u}}^i \mapsto \tilde{\boldsymbol{y}}^i$ is discrete-time passive.*

It then follows that the feasibility domain $\mathbb{F}_{\mathcal{M}_d}(\boldsymbol{x}_0, \boldsymbol{E}_0, N)$ is a convex set.

Proof. Assumption 4 states that performance measure J is a convex function of $\{\boldsymbol{u}_{0:N}, \boldsymbol{q}_{0:N}\}$. Theorem 4.2 shows that the upper energy constraint $\boldsymbol{c}^U_k(\cdot,\cdot,\cdot)$ is a concave function in $\boldsymbol{u}_{0:N}$. However, if $E^i_U \geqslant E^i_{max}$, which is defined in (4.13), for all $i \in \{1...p\}$, then the upper energy constraint is inactive for all $k \in \{0...N\}$ and for all $\{\boldsymbol{u}_{0:N}, \boldsymbol{q}_{0:N}\} \in (\mathbb{R}^m)^{(N+1)} \times (\mathbb{R}^p)^{(N+1)}$. It follows that the ECOCP is convex. A tighter bound, where $\hat{E}^i_U < E^i_{max}$, may exist. □

The requirement that the mapping $\tilde{\boldsymbol{u}}^i \mapsto \tilde{\boldsymbol{y}}^i$ be discrete-time passive $\forall i \in \{1...p\}$ is rather restrictive. To simplify matters, consider the case in which $\gamma^i = 1$, $\forall i \in \{1...p\}$. Then, this effectively requires discrete-time passivity of each mapping $\boldsymbol{u} \mapsto \boldsymbol{y}^i$, $\forall i \in \{1...p\}$. It is straight-forward to show that this is the case if $p = 1$, i.e., if there is only one storage system, because in this case the discrete-time passivity of $\boldsymbol{u} \mapsto \boldsymbol{y}^1$ is inherited from the continuous-time passivity of the plant, which we prove below. However, if $p > 1$, then this discrete-time passivity condition does not hold in general, irrespective of the passivity of the continuous-time system. And even if the mapping $\tilde{\boldsymbol{u}}^i \mapsto \tilde{\boldsymbol{y}}^i$ is discrete-time passive for $\gamma^i = 1$, it may fail to hold for γ^i below a certain threshold (see Section 4.2.1 for an extended discussion on this).

Lemma 4.1. *Consider the case with one energy storage unit $p = 1$ and where $T^1_S \to \infty$. If the mapping $\boldsymbol{u} \mapsto \boldsymbol{v}$ is continuous-time passive, which is the case for all $\mathcal{P} \in \mathbb{P}$, then the discrete-time mapping $\boldsymbol{u} \mapsto \boldsymbol{y}^1$ is discrete-time passive.*

Proof. It follows from the definition of continuous-time passivity in Definition 2.10 that for each initial condition $\boldsymbol{x}(0) \in \mathbb{R}^n$ and exogenous disturbance trajectory $\boldsymbol{a} \in (\mathbb{L}^2)^d$, there exists a $\beta \geqslant 0$ such that for all $\boldsymbol{u} \in (\mathbb{L}^2)^m$ and all $\ell \in \mathbb{Z}_{\geqslant 0}$:

$$\int_0^{(\ell+1)\Delta t} \boldsymbol{u}^T(\tau)\boldsymbol{v}(\tau)d\tau \geqslant -\beta.$$

Then, when $\boldsymbol{u}(\tau) = \boldsymbol{u}_k$ for $\tau \in [k\Delta t, (k+1)\Delta t)$ and for all $k \in \{0...\ell\}$, i.e., $\boldsymbol{u}$ is a ZOH trajectory, we can write the above as:

$$\boldsymbol{u}_0^T \int_0^{\Delta t} \boldsymbol{v}(\tau)d\tau + \boldsymbol{u}_1^T \int_{\Delta t}^{2\Delta t} \boldsymbol{v}(\tau)d\tau + \cdots + \boldsymbol{u}_\ell^T \int_{\ell\Delta t}^{(\ell+1)\Delta t} \boldsymbol{v}(\tau)d\tau \geqslant -\beta.$$

When $T_S^1 \to \infty$, $\boldsymbol{y}_k^1$ simplifies to $\boldsymbol{y}_k^1 = \int_{k\Delta t}^{(k+1)\Delta t} \boldsymbol{v}(\tau)d\tau$, and then it follows that:

$$\sum_{k=0}^{\ell} \boldsymbol{u}_k^T \boldsymbol{y}_k^1 \geqslant -\beta,$$

and therefore, the mapping $\boldsymbol{u} \mapsto \boldsymbol{y}^1$ is discrete-time passive via Definition 2.12. □

4.2 Special Cases of the Energy-Constrained Optimal Control Problem

4.2.1 Linear Time Invariant Plant

Consider the special case where the dynamics of the continuous-time plant $\mathcal{P}$ in (3.1) are LTI. Then, it follows that the discrete-time plant dynamics evolves according to the following discrete-time LTI difference equation:

$$\begin{aligned} \boldsymbol{x}_{k+1} =& \boldsymbol{A}\boldsymbol{x}_k + \boldsymbol{B}\boldsymbol{u}_k + \boldsymbol{a}_k \\ \boldsymbol{y}_k^i =& \boldsymbol{C}_E^i \boldsymbol{x}_k + \boldsymbol{D}_E^i \boldsymbol{u}_k + \boldsymbol{a}_{E,k}^i. \end{aligned} \tag{4.14}$$

where:

$$\begin{aligned} \boldsymbol{A} =& e^{\bar{\boldsymbol{A}}\Delta t}, \quad \boldsymbol{B} = \bar{\boldsymbol{A}}^{-1}(\boldsymbol{A} - \boldsymbol{I})\bar{\boldsymbol{B}} \\ \boldsymbol{D} =& \bar{\boldsymbol{D}}, \qquad \boldsymbol{C} = \bar{\boldsymbol{C}}. \end{aligned} \tag{4.15}$$

Then, the energy-preserving, discrete-time matrices in (3.16), (3.17), and (3.18) simplify to:

$$\begin{aligned}
\boldsymbol{C}_E^i =& \boldsymbol{K}^i \boldsymbol{C}(\bar{\boldsymbol{A}} + \tfrac{1}{T_S^i}\boldsymbol{I})^{-1}\left(\boldsymbol{A} - \gamma^i \boldsymbol{I}\right) \\
\boldsymbol{D}_E^i =& \boldsymbol{K}^i \left(\boldsymbol{C}(\bar{\boldsymbol{A}} + \tfrac{1}{T_S^i}\boldsymbol{I})^{-1}\left(\boldsymbol{B} - \bar{\boldsymbol{B}}\chi^i\right) + \boldsymbol{D}\chi^i\right) \\
\boldsymbol{a}_{E,k}^i =& \boldsymbol{K}^i \left(\boldsymbol{C}(\bar{\boldsymbol{A}} + \tfrac{1}{T_S^i}\boldsymbol{I})^{-1}\left(\bar{\boldsymbol{A}}^{-1}(\boldsymbol{A} - \boldsymbol{I})\bar{\boldsymbol{G}} - \bar{\boldsymbol{G}}\chi^i\right)\right)\boldsymbol{a}_k.
\end{aligned} \tag{4.16}$$

Now, we can represent the discrete-time mapping $\boldsymbol{u} \mapsto \boldsymbol{y}^i$ by the following transfer function:

$$\boldsymbol{T}^i(z) = \boldsymbol{C}_E^i \left(z\boldsymbol{I} - \boldsymbol{A}\right)^{-1} \boldsymbol{B} + \boldsymbol{D}_E^i, \tag{4.17}$$

and the discrete-time mapping $\tilde{\boldsymbol{u}}^i \mapsto \tilde{\boldsymbol{y}}^i$, where $\tilde{\boldsymbol{u}}^i$ and $\tilde{\boldsymbol{y}}^i$ are defined in (4.10), are represented by following transfer function:

$$\tilde{\boldsymbol{T}}^i(z) = \boldsymbol{C}_E^i \left((\gamma^i)^{\frac{1}{2}} z\boldsymbol{I} - \boldsymbol{A}\right)^{-1} \boldsymbol{B} + \boldsymbol{D}_E^i. \tag{4.18}$$

We specialize Theorem 4.1 and Corollary 4.3 for LTI systems using transfer functions (4.17) and (4.18).

Corollary 4.4. *Consider the case where the dynamics of the continuous-time plant $\mathcal{P}$ in* (3.1) *are LTI. There exists bounds $\{\hat{E}_U^1 \cdots \hat{E}_U^p\}$ such that the ECOCP is convex if for all $i \in \{1...p\}$:*

1. *$E_U^i \geqslant \hat{E}_U^i$*
2. *Transfer function $\tilde{\boldsymbol{T}}^i(z)$ in* (4.18) *is PR.*

Recall from Theorem 2.7 that a transfer function is PR if and only if the associated discrete-time LTI system is passive. Consider the case where mapping $\boldsymbol{u} \mapsto \boldsymbol{y}^i$ is discrete-time passive for $i \in \{1...p\}$. If $p = 1$, we can guarantee $\boldsymbol{u} \mapsto \boldsymbol{y}^1$ is discrete-time passive via Lemma 4.1; however, we cannot guarantee passivity for $p > 1$. As mentioned in Section 4.1.3, there exists a threshold for γ^i below which passivity of $\tilde{\boldsymbol{u}}^i \mapsto \tilde{\boldsymbol{y}}^i$ is lost. This result becomes more obvious in the LTI case because we can more easily analyze how transfer function $\tilde{\boldsymbol{T}}^i(z)$ changes with decreasing γ^i. First, consider the case where $\gamma^i = 1$. Then, $\tilde{\boldsymbol{T}}^i(z) = \boldsymbol{T}^i(z)$ and the mappings $\tilde{\boldsymbol{u}}^i \mapsto \tilde{\boldsymbol{y}}^i$ and $\boldsymbol{u} \mapsto \boldsymbol{y}^i$ are equivalent. Hence, for $\gamma^i = 1$, Corollary 4.4 requires $\boldsymbol{T}^i(z)$ to be PR. However, if $\gamma^i < 1$, we require a stronger condition on $\boldsymbol{T}^i(z)$ to hold. It follows directly from Definition 2.13 that for $\gamma^i \in (0, 1]$, $\tilde{\boldsymbol{T}}^i(z)$ is PR if:

1. all elements of $\boldsymbol{T}^i(z)$ are analytic for $\forall |z| > (\gamma^i)^{\frac{1}{2}}$
2. $\boldsymbol{T}^i(z) + (\boldsymbol{T}^i)^T(\bar{z}) \succeq 0, \ \forall |z| > (\gamma^i)^{\frac{1}{2}}$.

As γ^i decreases, the region over which the above requirements must be satisfied grows. Therefore, the conditions for $\tilde{\boldsymbol{T}}^i(z)$ to be PR become more restrictive with decreasing γ^i. For the case where $\gamma^i = 0$, there is no energy storage (see Section 4.2.4), and the ECOCP is always nonconvex.

4.2.2 Energy Harvesting Problem

In the *energy harvesting problem*, the goal is to maximize the total generated energy (i.e., the energy delivered from the transducers to the storage system, minus transmission losses) over a finite time horizon. Then, the energy harvesting performance measure is:

$$J(\boldsymbol{u}_{0:N}, \boldsymbol{x}^{\circ}_{0:N+1}(\boldsymbol{u}_{0:N}, \boldsymbol{x}_0)) = \sum_{i=1}^{p} \sum_{k=0}^{N} \boldsymbol{u}_k^T \boldsymbol{y}_k^i + \mu_k^i \left(\boldsymbol{u}_k, \boldsymbol{y}_k^i\right), \tag{4.19}$$

where $\boldsymbol{y}_k^i$ is defined in (3.15), and $\mu_k^i(\cdot, \cdot)$ is the quadratic transmission loss model in (3.22). Note that the energy harvesting performance measure can written as the quadratic form in (4.2).

Theorem 4.3. *Consider the energy harvesting performance measure in* (4.19)*. Let the mapping* $\boldsymbol{u} \mapsto \boldsymbol{y}^i$ *be discrete-time passive* $\forall i \in \{1...p\}$*, then the energy harvesting performance measure* (4.19) *is a convex function of* $\boldsymbol{u}_{0:N}$*.*

Proof. First, we show that the first term of performance measure $J(\cdot, \cdot)$ is a convex function of $\boldsymbol{u}_{0:N}$. We write this first term as a quadratic function of $\boldsymbol{u}_{0:N}$:

$$\sum_{i=1}^{p} \sum_{k=0}^{N} \boldsymbol{u}_k^T \boldsymbol{y}_k^i = \begin{bmatrix} \boldsymbol{u}_0 \\ \vdots \\ \boldsymbol{u}_N \end{bmatrix}^T \left(\sum_{i=1}^{p} \boldsymbol{V}^i \right) \begin{bmatrix} \boldsymbol{u}_0 \\ \vdots \\ \boldsymbol{u}_N \end{bmatrix} + \begin{bmatrix} \boldsymbol{u}_0 \\ \vdots \\ \boldsymbol{u}_N \end{bmatrix}^T \sum_{i=1}^{p} \boldsymbol{L}^i, \tag{4.20}$$

with:

$$\boldsymbol{V}^i = \frac{1}{2}\begin{bmatrix} (\boldsymbol{D}^i_{E,0})^T + \boldsymbol{D}^i_{E,0} & (\boldsymbol{C}^i_{E,1}\boldsymbol{\Psi}(1,0)\boldsymbol{B}_0)^T & \cdots & (\boldsymbol{C}^i_{E,N}\boldsymbol{\Psi}(N,0)\boldsymbol{B}_0)^T \\ \boldsymbol{C}^i_{E,1}\boldsymbol{\Psi}(1,0)\boldsymbol{B}_0 & (\boldsymbol{D}^i_{E,1})^T + \boldsymbol{D}^i_{E,1} & \cdots & (\boldsymbol{C}^i_{E,N}\boldsymbol{\Psi}(N,1)\boldsymbol{B}_1)^T \\ \vdots & \vdots & \ddots & \vdots \\ \boldsymbol{C}^i_{E,N}\boldsymbol{\Psi}(N,0)\boldsymbol{B}_0 & \boldsymbol{C}^i_{E,N}\boldsymbol{\Psi}(N,1)\boldsymbol{B}_1 & \cdots & (\boldsymbol{D}^i_{E,N})^T + \boldsymbol{D}^i_{E,N} \end{bmatrix}$$

$$\boldsymbol{L}^i = \begin{bmatrix} \boldsymbol{a}^i_{E,0} + \boldsymbol{C}^i_{E,0}\bar{\boldsymbol{x}}_0 \\ \boldsymbol{a}^i_{E,1} + \boldsymbol{C}^i_{E,1}\bar{\boldsymbol{x}}_1 \\ \vdots \\ \boldsymbol{a}^i_{E,N} + \boldsymbol{C}^i_{E,N}\bar{\boldsymbol{x}}_N \end{bmatrix},$$

and where $\bar{\boldsymbol{x}}_k$ is defined in (4.4). Because $\boldsymbol{V}^i$ is a matrix of Markov parameters (see Definition 2.6) and if $\boldsymbol{u} \mapsto \boldsymbol{y}^i$ is discrete-time passive, it follows that:

$$\sum_{k=0}^{N} \boldsymbol{u}_k^T \hat{\boldsymbol{y}}^i_k = \begin{bmatrix} \boldsymbol{u}_0 \\ \vdots \\ \boldsymbol{u}_N \end{bmatrix}^T \begin{bmatrix} \hat{\boldsymbol{y}}^i_0 \\ \vdots \\ \hat{\boldsymbol{y}}^i_N \end{bmatrix} = \begin{bmatrix} \boldsymbol{u}_0 \\ \vdots \\ \boldsymbol{u}_N \end{bmatrix}^T \boldsymbol{V}^i \begin{bmatrix} \boldsymbol{u}_0 \\ \vdots \\ \boldsymbol{u}_N \end{bmatrix} \geqslant 0.$$

Then, $\boldsymbol{V}^i \succeq 0$. The sum of positive semi-definite matrices is a positive semi-definite matrix, so it follows that $\sum_{i=1}^{p} \boldsymbol{V}^i \succeq 0$. We conclude that (4.20) is a convex function of $\boldsymbol{u}_{0:N}$

Now, we show that the second term of performance measure $J(\cdot,\cdot)$:

$$\sum_{i=1}^{p}\sum_{k=0}^{N} \mu^i_k\left(\boldsymbol{u}_k, \boldsymbol{y}^i_k\right) = \sum_{i=1}^{p}\sum_{k=0}^{N} \begin{bmatrix} \boldsymbol{u}_k \\ \boldsymbol{y}^i_k \end{bmatrix}^T \begin{bmatrix} \boldsymbol{M}^i_{uu,k} & \boldsymbol{M}^i_{uy,k} \\ (\boldsymbol{M}^i_{uy,k})^T & \boldsymbol{M}^i_{yy,k} \end{bmatrix} \begin{bmatrix} \boldsymbol{u}_k \\ \boldsymbol{y}^i_k \end{bmatrix}$$

is a convex function of $\boldsymbol{u}_{0:N}$. Let $\hat{\boldsymbol{y}}^i_k$ be the portion of $\boldsymbol{y}^i_k$ forced by the control input, and not by the initial condition or exogenous disturbance, i.e., $\hat{\boldsymbol{y}}^i_k = \boldsymbol{C}^i_{E,k}(\boldsymbol{x}_k - \bar{\boldsymbol{x}}_k) + \boldsymbol{D}^i_{E,k}\boldsymbol{u}_k$. Then:

$$\begin{aligned} \sum_{i=1}^{p}\sum_{k=0}^{N} \begin{bmatrix} \boldsymbol{u}_k \\ \boldsymbol{y}^i_k \end{bmatrix}^T \begin{bmatrix} \boldsymbol{M}^i_{uu,k} & \boldsymbol{M}^i_{uy,k} \\ (\boldsymbol{M}^i_{uy,k})^T & \boldsymbol{M}^i_{yy,k} \end{bmatrix} \begin{bmatrix} \boldsymbol{u}_k \\ \boldsymbol{y}^i_k \end{bmatrix} &= \sum_{i=1}^{p}\sum_{k=0}^{N} \begin{bmatrix} \boldsymbol{u}_k \\ \hat{\boldsymbol{y}}^i_k \end{bmatrix}^T \begin{bmatrix} \boldsymbol{M}^i_{uu,k} & \boldsymbol{M}^i_{uy,k} \\ (\boldsymbol{M}^i_{uy,k})^T & \boldsymbol{M}^i_{yy,k} \end{bmatrix} \begin{bmatrix} \boldsymbol{u}_k \\ \hat{\boldsymbol{y}}^i_k \end{bmatrix} \\ + 2\begin{bmatrix} \boldsymbol{u}_k \\ \hat{\boldsymbol{y}}^i_k \end{bmatrix}^T \begin{bmatrix} \boldsymbol{M}^i_{uy,k}\left(\boldsymbol{C}^i_{E,k}\bar{\boldsymbol{x}}_k + \boldsymbol{a}^i_{E,k}\right) \\ \boldsymbol{M}^i_{yy,k}\left(\boldsymbol{C}^i_{E,k}\bar{\boldsymbol{x}}_k + \boldsymbol{a}^i_{E,k}\right) \end{bmatrix} &+ \left(\boldsymbol{C}^i_{E,k}\bar{\boldsymbol{x}}_k + \boldsymbol{a}^i_{E,k}\right)^T \boldsymbol{M}^i_{yy,k}\left(\boldsymbol{C}^i_{E,k}\bar{\boldsymbol{x}}_k + \boldsymbol{a}^i_{E,k}\right) \end{aligned} \quad (4.21)$$

Because $\boldsymbol{M}^i \succeq 0$ and $\hat{\boldsymbol{y}}_k^i$ is a linear function of the control inputs, (4.21) is a convex function of $\boldsymbol{u}_{0:N}$. The sum of convex functions is a convex function, so we conclude that performance measure (4.19) is a convex function of $\boldsymbol{u}_{0:N}$. □

4.2.3 Passivity-Constrained Problem

In the *passivity-constrained problem*, we enforce the constraint:

$$\sum_{j=0}^{k} \boldsymbol{u}_j^T \boldsymbol{y}_j^i \geqslant 0, \quad \forall i \in \{1...p\}, \text{ and } \forall k \in \{0...N\},$$

which is equivalent to the lower energy constraint $\boldsymbol{c}_k^L(\cdot,\cdot,\cdot)$ with $\gamma^i = 0$ and $\mu^i(\cdot,\cdot) = 0$ for all $i \in \{1...p\}$. This type of constraint is useful for robust control, where the Passivity Theorem guarantees the feedback connection of two passive systems is stable. The passivity-constrained problem has the form:

$$\text{Passivity-Constrained} = \begin{cases} \textbf{Given:} & \boldsymbol{x}_0,\ \boldsymbol{E}_0 = 0, \boldsymbol{a}_k, \boldsymbol{A}_k, \boldsymbol{B}_k, \\ & \boldsymbol{C}_{E,k}^i, \boldsymbol{D}_{E,k}^i, \boldsymbol{a}_{E,k}^i\ \forall k \in \{0...N\} \\ \textbf{Minimize:} & J(\boldsymbol{u}_{0:N}, \boldsymbol{x}_{0:N+1}^{\circ}(\boldsymbol{u}_{0:N}, \boldsymbol{x}_0)) \\ \textbf{Domain:} & \boldsymbol{u}_{0:N} \\ \textbf{Constraints:} & \sum_{j=0}^{k} \boldsymbol{u}_j^T \boldsymbol{y}_j^i \geqslant 0, \\ & \forall i \in \{1...p\},\ \forall k \in \{0...N\}, \end{cases}$$

Previous research exploits passivity (or (Q,S,R)-dissipativity, which can be thought of as a more general version of passivity [38]) in MPC optimization problems. References [57, 77, 80] impose passivity-based state constraints to enforce closed loop stability, and [69] uses dissipativity conditions to implement distributed MPC. References [6, 48] exploit dissipativity to find the optimal steady-state operation in the context of economic MPC. Falugi in [22] implements passivity-constrained MPC for passive plants and focuses on ensuring feasibility of constrained trajectories for nonlinear plants, which ensures robustness in a continuous-time setting.

4.2.4 Zero Energy Storage Problem

Consider the case where all transducer ports are connected to a single energy storage system. In the *zero energy storage problem*, $E_L^1 = E_U^1 = 0$, meaning that energy cannot be stored from time-step to time-step. In this case, feasible trajectories require $E_k^1 = 0$, $\forall k \in \{0...N\}$. This is equivalent to enforcing a power directionality constraint, meaning that the aggregate power from all transducers must flow out of the ports, i.e., $\boldsymbol{u}_k^T \boldsymbol{y}_k^1 \leqslant 0$, $\forall k \in \{0...N\}$. This is also equivalent to the case with $\gamma = 0$, i.e., all energy in the energy storage system is dissipated during a single time step. In the zero energy storage problem the two inequality constraints $c_k^L(\cdot,\cdot,\cdot) \leqslant 0$ and $c_k^U(\cdot,\cdot,\cdot) \leqslant 0$ can be simplified to a single equality constraint: $c_k^L(\cdot,\cdot,\cdot) = c_k^U(\cdot,\cdot,\cdot) = 0$, and therefore it is always a nonconvex problem.

4.3 Barrier Method Approach

In this section, we present an overview of the barrier method approach to solve the nonconvex ECOCP and then demonstrate this algorithm on a piezoelectric wireless sensor node with the goal of maximizing transmitted data.

As previously mentioned in Section 1.3.1, barrier methods are used to solve a sequence of equality-constrained minimizations to which Newton's method can be applied to ultimately find a solution of the desired constrained problem [10]. Consider the general COCP in (2.16) with inequality constraint vector $\boldsymbol{c}_k(\boldsymbol{u}_{0:N}, \boldsymbol{x}_{0:N+1}) \leqslant 0$ of length i. Let $c_{k,j}(\cdot,\cdot)$ be the j^{th} constraint in this vector. Then, the indicator function of $c_{k,j}(\cdot,\cdot)$ is:

$$\mathbf{1}(c_{k,j}(\boldsymbol{u}_{0:N}, \boldsymbol{x}_{0:N+1})) = \begin{cases} 0, & c_{k,j}(\boldsymbol{u}_{0:N}, \boldsymbol{x}_{0:N+1}) \leqslant 0 \\ \infty, & c_{k,j}(\boldsymbol{u}_{0:N}, \boldsymbol{x}_{0:N+1}) > 0. \end{cases}$$

We can enforce compliance of the inequality constraints by adding the indicator function to the performance measure and instead minimizing this altered performance measure. The altered performance measure is:

$$\tilde{J}(\boldsymbol{u}_{0:N}, \boldsymbol{x}_{0:N+1}) = J(\boldsymbol{u}_{0:N}, \boldsymbol{x}_{0:N+1}) + \sum_{k=0}^{N} \sum_{j=1}^{i} \mathbf{1}(c_{k,j}(\boldsymbol{u}_{0:N}, \boldsymbol{x}_{0:N+1}))$$

However, the indicator function is not differentiable. Therefore, solution methods that make use of derivatives of the performance measure, like Newton's method, cannot be used

in conjunction with $\tilde{J}(\cdot,\cdot)$. We can approximate the indicator function with the following differentiable logarithmic function, which we refer to as a *log barrier*. Let the log barrier of $c_{k,j}(\cdot,\cdot)$ with constant $\beta > 0$ be:

$$\hat{\mathbf{1}}(\beta, c_{k,j}(\boldsymbol{u}_{0:N}, \boldsymbol{x}_{0:N+1})) = \begin{cases} -\frac{1}{\beta}\ln\left(c_{j,k}(\boldsymbol{u}_{0:N}, \boldsymbol{x}_{0:N+1})\right), & c_{k,j}(\boldsymbol{u}_{0:N}, \boldsymbol{x}_{0:N+1}) \leqslant 0 \\ \infty, & c_{k,j}(\boldsymbol{u}_{0:N}, \boldsymbol{x}_{0:N+1}) > 0. \end{cases} \tag{4.22}$$

Note that the approximation of the indicator function improves as β increases. Then, we can minimize the performance measure plus the log barriers of each constraint as:

$$\hat{J}(\beta, \boldsymbol{u}_{0:N}, \boldsymbol{x}_{0:N+1}) = J(\boldsymbol{u}_{0:N}, \boldsymbol{x}_{0:N+1}) + \sum_{k=0}^{N}\sum_{j=1}^{i} \hat{\mathbf{1}}(\beta, c_{k,j}(\boldsymbol{u}_{0:N}, \boldsymbol{x}_{0:N+1})).$$

When using barrier methods to solve an optimization problem, we do not need to enforce the inequality constraints explicitly, and instead we solve a sequence of equality-constrained minimizations, increasing the value of β in each successive minimization. With each successive minimization, the approximation of the indicator function improves with increasing β. We iterate on the inputs until desired convergence is achieved for a sufficiently large β. An advantage of the barrier method is that the optimization is performed completely within the primal, feasible domain so there is no activation and de-activation of the multipliers. Here we have described the basic methodology of barrier methods; however, [8, 10] can be used as references to provide extended commentary about this class of algorithm. Next we look at using barrier methods to solve trajectory optimizations for a self-powered system.

4.3.1 Example: Piezoelectric Wireless Sensor Node

This example is based off of work in [37]. We use the barrier method approach to find the optimal control solution which maximizes data transmitted by a piezoelectric wireless sensor node subject to base acceleration impulses. Consider the model of a piezoelectric energy harvesting single-user wireless communication system depicted in Figure 4.1. This system has five components: (1) a piezoelectric bimorph cantilever beam, (2) a power electronic energy conversion circuit, (3) an energy storage system (e.g., a rechargeable battery), (4) a data queue, and (5) a data transmitter.

Base acceleration $a(t)$ excites the piezoelectric beam, resulting in mechanical vibrations, and in turn, a voltage $v(t)$ at the transducer. The power-electronic circuit controls the en-

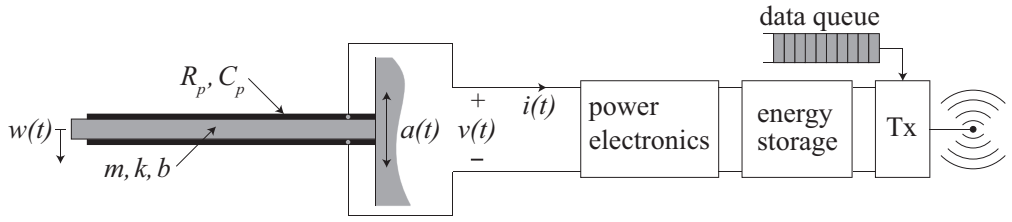

Figure 4.1: Wireless sensor node equipped with a piezoelectric bimorph cantilever beam, a power electronic circuit, an energy storage system, a data queue, and a transmitter.

ergy extracted from the transducer, and then delivers this harvested energy to the storage subsystem. By reciprocity, harvesting energy also removes mechanical energy, which imposes supplemental damping on the beam [40, 60]. If energy is harvested too aggressively, then the resulting high damping will suppress beam resonance, which may reduce the magnitude of future power injection to the beam from the disturbance. Oppositely, if energy is harvested too slowly, the injected disturbance energy will be lost due to mechanical damping. Consequently, the effectiveness of an energy harvesting system is strongly related to the dynamics of the control system used to extract power.

A commonly-used power-electronic circuit at the interface of the transducer is a diode bridge rectifier, which trickle-charges the energy storage system. This circuit cannot be controlled to maximize harvested energy, and hence it cannot adapt to optimize the damping imposed on the beam. Liu et al. in [43] use a PWM-controlled H-bridge circuit for piezoelectric energy harvesting, which is shown in Figure 4.2. Through high-frequency PWM switching of the circuit's four MOSFETs $\{S_1, S_2, S_3, S_4\}$, the H-bridge circuit can realize any desired transducer current, including trajectories that result in two-way power flow (i.e., absorbing energy from and injecting energy into the transducer). In this work, we assume the use of an H-bridge circuit at the interface between the transducer and storage system.

We consider the case where the wireless node is exclusively powered by energy harvested from a periodic chain of base acceleration impulses. We assume that the arrival times and magnitudes of these impulses are known *a priori*. Our goal is to determine the optimal off-line control of the transmission power and the transducer current that maximizes the number of bits transmitted over the wireless network in a fixed time period. Although we focus on piezoelectric transduction and impulsive disturbances, the techniques described in this paper may be applied to other energy harvesting technologies and/or disturbance regimes in an analogous manner.

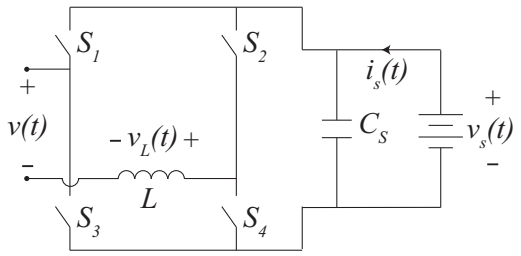

Figure 4.2: Circuit drawing of power electronics interfacing the piezoelectric transducer with the energy storage system, an H-bridge circuit

Recent work that identifies an optimal scheduling policy to maximize data transmission of an energy harvesting node abstracts the source and transduction method. Energy arrival is often treated as a discrete event, and energy is delivered to the harvester instantaneously in "energy packets" or "energy bursts" [50, 52, 54, 72, 78]. As described earlier, the dynamics of a piezoelectric transducer are affected by harvesting energy, and hence modeling a node without transducer dynamics may significantly vary the optimal solution. In addition, modeling energy arrival as a discrete event does not account for the time period over which that energy is harvested. For example, it may take x time units to harvest y energy units, but if we model all y units arriving instantaneously, we may schedule the use of those y energy units before they have actually been harvested.

Many studies also do not account for the energy consumed by the harvesting process, i.e., the parasitic losses of the power electronics [50, 52, 54, 72, 78]. Although transmitting data over a wireless network is a particularly energy-intensive task, operating power electronics does not come without an energy cost as well. [79] and [18] account for the energy consumption of the circuitry by including a constant penalty term for each unit time when the system is ON, however, this consumption model may not be conservative. For a general vibration energy harvesting system, [63] studies the parasitic losses of the power electronics. They show that loss models that are quadratic in the transducer current overbound the parasitic dissipation. In this study, we assume non-negligible parasitic losses and model these losses conservatively as shown in [63]. Our optimal scheduling policy must allocate energy resources between two energy-consuming tasks: harvesting energy and transmitting data.

We examine this problem in the context of full-information optimal control, in a manner that accounts for the transducer dynamics and parasitic losses associated with the recharge circuit. Although outside the scope, this technique can be compared to the more abstracted

solutions that currently exist in the literature. In addition, the optimal off-line control solution considered here provides intuition about the optimal real-time controller. Finally, the analysis presented here establishes an upper bound on the performance of any real-time controller, for which *a priori* disturbance information would likely be unavailable, and which would also have to contend with uncertainty in the model and feedback measurements.

Modeling

Reference the general model of a self-powered system in Figure 1.4, and the definition of model $\mathcal{M}$ in Definition 3.2. Here we consider the case with a single piezoelectric beam ($m = 1$) connected to one energy storage system ($p = 1$). As shown in Figure 4.1, our control input is the current $i(t)$ into the transducer, the potential variable is the transducer voltage $v(t)$, and the exogenous disturbance is a periodic chain of base acceleration impulses to the piezoelectric beam each with a magnitude a_0. Then, the rest of the components of the model are as follows:

1. **Plant:** Here we model $\mathcal{P} \in \mathbb{P}$, the dynamic response of the piezoelectric cantilever beam in Figure 4.1, by the following set of dynamic equations:

$$\mathcal{P} : \begin{cases} m_w \ddot{w}(t) + d_w \dot{w}(t) + k_w w(t) = \zeta_w a(t) - \theta_w v(t) \\ C_w \dot{v}(t) + \frac{1}{R_w} v(t) = \theta_w \dot{w}(t) + i(t), \end{cases} \tag{4.23}$$

   where $w(t)$ is the displacement of the piezoelectric beam, $v(t)$ is the transducer voltage, $i(t)$ is the transducer current, $a(t)$ is the base acceleration, m_w is the mass of the beam, d_w is the beam damping, k_w is the beam stiffness, ζ_w is the disturbance input coefficient, θ_w is the electro-mechanical coupling factor, C_w is the equivalent capacitance, and R_w is the dielectric leakage resistance. Note that the subscript w is meant to distinguish the model parameters from the other parameters used in this thesis. The electro-mechanical dynamics of a piezoelectric beam are constructed in [29], and the set of equations in (4.23) are based on simplifications of this model described in [66] and [64].

   Next, we nondimensionalize plant $\mathcal{P}$ by making the following variable substitutions

$$\begin{aligned} t &= \sqrt{\tfrac{m_w}{k_w}}\hat{t} & w(t) &= \tfrac{\zeta_w a_0}{k_w}\hat{w}(\hat{t}) & v(t) &= \tfrac{\zeta a_0}{\sqrt{C_w k_w}}\hat{v}(\hat{t}) \\ a(t) &= a_0\sqrt{\tfrac{k_w}{m_w}}\hat{a}(\hat{t}) & R_w &= \tfrac{1}{C_w}\sqrt{\tfrac{m_w}{k_w}}\hat{R}_w & i(t) &= \zeta_w a_0\sqrt{\tfrac{C_w}{m_w}}\hat{i}(\hat{t}), \end{aligned} \tag{4.24}$$

   where the hat indicates the nondimensional version of that variable. The nondimen-

sional mechanical damping $\hat{d}_w$, electromechanical coupling factor $\hat{\theta}_w$, and dielectric leakage coefficient $\hat{\kappa}_w$ are equal to:

$$\hat{d}_w = \frac{d_w}{\sqrt{k_w m_w}} \qquad \hat{\theta}_w = \frac{\theta_w}{\sqrt{C_w k_w}} \qquad \hat{\kappa}_w = \frac{C_w}{R_w}\sqrt{\frac{k_w}{m_w}}$$

We represent the plant in continuous-time with states $\boldsymbol{x}(t) = \begin{bmatrix}\hat{w}(t) & \dot{\hat{w}}(t) & v(t)\end{bmatrix}^T$, where $\hat{w}(t)$ and $\dot{\hat{w}}(t)$ are the nondimensionalized displacement and velocity of beam tip, respectively. The states evolve according to (3.1) with LTI matrices:

$$\bar{\boldsymbol{A}} = \begin{bmatrix} 0 & 1 & 0 \\ -1 & -\hat{d}_w & -\hat{\theta}_w \\ 0 & \hat{\theta}_w & -\hat{\kappa}_w \end{bmatrix}, \quad \bar{\boldsymbol{B}} = \begin{bmatrix} 0 \\ 0 \\ -1 \end{bmatrix}, \quad \bar{\boldsymbol{G}} = \begin{bmatrix} 0 \\ 1 \\ 0 \end{bmatrix}, \quad \bar{\boldsymbol{C}} = -\bar{\boldsymbol{B}}^T, \quad \bar{D} = 0,$$

where control input is the transducer current, $u(t) = i(t)$.

2. **Transmission Losses:** For the PWM-controlled H-bridge circuit, we assume it is equipped with a high-bandwidth current-tracking loop. This enables us to assume that at the time scale of the electromechanical beam dynamics, transducer current $i(t)$ can be made to track any desired signal with negligible error, allowing us to treat it as a control input. This versatility of the H-bridge circuit does not come without a price, as it exhibits higher parasitic losses than other popular power electronic circuits used for this interface (e.g., a diode bridge rectifier, or a buck-boost DC/DC converter). The higher parasitic losses are due to presence of four MOSFETs, which must be gated in PWM, and use of feedback control. We model the power electronics' parasitic dissipation quadratically as:

$$\mu^1(t) = R_c i(t)^2, \tag{4.25}$$

where R_c is the circuit resistance. To nondimensionalize $\mu^1(t)$, we use the relations in (4.24), and $R_c = \frac{1}{C_w}\sqrt{\frac{m_w}{k_w}}\hat{R}_c$.

3. **Dissipated Power From Energy Storage:** In this example, let $q^1(t)$ be the transmission power of the communication system. Define $r(t)$ as the transmission rate in bits per second. Assuming an additive white Gaussian noise data channel with zero-mean and unit variance, the transmission rate and transmission power are related through the following function:

$$q^1(t) = \tau(e^{\alpha r(t)} - 1),$$

where $\tau > 0$ and $\alpha > 0$ are physical constants (with units of power and time, respectively) that are dependent on the proprieties of the transmitter hardware. The transmission rate is a non-negative value, i.e., $r(t) \geqslant 0$. The power terms $q^1(t)$ and τ is nondimensionalized via the relation $q^1(t) = \frac{(\zeta a_0)^2}{\sqrt{m_w k_w}} \hat{q}^1(\hat{t})$, and α is nondimensionalized via the relations in (4.24).

4. **Energy Storage System:** We assume the evolution of the energy in the storage system $E^1(t)$ is governed by Equation (3.2), where the lower energy constraint is $E_L^1 = 0$. We vary the upper energy constraint E_U^1 in the following analysis. Note that the energy in the storage system is nondimensionalized via the relation $E^1(t) = \frac{(\zeta_w a_0)^2}{k_w} \hat{E}^1(\hat{t})$.

We suppress the hat notation for the remainder of the example, and exclusively use the nondimensional parameters and variables from here on. The discretized state space is of the form (4.14) with matrices (4.15) and (4.16), and the discrete-time dynamics of the energy in the storage system are of the form (3.19).

ECOCP Formulation

Our goal is to maximize the number of bits transmitted to the receiver over a finite time period without violating the input and energy constraints. Framed as a minimization objective, the resultant optimal control problem is then:

$$
\begin{cases}
\textbf{Given:} & \boldsymbol{x}_0, E_0^1, \boldsymbol{A}, \boldsymbol{B}, \boldsymbol{C}_E^1, \boldsymbol{D}_E^1, \gamma^1, \\
& a_k, a_{E,k}^1, \mu_k^1, \forall k \in \{0...N\}, \\
\textbf{Minimize:} & J(q_{0:N}^1) = -\sum_{k=0}^{N} \ln\left(\frac{1}{\tau} q_k^1 + 1\right) \\
\textbf{Domain:} & u_{0:N},\ q_{0:N}^1 \\
\textbf{Constraints:} & c_k^L(u_{0:N}, q_{0:N}^1, \boldsymbol{x}_{0:N}^\circ(u_{0:N}, \boldsymbol{x}_0)) \leqslant 0, \\
& c_k^U(u_{0:N}, q_{0:N}^1, \boldsymbol{x}_{0:N}^\circ(u_{0:N}, \boldsymbol{x}_0)) \leqslant 0, \\
& q_k^1 \geqslant 0, \\
& \forall k \in \{0...N\},
\end{cases}
$$

Note that to simplify the analysis, we assume zero initial conditions, i.e., $E_0^1 = 0$, and $\boldsymbol{x}_0 = 0$. However, the development is not fundamentally different when other (known) initial conditions are assumed. Now, we eliminate the explicitly enforced inequality constraints by

implementing log barriers as:

$$\begin{cases} \textbf{Given:} & \boldsymbol{x}_0, E_0^1, \boldsymbol{A}, \boldsymbol{B}, \boldsymbol{C}_E^1, \boldsymbol{D}_E^1, \gamma^1, \beta, a_k, a_{E,k}^1, \mu_k^1, \forall k \in \{0...N\}, \\ \textbf{Minimize:} & J(q_{0:N}^1) = -\sum_{k=0}^{N} \ln\left(\frac{1}{\tau} q_k^1 + 1\right) + \hat{\mathbf{1}}(\beta, c_k^L(u_{0:N}, q_{0:N}^1, \boldsymbol{x}_{0:N}^\circ(u_{0:N}, \boldsymbol{x}_0)) \\ & \qquad + \hat{\mathbf{1}}(\beta, c_k^U(u_{0:N}, q_{0:N}^1, \boldsymbol{x}_{0:N}^\circ(u_{0:N}, \boldsymbol{x}_0)) + \hat{\mathbf{1}}(\beta, -q_k^1) \\ \textbf{Domain:} & u_{0:N},\ q_{0:N}^1 \end{cases}$$

where $\hat{\mathbf{1}}(\cdot,\cdot)$ is the log barrier and β is the log barrier constraint defined in Definition 4.22. However, due to the computational complexity of the energy constraints, we introduce two slack variables, $\underline{\sigma}_k$ and $\bar{\sigma}_k$, to enforce them. We require that for all $k \in \mathbb{Z}_{0:N}$:

$$\underline{\sigma}_k \leqslant -\left(u_k^T y_k^1 + \mu_k^1\right) \leqslant \bar{\sigma}_k.$$

Then, let $\underline{E}_{k+1}^1$ be a lower approximation of the stored energy and $\bar{E}_{k+1}^1$ be an upper approximation of the stored energy using these slack variables, i.e.,

$$\underline{E}_{k+1}^1 = \gamma^1 \underline{E}_k^1 + \underline{\sigma}_k - q_k^1, \qquad \bar{E}_{k+1}^1 = \gamma^1 \bar{E}_k^1 + \bar{\sigma}_k - q_k^1,$$

which implies that $\underline{E}_k^1 \leqslant E_k^1 \leqslant \bar{E}_k^1$. We enforce new constraints containing these slack variables instead of the original constraints $c_k^L(\cdot,\cdot,\cdot)$ and $c_k^U(\cdot,\cdot,\cdot)$. Let $\tilde{\boldsymbol{c}}_k^L(\cdot,\cdot,\cdot,\cdot)$ and $\tilde{\boldsymbol{c}}_k^U(\cdot,\cdot,\cdot,\cdot)$ be:

$$\tilde{\boldsymbol{c}}_k^L(u_{0:N}, q_{0:N}^1, \boldsymbol{x}_{0:N}^\circ(u_{0:N}, \boldsymbol{x}_0), \underline{\sigma}_k) = \begin{bmatrix} \underline{\sigma}_k + \left(u_k^T y_k^1 + \mu_k^1\right) \\ -\underline{E}_{k+1}^1 \end{bmatrix}$$

$$\tilde{\boldsymbol{c}}_k^U(u_{0:N}, q_{0:N}^1, \boldsymbol{x}_{0:N}^\circ(u_{0:N}, \boldsymbol{x}_0), \bar{\sigma}_k) = \begin{bmatrix} -\bar{\sigma}_k - \left(u_k^T y_k^1 + \mu_k^1\right) \\ \bar{E}_{k+1}^1 - E_U^1 \end{bmatrix}.$$

We modify the optimal control problem to reflect the addition of these new slack variables and constraints:

$$\begin{cases} \textbf{Given:} & \boldsymbol{x}_0, E_0^1, \boldsymbol{A}, \boldsymbol{B}, \boldsymbol{C}_E^1, \boldsymbol{D}_E^1, \gamma^1, \beta, a_k, a_{E,k}^1, \mu_k^1, \forall k \in \{0...N\}, \\ \textbf{Minimize:} & J(q_{0:N}^1) = -\sum_{k=0}^{N} \ln\left(\frac{1}{\tau} q_k^1 + 1\right) + \hat{\mathbf{1}}(\beta, -q_k^1) \\ & \qquad + \sum_{j=1}^{2} \hat{\mathbf{1}}(\beta, \tilde{c}_{k,j}^L(u_{0:N}, q_{0:N}^1, \boldsymbol{x}_{0:N}^\circ(u_{0:N}, \boldsymbol{x}_0), \underline{\sigma}_k) \\ & \qquad\qquad + \hat{\mathbf{1}}(\beta, \tilde{c}_{k,j}^U(u_{0:N}, q_{0:N}^1, \boldsymbol{x}_{0:N}^\circ(u_{0:N}, \boldsymbol{x}_0), \bar{\sigma}_k) \\ \textbf{Domain:} & u_{0:N}, q_{0:N}^1, \underline{\sigma}_{0:N}, \bar{\sigma}_{0:N} \end{cases}$$

Now, we can solve the above optimization by iterating on the inputs $\{u_{0:N}, q_{0:N}^1, \underline{\sigma}_{0:N}, \bar{\sigma}_{0:N}\}$ by using a conjugate gradient algorithm paired with a line search. Once desired convergence is achieved, β is increased and another optimization is performed. [10] gives stopping criteria as a function of β.

Results

We emphasize that this example is primarily demonstrative, and is not meant to be an accurate depiction of any realistic hardware. All parameters are treated in their nondimensional units. Let time step $\Delta t = 1$, number of time steps $N = 299$, mechanical damping $d_w = 0.05$, electromechanical coupling factor $\theta_w = 0.2$, dielectric leakage coefficient $\kappa_w = 0.001$, circuit resistance $R_c = 0.001$, and $\gamma^1 = 0.99$. The system is excited every $T = \lfloor j\frac{2\pi}{\Delta t} \rfloor$ for $j \in \mathbb{Z}$ by acceleration impulses with magnitude $a_0 = 1$.

We compare the cases where storage capacity is $E_U^1 \to \infty$, $E_U^1 = 1$, $E_U^1 = 0.5$, and $E_U^1 = 0.1$. These four considered cases are marked in black, blue, green and red, respectively, in the following figures. Figure 4.3 shows the energy in the storage system, transmission energy, and transducer current for the considered cases over the entire time period. Figure 4.4 shows these same variables in addition to the transducer power, i.e., $p_{T,k} = i_k v_k$ for times 150 to 180.

For cases $E_U^1 = 0.5$ and $E_U^1 = 0.1$, the transducer power is negative for all time, meaning that power is only flowing into the energy storage system. For cases $E_U^1 \to \infty$ and $E_U^1 = 1$, the transducer current cycles energy into and out of the transducer (i.e., this current could not be realized by a circuit that trickle-charges the storage system). From a design standpoint,

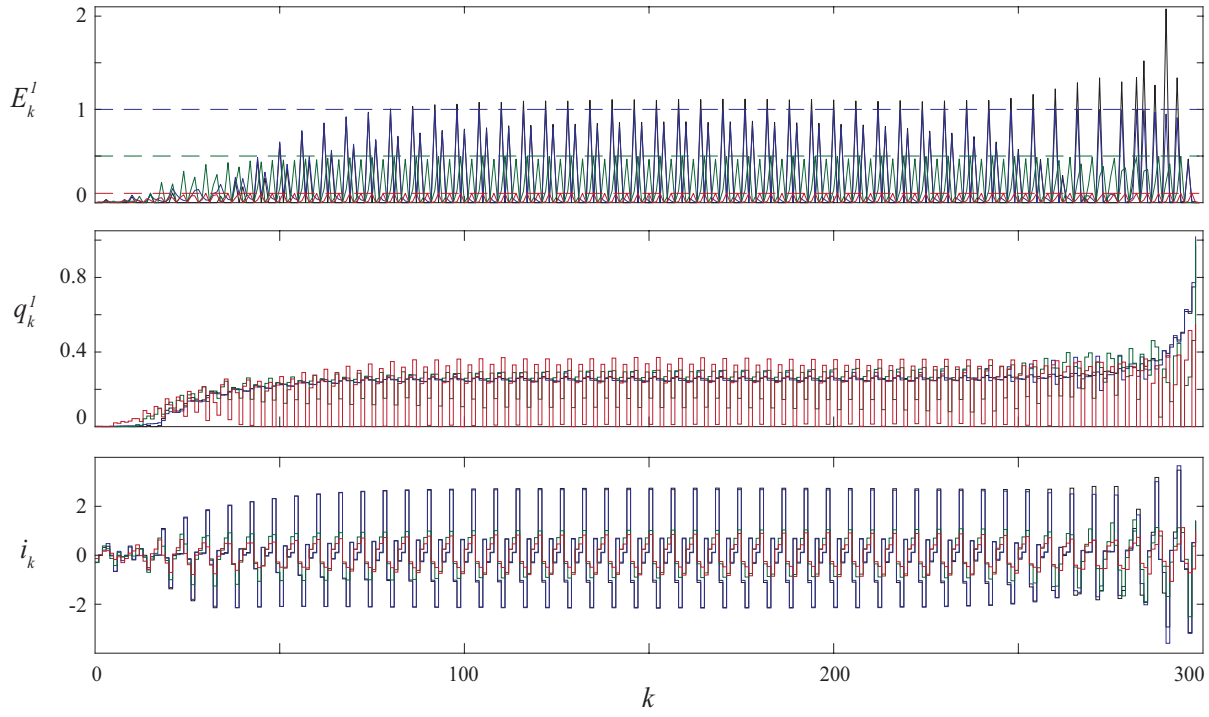

Figure 4.3: The energy in storage system E^1, transmission energy q^1, and transducer current i over the entire time series. The capacity of the energy storage system is marked as a dashed line in the color corresponding to each case in the energy plot.

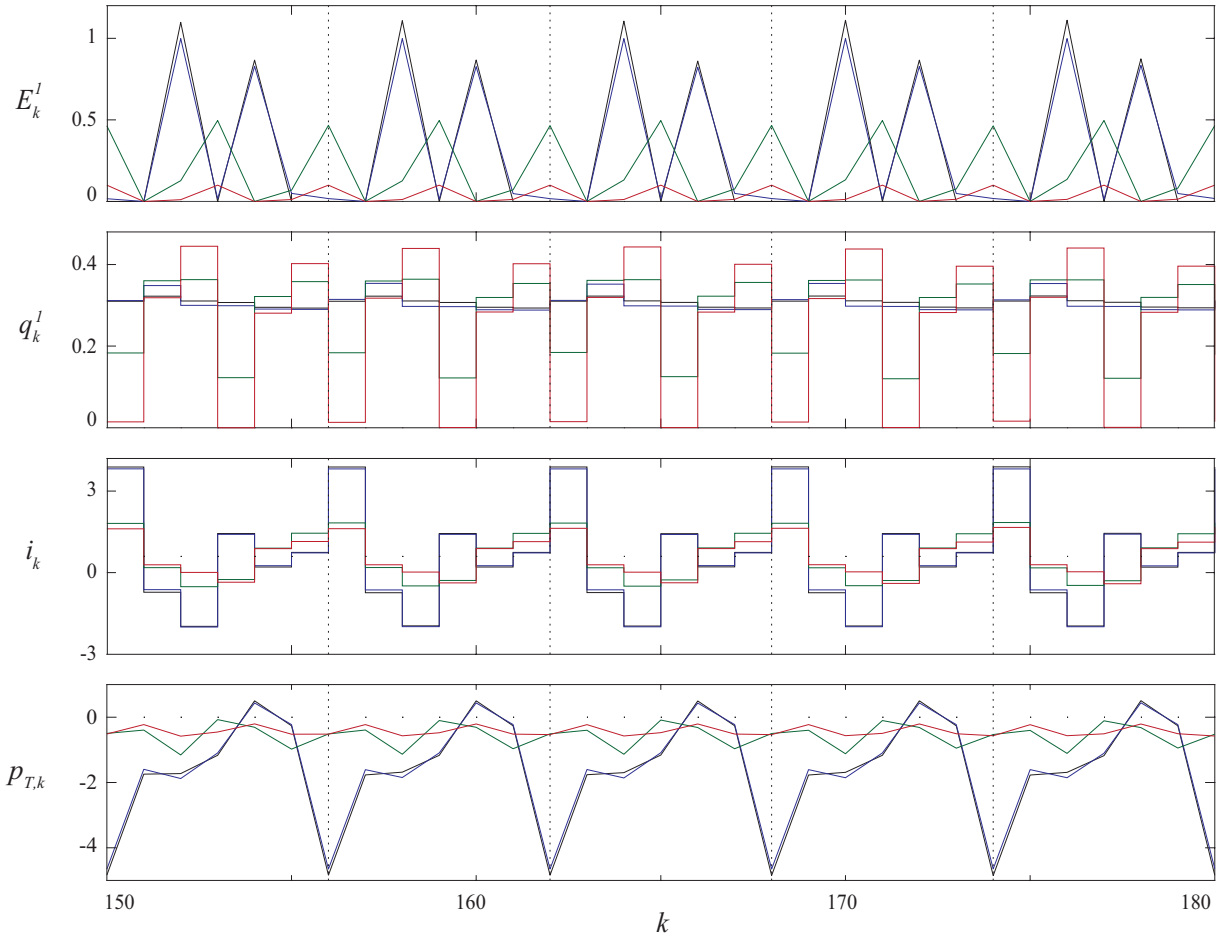

Figure 4.4: The energy in storage system E^1, transmission energy q^1, transducer current i, and transducer power $p_{T,k}$ from times 150 to 180. The dashed vertical lines indicates the arrival of a base acceleration impulse.

it is necessary to implement a recharge circuit with two-way power flow for these larger E_U^1 cases to achieve optimally, however, for the smaller E_U^1 cases, a trickle-charge circuit is sufficient. In Figure 4.4, note that energy is produced and then completely consumed in all cases. Although the magnitude of the transmission power and transducer current differs for each case, the shape of the trajectories are similar.

Chapter 5

The Dual Problem

As shown in Chapter 3, ECOCPs are nonconvex in general. Nonconvex optimal control problems can be challenging to solve as they may be computationally expensive, and only local optima can be assured. However, constrained optimal control problems can be viewed from two perspectives: the primal problem (in which we minimize over the control variables, as demonstrated in Section 4.3.1), and the dual problem (in which we maximize over the Lagrange multipliers). As discussed in Chapter 2, dual problems are always convex, regardless of the convexity of the primal problem, and hence, global solutions to the dual problem can often be found in polynomial time. Furthermore, the dual problem provides a lower bound on the optimal solution of the primal problem [10].

The *duality gap* is the difference between the optimal primal and dual solutions (see Definition 2.26). In the case where the optimal primal and dual solutions are coincident, the duality gap is zero. Therefore, we investigate the use of duality techniques to aid in finding the primal optimal solution (when the duality gap is zero) or a lower bound on the primal optimal performance measure (when the duality gap is nonzero). In this chapter, we develop the dual problem (which we also refer to as the dual relaxation) for a ECOCP with quadratic performance measures (see Section 4.1.1), and present easy-to-check sufficient conditions for zero duality gap. The work in this chapter expands on ideas originally presented in [36].

5.1 Formulating the Dual Problem for the Energy-Constrained Optimal Control Problem with Quadratic Performance Measures

Let $G(\cdot)$ be the *dual function* of the ECOCP, which is:

$$G(\boldsymbol{\lambda}_{0:N}) = \inf_{\boldsymbol{u}_{0:N},\, \boldsymbol{q}_{0:N} \geqslant 0} \bar{J}(\boldsymbol{u}_{0:N}, \boldsymbol{q}_{0:N}, \boldsymbol{x}^{\circ}_{0:N}(\boldsymbol{u}_{0:N}, \boldsymbol{x}_0), \boldsymbol{\lambda}_{0:N}), \tag{5.1}$$

where $\bar{J}(\cdot,\cdot,\cdot,\cdot)$ is the augmented performance measure defined in (4.8). Then, as discussed in Section 2.5, the *dual problem* of the ECOCP constitutes a reversal of the infimum and supremum in primal minimax problem (4.9) as:

$$G^* = \sup_{\boldsymbol{\lambda}_{0:N} \geqslant 0} G(\boldsymbol{\lambda}_{0:N}). \tag{5.2}$$

In this section, we solve the dual problem in lieu of the primal problem, as a means of determining a trajectory $\{\boldsymbol{u}_{0:N}, \boldsymbol{q}_{0:N}\}$. It is a classical result that dual problems are always convex [10], and consequently this approach eliminates the nonconvexity of the primal problem, leading to efficient determination of a global optimum for $G(\boldsymbol{\lambda}_{0:N})$. However, (5.2) may exhibit a *duality gap* in which case $J^* > G^*$. In this circumstance, the optimum $\boldsymbol{\lambda}_{0:N}$ does not correspond to a feasible trajectory for $\{\boldsymbol{u}_{0:N}, \boldsymbol{q}_{0:N}\}$.

5.1.1 Feasibility of the Dual Solution

We begin by showing that for the assumptions made in this paper, $G^* > -\infty$.

Lemma 5.1. *Let $\mathcal{M}_d = \mathcal{D}(\mathcal{M}, \Delta t, \boldsymbol{a})$ be the discrete-time model under consideration. Let $J(\cdot,\cdot)$ be defined as in* (4.2)*. Given that Assumption 4 holds, then $G^* > -\infty$.*

Proof. Evaluating $G(\boldsymbol{\lambda}_{0:N})$ at $\boldsymbol{\lambda}_{0:N} = 0$ gives the minimal unconstrained performance; i.e.,

$$G(0) = \operatorname*{arginf}_{\boldsymbol{u}_{0:N}} J(\boldsymbol{u}_{0:N}, \boldsymbol{x}^{\circ}_{0:N+1}(\boldsymbol{u}_{0:N})).$$

From Corollary 4.1, it is known that under the stated conditions the above infimium has finite value. Because G^* is the supremum of $G(\boldsymbol{\lambda}_{0:N})$ over $\boldsymbol{\lambda}_{0:N}$, this finite value is a lower bound, i.e., $-\infty < G(0) < G^*$. □

5.1.2 Closed-Form Expression of the Dual Function

Let:

$$\nu_k^i = \sum_{j=k}^{N} (\gamma^i)^{j-k} \left(\lambda_j^{U,i} - \lambda_j^{L,i} \right), \tag{5.3}$$

and define $\boldsymbol{\nu}_k = \begin{bmatrix} \nu_k^1 & \cdots & \nu_k^p \end{bmatrix}^T$ and $\boldsymbol{\nu} = \begin{bmatrix} \boldsymbol{\nu}_0^T & \cdots & \boldsymbol{\nu}_N^T \end{bmatrix}^T$. Now, we can write the augmented performance measure $\bar{J}(\cdot,\cdot,\cdot,\cdot)$ in quadratic form as:

$$\begin{aligned} \bar{J}(\boldsymbol{u}_{0:N}, \boldsymbol{q}_{0:N}, \boldsymbol{x}^{\circ}_{0:N}(\boldsymbol{u}_{0:N}, \boldsymbol{x}_0), \boldsymbol{\lambda}_{0:N}) = \begin{bmatrix} \boldsymbol{u}_0 \\ \vdots \\ \boldsymbol{u}_N \end{bmatrix}^T \boldsymbol{H}(\boldsymbol{\lambda}_{0:N}) \begin{bmatrix} \boldsymbol{u}_0 \\ \vdots \\ \boldsymbol{u}_N \end{bmatrix} + 2\boldsymbol{b}^T(\boldsymbol{\lambda}_{0:N}) \begin{bmatrix} \boldsymbol{u}_0 \\ \vdots \\ \boldsymbol{u}_N \end{bmatrix} \\ + f(\boldsymbol{\lambda}_{0:N}) - \sum_{k=0}^{N} \boldsymbol{\nu}_k^T \boldsymbol{q}_k, \end{aligned} \tag{5.4}$$

where the $(i,j)^{th}$ $m \times m$ block of the symmetric $m(N+1) \times m(N+1)$ matrix $\boldsymbol{H}(\cdot)$ is:

$$\begin{aligned} \boldsymbol{H}_{jk}(\boldsymbol{\lambda}_{0:N}) = \boldsymbol{g}_{N+1,j}^T \boldsymbol{P}_{N+1} \boldsymbol{g}_{N+1,k} + \boldsymbol{R}_j \delta_{jk} + \boldsymbol{g}_{kj}^T \boldsymbol{S}_k + \boldsymbol{S}_j^T \boldsymbol{g}_{jk} - \boldsymbol{g}_{E,jk} + \sum_{h=0}^{N} \boldsymbol{g}_{hj}^T \boldsymbol{Q}_h \boldsymbol{g}_{hk} \\ - \boldsymbol{\Psi}^T(h,j) \left(\sum_{i=1}^{p} \nu_h^i (\boldsymbol{C}_{E,h}^i)^T \boldsymbol{M}_{yy,h}^i \boldsymbol{C}_{E,h}^i \right) \boldsymbol{\Psi}(h,k), \end{aligned} \tag{5.5}$$

the j^{th} subvector of length m of the $m(N+1)$ vector $\boldsymbol{b}(\cdot)$ is:

$$\begin{aligned} \boldsymbol{b}_j(\boldsymbol{\lambda}_{0:N}) = \boldsymbol{g}_{N+1,j}^T \boldsymbol{P}_{N+1} \bar{\boldsymbol{x}}_{N+1} + \boldsymbol{S}_j^T \bar{\boldsymbol{x}}_j + \boldsymbol{U}_j \boldsymbol{a}_j \\ - \sum_{i=1}^{p} \nu_j^i \Bigg(\left(\frac{1}{2} \boldsymbol{C}_{E,j}^i + (\boldsymbol{M}_{uy,j}^i)^T \boldsymbol{C}_{E,j}^i + (\boldsymbol{D}_{E,j}^i)^T \boldsymbol{M}_{yy,j}^i \boldsymbol{C}_{E,j}^i \right) \bar{\boldsymbol{x}}_j \\ + \left(\frac{1}{2} \boldsymbol{I} + \boldsymbol{M}_{uy,j}^i + (\boldsymbol{D}_{E,j}^i)^T \boldsymbol{M}_{yy,j}^i \right) \boldsymbol{a}_{E,j} \Bigg) + \sum_{k=0}^{N} \boldsymbol{g}_{kj}^T \left(\boldsymbol{Q}_k \bar{\boldsymbol{x}}_k + \boldsymbol{T}_k \boldsymbol{a}_k \right) \\ - \boldsymbol{\Psi}^T(k,j) \sum_{i=1}^{p} \nu_j^i \left((\boldsymbol{C}_{E,k}^i)^T \boldsymbol{M}_{yy,k}^i \boldsymbol{a}_{E,k}^i + (\boldsymbol{C}_{E,k}^i)^T \boldsymbol{M}_{yy,k}^i \boldsymbol{C}_{E,k}^i \bar{\boldsymbol{x}}_k \right) \end{aligned} \tag{5.6}$$

and the scalar term $f(\cdot)$ is:

$$f(\boldsymbol{\lambda}_{0:N}) = \bar{\boldsymbol{x}}_{N+1}^T \boldsymbol{P}_{N+1} \bar{\boldsymbol{x}}_{N+1} + \sum_{k=0}^{N} \bar{\boldsymbol{x}}_k^T \boldsymbol{Q}_k \bar{\boldsymbol{x}}_k + \boldsymbol{a}_k^T \boldsymbol{V}_k \boldsymbol{a}_k + \left((\boldsymbol{\lambda}_k^L)^T \boldsymbol{E}_L - (\boldsymbol{\lambda}_k^U)^T \boldsymbol{E}_U\right) + \sum_{i=1}^{p} \gamma^i E_0^i \nu_0^i$$
$$- \nu_k^i \left(\bar{\boldsymbol{x}}_k^T (\boldsymbol{C}_{E,k}^i)^T \boldsymbol{M}_{yy,k}^i \boldsymbol{C}_{E,k}^i \bar{\boldsymbol{x}}_k + 2\bar{\boldsymbol{x}}_k^T (\boldsymbol{C}_{E,k}^i)^T \boldsymbol{M}_{yy,k}^i \boldsymbol{a}_{E,k}^i + (\boldsymbol{a}_{E,k}^i)^T \boldsymbol{M}_{yy,k}^i \boldsymbol{a}_{E,k}^i \right). \quad (5.7)$$

Parameters $\boldsymbol{g}_{jk}$ and $\boldsymbol{g}_{E,jk}$ have the following forms:

$$\boldsymbol{g}_{jk} = \begin{cases} 0, & j \leqslant k \\ \boldsymbol{\Psi}(j,k)\boldsymbol{B}_k, & j > k \end{cases},$$

$$\boldsymbol{g}_{E,jk} = \begin{cases} 0, & j < k \\ \sum_{i=1}^{p} \nu_j^i \left(\boldsymbol{D}_{E,j}^i + \boldsymbol{M}_{uu,j}^i \right), & j = k \\ \sum_{i=1}^{p} \nu_j^i \left(\boldsymbol{C}_{E,j}^i + 2\boldsymbol{M}_{ux,j}^i \right) \boldsymbol{\Psi}(k,j)\boldsymbol{B}_k, & j > k, \end{cases}$$

where $\boldsymbol{\Psi}(k,j)$ is the discrete-time state transition matrix defined in (4.3).

Let $\{\boldsymbol{u}_{0:N}^*(\boldsymbol{\lambda}_{0:N}), \boldsymbol{q}_{0:N}^*(\boldsymbol{\lambda}_{0:N})\}$ be the primal trajectory as a function of the Lagrange multipliers that minimizes $\bar{J}(\cdot,\cdot,\cdot,\cdot)$, i.e.,

$$\{\boldsymbol{u}_{0:N}^*(\boldsymbol{\lambda}_{0:N}), \boldsymbol{q}_{0:N}^*(\boldsymbol{\lambda}_{0:N})\} = \underset{\boldsymbol{u}_{0:N},\, \boldsymbol{q}_{0:N} \geqslant 0}{\operatorname{arginf}} \bar{J}(\boldsymbol{u}_{0:N}, \boldsymbol{q}_{0:N}, \boldsymbol{x}_{0:N}^\circ(\boldsymbol{u}_{0:N}, \boldsymbol{x}_0), \boldsymbol{\lambda}_{0:N}).$$

Then, we have the following result.

Lemma 5.2. *Reference the definition of ν_k^i in* (5.3) *and the dual function in* (5.1)*. Then, the following are true:*

1. *If $\nu_k^i > 0$ for some $k \in \{0...N\}$ and $i \in \{1...p\}$, then $G(\boldsymbol{\lambda}_{0:N}) \to -\infty$.*
2. *If $G(\boldsymbol{\lambda}_{0:N})$ is finite then $\boldsymbol{\nu}_k^T \boldsymbol{q}_k^*(\boldsymbol{\lambda}_{0:N}) = 0$, $\forall k \in \{0...N\}$.*

Proof. To prove statement 1, we note that $\boldsymbol{q}_{0:N}$ appears only affinely in the last term in (5.4), and independently of $\boldsymbol{u}_{0:N}$. We have that:

$$\boldsymbol{q}_{0:N}^*(\boldsymbol{\lambda}_{0:N}) = \underset{\boldsymbol{q}_{0:N} \geqslant 0}{\operatorname{arginf}} \sum_{k=0}^{N} \left\{ -\boldsymbol{\nu}_k^T \boldsymbol{q}_k \right\}.$$

Clearly if any $\nu_k^i > 0$, then the objective being infimized decreases linearly with q_k^i, which is constrained to be positive. Consequently, the infimizing solution is $q_k^i \to \infty$, rendering an objective which is $-\infty$.

To prove statement 2, we note that in the equation above, if $\nu_k^i < 0$, then the objective increases linearly with q_k^i. Consequently, because q_k^i is constrained, the infimium is achieved at $q_k^i = 0$. □

An interpretation of the results of Lemma 5.2, is that the $\boldsymbol{q}_{0:N} \geqslant 0$ sequence acts as Lagrange multipliers to enforce the constraint $\boldsymbol{\nu}_{0:N} \leqslant 0$, i.e. for all $k \in \{0...N\}$ and $i \in \{1...p\}$:

$$(q_k^i)^* \begin{cases} = 0, & \nu_k^i < 0 \\ \geqslant 0, & \nu_k^i = 0 \\ \to \infty, & \nu_k^i > 0. \end{cases}$$

Also as a result of Lemma 5.2, we can disregard $\boldsymbol{q}$ when formulating the dual function $G(\cdot)$. Let a prime, i.e. $\bar{J}'(\boldsymbol{u}_{0:N}, \boldsymbol{x}_{0:N}^{\circ}(\boldsymbol{u}_{0:N}, \boldsymbol{x}_0), \boldsymbol{\lambda}_{0:N})$, denote the evaluation of $\bar{J}(\cdot,\cdot,\cdot,\cdot)$ with $\boldsymbol{q}_k^T \boldsymbol{\nu}_k = 0$, $\forall k \in \{0...N\}$. Then it follows that we can write the dual function in (5.1) to reflect this:

$$G(\boldsymbol{\lambda}_{0:N}) = \inf_{\boldsymbol{u}_{0:N}} \bar{J}'(\boldsymbol{u}_{0:N}, \boldsymbol{x}_{0:N}^{\circ}(\boldsymbol{u}_{0:N}, \boldsymbol{x}_0), \boldsymbol{\lambda}_{0:N}). \tag{5.8}$$

It is worth emphasizing that $\boldsymbol{H}(\boldsymbol{\lambda}_{0:N})$ is the $m(N+1) \times m(N+1)$ Hessian of $\bar{J}'(\cdot,\cdot,\cdot)$ with respect to the control inputs $\boldsymbol{u}_{0:N}$, evaluated at a given value of $\boldsymbol{\lambda}_{0:N}$, i.e.,

$$\boldsymbol{H}(\boldsymbol{\lambda}_{0:N}) = \begin{bmatrix} \frac{\partial^2 \bar{J}'}{\partial \boldsymbol{u}_0 \partial \boldsymbol{u}_0} & \frac{\partial^2 \bar{J}'}{\partial \boldsymbol{u}_1 \partial \boldsymbol{u}_0} & \cdots & \frac{\partial^2 \bar{J}'}{\partial \boldsymbol{u}_N \partial \boldsymbol{u}_0} \\ \frac{\partial^2 \bar{J}'}{\partial \boldsymbol{u}_0 \partial \boldsymbol{u}_1} & \frac{\partial^2 \bar{J}'}{\partial \boldsymbol{u}_1 \partial \boldsymbol{u}_1} & \cdots & \frac{\partial^2 \bar{J}'}{\partial \boldsymbol{u}_N \partial \boldsymbol{u}_1} \\ \vdots & \vdots & \ddots & \vdots \\ \frac{\partial^2 \bar{J}'}{\partial \boldsymbol{u}_0 \partial \boldsymbol{u}_N} & \frac{\partial^2 \bar{J}'}{\partial \boldsymbol{u}_1 \partial \boldsymbol{u}_N} & \cdots & \frac{\partial^2 \bar{J}'}{\partial \boldsymbol{u}_N \partial \boldsymbol{u}_N} \end{bmatrix}. \tag{5.9}$$

Definition 5.1. *For an initial condition $\boldsymbol{x}_0 \in \mathbb{R}^n$ and exogenous disturbance $\boldsymbol{a} \in (\mathbb{L}^2)^d$, the set $\mathbb{G}(\boldsymbol{x}_0, \boldsymbol{a})$ is comprised of all $\boldsymbol{\lambda}_{0:N}$ for which the following conditions hold:*

1. $\boldsymbol{\lambda}_{0:N} \geqslant 0$
2. $\boldsymbol{\nu}_{0:N} \leqslant 0$

3. $\boldsymbol{H}(\boldsymbol{\lambda}_{0:N}) \succ 0$ *or* $\Big(\boldsymbol{H}(\boldsymbol{\lambda}_{0:N}) \succeq 0$ *and* $\boldsymbol{b}(\boldsymbol{\lambda}_{0:N}) \in \mathcal{N}(\boldsymbol{H}(\boldsymbol{\lambda}_{0:N}))\Big)$.

Theorem 5.1. *The dual function* $G(\boldsymbol{\lambda}_{0:N})$ *can be expressed in the following closed-form solution:*

$$G(\boldsymbol{\lambda}_{0:N}) = \begin{cases} -\boldsymbol{b}^T(\boldsymbol{\lambda}_{0:N})\boldsymbol{H}^\dagger(\boldsymbol{\lambda}_{0:N})\boldsymbol{b}(\boldsymbol{\lambda}_{0:N}) + f(\boldsymbol{\lambda}_{0:N}), & \boldsymbol{\lambda}_{0:N} \in \mathbb{G}(\boldsymbol{x}_0, \boldsymbol{a}) \\ -\infty, & else, \end{cases} \tag{5.10}$$

where $(\cdot)^\dagger$ *denotes the Moore-Penrose inverse. The dual function is finite if and only if* $\boldsymbol{\lambda}_{0:N} \in \mathbb{G}(\boldsymbol{x}_0, \boldsymbol{a})$. *For finite* $G(\boldsymbol{\lambda}_{0:N})$, *the associated optimal control input for a given* $\boldsymbol{\lambda}_{0:N}$ *is:*

$$\boldsymbol{u}^*(\boldsymbol{\lambda}_{0:N}) = -\boldsymbol{H}^\dagger(\boldsymbol{\lambda}_{0:N})\boldsymbol{b}(\boldsymbol{\lambda}_{0:N}).$$

Proof. From Lemma 5.2, we know if there exists a $k \in \{0...N\}$ and $i \in \{1...p\}$ such that $\nu_k^i > 0$, then $G(\boldsymbol{\lambda}_{0:N}) \to -\infty$. Now, consider $\bar{J}'(\cdot,\cdot,\cdot)$, which has the quadratic term $\boldsymbol{H}(\boldsymbol{\lambda}_{0:N})$. From (5.8), it follows that $G(\boldsymbol{\lambda}_{0:N})$ is finite if $\boldsymbol{H}(\boldsymbol{\lambda}_{0:N}) \succ 0$, and equal to $-\infty$ if $\boldsymbol{H}(\boldsymbol{\lambda}_{0:N})$ has at least one negative eigenvalue. When $\boldsymbol{H}(\boldsymbol{\lambda}_{0:N})$ has a null space, the boundedness of $G(\boldsymbol{\lambda}_{0:N})$ requires that $\boldsymbol{b}$ be in the null space. □

5.2 Numerical Methods to Solve the Dual Problem

In this section, we outline a method to solve the dual problem by solving a series of QPs. Newton's method is an iterative algorithm that can be used to find the direction in which to modify the Lagrange multipliers $\boldsymbol{\lambda}_{0:N}$ that maximizes the second-order approximation of $G(\cdot)$. Let $\boldsymbol{\lambda}_{0:N}^{(j)}$ be the j^{th} iteration of the Lagrange multpliers. Then, let the second-order Taylor approximation of the dual function about $\boldsymbol{\lambda}_{0:N}^{(j)}$ be $\hat{G}^{(j)}(\boldsymbol{\zeta}^{(j)})$ where $\boldsymbol{\zeta}^{(j)}$ is the direction that we optimize. The second-order approximation $\hat{G}^{(j)}(\boldsymbol{\zeta}^{(j)})$ is:

$$\hat{G}^{(j)}\left(\boldsymbol{\zeta}^{(j)}\right) = G\left(\boldsymbol{\lambda}_{0:N}^{(j)}\right) + \left(\frac{\partial G}{\partial \boldsymbol{\lambda}_{0:N}^{(j)}}\right)^T \boldsymbol{\zeta}^{(j)} + \frac{1}{2}\left(\boldsymbol{\zeta}^{(j)}\right)^T \left(\frac{\partial^2 G}{\partial \boldsymbol{\lambda}_{0:N}^{(j)} \left(\partial \boldsymbol{\lambda}_{0:N}^{(j)}\right)^T}\right) \boldsymbol{\zeta}^{(j)},$$

where the gradient has the following form:

$$\frac{\partial G}{\partial \boldsymbol{\lambda}_k} = \begin{bmatrix} \frac{\partial G}{\partial \lambda_k^{L,1}} & \cdots & \frac{\partial G}{\partial \lambda_k^{L,p}} & \frac{\partial G}{\partial \lambda_k^{U,1}} & \cdots & \frac{\partial G}{\partial \lambda_k^{U,p}} \end{bmatrix}^T, \qquad \frac{\partial G}{\partial \boldsymbol{\lambda}_{0:N}} = \begin{bmatrix} (\frac{\partial G}{\partial \boldsymbol{\lambda}_0})^T & \cdots & (\frac{\partial G}{\partial \boldsymbol{\lambda}_N})^T \end{bmatrix}^T,$$

and where the Hessian has the following form:

$$\frac{\partial^2 G}{\partial \boldsymbol{\lambda}_{0:N}^2} = \begin{bmatrix} \frac{\partial^2 G}{\partial \lambda_0^{L,1} \partial \lambda_0^{L,1}} & \cdots & \frac{\partial^2 G}{\partial \lambda_0^{L,p} \partial \lambda_0^{L,1}} & \frac{\partial^2 G}{\partial \lambda_0^{U,1} \partial \lambda_0^{L,1}} & \cdots & \frac{\partial^2 G}{\partial \lambda_0^{U,p} \partial \lambda_0^{L,1}} & \cdots & \frac{\partial^2 G}{\partial \lambda_N^{L,1} \partial \lambda_0^{L,1}} & \cdots & \frac{\partial^2 G}{\partial \lambda_N^{L,p} \partial \lambda_0^{L,1}} & \frac{\partial^2 G}{\partial \lambda_N^{U,1} \partial \lambda_0^{L,1}} & \cdots & \frac{\partial^2 G}{\partial \lambda_N^{U,p} \partial \lambda_0^{L,1}} \\ \vdots & & \vdots & \vdots & & \vdots & & \vdots & & \vdots & \vdots & & \vdots \\ \frac{\partial^2 G}{\partial \lambda_0^{L,1} \partial \lambda_0^{L,p}} & \cdots & \frac{\partial^2 G}{\partial \lambda_0^{L,p} \partial \lambda_0^{L,p}} & \frac{\partial^2 G}{\partial \lambda_0^{U,1} \partial \lambda_0^{L,p}} & \cdots & \frac{\partial^2 G}{\partial \lambda_0^{U,p} \partial \lambda_0^{L,p}} & \cdots & \frac{\partial^2 G}{\partial \lambda_N^{L,1} \partial \lambda_0^{L,p}} & \cdots & \frac{\partial^2 G}{\partial \lambda_N^{L,p} \partial \lambda_0^{L,p}} & \frac{\partial^2 G}{\partial \lambda_N^{U,1} \partial \lambda_0^{L,p}} & \cdots & \frac{\partial^2 G}{\partial \lambda_N^{U,p} \partial \lambda_0^{L,p}} \\ \frac{\partial^2 G}{\partial \lambda_0^{L,1} \partial \lambda_0^{U,1}} & \cdots & \frac{\partial^2 G}{\partial \lambda_0^{L,p} \partial \lambda_0^{U,1}} & \frac{\partial^2 G}{\partial \lambda_0^{U,1} \partial \lambda_0^{U,1}} & \cdots & \frac{\partial^2 G}{\partial \lambda_0^{U,p} \partial \lambda_0^{U,1}} & \cdots & \frac{\partial^2 G}{\partial \lambda_N^{L,1} \partial \lambda_0^{U,1}} & \cdots & \frac{\partial^2 G}{\partial \lambda_N^{L,p} \partial \lambda_0^{U,1}} & \frac{\partial^2 G}{\partial \lambda_N^{U,1} \partial \lambda_0^{U,1}} & \cdots & \frac{\partial^2 G}{\partial \lambda_N^{U,p} \partial \lambda_0^{U,1}} \\ \vdots & & \vdots & \vdots & & \vdots & & \vdots & & \vdots & \vdots & & \vdots \\ \frac{\partial^2 G}{\partial \lambda_0^{L,1} \partial \lambda_0^{U,1}} & \cdots & \frac{\partial^2 G}{\partial \lambda_0^{L,p} \partial \lambda_0^{U,p}} & \frac{\partial^2 G}{\partial \lambda_0^{U,1} \partial \lambda_0^{U,p}} & \cdots & \frac{\partial^2 G}{\partial \lambda_0^{U,p} \partial \lambda_0^{U,p}} & \cdots & \frac{\partial^2 G}{\partial \lambda_N^{L,1} \partial \lambda_0^{U,p}} & \cdots & \frac{\partial^2 G}{\partial \lambda_N^{L,p} \partial \lambda_0^{U,p}} & \frac{\partial^2 G}{\partial \lambda_N^{U,1} \partial \lambda_0^{U,p}} & \cdots & \frac{\partial^2 G}{\partial \lambda_N^{U,p} \partial \lambda_0^{U,p}} \\ \vdots & & \vdots & \vdots & & \vdots & & \vdots & & \vdots & \vdots & & \vdots \\ \frac{\partial^2 G}{\partial \lambda_0^{L,1} \partial \lambda_N^{L,1}} & \cdots & \frac{\partial^2 G}{\partial \lambda_0^{L,p} \partial \lambda_N^{L,1}} & \frac{\partial^2 G}{\partial \lambda_0^{U,1} \partial \lambda_N^{L,1}} & \cdots & \frac{\partial^2 G}{\partial \lambda_0^{U,p} \partial \lambda_N^{L,1}} & \cdots & \frac{\partial^2 G}{\partial \lambda_N^{L,1} \partial \lambda_N^{L,1}} & \cdots & \frac{\partial^2 G}{\partial \lambda_N^{L,p} \partial \lambda_N^{L,1}} & \frac{\partial^2 G}{\partial \lambda_N^{U,1} \partial \lambda_N^{L,1}} & \cdots & \frac{\partial^2 G}{\partial \lambda_N^{U,p} \partial \lambda_N^{L,1}} \\ \vdots & & \vdots & \vdots & & \vdots & & \vdots & & \vdots & \vdots & & \vdots \\ \frac{\partial^2 G}{\partial \lambda_0^{L,1} \partial \lambda_N^{L,p}} & \cdots & \frac{\partial^2 G}{\partial \lambda_0^{L,p} \partial \lambda_N^{L,p}} & \frac{\partial^2 G}{\partial \lambda_0^{U,1} \partial \lambda_N^{L,p}} & \cdots & \frac{\partial^2 G}{\partial \lambda_0^{U,p} \partial \lambda_N^{L,p}} & \cdots & \frac{\partial^2 G}{\partial \lambda_N^{L,1} \partial \lambda_N^{L,p}} & \cdots & \frac{\partial^2 G}{\partial \lambda_N^{L,p} \partial \lambda_N^{L,p}} & \frac{\partial^2 G}{\partial \lambda_N^{U,1} \partial \lambda_N^{L,p}} & \cdots & \frac{\partial^2 G}{\partial \lambda_N^{U,p} \partial \lambda_N^{L,p}} \\ \frac{\partial^2 G}{\partial \lambda_0^{L,1} \partial \lambda_N^{U,1}} & \cdots & \frac{\partial^2 G}{\partial \lambda_0^{L,p} \partial \lambda_N^{U,1}} & \frac{\partial^2 G}{\partial \lambda_0^{U,1} \partial \lambda_N^{U,1}} & \cdots & \frac{\partial^2 G}{\partial \lambda_0^{U,p} \partial \lambda_N^{U,1}} & \cdots & \frac{\partial^2 G}{\partial \lambda_N^{L,1} \partial \lambda_N^{U,1}} & \cdots & \frac{\partial^2 G}{\partial \lambda_N^{L,p} \partial \lambda_N^{U,1}} & \frac{\partial^2 G}{\partial \lambda_N^{U,1} \partial \lambda_N^{U,1}} & \cdots & \frac{\partial^2 G}{\partial \lambda_N^{U,p} \partial \lambda_N^{U,1}} \\ \vdots & & \vdots & \vdots & & \vdots & & \vdots & & \vdots & \vdots & & \vdots \\ \frac{\partial^2 G}{\partial \lambda_0^{L,1} \partial \lambda_N^{U,1}} & \cdots & \frac{\partial^2 G}{\partial \lambda_0^{L,p} \partial \lambda_N^{U,p}} & \frac{\partial^2 G}{\partial \lambda_0^{U,1} \partial \lambda_N^{U,p}} & \cdots & \frac{\partial^2 G}{\partial \lambda_0^{U,p} \partial \lambda_N^{U,p}} & \cdots & \frac{\partial^2 G}{\partial \lambda_N^{L,1} \partial \lambda_N^{U,p}} & \cdots & \frac{\partial^2 G}{\partial \lambda_N^{L,p} \partial \lambda_N^{U,p}} & \frac{\partial^2 G}{\partial \lambda_N^{U,1} \partial \lambda_N^{U,p}} & \cdots & \frac{\partial^2 G}{\partial \lambda_N^{U,p} \partial \lambda_N^{U,p}} \end{bmatrix}.$$

Given $\boldsymbol{\lambda}_{0:N}^{(j)}$, we solve the following QP to find the vector $\boldsymbol{\zeta}^{(j)}$ that maximizes $\hat{G}^{(j)}(\cdot)$:

$$\text{Dual QP} = \begin{cases} \textbf{Given:} & \boldsymbol{\lambda}_{0:N}^{(j)} \\ \textbf{Maximize:} & \hat{G}^{(j)}\left(\boldsymbol{\zeta}^{(j)}\right) \\ \textbf{Domain:} & \boldsymbol{\zeta}^{(j)} \\ \textbf{Constraints:} & \boldsymbol{\lambda}_{0:N}^{(j)} + \boldsymbol{\zeta}^{(j)} \geqslant 0. \end{cases} \tag{5.11}$$

The Newton step is the value that maximizes $\hat{G}^{(j)}(\cdot)$ without the non-negativity constraints on the Lagrange multipliers, which is:

$$\boldsymbol{\zeta}^{(j)} = -\left(\frac{\partial^2 G}{\partial \boldsymbol{\lambda}_{0:N}^{(j)} \left(\partial \boldsymbol{\lambda}_{0:N}^{(j)}\right)^T}\right)^{-1} \frac{\partial G}{\partial \boldsymbol{\lambda}_{0:N}^{(j)}}.$$

However, given the constraints on the Lagrange multipliers, we cannot guarantee that the Newton step is the solution to (5.11). Therefore, a common method used to solve these QPs are interior-point algorithms, which can enforce the non-negativity constraints on the Lagrange multipliers [10].

After solving (5.11) for the optimal value of $\boldsymbol{\zeta}^{(j)}$, which we designate as $\boldsymbol{\zeta}^{(j)*}$, a scalar line search is performed over $\alpha^{(j)}$ to maximize the original dual function $G(\boldsymbol{\lambda}_{0:N}^{(j)} + \alpha^{(j)}\boldsymbol{\zeta}^{(j)*})$

subject to the nonnegativity constraints on the Lagrange multipliers, that is:

$$\alpha^{(j)*} = \underset{\alpha^{(j)}}{\operatorname{argmax}} \left\{ G\left(\boldsymbol{\lambda}_{0:N}^{(j)} + \alpha^{(j)}\boldsymbol{\zeta}^{(j)*}\right) \quad | \quad \boldsymbol{\lambda}_{0:N}^{(j)} + \alpha^{(j)}\boldsymbol{\zeta}^{(j)*} \geqslant 0 \right\}.$$

Then, the $(j+1)^{th}$ iteration of the Lagrange multipliers is:

$$\boldsymbol{\lambda}_{0:N}^{(j+1)} = \boldsymbol{\lambda}_{0:N}^{(j)} + \alpha^{(j)*}\boldsymbol{\zeta}^{(j)*}.$$

We continue this iteration process until iteration h where $\alpha^{(h)*} = \epsilon$. Then, the maximum dual function is $G^* = G\left(\boldsymbol{\lambda}_{0:N}^{(h)}\right)$. In the following section, we formulate the gradient and Hessian of the dual function with respect to $\boldsymbol{\lambda}_{0:N}$.

5.2.1 Formulating the Dual Gradient and Hessian

Due to the structure of the dual function, it is easier to take derivatives with respect to $\boldsymbol{\nu}_{0:N}$, which is defined in (5.3), than $\boldsymbol{\lambda}_{0:N}$. Reference the equations for $\boldsymbol{H}(\cdot)$ and $\boldsymbol{b}(\cdot)$ in (5.5) and (5.6), respectively, where $\boldsymbol{\lambda}_{0:N}$ only appears in $\boldsymbol{H}(\cdot)$ and $\boldsymbol{b}(\cdot)$ in the form of $\boldsymbol{\nu}_{0:N}$. Let $\hat{G}(\cdot)$ be the portion of dual function $G(\cdot)$ that directly dependent on $\boldsymbol{\nu}_{0:N}$, i.e.,

$$G(\boldsymbol{\lambda}_{0:N}) = \hat{G}(\boldsymbol{\nu}_{0:N}) + \sum_{k=0}^{N} (\boldsymbol{\lambda}_k^L)^T \boldsymbol{E}_L - (\boldsymbol{\lambda}_k^U)^T \boldsymbol{E}_U.$$

First, we determine the Hessian of $\hat{G}(\cdot)$ with respect to $\boldsymbol{\nu}_{0:N}$, which has the following form:

$$\frac{\partial^2 \hat{G}}{\partial \boldsymbol{\nu}_{0:N}^2} = \begin{bmatrix} \frac{\partial^2 \hat{G}}{\partial \nu_0^1 \partial \nu_0^1} & \cdots & \frac{\partial^2 \hat{G}}{\partial \nu_0^p \partial \nu_0^1} & \cdots & \frac{\partial^2 \hat{G}}{\partial \nu_N^1 \partial \nu_0^1} & \cdots & \frac{\partial^2 \hat{G}}{\partial \nu_N^p \partial \nu_0^1} \\ \vdots & & \vdots & & \vdots & & \vdots \\ \frac{\partial^2 \hat{G}}{\partial \nu_0^1 \partial \nu_0^p} & \cdots & \frac{\partial^2 \hat{G}}{\partial \nu_0^p \partial \nu_0^p} & \cdots & \frac{\partial^2 \hat{G}}{\partial \nu_N^1 \partial \nu_0^p} & \cdots & \frac{\partial^2 \hat{G}}{\partial \nu_N^p \partial \nu_0^p} \\ \vdots & & \vdots & & \vdots & & \vdots \\ \frac{\partial^2 \hat{G}}{\partial \nu_0^1 \partial \nu_N^1} & \cdots & \frac{\partial^2 \hat{G}}{\partial \nu_0^p \partial \nu_N^1} & \cdots & \frac{\partial^2 \hat{G}}{\partial \nu_N^1 \partial \nu_N^1} & \cdots & \frac{\partial^2 \hat{G}}{\partial \nu_N^p \partial \nu_N^1} \\ \vdots & & \vdots & & \vdots & & \vdots \\ \frac{\partial^2 \hat{G}}{\partial \nu_0^1 \partial \nu_N^p} & \cdots & \frac{\partial^2 \hat{G}}{\partial \nu_0^p \partial \nu_N^p} & \cdots & \frac{\partial^2 \hat{G}}{\partial \nu_N^1 \partial \nu_N^p} & \cdots & \frac{\partial^2 \hat{G}}{\partial \nu_N^p \partial \nu_N^p} \end{bmatrix},$$

where the $((k-1)p+h,(j-1)p+i)^{th}$ element of the Hessian is:

$$\frac{\partial^2 \hat{G}}{\partial \nu_k^h \partial \nu_j^i} = 4\left(\frac{\partial \boldsymbol{b}}{\partial \nu_j^i}\right)^T \boldsymbol{H}^\dagger \frac{\partial \boldsymbol{H}}{\partial \nu_k^h} \boldsymbol{H}^\dagger \boldsymbol{b} - 2\left(\frac{\partial \boldsymbol{b}}{\partial \nu_j^i}\right)^T \boldsymbol{H}^\dagger \frac{\partial \boldsymbol{b}}{\partial \nu_k^h} - 2\boldsymbol{b}^T \boldsymbol{H}^\dagger \frac{\partial \boldsymbol{H}}{\partial \nu_j^i} \boldsymbol{H}^\dagger \frac{\partial \boldsymbol{H}}{\partial \nu_k^h} \boldsymbol{H}^\dagger \boldsymbol{b}.$$

Note that the second derivatives of $\boldsymbol{H}(\boldsymbol{\nu}_{0:N})$ and $\boldsymbol{b}(\boldsymbol{\nu}_{0:N})$ both zero, i.e., $\frac{\partial^2 \boldsymbol{H}}{\partial \nu_k^h \partial \nu_j^i} = \frac{\partial^2 \boldsymbol{b}}{\partial \nu_k^h \partial \nu_j^i} = 0$. The gradient of $\hat{G}(\cdot)$ with respect to $\boldsymbol{\nu}_{0:N}$ has the form:

$$\frac{\partial \hat{G}}{\partial \boldsymbol{\nu}_{0:N}} = \begin{bmatrix} \frac{\partial \hat{G}}{\partial \nu_0^1} & \cdots & \frac{\partial \hat{G}}{\partial \nu_0^p} & \cdots & \frac{\partial \hat{G}}{\partial \nu_N^1} & \cdots & \frac{\partial \hat{G}}{\partial \nu_N^p} \end{bmatrix}^T,$$

where the $((j-1)p+i)^{th}$ element of the gradient of $\hat{G}(\cdot)$ is:

$$\frac{\partial \hat{G}}{\partial \nu_j^i} = -2\left(\frac{\partial \boldsymbol{b}}{\partial \nu_j^i}\right)^T \boldsymbol{H}^\dagger \boldsymbol{b} + \boldsymbol{b}^T \boldsymbol{H}^\dagger \frac{\partial \boldsymbol{H}}{\partial \nu_j^i} \boldsymbol{H}^\dagger \boldsymbol{b} + \frac{\partial \tilde{f}}{\partial \nu_j^i},$$

where $\tilde{f}(\cdot)$ is:

$$\begin{aligned} \tilde{f}(\boldsymbol{\nu}_{0:N}) = \bar{\boldsymbol{x}}_{N+1}^T \boldsymbol{P}_{N+1} \bar{\boldsymbol{x}}_{N+1} + \sum_{k=0}^{N} \bar{\boldsymbol{x}}_k^T \boldsymbol{Q}_k \bar{\boldsymbol{x}}_k + \boldsymbol{a}_k^T \boldsymbol{V}_k \boldsymbol{a}_k + \sum_{i=1}^{p} \gamma^i E_0^i \nu_0^i \\ - \nu_k^i \left(\bar{\boldsymbol{x}}_k^T (\boldsymbol{C}_{E,k}^i)^T \boldsymbol{M}_{yy,k}^i \boldsymbol{C}_{E,k}^i \bar{\boldsymbol{x}}_k + 2\bar{\boldsymbol{x}}_k^T (\boldsymbol{C}_{E,k}^i)^T \boldsymbol{M}_{yy,k}^i \boldsymbol{a}_{E,k}^i + (\boldsymbol{a}_{E,k}^i)^T \boldsymbol{M}_{yy,k}^i \boldsymbol{a}_{E,k}^i \right). \end{aligned}$$

The gradient of the dual function $G(\cdot)$ with respect to $\boldsymbol{\lambda}_{0:N}$ is:

$$\frac{\partial G}{\partial \boldsymbol{\lambda}_{0:N}} = \left(\frac{\partial \boldsymbol{\nu}_{0:N}}{\partial \boldsymbol{\lambda}_{0:N}}\right)^T \frac{\partial \hat{G}}{\partial \boldsymbol{\nu}_{0:N}} + \frac{\partial}{\partial \boldsymbol{\lambda}_{0:N}} \left(\sum_{k=0}^{N} (\boldsymbol{\lambda}_k^L)^T \boldsymbol{E}_L - (\boldsymbol{\lambda}_k^U)^T \boldsymbol{E}_U \right),$$

and the Hessian of the dual function with respect to $\boldsymbol{\lambda}_{0:N}$ is:

$$\frac{\partial^2 G}{\partial \boldsymbol{\lambda}_{0:N}^2} = \left(\frac{\partial \boldsymbol{\nu}_{0:N}}{\partial \boldsymbol{\lambda}_{0:N}}\right)^T \frac{\partial^2 \hat{G}}{\partial \boldsymbol{\nu}_{0:N}^2} \left(\frac{\partial \boldsymbol{\nu}_{0:N}}{\partial \boldsymbol{\lambda}_{0:N}}\right).$$

It is notationally cumbersome to present $\frac{\partial \boldsymbol{\nu}_{0:N}}{\partial \boldsymbol{\lambda}_{0:N}}$ for general p, so we instead present the case

with $p = 1$. Let $\boldsymbol{\varphi}^i = \boldsymbol{\lambda}^{L,i} - \boldsymbol{\lambda}^{U,i}$, and then:

$$\frac{\partial \boldsymbol{\nu}_{0:N}}{\partial \boldsymbol{\varphi}_{0:N}} = \begin{bmatrix} \frac{\partial \nu_0^1}{\partial \varphi_0^1} & \frac{\partial \nu_0^1}{\partial \varphi_1^1} & \cdots & \frac{\partial \nu_0^1}{\partial \varphi_N^1} \\ \frac{\partial \nu_1^1}{\partial \varphi_0^1} & \frac{\partial \nu_1^1}{\partial \varphi_1^1} & \cdots & \frac{\partial \nu_1^1}{\partial \varphi_N^1} \\ \vdots & \vdots & \ddots & \vdots \\ \frac{\partial \nu_N^1}{\partial \varphi_0^1} & \frac{\partial \nu_N^1}{\partial \varphi_1^1} & \cdots & \frac{\partial \nu_N^1}{\partial \varphi_N^1} \end{bmatrix} = \begin{bmatrix} 1 & (\gamma^1) & \cdots & (\gamma^1)^N \\ 0 & 1 & \cdots & (\gamma^1)^{N-1} \\ \vdots & \vdots & \ddots & \vdots \\ 0 & 0 & \cdots & 1 \end{bmatrix},$$

and:

$$\frac{\partial \boldsymbol{\varphi}_{0:N}}{\partial \boldsymbol{\lambda}_{0:N}} = \begin{bmatrix} \frac{\partial \varphi_0^1}{\partial \lambda_0^{L,1}} & \frac{\partial \varphi_0^1}{\partial \lambda_0^{U,1}} & \frac{\partial \varphi_0^1}{\partial \lambda_1^{L,1}} & \frac{\partial \varphi_0^1}{\partial \lambda_1^{U,1}} & \cdots & \frac{\partial \varphi_0^1}{\partial \lambda_N^{L,1}} & \frac{\partial \varphi_0^1}{\partial \lambda_N^{U,1}} \\ \frac{\partial \varphi_1^1}{\partial \lambda_0^{L,1}} & \frac{\partial \varphi_1^1}{\partial \lambda_0^{U,1}} & \frac{\partial \varphi_1^1}{\partial \lambda_1^{L,1}} & \frac{\partial \varphi_1^1}{\partial \lambda_1^{U,1}} & \cdots & \frac{\partial \varphi_1^1}{\partial \lambda_N^{L,1}} & \frac{\partial \varphi_1^1}{\partial \lambda_N^{U,1}} \\ \vdots & \vdots & \vdots & \vdots & \ddots & \vdots & \vdots \\ \frac{\partial \varphi_N^1}{\partial \lambda_0^{L,1}} & \frac{\partial \varphi_N^1}{\partial \lambda_0^{U,1}} & \frac{\partial \varphi_N^1}{\partial \lambda_1^{L,1}} & \frac{\partial \varphi_N^1}{\partial \lambda_1^{U,1}} & \cdots & \frac{\partial \varphi_N^1}{\partial \lambda_N^{L,1}} & \frac{\partial \varphi_N^1}{\partial \lambda_N^{U,1}} \end{bmatrix} = \begin{bmatrix} -1 & 1 & 0 & 0 & \cdots & 0 & 0 \\ 0 & 0 & -1 & 1 & \cdots & 0 & 0 \\ \vdots & \vdots & \vdots & \vdots & \ddots & \vdots & \vdots \\ 0 & 0 & 0 & 0 & \cdots & -1 & 1 \end{bmatrix},$$

and it follows that:

$$\frac{\partial \boldsymbol{\nu}_{0:N}}{\partial \boldsymbol{\lambda}_{0:N}} = \left(\frac{\partial \boldsymbol{\nu}_{0:N}}{\partial \boldsymbol{\varphi}_{0:N}}\right)\left(\frac{\partial \boldsymbol{\varphi}_{0:N}}{\partial \boldsymbol{\lambda}_{0:N}}\right).$$

For the case with $p = 1$, we have that:

$$\frac{\partial}{\partial \boldsymbol{\lambda}_{0:N}}\left(\sum_{k=0}^{N}(\boldsymbol{\lambda}_k^L)^T \boldsymbol{E}_L - (\boldsymbol{\lambda}_k^U)^T \boldsymbol{E}_U\right) = \begin{bmatrix} E_L^1 & -E_U^1 & E_L^1 & -E_U^1 & \cdots & E_L^1 & -E_U^1 \end{bmatrix}^T.$$

Note that for the zero energy storage case (see Section 4.2.4), we can optimize directly over the $\boldsymbol{\nu}_{0:N}$ because the above derivative is zero.

5.3 Alternative Method Using Costates

The method outlined in the last section to formulate the dual function, gradient, and Hessian can be computationally intractable because it requires the construction and inversion of Hessian $\boldsymbol{H}(\cdot)$. A less computationally expensive method is to instead formulate the dual function, gradient, and Hessian using costates. Let $\boldsymbol{\rho}_{k+1}$ be the $(k+1)^{th}$ costate which enforces the $(k+1)^{th}$ difference equation modeling the evolution of the states, i.e., $\boldsymbol{x}_{k+1} = \boldsymbol{A}_k \boldsymbol{x}_k + \boldsymbol{B}_k \boldsymbol{u}_k + \boldsymbol{a}_k$.

5.3.1 Closed-Form Expression of the Dual Function

Let $J'_\rho(\cdot,\cdot,\cdot,\cdot)$ be the modified performance measure incorporating the costates and disregarding the term with $\boldsymbol{q}$ as discussed in Lemma 5.2:

$$J'_\rho(\boldsymbol{u}_{0:N}, \boldsymbol{x}_{0:N+1}, \boldsymbol{\lambda}_{0:N}, \boldsymbol{\rho}_{1:N+1}) = \sum_{i=1}^{p} \nu_0^i \gamma^i E_0^i + \sum_{k=0}^{N} \boldsymbol{\xi}_k^T \boldsymbol{\Pi}_k \boldsymbol{\xi}_k + (\boldsymbol{\lambda}_k^L)^T \boldsymbol{E}_L \\ - (\boldsymbol{\lambda}_k^U)^T \boldsymbol{E}_U + \boldsymbol{\rho}_{k+1}^T (\boldsymbol{A}_k \boldsymbol{x}_k + \boldsymbol{B}_k \boldsymbol{u}_k + \boldsymbol{a}_k - \boldsymbol{x}_{k+1}),$$

where:

$$\boldsymbol{\xi}_k = \begin{bmatrix} \boldsymbol{x}_k^\circ(\boldsymbol{u}_{0:N}, \boldsymbol{x}_0) \\ \boldsymbol{u}_k \\ 1 \end{bmatrix}, \quad \boldsymbol{\Pi}_k = \begin{bmatrix} \boldsymbol{X}_k & \boldsymbol{\Omega}_k & \boldsymbol{\Lambda}_k \\ \boldsymbol{\Omega}_k^T & \boldsymbol{Z}_k & \boldsymbol{\Xi}_k \\ \boldsymbol{\Lambda}_k^T & \boldsymbol{\Xi}_k^T & Y_k \end{bmatrix}$$

with:

$$\boldsymbol{X}_k = \boldsymbol{Q}_k - \sum_{i=1}^{p} \nu_k^i (\boldsymbol{C}_{E,k}^i)^T \boldsymbol{M}_{yy,k}^i \boldsymbol{C}_{E,k}^i$$

$$\boldsymbol{\Omega}_k = \boldsymbol{S}_k - \sum_{i=1}^{p} \nu_k^i \left(\frac{1}{2} (\boldsymbol{C}_{E,k}^i)^T + (\boldsymbol{C}_{E,k}^i)^T \boldsymbol{M}_{uy,k}^i + (\boldsymbol{C}_{E,k}^i)^T \boldsymbol{M}_{yy,k}^i \boldsymbol{D}_{E,k}^i \right)$$

$$\boldsymbol{\Lambda}_k = \boldsymbol{U}_k \boldsymbol{a}_k - \sum_{i=1}^{p} \nu_k^i (\boldsymbol{C}_{E,k}^i)^T \boldsymbol{M}_{yy,k}^i \boldsymbol{a}_{E,k}^i$$

$$\boldsymbol{Z}_k = \boldsymbol{R}_k - \sum_{i=1}^{p} \nu_k^i \left((\boldsymbol{D}_{E,k}^i)^T + \boldsymbol{M}_{uu,k}^i + \boldsymbol{M}_{uy,k}^i \boldsymbol{D}_{E,k}^i + (\boldsymbol{D}_{E,k}^i)^T \boldsymbol{M}_{yy,k}^i \boldsymbol{D}_{E,k}^i \right)$$

$$\boldsymbol{\Xi}_k = \boldsymbol{T}_k \boldsymbol{a}_k - \sum_{i=1}^{p} \nu_k^i \left(\frac{1}{2} \boldsymbol{I} + \boldsymbol{M}_{uy,k}^i + (\boldsymbol{D}_{E,k}^i)^T \boldsymbol{M}_{yy,k}^i \right) \boldsymbol{a}_{E,k}^i$$

$$Y_k = \boldsymbol{a}_k^T \boldsymbol{V}_k \boldsymbol{a}_k - \sum_{i=1}^{p} \nu_k^i (\boldsymbol{a}_{E,k}^i)^T \boldsymbol{M}_{yy,k}^i \boldsymbol{a}_{E,k}^i.$$

Note that $\boldsymbol{M}_{uu,k}^i$, $\boldsymbol{M}_{yy,k}^i$, and $\boldsymbol{M}_{uy,k}^i$ are components of the quadratic loss model in (3.22). Then, the associated dual function is:

$$G(\boldsymbol{\lambda}_{0:N}) = \sup_{\boldsymbol{p}_{1:N+1}} \inf_{\boldsymbol{u}_{0:N},\, \boldsymbol{x}_{0:N+1}} J'_\rho(\boldsymbol{u}_{0:N}, \boldsymbol{x}_{0:N+1}, \boldsymbol{\lambda}_{0:N}, \boldsymbol{\rho}_{1:N+1}).$$

The Hamiltonian (see Definition 2.17) associated with $J'_\rho(\cdot,\cdot,\cdot,\cdot)$ is:

$$\mathcal{H}_k(\boldsymbol{u}_k, \boldsymbol{x}_k, \boldsymbol{\lambda}_{k:N}, \boldsymbol{\rho}_{k+1}) = \boldsymbol{\xi}_k^T \boldsymbol{\Pi}_k \boldsymbol{\xi}_k + (\boldsymbol{\lambda}_k^L)^T \boldsymbol{E}_L - (\boldsymbol{\lambda}_k^U)^T \boldsymbol{E}_U + \boldsymbol{\rho}_{k+1}^T \left(\boldsymbol{A}_k \boldsymbol{x}_k + \boldsymbol{B}_k \boldsymbol{u}_k + \boldsymbol{a}_k - \boldsymbol{x}_{k+1}\right).$$

Then, from Pontryagin's minimum principle [15, 41] we require that $\boldsymbol{u}^*_{0:N}$, $\boldsymbol{x}^*_{0:N}$, and $\boldsymbol{\rho}^*_{1:N+1}$ satisfy the following first order necessary conditions for optimality, $\forall k \in \{0...N\}$:

$$\frac{\partial \mathcal{H}_k}{\partial \boldsymbol{u}_k} = \boldsymbol{\Sigma}_k \boldsymbol{u}_k + 2\boldsymbol{\Omega}_k^T \boldsymbol{x}_k + 2\boldsymbol{\Xi}_k + \boldsymbol{B}_k^T \boldsymbol{\rho}_{k+1} = 0 \tag{5.12}$$

$$\frac{\partial \mathcal{H}_k}{\partial \boldsymbol{x}_k} = 2\boldsymbol{X}_k \boldsymbol{x}_k + 2\boldsymbol{\Omega}_k \boldsymbol{u}_k + 2\boldsymbol{\Lambda}_k + \boldsymbol{A}_k^T \boldsymbol{\rho}_{k+1} = \boldsymbol{\rho}_k \tag{5.13}$$

$$\frac{\partial \mathcal{H}_k}{\partial \boldsymbol{\rho}_{k+1}} = \boldsymbol{A}_k \boldsymbol{x}_k + \boldsymbol{B}_k \boldsymbol{u}_k + \boldsymbol{a}_k = \boldsymbol{x}_{k+1} \tag{5.14}$$

and final costate condition:

$$\frac{\partial \Phi}{\partial \boldsymbol{x}_{N+1}} = 2\boldsymbol{P}_{N+1} \boldsymbol{x}_{N+1} = \boldsymbol{\rho}_{N+1}, \tag{5.15}$$

where $\boldsymbol{\Sigma}_k = \left(\boldsymbol{Z}_k + \boldsymbol{Z}_k^T\right)$. To find the optimal control input, we solve for $\boldsymbol{u}_k$ in (5.12) as:

$$\boldsymbol{u}_k^*(\boldsymbol{\lambda}_{0:N}) = -\boldsymbol{\Sigma}_k^{-1} \left(2\boldsymbol{\Omega}_k^T \boldsymbol{x}_k^* + \boldsymbol{B}_k^T \boldsymbol{\rho}_{k+1}^* + 2\boldsymbol{\Xi}_k\right). \tag{5.16}$$

Let $\{\boldsymbol{x}^\circ_{0:N}, \boldsymbol{\rho}^\circ_{0:N}\}$ be the unique solutions to the following two-point boundary value problem, which follows from (5.13)–(5.15):

$$\begin{bmatrix} \boldsymbol{x}^\circ_{k+1} \\ \boldsymbol{\rho}^\circ_k \end{bmatrix} = \begin{bmatrix} \boldsymbol{A}_k \boldsymbol{x}^\circ_k + \boldsymbol{B}_k \boldsymbol{u}_k + \boldsymbol{a}_k \\ 2\boldsymbol{X}_k \boldsymbol{x}^\circ_k + 2\boldsymbol{\Omega}_k \boldsymbol{u}_k + 2\boldsymbol{\Lambda}_k + \boldsymbol{A}_k^T \boldsymbol{\rho}^\circ_{k+1} \end{bmatrix}, \quad \begin{bmatrix} \boldsymbol{x}^\circ_0 \\ \boldsymbol{\rho}^\circ_{N+1} \end{bmatrix} = \begin{bmatrix} \boldsymbol{x}_0 \\ \boldsymbol{2P_{N+1} x_{N+1}} \end{bmatrix}, \tag{5.17}$$

and then:

$$\begin{bmatrix} \boldsymbol{x}^*_k(\boldsymbol{\lambda}_{0:N}) \\ \boldsymbol{\rho}^*_k(\boldsymbol{\lambda}_{0:N}) \end{bmatrix} = \begin{bmatrix} \boldsymbol{x}^\circ_k(\boldsymbol{\lambda}_{0:N}, \boldsymbol{u}^*_{0:N}(\boldsymbol{\lambda}_{0:N})) \\ \boldsymbol{\rho}^\circ_k(\boldsymbol{\lambda}_{0:N}, \boldsymbol{u}^*_{0:N}(\boldsymbol{\lambda}_{0:N})) \end{bmatrix}.$$

Now since we have established the optimal trajectories of $\boldsymbol{u}_{0:N}$, $\boldsymbol{x}_{0:N}$, and $\boldsymbol{\rho}_{1:N+1}$ as a function of $\boldsymbol{\lambda}_{0:N}$, we can now formulate the closed-form expression of $G(\boldsymbol{\lambda}_{0:N})$. First, we multiply both sides of (5.13), the partial derivative of the Hessian with respect to the states,

by $\frac{1}{2}(\boldsymbol{x}_k^*)^T$:

$$\begin{aligned}\frac{1}{2}(\boldsymbol{x}_k^*)^T\frac{\partial \mathcal{H}_k}{\partial \boldsymbol{x}_k^*} =&(\boldsymbol{x}_k^*)^T\boldsymbol{X}_k\boldsymbol{x}_k^* + (\boldsymbol{x}_k^*)^T\boldsymbol{\Omega}_k\boldsymbol{u}_k^* + (\boldsymbol{x}_k^*)^T\boldsymbol{\Lambda}_k + \frac{1}{2}(\boldsymbol{x}_k^*)^T\boldsymbol{A}_k^T\boldsymbol{\rho}_{k+1}^*\\ =&(\boldsymbol{\xi}_k^*)^T\boldsymbol{\Pi}_k\boldsymbol{\xi}_k^* - (\boldsymbol{u}_k^*)^T\boldsymbol{\Omega}_k^T\boldsymbol{x}_k^* - (\boldsymbol{u}_k^*)^T\boldsymbol{Z}_k\boldsymbol{u}_k^* + \frac{1}{2}(\boldsymbol{\rho}_{k+1}^*)^T\left(\frac{\partial \mathcal{H}_k}{\partial \boldsymbol{\rho}_{k+1}^*} - \boldsymbol{B}_k\boldsymbol{u}_k^* - \boldsymbol{a}_k\right)\\ &- 2(\boldsymbol{u}_k^*)^T\boldsymbol{\Xi}_k - \boldsymbol{\Lambda}_k^T\boldsymbol{x}_k^* - Y_k.\end{aligned}$$

Gathering terms, and then using the relation $\boldsymbol{\Sigma}_k\boldsymbol{u}_k^* = \left(2\boldsymbol{\Omega}_k^T\boldsymbol{x}_k^* + \boldsymbol{B}_k^T\boldsymbol{\rho}_{k+1}^* + 2\boldsymbol{\Xi}_k\right)$ from (5.16), we have:

$$\begin{aligned}\frac{1}{2}(\boldsymbol{x}_k^*)^T\frac{\partial \mathcal{H}_k}{\partial \boldsymbol{x}_k^*} =&(\boldsymbol{\xi}_k^*)^T\boldsymbol{\Pi}_k\boldsymbol{\xi}_k^* - (\boldsymbol{u}_k^*)^T\boldsymbol{Z}_k\boldsymbol{u}_k^* - \frac{1}{2}(\boldsymbol{u}_k^*)^T\left(2\boldsymbol{\Omega}_k^T\boldsymbol{x}_k^* + \boldsymbol{B}_k^T\boldsymbol{\rho}_{k+1}^* + 2\boldsymbol{\Xi}_k\right)\\ &+ \frac{1}{2}(\boldsymbol{\rho}_{k+1}^*)^T\left(\frac{\partial \mathcal{H}_k}{\partial \boldsymbol{\rho}_{k+1}^*} - \boldsymbol{a}_k\right) - (\boldsymbol{u}_k^*)^T\boldsymbol{\Xi}_k - \boldsymbol{\Lambda}_k^T\boldsymbol{x}_k^* - Y_k\\ =&(\boldsymbol{\xi}_k^*)^T\boldsymbol{\Pi}_k\boldsymbol{\xi}_k^* - (\boldsymbol{u}_k^*)^T\boldsymbol{Z}_k\boldsymbol{u}_k^* + \frac{1}{2}(\boldsymbol{u}_k^*)^T\boldsymbol{\Sigma}_k\boldsymbol{u}_k^* + \frac{1}{2}(\boldsymbol{\rho}_{k+1}^*)^T\left(\frac{\partial \mathcal{H}_k}{\partial \boldsymbol{\rho}_{k+1}^*} - \boldsymbol{a}_k\right)\\ &- (\boldsymbol{u}_k^*)^T\boldsymbol{\Xi}_k - \boldsymbol{\Lambda}_k^T\boldsymbol{x}_k^* - Y_k\\ =&(\boldsymbol{\xi}_k^*)^T\boldsymbol{\Pi}_k\boldsymbol{\xi}_k^* + \frac{1}{2}(\boldsymbol{\rho}_{k+1}^*)^T\frac{\partial \mathcal{H}_k}{\partial \boldsymbol{\rho}_{k+1}^*} - \left(\frac{1}{2}(\boldsymbol{\rho}_{k+1}^*)^T\boldsymbol{a}_k + (\boldsymbol{u}^*)_k^T\boldsymbol{\Xi}_k + \boldsymbol{x}_k^*\boldsymbol{\Lambda}_k + Y_k\right).\end{aligned}$$

Solving for $(\boldsymbol{\xi}_k^*)^T\boldsymbol{\Pi}_k\boldsymbol{\xi}_k^*$, and using the relations in (5.13) and (5.14), we have that

$$\begin{aligned}(\boldsymbol{\xi}_k^*)^T\boldsymbol{\Pi}_k\boldsymbol{\xi}_k^* =&\frac{1}{2}(\boldsymbol{x}_k^*)^T\frac{\partial \mathcal{H}_k}{\partial \boldsymbol{x}_k^*} - \frac{1}{2}(\boldsymbol{\rho}_{k+1}^*)^T\frac{\partial \mathcal{H}_k}{\partial \boldsymbol{\rho}_{k+1}^*} + \left(\frac{1}{2}\boldsymbol{a}_k^T\boldsymbol{\rho}_{k+1}^* + \boldsymbol{\Xi}_k^T\boldsymbol{u}_k^* + \boldsymbol{\Lambda}^T\boldsymbol{x}_k^* + Y_k\right)\\ =&\frac{1}{2}(\boldsymbol{x}_k^*)^T\boldsymbol{\rho}_k^* - \frac{1}{2}(\boldsymbol{\rho}_{k+1}^*)^T\boldsymbol{x}_{k+1}^* + \left(\frac{1}{2}\boldsymbol{a}_k^T\boldsymbol{\rho}_{k+1}^* + \boldsymbol{\Xi}_k^T\boldsymbol{u}_k^* + \boldsymbol{\Lambda}_k^T\boldsymbol{x}_k^* + Y_k\right).\end{aligned} \tag{5.18}$$

Now, we plug relations (5.18), (5.13), and (5.14) into (4.8) to derive the dual function $G(\boldsymbol{\lambda}_{0:N})$, and then from Theorem 5.1, we have that:

$$G(\boldsymbol{\lambda}_{0:N}) = \begin{cases}\frac{1}{2}\boldsymbol{x}_0^T\boldsymbol{\rho}_0^* + \sum_{i=1}^{p}\nu_0^i\gamma^iE_0^i + \sum_{k=0}^{N}(\boldsymbol{\lambda}_k^L)^T\boldsymbol{E}_L & \\ \qquad - (\boldsymbol{\lambda}_k^U)^T\boldsymbol{E}_U + \frac{1}{2}\boldsymbol{a}_k^T\boldsymbol{\rho}_{k+1}^* + \boldsymbol{\Xi}_k^T\boldsymbol{u}_k^* + \boldsymbol{\Lambda}_k^T\boldsymbol{x}_k^* + Y_k, & \boldsymbol{\lambda}_{0:N} \in \mathbb{G}(\boldsymbol{x}_0, \boldsymbol{a})\\ -\infty, & \text{else.}\end{cases} \tag{5.19}$$

5.3.2 Decoupling the Two-Point Boundary Value Problem

In this section, we present a method to decouple the two-point boundary value problem (5.17) through a change-of-basis, which provides of means of efficiently calculating $\boldsymbol{u}^*_{0:N}$, $\boldsymbol{x}^*_{1:N+1}$, and $\boldsymbol{\rho}^*_{1:N+1}$. First, we substitute $\boldsymbol{u}^*_k$, which is defined in (5.16), into (5.17) as:

$$\begin{bmatrix} \boldsymbol{x}^*_{k+1} \\ \boldsymbol{\rho}^*_k \end{bmatrix} = \begin{bmatrix} \boldsymbol{T}_{11,k} & \boldsymbol{T}_{12,k} \\ \boldsymbol{T}_{21,k} & \boldsymbol{T}^T_{11,k} \end{bmatrix} \begin{bmatrix} \boldsymbol{x}^*_k \\ \boldsymbol{\rho}^*_{k+1} \end{bmatrix} + \begin{bmatrix} \boldsymbol{W}_{1,k} \\ \boldsymbol{W}_{2,k} \end{bmatrix}, \qquad \begin{bmatrix} \boldsymbol{x}^*_0 \\ \boldsymbol{\rho}^*_{N+1} \end{bmatrix} = \begin{bmatrix} \boldsymbol{x}_0 \\ 2\boldsymbol{P}_{N+1} \end{bmatrix}, \tag{5.20}$$

where

$$\begin{aligned} \boldsymbol{T}_{11,k} =& \boldsymbol{A}_k - 2\boldsymbol{B}_k\boldsymbol{\Sigma}_k^{-1}\boldsymbol{\Omega}_k^T, & \boldsymbol{W}_{1,k} =& \boldsymbol{a}_k - 2\boldsymbol{B}_k\boldsymbol{\Sigma}_k^{-1}\boldsymbol{\Xi}_k \\ \boldsymbol{T}_{12,k} =& -\boldsymbol{B}_k\boldsymbol{\Sigma}_k^{-1}\boldsymbol{B}_k^T, & \boldsymbol{W}_{2,k} =& 2\boldsymbol{\Omega}_k - 4\boldsymbol{\Omega}\boldsymbol{\Sigma}_k^{-1}\boldsymbol{\Xi}_k \\ \boldsymbol{T}_{21,k} =& 2\boldsymbol{X}_k - 4\boldsymbol{\Omega}_k\boldsymbol{\Sigma}_k^{-1}\boldsymbol{\Omega}_k^T. \end{aligned} \tag{5.21}$$

Let $\tilde{\boldsymbol{\rho}}_{k+1}$ be the altered costate, which we define as:

$$\begin{aligned} \tilde{\boldsymbol{\rho}}_{k+1} =& \boldsymbol{\rho}^*_{k+1} - \boldsymbol{\Delta}_k x^*_{k+1} \\ =& \left(\boldsymbol{I} - \boldsymbol{\Delta}_k\boldsymbol{T}_{12,k}\right)\boldsymbol{\rho}^*_{k+1} - \boldsymbol{\Delta}_k\boldsymbol{T}_{11,k}\boldsymbol{x}^*_k - \boldsymbol{\Delta}_k\boldsymbol{W}_{1,k}, \end{aligned} \tag{5.22}$$

where $\{\boldsymbol{\Delta}_0, \boldsymbol{\Delta}_1, \ldots, \boldsymbol{\Delta}_N\}$ is a series of $n \times n$ matrices, and the second equality is derived using the relation $\boldsymbol{x}^*_{k+1} = \boldsymbol{T}_{11,k}\boldsymbol{x}^*_k + \boldsymbol{T}_{12,k}\boldsymbol{\rho}^*_{k+1} + \boldsymbol{W}_{1,k}$ in (5.20). We define the final condition as $\tilde{\boldsymbol{\rho}}_{N+1} = 0$ by letting $\boldsymbol{\Delta}_N = 2\boldsymbol{P}_{N+1}$, i.e.,

$$\begin{aligned} \tilde{\boldsymbol{\rho}}_{N+1} &= \boldsymbol{\rho}^*_{N+1} - \boldsymbol{\Delta}_N\boldsymbol{x}^*_{N+1} \\ &= \left(2\boldsymbol{P}_{N+1} - \boldsymbol{\Delta}_N\right)\boldsymbol{x}^*_{N+1} \\ &= 0. \end{aligned}$$

Solving for $\boldsymbol{\rho}^*_{k+1}$ in equation (5.22), we have:

$$\boldsymbol{\rho}^*_{k+1} = \left(\boldsymbol{I} - \boldsymbol{\Delta}_k\boldsymbol{T}_{12,k}\right)^{-1}\left(\tilde{\boldsymbol{\rho}}_{k+1} + \boldsymbol{\Delta}_k\boldsymbol{T}_{11,k}\boldsymbol{x}^*_k + \boldsymbol{\Delta}_k\boldsymbol{W}_{1,k}\right).$$

Then, $\tilde{\boldsymbol{\rho}}_k$ is defined as $\tilde{\boldsymbol{\rho}}_k = \boldsymbol{\rho}^*_k - \boldsymbol{\Delta}_{k-1}\boldsymbol{x}^*_k$, and we use relations in (5.20) to expand $\tilde{\boldsymbol{\rho}}_k$ as:

$$\begin{aligned} \tilde{\boldsymbol{\rho}}_k = &\left(\boldsymbol{T}_{21,k} + \boldsymbol{T}^T_{11,k}\left(\boldsymbol{I} - \boldsymbol{\Delta}_k\boldsymbol{T}_{12,k}\right)^{-1}\boldsymbol{\Delta}_k\boldsymbol{T}_{11,k} - \boldsymbol{\Delta}_{k-1}\right)\boldsymbol{x}^*_k \\ &+ \boldsymbol{T}^T_{11,k}\left(\boldsymbol{I} - \boldsymbol{\Delta}_k\boldsymbol{T}_{12,k}\right)^{-1}\tilde{\boldsymbol{\rho}}_{k+1} + \boldsymbol{T}^T_{11,k}\left(\boldsymbol{I} - \boldsymbol{\Delta}_k\boldsymbol{T}_{12,k}\right)^{-1}\boldsymbol{\Delta}_k\boldsymbol{W}_{1,k} + \boldsymbol{W}_{2,k}. \end{aligned}$$

We force $\boldsymbol{\Delta}_k$ to evolve backwards according to the following difference equation:

$$\boldsymbol{\Delta}_{k-1} = \boldsymbol{T}_{21,k} + \boldsymbol{T}_{11,k}^T \left(\boldsymbol{I} - \boldsymbol{\Delta}_k \boldsymbol{T}_{12,k}\right)^{-1} \boldsymbol{\Delta}_k \boldsymbol{T}_{11,k}, \tag{5.23}$$

with final condition $\boldsymbol{\Delta}_N = 2P_{N+1}$. We decouple the altered costate from the state as:

$$\tilde{\boldsymbol{\rho}}_k = \boldsymbol{T}_{11,k}^T \left(\boldsymbol{I} - \boldsymbol{\Delta}_k \boldsymbol{T}_{12,k}\right)^{-1} \tilde{\boldsymbol{\rho}}_{k+1} + \boldsymbol{T}_{11,k}^T \left(\boldsymbol{I} - \boldsymbol{\Delta}_k \boldsymbol{T}_{12,k}\right)^{-1} \boldsymbol{\Delta}_k \boldsymbol{W}_{1,k} + \boldsymbol{W}_{2,k}. \tag{5.24}$$

Now, we rewrite (5.20) as a time-varying, decoupled linear system as:

$$\begin{bmatrix} \boldsymbol{x}_{k+1}^* \\ \tilde{\boldsymbol{\rho}}_k \end{bmatrix} = \begin{bmatrix} \tilde{\boldsymbol{T}}_{11,k} & \tilde{\boldsymbol{T}}_{12,k} \\ \boldsymbol{0} & \tilde{\boldsymbol{T}}_{11,k}^T \end{bmatrix} \begin{bmatrix} \boldsymbol{x}_k^* \\ \tilde{\boldsymbol{\rho}}_{k+1} \end{bmatrix} + \begin{bmatrix} \tilde{\boldsymbol{W}}_{1,k} \\ \tilde{\boldsymbol{W}}_{2,k} \end{bmatrix}, \qquad \begin{bmatrix} \boldsymbol{x}_0^* \\ \tilde{\boldsymbol{\rho}}_{N+1} \end{bmatrix} = \begin{bmatrix} \boldsymbol{x}_0 \\ 0 \end{bmatrix}, \tag{5.25}$$

where

$$\begin{aligned} \tilde{\boldsymbol{T}}_{11,k} &= \left(\boldsymbol{I} - \boldsymbol{T}_{12,k}\boldsymbol{\Delta}_k\right)^{-1} \boldsymbol{T}_{11,k}, \quad \tilde{\boldsymbol{W}}_{1,k} = \left(\boldsymbol{I} - \boldsymbol{T}_{12,k}\boldsymbol{\Delta}_k\right)^{-1} \boldsymbol{W}_{k,1} \\ \tilde{\boldsymbol{T}}_{12,k} &= \left(\boldsymbol{I} - \boldsymbol{T}_{12,k}\boldsymbol{\Delta}_k\right)^{-1} \boldsymbol{T}_{12,k}, \quad \tilde{\boldsymbol{W}}_{k,2} = \boldsymbol{T}_{22,k} \left(\boldsymbol{I} - \boldsymbol{\Delta}_k \boldsymbol{T}_{12,k}\right)^{-1} \left(\boldsymbol{\Delta}_k \boldsymbol{W}_{1,k}\right) + \boldsymbol{W}_{2,k}. \end{aligned} \tag{5.26}$$

We can expand the difference equation for $\boldsymbol{\Delta}_{k-1}$ in (5.23) using (5.21) and the Matrix Inversion Lemma (see Theorem 2.1) as:

$$\begin{aligned} \boldsymbol{\Delta}_{k-1} &= \left(2\boldsymbol{X}_k - 4\boldsymbol{\Omega}_k \boldsymbol{\Sigma}_k^{-1} \boldsymbol{\Omega}_k^T\right) \\ &\qquad + \left(\boldsymbol{A}_k^T - 2\boldsymbol{\Omega}_k \boldsymbol{\Sigma}_k^{-1} \boldsymbol{B}_k^T\right) \left(\boldsymbol{I} + \boldsymbol{\Delta}_k \boldsymbol{B}_k \boldsymbol{\Sigma}_k^{-1} \boldsymbol{B}_k^T\right)^{-1} \boldsymbol{\Delta}_k \left(\boldsymbol{A}_k - 2\boldsymbol{B}_k \boldsymbol{\Sigma}_k^{-1} \boldsymbol{\Omega}_k^T\right) \\ &= \left(2\boldsymbol{X}_k - 4\boldsymbol{\Omega}_k \boldsymbol{\Sigma}_k^{-1} \boldsymbol{\Omega}_k^T\right) \\ &\qquad + \left(\boldsymbol{A}_k^T - 2\boldsymbol{\Omega}_k \boldsymbol{\Sigma}_k^{-1} \boldsymbol{B}_k^T\right) \left(\boldsymbol{I} - \boldsymbol{\Delta}_k \boldsymbol{B}_k \boldsymbol{\Upsilon}^{-1} \boldsymbol{B}_k^T\right) \boldsymbol{\Delta}_k \left(\boldsymbol{A}_k - 2\boldsymbol{B}_k \boldsymbol{\Sigma}_k^{-1} \boldsymbol{\Omega}_k^T\right), \end{aligned}$$

where we let $\boldsymbol{\Upsilon}_k$ be the following $m \times m$ matrix:

$$\boldsymbol{\Upsilon}_k = \boldsymbol{\Sigma}_k + \boldsymbol{B}_k^T \boldsymbol{\Delta}_k \boldsymbol{B}_k. \tag{5.27}$$

Expanding the second term in the above equation:

$$\begin{aligned}\boldsymbol{\Delta}_{k-1} = &\left(2\boldsymbol{X}_k - 4\boldsymbol{\Omega}_k\boldsymbol{\Sigma}_k^{-1}\boldsymbol{\Omega}_k^T\right) + \left(\boldsymbol{A}_k^T - 2\boldsymbol{\Omega}_k\boldsymbol{\Sigma}_k^{-1}\boldsymbol{B}_k^T\right)\boldsymbol{\Delta}_k\left(\boldsymbol{A}_k - 2\boldsymbol{B}_k\boldsymbol{\Sigma}_k^{-1}\boldsymbol{\Omega}_k^T\right)\\ -&\boldsymbol{A}_k^T\boldsymbol{\Delta}_k\boldsymbol{B}_d\left(\boldsymbol{\Sigma}_k + \boldsymbol{B}_k^T\boldsymbol{\Delta}_k\boldsymbol{B}_k\right)^{-1}\boldsymbol{B}_k^T\boldsymbol{\Delta}_k\boldsymbol{A}_k + 2\boldsymbol{A}_k^T\boldsymbol{\Delta}_k\boldsymbol{B}_k\left(\boldsymbol{\Sigma}_k + \boldsymbol{B}_k^T\boldsymbol{\Delta}_k\boldsymbol{B}_k\right)^{-1}\boldsymbol{B}_k^T\boldsymbol{\Delta}_k\boldsymbol{B}_k\boldsymbol{\Sigma}_k^{-1}\boldsymbol{\Omega}_k^T\\ &+ 2\boldsymbol{\Omega}_k\boldsymbol{\Sigma}_k^{-1}\boldsymbol{B}_k^T\boldsymbol{\Delta}_k\boldsymbol{B}_k\left(\boldsymbol{\Sigma}_k + \boldsymbol{B}_k^T\boldsymbol{\Delta}_k\boldsymbol{B}_k\right)^{-1}\boldsymbol{B}_k^T\boldsymbol{\Delta}_k\boldsymbol{A}_k\\ &- 4\boldsymbol{\Omega}_k\boldsymbol{\Sigma}_k^{-1}\boldsymbol{B}_k^T\boldsymbol{\Delta}_k\boldsymbol{B}_k\left(\boldsymbol{\Sigma}_k + \boldsymbol{B}_k^T\boldsymbol{\Delta}_k\boldsymbol{B}_k\right)^{-1}\boldsymbol{B}_k^T\boldsymbol{\Delta}_k\boldsymbol{B}_k\boldsymbol{\Sigma}_k^{-1}\boldsymbol{\Omega}_k^T,\end{aligned}$$

and then adding a zero matrix ($\boldsymbol{\Sigma}_k - \boldsymbol{\Sigma}_k = \mathbf{0}$) in strategic places results in:

$$\begin{aligned}\boldsymbol{\Delta}_{k-1} = &\left(2\boldsymbol{X}_k - 4\boldsymbol{\Omega}_k\boldsymbol{\Sigma}_k^{-1}\boldsymbol{\Omega}_k^T\right) + \left(\boldsymbol{A}_k^T - 2\boldsymbol{\Omega}_k\boldsymbol{\Sigma}_k^{-1}\boldsymbol{B}_k^T\right)\boldsymbol{\Delta}_k\left(\boldsymbol{A}_k - 2\boldsymbol{B}_k\boldsymbol{\Sigma}_k^{-1}\boldsymbol{\Omega}_k^T\right)\\ &- \boldsymbol{A}_j^T\boldsymbol{\Delta}_j\boldsymbol{B}_k\left(\boldsymbol{\Sigma}_j + \boldsymbol{B}_k^T\boldsymbol{\Delta}_j\boldsymbol{B}_j\right)^{-1}\boldsymbol{B}_j^T\boldsymbol{\Delta}_j\boldsymbol{A}_j\\ &+ 2\boldsymbol{A}_j^T\boldsymbol{\Delta}_j\boldsymbol{B}_j\left(\boldsymbol{\Sigma}_j + \boldsymbol{B}_j^T\boldsymbol{\Delta}_j\boldsymbol{B}_j\right)^{-1}\left(-\boldsymbol{\Sigma}_j + \boldsymbol{\Sigma}_j + \boldsymbol{B}_j^T\boldsymbol{\Delta}_j\boldsymbol{B}_j\right)\boldsymbol{\Sigma}_j^{-1}\boldsymbol{\Omega}_j^T\\ &+ 2\boldsymbol{\Omega}_j\boldsymbol{\Sigma}_j^{-1}\left(-\boldsymbol{\Sigma}_j + \boldsymbol{\Sigma}_j + \boldsymbol{B}_j^T\boldsymbol{\Delta}_j\boldsymbol{B}_j\right)\left(\boldsymbol{\Sigma}_j + \boldsymbol{B}_j^T\boldsymbol{\Delta}_j\boldsymbol{B}_j\right)^{-1}\boldsymbol{B}_j^T\boldsymbol{\Delta}_j\boldsymbol{A}_j\\ &- 4\boldsymbol{\Omega}_j\boldsymbol{\Sigma}_j^{-1}\left(-\boldsymbol{\Sigma}_j + \boldsymbol{\Sigma}_j + \boldsymbol{B}_j^T\boldsymbol{\Delta}_j\boldsymbol{B}_j\right)\left(\boldsymbol{\Sigma}_j + \boldsymbol{B}_j^T\boldsymbol{\Delta}_j\boldsymbol{B}_j\right)^{-1}\left(-\boldsymbol{\Sigma}_j + \boldsymbol{\Sigma}_j + \boldsymbol{B}_j^T\boldsymbol{\Delta}_j\boldsymbol{B}_j\right)\boldsymbol{\Sigma}_j^{-1}\boldsymbol{\Omega}_j^T\end{aligned}$$

Finally, collecting and cancelling terms results in the following:

$$\boldsymbol{\Delta}_{k-1} = \boldsymbol{A}_k^T\boldsymbol{\Delta}_k\boldsymbol{A}_k - \left(\boldsymbol{A}_k^T\boldsymbol{\Delta}_k\boldsymbol{B}_k + 2\boldsymbol{\Omega}_k^T\right)\left(\boldsymbol{\Sigma}_k + \boldsymbol{B}_k^T\boldsymbol{\Delta}_k\boldsymbol{B}_k\right)^{-1}\left(\boldsymbol{B}_k^T\boldsymbol{\Delta}_k\boldsymbol{A}_k + 2\boldsymbol{\Omega}_k\right) + 2\boldsymbol{X}_k. \tag{5.28}$$

Therefore, the series of $n \times n$ matrices $\{\boldsymbol{\Delta}_0, \boldsymbol{\Delta}_1, \ldots, \boldsymbol{\Delta}_N\}$ evolve according to the above Riccati difference equation.

5.3.3 Formulating the Dual Gradient and Hessian

Let the performance measure $\hat{J}'_\rho$ be:

$$\hat{J}'_\rho(\boldsymbol{u}_{0:N}, \boldsymbol{x}_{0:N+1}, \boldsymbol{\nu}_{0:N}, \boldsymbol{\rho}_{1:N+1}) = J'_\rho(\boldsymbol{u}_{0:N}, \boldsymbol{x}_{0:N+1}, \boldsymbol{\lambda}_{0:N}, \boldsymbol{\rho}_{1:N+1}) - \sum_{k=0}^{N}\left((\boldsymbol{\lambda}_k^L)^T\boldsymbol{E}_L - (\boldsymbol{\lambda}_k^U)^T\boldsymbol{E}_U\right),$$

and then $\hat{G}(\cdot)$ is:

$$\hat{G}(\boldsymbol{\nu}_{0:N}) = \sup_{\boldsymbol{p}_{1:N+1}} \inf_{\boldsymbol{u}_{0:N},\, \boldsymbol{x}_{0:N+1}} \hat{J}'_\rho(\boldsymbol{u}_{0:N}, \boldsymbol{x}_{0:N+1}, \boldsymbol{\nu}_{0:N}, \boldsymbol{\rho}_{1:N+1}), \tag{5.29}$$

and the $((j-1)p+i)^{th}$ element of the gradient of $\hat{G}(\cdot)$ is:

$$\frac{\partial \hat{G}}{\partial \nu_j^i} = \frac{\partial \hat{J}'_\rho}{\partial \nu_j^i} + \sum_{k=1}^{N} \frac{\partial \hat{J}'_\rho}{\partial \boldsymbol{x}_k^*} \frac{\partial \boldsymbol{x}_k^*}{\partial \nu_j^i} + \sum_{k=0}^{N} \frac{\partial \hat{J}'_\rho}{\partial \boldsymbol{u}_k^*} \frac{\partial \boldsymbol{u}_k^*}{\partial \nu_j^i} + \sum_{k=0}^{N-1} \frac{\partial \hat{J}'_\rho}{\partial \boldsymbol{\rho}_{k+1}^*} \frac{\partial \boldsymbol{\rho}_{k+1}^*}{\partial \nu_j^i}.$$

From classic Euler-Lagrange theory [15] and (5.29), we know that $\boldsymbol{x}_k^*(\boldsymbol{\nu}_{0:N})$, $\boldsymbol{u}_k^*(\boldsymbol{\nu}_{0:N})$, and $\boldsymbol{\rho}_k^*(\boldsymbol{\nu}_{0:N})$ are at their optimums, so it follows that:

$$\frac{\partial \hat{J}'_\rho}{\partial \boldsymbol{x}_k^*} = 0, \quad \forall k \in \{1...N\}, \quad \frac{\partial \hat{J}'_\rho}{\partial \boldsymbol{u}_k^*} = 0, \quad \forall k \in \{0...N\}, \quad \frac{\partial \hat{J}'_\rho}{\partial \boldsymbol{\rho}_{k+1}^*} = 0, \quad \forall k \in \{0...N-1\}.$$

Then, the $((j-1)p+i)^{th}$ element of the gradient of $\hat{G}(\cdot)$ is:

$$\frac{\partial \hat{G}}{\partial \nu_j^i} = \frac{\partial \hat{J}'_\rho}{\partial \nu_j^i} = \delta_{j0}\gamma^i E_0^i + \begin{bmatrix} \boldsymbol{x}_j^* \\ \boldsymbol{u}_j^* \\ 1 \end{bmatrix}^T \begin{bmatrix} \frac{\partial \boldsymbol{X}_j}{\partial \nu_j^i} & \frac{\partial \boldsymbol{\Omega}_j}{\partial \nu_j^i} & \frac{\partial \boldsymbol{\Lambda}_j}{\partial \nu_j^i} \\ \left(\frac{\partial \boldsymbol{\Omega}_j}{\partial \nu_j^i}\right)^T & \frac{\partial \boldsymbol{Z}_j}{\partial \nu_j^i} & \frac{\partial \boldsymbol{\Xi}_j}{\partial \nu_j^i} \\ \left(\frac{\partial \boldsymbol{\Lambda}_j}{\partial \nu_j^i}\right)^T & \left(\frac{\partial \boldsymbol{\Xi}_j}{\partial \nu_j^i}\right)^T & \frac{\partial \boldsymbol{Y}_j}{\partial \nu_j^i} \end{bmatrix} \begin{bmatrix} \boldsymbol{x}_j^* \\ \boldsymbol{u}_j^* \\ 1 \end{bmatrix},$$

where δ_{j0} is the Kronecker delta, and where:

$$\frac{\partial \boldsymbol{X}_k}{\partial \nu_j^i} = \begin{cases} -(\boldsymbol{C}_{E,k}^i)^T \boldsymbol{M}_{yy,k}^i \boldsymbol{C}_{E,k}^i, & j = k \\ 0, & j \neq k \end{cases}$$

$$\frac{\partial \boldsymbol{\Omega}_k}{\partial \nu_k^i} = \begin{cases} -\left(\frac{1}{2}(\boldsymbol{C}_{E,k}^i)^T + (\boldsymbol{C}_{E,k}^i)^T \boldsymbol{M}_{uy,k}^i + (\boldsymbol{C}_{E,k}^i)^T \boldsymbol{M}_{yy,k}^i \boldsymbol{D}_{E,k}^i\right), & j = k \\ 0, & j \neq k \end{cases}$$

$$\frac{\partial \boldsymbol{\Lambda}_k}{\partial \nu_j^i} = \begin{cases} -(\boldsymbol{C}_{E,k}^i)^T \boldsymbol{M}_{yy,k}^i \boldsymbol{a}_{E,k}^i, & j = k \\ 0, & j \neq k \end{cases}$$

$$\frac{\partial \boldsymbol{Z}_k}{\partial \nu_j^i} = \begin{cases} -\left((\boldsymbol{D}_{E,k}^i)^T + \boldsymbol{M}_{uu,k}^i + \boldsymbol{M}_{uy,k} \boldsymbol{D}_{E,k}^i + (\boldsymbol{D}_{E,k}^i)^T \boldsymbol{M}_{yy,k}^i \boldsymbol{D}_{E,k}^i\right), & j = k \\ 0, & j \neq k \end{cases}$$

$$\frac{\partial \boldsymbol{\Xi}_k}{\partial \nu_j^i} = \begin{cases} -\left(\frac{1}{2}\boldsymbol{I} + \boldsymbol{M}_{uy,k}^i + (\boldsymbol{D}_{E,k}^i)^T \boldsymbol{M}_{yy,k}^i\right) \boldsymbol{a}_{E,k}^i, & j = k \\ 0, & j \neq k \end{cases}$$

$$\frac{\partial Y_k}{\partial \nu_j^i} = \begin{cases} -(\boldsymbol{a}_{E,k}^i)^T \boldsymbol{M}_{yy,k}^i \boldsymbol{a}_{E,k}^i, & j = k. \\ 0, & j \neq k \end{cases}$$

Note that we can then rewrite $\frac{\partial \hat{G}}{\partial \nu_j^i}$ in terms of variable $(\boldsymbol{y}_j^i)^* = \boldsymbol{C}_{E,j}^i \boldsymbol{x}_j^* + \boldsymbol{D}_{E,j}^i \boldsymbol{u}_j^* + \boldsymbol{a}_{E,j}^i$ as:

$$\frac{\partial \hat{G}}{\partial \nu_j^i} = \delta_{j0} \gamma^i E_0^i - (\boldsymbol{u}_j^*)^T (\boldsymbol{y}_j^i)^* - \mu_j(\boldsymbol{u}_j^*, (\boldsymbol{y}_j^i)^*).$$

The $((k-1)p+h, (j-1)p+1)^{th}$ element of the Hessian is:

$$\frac{\partial^2 \hat{G}}{\partial \nu_k^h \nu_j^i} = 2 \begin{bmatrix} \boldsymbol{x}_j^* \\ \boldsymbol{u}_j^* \\ 1 \end{bmatrix}^T \begin{bmatrix} \frac{\partial \boldsymbol{X}_j}{\partial \nu_j^i} & \frac{\partial \boldsymbol{\Omega}_j}{\partial \nu_j^i} \\ \left(\frac{\partial \boldsymbol{\Omega}_j}{\partial \nu_j^i}\right)^T & \frac{1}{2}\frac{\partial \boldsymbol{\Sigma}_j}{\partial \nu_j^i} \\ \left(\frac{\partial \boldsymbol{\Lambda}_j}{\partial \nu_j^i}\right)^T & \left(\frac{\partial \boldsymbol{\Xi}_j}{\partial \nu_j^i}\right)^T \end{bmatrix} \begin{bmatrix} \frac{\partial \boldsymbol{x}_j^*}{\partial \nu_k^h} \\ \frac{\partial \boldsymbol{u}_j^*}{\partial \nu_k^h} \\ 1 \end{bmatrix}.$$

The derivative of the optimal control input $\boldsymbol{u}_j^*$ with respect to ν_k^h is:

$$\frac{\partial \boldsymbol{u}_j^*}{\partial \nu_k^h} = \begin{cases} -\boldsymbol{\Sigma}_j^{-1} \left(2\boldsymbol{\Omega}_j^T \frac{\partial \boldsymbol{x}_j^*}{\partial \nu_k^h} + \boldsymbol{B}_j^T \frac{\partial \boldsymbol{\rho}_{j+1}^*}{\partial \nu_k^h}\right), & k \neq j \\ \boldsymbol{\Sigma}_j^{-1} \left(\frac{\partial \boldsymbol{\Sigma}_j}{\partial \nu_k^h}\right) \boldsymbol{\Sigma}_j^{-1} \left(2\boldsymbol{\Omega}_j^T \boldsymbol{x}_j^* + \boldsymbol{B}_j^T \boldsymbol{\rho}_{j+1}^* + 2\boldsymbol{\Xi}_j\right) & \\ \quad -\boldsymbol{\Sigma}_j^{-1} \left(2\frac{\partial \boldsymbol{\Omega}_j^T}{\partial \nu_k^h} \boldsymbol{x}_j^* + 2\boldsymbol{\Omega}_j^T \frac{\partial \boldsymbol{x}_j^*}{\partial \nu_k^h} + \boldsymbol{B}_j^T \frac{\partial \boldsymbol{\rho}_{j+1}^*}{\partial \nu_k^h} + 2\frac{\partial \boldsymbol{\Xi}_j}{\partial \nu_k^h}\right), & k = j, \end{cases}.$$

To solve for $\frac{\partial \boldsymbol{x}_j^*}{\partial \nu_k^h}$ and $\frac{\partial \boldsymbol{\rho}_j^*}{\partial \nu_k^h}$, we take the derivative of (5.20) with respect to ν_k^h, and solve the resulting two-point boundary value problem:

$$\begin{bmatrix} \frac{\partial \boldsymbol{x}_{j+1}^*}{\partial \nu_k^h} \\ \frac{\partial \boldsymbol{\rho}_j^*}{\partial \nu_k^h} \end{bmatrix} = \begin{bmatrix} \boldsymbol{T}_{11,} & \boldsymbol{T}_{12,j} \\ \boldsymbol{T}_{21,j} & \boldsymbol{T}_{11,j}^T \end{bmatrix} \begin{bmatrix} \frac{\partial x_j^*}{\partial \nu_k^h} \\ \frac{\partial \rho_{j+1}^*}{\partial \nu_k^h} \end{bmatrix} + \left(\begin{bmatrix} \frac{\partial \boldsymbol{T}_{11,j}}{\partial \nu_k^h} & \frac{\partial \boldsymbol{T}_{12,j}}{\partial \nu_k^h} \\ \frac{\partial \boldsymbol{T}_{21,j}}{\partial \nu_k^h} & \frac{\partial \boldsymbol{T}_{11,j}^T}{\partial \nu_k^h} \end{bmatrix} \begin{bmatrix} \boldsymbol{x}_j^* \\ \boldsymbol{\rho}_{j+1}^* \end{bmatrix} + \begin{bmatrix} \frac{\partial \boldsymbol{W}_{1,j}}{\partial \nu_k^h} \\ \frac{\partial \boldsymbol{W}_{2,j}}{\partial \nu_k^h} \end{bmatrix} \right),$$

with:

$$\frac{\partial \boldsymbol{T}_{11,j}}{\partial \nu_k^h} = \begin{cases} 2\boldsymbol{B}_j\boldsymbol{\Sigma}_j^{-1}\frac{\partial \boldsymbol{\Sigma}_j}{\partial \nu_k^h}\boldsymbol{\Sigma}_j^{-1}\boldsymbol{\Omega}_j^T - 2\boldsymbol{B}_j\boldsymbol{\Sigma}_j^{-1}\frac{\partial \boldsymbol{\Omega}_j^T}{\partial \nu_k^h}, & k = j \\ 0, & k \neq j \end{cases}$$

$$\frac{\partial \boldsymbol{T}_{12,j}}{\partial \nu_k^h} = \begin{cases} \boldsymbol{B}_j\boldsymbol{\Sigma}_j^{-1}\frac{\partial \boldsymbol{\Sigma}_j}{\partial \nu_k^h}\boldsymbol{\Sigma}_j^{-1}\boldsymbol{B}_j^T, & k = j \\ 0, & k \neq j \end{cases}$$

$$\frac{\partial \boldsymbol{T}_{21,j}}{\partial \nu_k^h} = \begin{cases} 2\frac{\partial \boldsymbol{X}_j}{\partial \nu_k^h} - 4\frac{\partial \boldsymbol{\Omega}_j}{\partial \nu_k^h}\boldsymbol{\Sigma}_j^{-1}\boldsymbol{\Omega}_j^T + 4\boldsymbol{\Omega}_j\boldsymbol{\Sigma}_j^{-1}\frac{\partial \boldsymbol{\Sigma}_j}{\partial \nu_k^h}\boldsymbol{\Sigma}_j^{-1}\boldsymbol{\Omega}_j^T - 4\boldsymbol{\Omega}_j\boldsymbol{\Sigma}_j^{-1}\frac{\partial \boldsymbol{\Omega}_j^T}{\partial \nu_k^h}, & k = j \\ 0, & k \neq j \end{cases}$$

and:

$$\frac{\partial \boldsymbol{W}_{1,j}}{\partial \nu_k^h} = \begin{cases} 2\boldsymbol{B}_j\boldsymbol{\Sigma}_j^{-1}\frac{\partial \boldsymbol{\Sigma}_j}{\partial \nu_k^h}\boldsymbol{\Sigma}_j^{-1}\boldsymbol{\Xi}_j - 2\boldsymbol{B}_j\boldsymbol{\Sigma}_j^{-1}\frac{\partial \boldsymbol{\Xi}_j}{\partial \nu_k^h}, & k = j \\ 0, & k \neq j \end{cases}$$

$$\frac{\partial \boldsymbol{W}_{2,j}}{\partial \nu_k^h} = \begin{cases} 2\frac{\partial \boldsymbol{\Omega}_j}{\partial \nu_k^h} - 4\frac{\partial \boldsymbol{\Omega}_j}{\partial \nu_k^h}\boldsymbol{\Sigma}_j^{-1}\boldsymbol{\Xi}_j + 4\boldsymbol{\Omega}_j\boldsymbol{\Sigma}_j^{-1}\frac{\partial \boldsymbol{\Sigma}_j}{\partial \nu_k^h}\boldsymbol{\Sigma}_j^{-1}\boldsymbol{\Xi}_j - 4\boldsymbol{\Omega}_j\boldsymbol{\Sigma}_j^{-1}\frac{\partial \boldsymbol{\Xi}_j}{\partial \nu_k^h}, & k = j. \\ 0, & k \neq j \end{cases}$$

Then, we can decouple this two point boundary value problem by using the same procedure as described in Section 5.3.2. Let:

$$\hat{\boldsymbol{\rho}}_{j+1,k}^h = \frac{\partial \boldsymbol{\rho}_{j+1}^*}{\partial \nu_k^h} - \boldsymbol{\Delta}_j\frac{\partial \boldsymbol{x}_{j+1}^*}{\partial \nu_k^h},$$

where if $\boldsymbol{\Delta}_j$ is defined as the backward Riccati equation in (5.23) with final condition $\boldsymbol{\Delta}_N = 2\boldsymbol{P}_{N+1}$, then the two-point boundary value problem decouples as:

$$\begin{bmatrix} \frac{\partial \boldsymbol{x}_{j+1}^*}{\partial \nu_k^h} \\ \hat{\boldsymbol{\rho}}_{j,k}^h \end{bmatrix} = \begin{bmatrix} \tilde{\boldsymbol{T}}_{11,j} & \tilde{\boldsymbol{T}}_{12,j} \\ \boldsymbol{0} & \tilde{\boldsymbol{T}}_{11,j}^T \end{bmatrix} \begin{bmatrix} \frac{\partial \boldsymbol{x}_j^*}{\partial \nu_k^h} \\ \hat{\boldsymbol{\rho}}_{j+1,k}^h \end{bmatrix} + \begin{bmatrix} (\boldsymbol{I} - \boldsymbol{T}_{12,j}\boldsymbol{\Delta}_j)^{-1} & \boldsymbol{0} \\ \tilde{\boldsymbol{T}}_{11,j}^T\boldsymbol{\Delta}_j & \boldsymbol{I} \end{bmatrix} \left(\begin{bmatrix} \frac{\partial \boldsymbol{T}_{11,j}}{\partial \nu_k^h} & \frac{\partial \boldsymbol{T}_{12,j}}{\partial \nu_k^h} \\ \frac{\partial \boldsymbol{T}_{21,j}}{\partial \nu_k^h} & \frac{\partial \boldsymbol{T}_{11,j}^T}{\partial \nu_k^h} \end{bmatrix} \begin{bmatrix} \boldsymbol{x}_j^* \\ \boldsymbol{\rho}_{j+1}^* \end{bmatrix} + \begin{bmatrix} \frac{\partial \boldsymbol{W}_{1,j}}{\partial \nu_k^h} \\ \frac{\partial \boldsymbol{W}_{2,j}}{\partial \nu_k^h} \end{bmatrix} \right),$$

where $\tilde{\boldsymbol{T}}_{11,j}$ and $\tilde{\boldsymbol{T}}_{12,j}$ are defined in (5.26).

5.4 Evaluating the Duality Gap

Now, we explore one of the most interesting questions in this analysis, which is whether the dual optimum exhibits a duality gap. Let $\boldsymbol{u}^p$ be the primal optimal input sequence, and $\boldsymbol{\lambda}^{dual}$ be the dual optimal Lagrange multiplier sequence. Then, when strong duality holds, we have that:

$$\boldsymbol{u}^p_{0:N} = \boldsymbol{u}^*_{0:N}(\boldsymbol{\lambda}^{dual}_{0:N}), \tag{5.30}$$

which implies that the (potentially nonconvex) primal problem is solved via its convex dual relaxation.

Corollary 5.1. *Let $\boldsymbol{H}(\boldsymbol{\lambda}_{0:N})$ be defined according to* (5.9)*. Then, the following statements are equivalent:*

1. $\boldsymbol{H}(\boldsymbol{\lambda}_{0:N}) \succ 0$
2. $\boldsymbol{\Upsilon}_k(\boldsymbol{\lambda}_{0:N}) = \boldsymbol{Z}_k + \boldsymbol{Z}_k^T - \boldsymbol{B}_k^T \boldsymbol{\Delta}_k \boldsymbol{B}_k \succ 0$, $\forall k \in \{0...N\}$, *where $\boldsymbol{\Delta}_k$ is the solution to Riccati equation in* (5.28) *with final value $\boldsymbol{\Delta}_N = 2\boldsymbol{P}_{N+1}$.*

Proof. The proof is analogous to the proof of Theorem 4.1, where instead we consider whether $\bar{J}'(\cdot,\cdot,\cdot)$ has a unique, finite minimum. □

Theorem 5.2. *If $\boldsymbol{\Upsilon}_k(\boldsymbol{\lambda}^{dual}_{0:N}) \succ 0$, $\forall k \in \{0...N\}$, as described in condition 2 of Corollary 5.1, then the duality gap is zero and* (5.30) *holds.*

Proof. Via Corollary 5.1, $\boldsymbol{H}(\boldsymbol{\lambda}^{dual}_{0:N}) \succ 0$ and then it follows that $\boldsymbol{\lambda}^{dual}_{0:N} \in \text{int}(\mathbb{G}(\boldsymbol{x}_0, \boldsymbol{a}))$. It is straight-forward to verify that $G(\boldsymbol{\lambda}_{0:N})$ is twice differentiable when not on the boundary of $\mathbb{G}(\boldsymbol{x}_0, \boldsymbol{a})$. Then, it is a classical result (see, e.g., [10]) that if a dual function is twice differentiable at its optimum, the duality gap is zero. □

Then, the duality gap can be checked by determining if the minimum singular values of the sequence $\boldsymbol{\Upsilon}_{0:N}(\boldsymbol{\lambda}^{dual}_{0:N})$ are uniformly positive; i.e., if there exists an $\epsilon > 0$ such that:

$$\boldsymbol{\Upsilon}_k(\boldsymbol{\lambda}^{dual}_{0:N}) - \epsilon \boldsymbol{I} \succ 0, \quad \forall k \in \{0...N\}. \tag{5.31}$$

Note that $\boldsymbol{\Upsilon}_{0:N}(\cdot)$ is also calculated in (5.27) of Section 5.3.2 when decoupling the states and costates, and then calculating the control inputs. When the dual optimal Lagrange multipliers $\boldsymbol{\lambda}^{dual}_{0:N}$ are determined, for a small computational cost, we can check the definiteness of these matrices to gain additional information on the primal optimality of this dual solution.

Because $\boldsymbol{\Upsilon}_k$ is an $m \times m$ matrix, for the case with $m = 1$, $\boldsymbol{\Upsilon}_k$ reduces to scalar value and we instead test its positiveness.

It is well-known (see, e.g., [10]) that if $\boldsymbol{\lambda}_{0:N}^{dual} \in \text{int}(\mathbb{G}(\boldsymbol{x}_0, \boldsymbol{a}))$ and there is a nonzero duality gap, then $G(\boldsymbol{\lambda}_{0:N})$ is not differentiable at $\boldsymbol{\lambda}_{0:N}^{dual}$. From inspection of (5.1), the dual function $G(\boldsymbol{\lambda}_{0:N})$ is differentiable with respect to all $\boldsymbol{\lambda}_{0:N} \in \mathbb{G}(\boldsymbol{x}_0, \boldsymbol{a})$. Therefore, if a nonzero duality gap exists, $\boldsymbol{\lambda}_{0:N}^{dual}$ is on the boundary of $\mathbb{G}(\boldsymbol{x}_0, \boldsymbol{a})$, i.e., $\boldsymbol{\lambda}_{0:N}^{dual} \in \partial\mathbb{G}(\boldsymbol{x}_0, \boldsymbol{a})$.

We can guarantee zero duality gap for any exogenous disturbance or initial condition for problems with special structures as shown in the Theorem below.

Theorem 5.3. *Consider a convex ECOCP, which satisfies Corollary 4.3. Then, if for each $i \in \{1...p\}$, either $E_L^i = 0$ or $\gamma^i = 1$, there is zero duality gap for all initial conditions $\boldsymbol{x}_0 \in \mathbb{R}^n$ and $\boldsymbol{E}_0 \in \mathbb{R}_E$, and for all exogenous disturbances $\boldsymbol{a} \in (\mathbb{L}^2)^d$.*

Proof. From Corollary 4.3, we assume that the upper energy constraints are inactive for all $k \in \{0...N\}$, and can therefore be excluded them from this analysis. We also assume that the system takes no action (i.e., $\boldsymbol{u}_0 = 0$) unless energy is available, so without loss of generality, let $\check{\boldsymbol{y}}_0^i = \boldsymbol{C}_{E,0}^i \boldsymbol{x}_0 + \boldsymbol{a}_{E,0}^i \neq 0$. To use Slater's constraint qualification (Theorem 2.9), we must show that there exists a $\boldsymbol{u}_{0:N} \in \text{relint}(\mathbb{F}_{\mathcal{M}_d})$ that strictly satisfies the lower energy storage constraints, i.e., $E_k^i > E_L^i$ for all $k \in \{0...N\}$ and all $i \in \{1...p\}$.

First, let $E_L^i = 0$. If $E_0^i > 0$, then $\boldsymbol{u}_{0:N} = 0$ strictly satisfies the constraints. If the storage decay term $\gamma^i < 1$, the energy in the storage system asymptotically approachs zero, however, because N is finite, $E_k^i > 0$ for all $k \in \{0...N\}$. If $E_0^i = 0$, the energy at the next time-step is:

$$\begin{aligned} E_1^i &= -\boldsymbol{u}_0 \boldsymbol{y}_0^i - \mu_0^i(\boldsymbol{u}_0, \boldsymbol{y}_0^i) \\ &= -\begin{bmatrix} \boldsymbol{u}_0 \\ \boldsymbol{y}_0^i \end{bmatrix}^T \begin{bmatrix} \boldsymbol{M}_{uu,0}^i & \boldsymbol{M}_{uy,0}^i + \frac{1}{2}\boldsymbol{I} \\ (\boldsymbol{M}_{uy,0}^i)^T + \frac{1}{2}\boldsymbol{I} & \boldsymbol{M}_{yy,0}^i \end{bmatrix} \begin{bmatrix} \boldsymbol{u}_0 \\ \boldsymbol{y}_0^i \end{bmatrix}. \end{aligned}$$

From Assumption 3 it follows that for all $i \in \{1...p\}$ and each $\check{\boldsymbol{y}}_0^i \in \mathbb{R}^m \setminus 0$ (where $\boldsymbol{y}_0^i = \check{\boldsymbol{y}}_0^i + \boldsymbol{D}_{E,0}^i \boldsymbol{u}_0$), there exists a $\boldsymbol{u}_0 \in \mathbb{R}^m$ such that $E_1^i > 0$. Setting the rest of the trajectory $\boldsymbol{u}_{1:N} = 0$ strictly satisfies the constraints.

Now, let $\gamma^i = 1$. If $E_0^i > E_L^i$, then $\boldsymbol{u}_{0:N} = 0$ strictly satisfies the constraints. If $E_0^i = E_L^i$, we again invoke Assumption 3 as shown above to guarantee that there exists a $\boldsymbol{u}_0 \in \mathbb{R}^m$ such that $E_1^i > E_L^i$. □

5.5 Example: Piezoelectric Energy Harvester

In this section, we present an example using a piezoelectric energy harvester. The process of formulating the model for this device, and then discretizing and nondimensionalizing it is outlined in Section 4.3.1. In this case, we assume there is no transmitter and instead $q^1(t)$ sends power to a resistor bank. Our goal is to maximize the energy generated by this device (see Section 4.2.2). The associated ECOCP is:

$$\begin{cases} \textbf{Given:} & \boldsymbol{x}_0, E_0^1, \boldsymbol{A}, \boldsymbol{B}, \boldsymbol{C}_E, \boldsymbol{D}_E, \gamma^1, \\ & a_k, a_{E,k}^1, \mu_k^1(\cdot,\cdot), \forall k \in \{0...N\}, \\ \textbf{Minimize:} & J(u_{0:N}) = \sum_{k=0}^{N} u_k y_k^1 + \mu_k^1(u_k, y_k^1) \\ \textbf{Domain:} & u_{0:N},\ q_{0:N}^1 \\ \textbf{Constraints:} & c_k^L(u_{0:N}, q_{0:N}^1, \boldsymbol{x}_{0:N}^\circ(u_{0:N})) \leqslant 0, \\ & c_k^U(u_{0:N}, q_{0:N}^1, \boldsymbol{x}_{0:N}^\circ(u_{0:N})) \leqslant 0, \\ & q_k^1 \geqslant 0, \\ & \forall k \in \{0...N\}. \end{cases}$$

Let the time step $\Delta t = 1$, number of time steps $N = 100$, nondimensionalized mechanical damping $d_p = 0.005$, electromechanical coupling factor $\theta_p = 0.1$, dielectric leakage coefficient $\kappa_p = 0.001$, circuit resistance $R_c = 0.4$, and $\gamma^1 = 1$ (note that we have suppressed the overbar to indicate nondimensional factors, and assume all factors are nondimensional). The beam is excited by a base acceleration $\boldsymbol{a} \sim \mathcal{N}(0, 1)$. Let $E_L^1 = 0$, and consider four different energy storage values: $E_U^1 = \{\infty,\ 2,\ 0.2,\ 0.02\}$.

Figure 5.1 shows the trajectories for the energy in storage system E_k^1, the control input u_k, and power sent to the resistor bank q_k^1 for various nondimensional values of E_U^1. These trajectories have been modified for feasibility when necessary. The control input trajectories $u_{0:N}$ are the same for the $E_U^1 = \infty$ and $E_U^1 = 2$ cases. However, the energy sent to the resistor bank $q_{0:N}^1$ is nonzero for the $E_U^1 = 2$ case to satisfy the upper energy storage constraint, while for the $E_U^1 = \infty$ case, no energy is sent to the resistor bank. Note that the control input trajectories $u_{0:N}$ differ from the infinite energy storage case for $E_U^1 = 0.2$ and $E_U^1 = 0.02$.

Because $m = 1$ for this example, $\Upsilon_{0:N}$ simplifies to a sequence of scalar values. Therefore, we can verify zero duality gap by checking that each scalar $\Upsilon_k > 0$, for all $k \in \{0...N\}$. However, due to finite numerical tolerance, we assume that Theorem 5.2 is satisfied if $\Upsilon_k >$

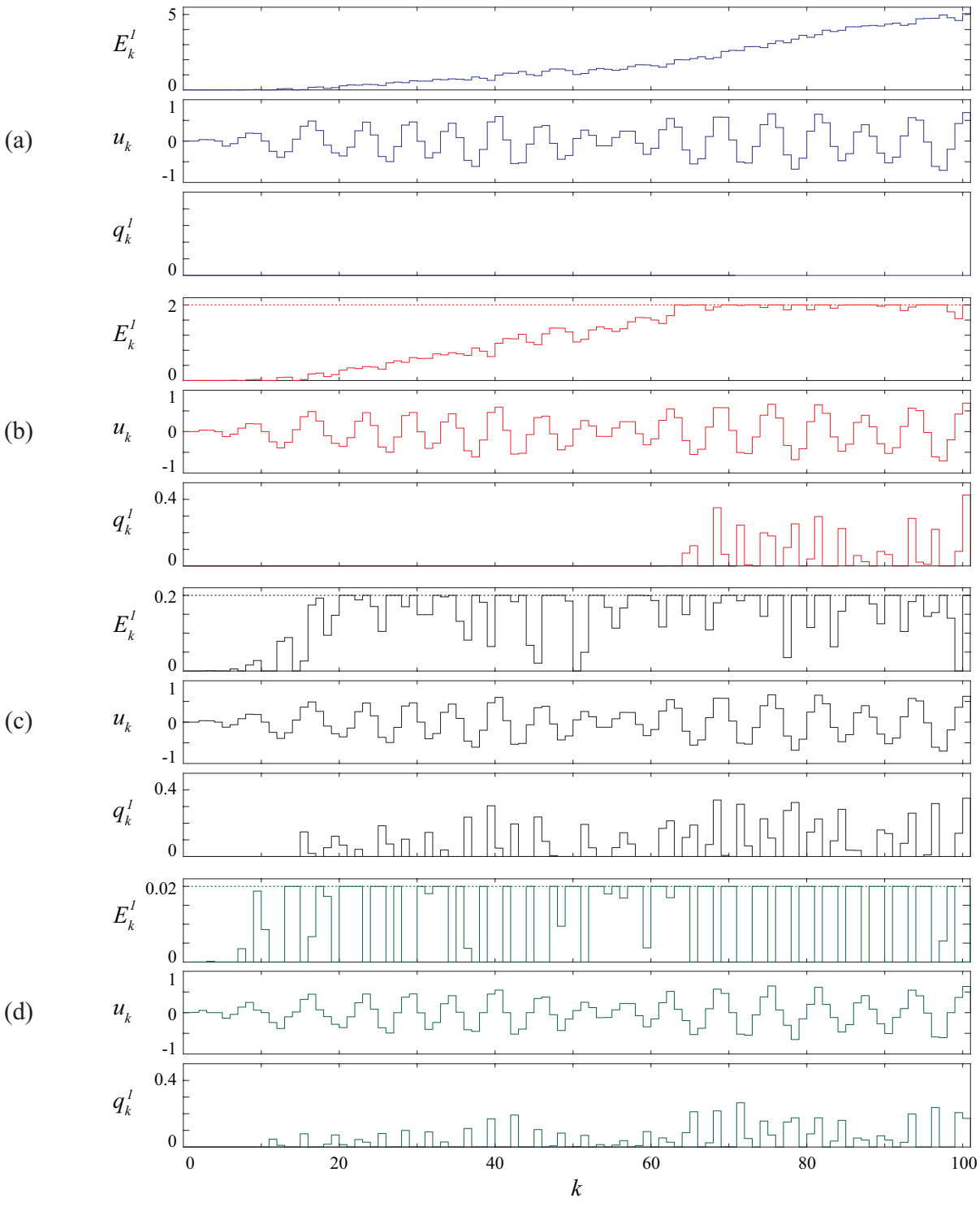

Figure 5.1: The energy in storage system E_k^1, the control input u_k^1, and energy sent to the resistor bank q_k^1 for a piezoelectric energy harvester with various values of upper energy constraint: $E_U^1 = \infty$ (red), $E_U^1 = 2$ (blue), $E_U^1 = 0.2$ (black), and $E_U^1 = 0.02$ (green).

10^{-8}, for all $k \in \{0...N\}$. For $E_U^1 = \{\infty,\ 2,\ 0.2\}$, $\Upsilon_k > 0$ at each time step, and we can conclude that strong duality holds for these cases. However, for the $E_U^1 = 0.02$ case, Υ_0 is below the threshold stated above, and therefore, we conclude that it has nonzero duality gap.

Figure 5.2 plots E_U^1 versus the saturated primal performance measure, J_{sat}. If the dual optimum results in a feasible trajectory, which is the case when strong duality holds, then $J_{sat} = J$. However, if the dual optimum results in an infeasible trajectory, which is the case when a nonzero duality gap is present, we modify the resulting $\boldsymbol{u}^*(\boldsymbol{\lambda}^d)$ so that the constraints are satisfied.

In Figure 5.2, the blue arrow spans the values of E_U^1 that have the same optimal solution as the infinite storage case, as described above with $E_U^1 = 2$. The $q_{0:N}^1$ trajectories differ for values of E_U^1 in this region in order to satisfy the upper energy constraints. The red arrow spans the region that results in zero duality gap, meaning that solving the dual problem results in the optimal solution to the primal problem. The green arrow spans the values of E_U^1 that result in nonzero duality gap, and hence the resulting trajectory from the dual optimization is infeasible. Therefore, we must modify these trajectories for feasibility. The $E_U^1 = 0.02$ case falls within this region, meaning it is the only suboptimal solution of the four considered cases.

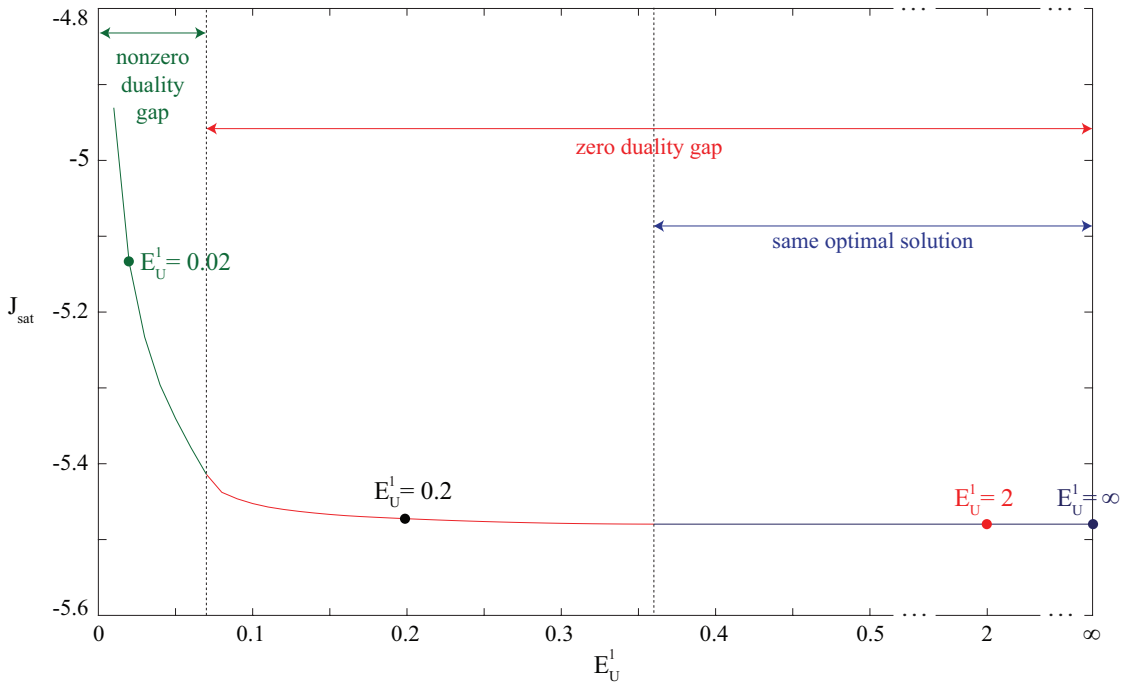

Figure 5.2: Plot of J_{sat} versus E_U^1. The blue, red, and green arrows spans the values of E_U^1 that have the same optimal solution as the infinite storage case, result in zero duality gap, and result in nonzero duality gap, respectively.

Chapter 6

Implementation via Model Predictive Control

In this chapter, we first provide an overview of MPC. We then discuss how to implement the solution from the dual relaxation introduced in Chapter 5 in real-time via MPC. When the optimal control problem has nonzero duality gap, the solution to the dual relaxation is infeasible, meaning the primal constraints are not satisfied. Therefore, we introduce an algorithm to derive a feasible input from the dual relaxation solution. We demonstrate these techniques on a spherical buoy WEC, with the goal of maximizing generated energy, and a multi-energy-storage-system vibration suppression system.

6.1 Overview of Model Predictive Control

MPC, which is also referred to as receding horizon control, is an on-line closed-loop iterative control method [9, 46]. At time k, an open-loop optimal control problem is solved over time interval $\{k, ..k+N\}$, starting from (known) initial condition $\boldsymbol{x}_k$. This optimal control problem yields a sequence of $N+1$ control inputs. The first control input (for time k) is implemented. Then at time $k+1$, the process is repeated over the new interval $\{k+1, ...k+1+N\}$, with known initial condition $\boldsymbol{x}_{k+1}$. Figure 1.6 shows how the system intelligence of a self-powered system may be structured to enable MPC.

Figure 6.1 depicts the procedure for implementing MPC. In this figure, we assume that the control input is ZOH, and the performance objective is measured at discretized points. Let the solid blue lines represent the past control inputs, and the dashed blue lines represent the $N+1$ future control inputs determined from the optimal control problem. The solid red

lines represent the past objective functions, and the dashed red lines represent the $N+1$ predicted objective functions based on the future control inputs.

In Figure 6.1a, the current time-step is k. The control inputs from time-steps k to $k+10$ are calculated. In Figure 6.1b, the control input at time k was implemented, and the current time-step is now $k+1$. The control inputs from $k+1$ to $k+11$ and the corresponding values of the objective function are calculated. Note that the measured objective function in Figure 6.1b at time k is different from the predicted objection function in Figure 6.1a at time-step k. Differences between the predicted and measured objective function could result from errors in the exogenous disturbance predictions, or from modeling errors. In 6.1c, the control input at time $k+1$ was implemented, and the current time-step is now $k+2$. Again, the control inputs from $k+2$ to $k+12$ and the corresponding values of the objective function are calculated as the prediction horizon is shifted forward one time-step.

A benefit of MPC is that it can account for hard and soft constraints, which nearly all engineering applications require. However, as described above, in MPC, an optimal control problem is solved every time step Δt, meaning that either the dynamics of the plant must be sufficiently slow to accommodate this or the optimal control algorithm sufficiently fast. When using MPC techniques, the introduction of uncertainty via, for example, poor disturbance prediction or large modeling errors, may cause MPC algorithms to perform poorly. Therefore, robustness of MPC algorithms is an ongoing research area [27, 46]. Here we have provided a brief overview of MPC; however, [24, 46, 57] can be used as references.

In the context of the self-powered system control problem, we implement our control strategy using MPC because it allows us to strictly enforce the physical constraints of the energy storage units. However, as mentioned earlier, using MPC requires that the ECOCP be solved every time step Δt. We prove in Chapter 4 that the ECOCP is nonconvex in general, meaning it may be computationally expensive to solve and only local minima can be ensured. Therefore, we explore the use of the convex dual relaxation in Chapter 5 to solve the ECOCP, where the global optimum can be found in polynomial time. However, in general, we cannot guarantee that the solution to the dual relaxation is feasible, and obviously, MPC requires feasible inputs to satisfy constraints. Therefore, in the following sections, we formulate an algorithm to modify infeasible trajectories resulting from the dual relaxation to implement via MPC .

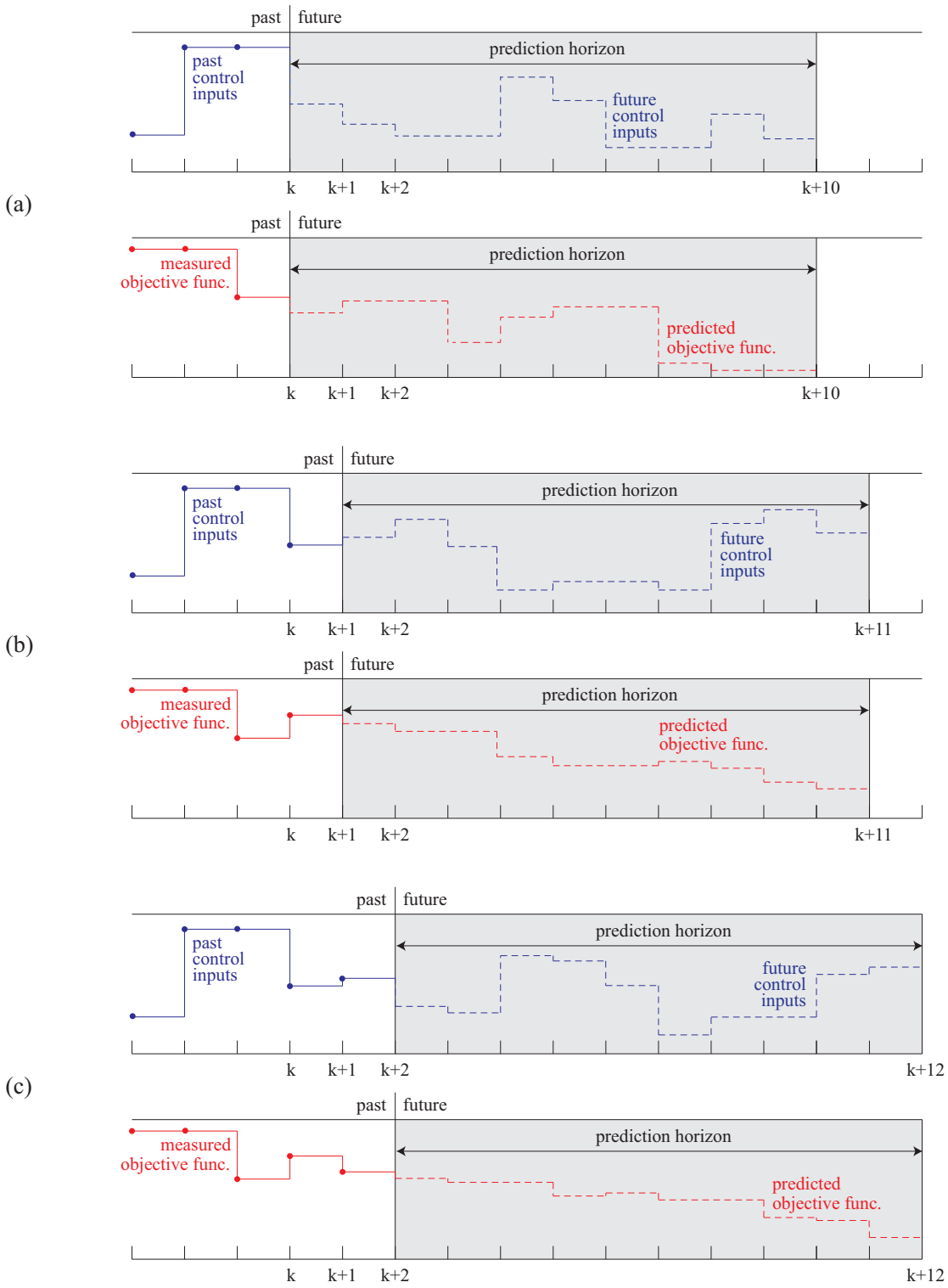

Figure 6.1: Diagram depicting model predictive control procedure: (a) prediction horizon starting at time step k, (b) starting at time step $k+1$, and (c) starting at time step $k+2$.

6.2 Modifying Infeasible Trajectories

In the case where the ECOCP has nonzero duality gap, the resulting optimal trajectory found from solving the dual problem $\{\boldsymbol{u}^*_{k:k+N}(\boldsymbol{\lambda}^{dual}_{k:k+N}),\ \boldsymbol{q}^*_{k:k+N}(\boldsymbol{\lambda}^{dual}_{k:k+N})\}$ is infeasible (i.e., violates the constraints). Let k be the first time step in the ECOCP. In MPC, we only implement the first time step of the dual optimal trajectory, i.e., $\{\boldsymbol{u}^*_k(\boldsymbol{\lambda}^{dual}_{k:k+N}),\ \boldsymbol{q}^*_k(\boldsymbol{\lambda}^{dual}_{k:k+N})\}$. Therefore, we are specifically interested in modifying these to guarantee feasibility. Recall from Definition 3.7, that $\mathbb{F}(\boldsymbol{x}_k, \boldsymbol{E}_k, N)$ is the domain of all finite-horizon discrete-time feasible inputs. Now let $\mathbb{F}_k(\boldsymbol{x}_k, \boldsymbol{E}_k, N)$ be the set of all inputs at the k^{th} time step $\{\boldsymbol{u}_k, \boldsymbol{q}_k\}$ that satisfy the constraints at time-step k, i.e.,

$$\mathbb{F}_k(\boldsymbol{x}_k, \boldsymbol{E}_k, N) = \Big\{ \{\boldsymbol{u}_k, \boldsymbol{q}_k\} \ :\ \boldsymbol{c}^L_k(\boldsymbol{u}_k, \boldsymbol{q}_k, \boldsymbol{x}_k) \leqslant 0,\ \boldsymbol{c}^U_k(\boldsymbol{u}_k, \boldsymbol{q}_k, \boldsymbol{x}_k) \leqslant 0,\ \text{and } \boldsymbol{q}_k \geqslant 0 \Big\},$$

which we reference as $\mathbb{F}_k$ for brevity. If $\{\boldsymbol{u}^*_k(\boldsymbol{\lambda}^{dual}_{k:k+N}),\ \boldsymbol{q}^*_k(\boldsymbol{\lambda}^{dual}_{k:k+N})\} \in \mathbb{F}_k$, then regardless of the feasibility of the rest of the dual optimal trajectory, we implement $\{\boldsymbol{u}^*_k(\boldsymbol{\lambda}^{dual}_{k:k+N}),\ \boldsymbol{q}^*_k(\boldsymbol{\lambda}^{dual}_{k:k+N})\}$ as is. However, if $\{\boldsymbol{u}^*_k(\boldsymbol{\lambda}^{dual}_{k:k+N}),\ \boldsymbol{q}^*_k(\boldsymbol{\lambda}^{dual}_{k:k+N})\} \notin \mathbb{F}_k$, then we modify for feasibility.

Given how $\boldsymbol{q}_k$, the energy sent from the storage system, can be treated a Lagrange multiplier in the dual domain (see Section 5.1.2), it does not violate the constraint $\boldsymbol{q}_k \geqslant 0$. If $\{\boldsymbol{u}^*_k(\boldsymbol{\lambda}^{dual}_{k:k+N}),\ \boldsymbol{q}^*_k(\boldsymbol{\lambda}^{dual}_{k:k+N})\}$ violates the upper energy storage constraint of the i^{th} storage unit $c^{U,i}_k(\cdot,\cdot,\cdot) \leqslant 0$, the constraint can be satisfied by increasing q^i_k so that $c^{U,i}_k(\cdot,\cdot,\cdot) = 0$. If $\{\boldsymbol{u}^*_k(\boldsymbol{\lambda}^{dual}_{k:k+N}),\ \boldsymbol{q}^*_k(\boldsymbol{\lambda}^{dual}_{k:k+N})\}$ violates the lower energy storage constraint of the i^{th} storage unit $c^{L,i}_k(\cdot,\cdot,\cdot) \leqslant 0$, modifying the inputs to satisfy this constraint is more complex.

When there is a lower energy storage constraint, we modify $\boldsymbol{u}_k$ such that it minimizes the difference between the (infeasible) dual optimum, under a quadratic performance measure, such that the lower energy constraints are satisfied for all of the energy storage systems. We refer to this as the Modification Quadratically Constrained Quadratic Program (MQCQP) and it has the form:

$$\text{MQCQP}: \begin{cases} \textbf{Given:} & \boldsymbol{x}_k, \boldsymbol{E}_k, \boldsymbol{A}, \boldsymbol{B}, \\ & \boldsymbol{C}^i_E, \boldsymbol{D}^i_E, \gamma^i, \boldsymbol{a}^i_{E,k}, \mu^i_k(\cdot,\cdot),\ \forall i \in \{1...p\} \\ \textbf{Minimize:} & \big(\hat{\boldsymbol{u}} - \boldsymbol{u}^*_k(\boldsymbol{\lambda}^{dual}_{k:k+N})\big)^T \left(\sum_{i=1}^{p} \boldsymbol{M}^i_{uu,k}\right) \big(\hat{\boldsymbol{u}} - \boldsymbol{u}^*_k(\boldsymbol{\lambda}^{dual}_{k:k+N})\big) \\ \textbf{Domain:} & \hat{\boldsymbol{u}} \\ \textbf{Constraints:} & \boldsymbol{c}^L_k(\hat{\boldsymbol{u}}_k, 0, \boldsymbol{x}_k) \leqslant 0. \end{cases}$$

Corollary 6.1. *The MQCQP is convex if for all $i \in \{1...p\}$:*

$$\begin{bmatrix} \frac{1}{2}\left(\boldsymbol{D}^i_{E,k} + (\boldsymbol{D}^i_{E,k})^T\right) + \boldsymbol{M}^i_{uu,k} & \boldsymbol{M}^i_{uy,k} \\ (\boldsymbol{M}^i_{uy,k})^T & \boldsymbol{M}^i_{yy,k} \end{bmatrix} \succeq 0. \tag{6.1}$$

Proof. It is trivial to show that the quadratic performance measure is convex. We turn our attention to the constraint function $c^{L,i}_k(\cdot,\cdot,\cdot) \leqslant 0$, which can be written as:

$$\begin{aligned} c^{L,i}_k(\boldsymbol{u}_k, 0, \boldsymbol{x}_k) &= E^i_L - \gamma^i E^i_k + (\check{\boldsymbol{y}}^i_k)^T \boldsymbol{u}_k \\ &+ \begin{bmatrix} \boldsymbol{u}_k \\ \check{\boldsymbol{y}}^i_k + \boldsymbol{D}^i_{E,k}\boldsymbol{u}_k \end{bmatrix}^T \begin{bmatrix} \frac{1}{2}\left(\boldsymbol{D}^i_{E,k} + (\boldsymbol{D}^i_{E,k})^T\right) + \boldsymbol{M}^i_{uu,k} & \boldsymbol{M}^i_{uy,k} \\ (\boldsymbol{M}^i_{uy,k})^T & \boldsymbol{M}^i_{yy,k} \end{bmatrix} \begin{bmatrix} \boldsymbol{u}_k \\ \check{\boldsymbol{y}}^i_k + \boldsymbol{D}^i_{E,k}\boldsymbol{u}_k \end{bmatrix}. \end{aligned}$$

Now, assume (6.1) holds, and then we can write the matrix in the following form:

$$\begin{bmatrix} \frac{1}{2}\left(\boldsymbol{D}^i_{E,k} + (\boldsymbol{D}^i_{E,k})^T\right) + \boldsymbol{M}^i_{uu,k} & \boldsymbol{M}^i_{uy,k} \\ (\boldsymbol{M}^i_{uy,k})^T & \boldsymbol{M}^i_{yy,k} \end{bmatrix} = \boldsymbol{V}\boldsymbol{V}^T,$$

where $\boldsymbol{V} \in \mathbb{S}^{2m}$. Then via Theorem 2.3, it follows that $c^{L,i}_k(\boldsymbol{u}_k, 0, \boldsymbol{x}_k) \leqslant 0$ if and only if:

$$\begin{bmatrix} E^i_L - \gamma^i E^i_k + (\check{\boldsymbol{y}}^i_k)^T \boldsymbol{u}_k & \begin{bmatrix} \boldsymbol{u}_k \\ \check{\boldsymbol{y}}^i_k + \boldsymbol{D}^i_{E,k}\boldsymbol{u}_k \end{bmatrix}^T \boldsymbol{V} \\ \boldsymbol{V}^T \begin{bmatrix} \boldsymbol{u}_k \\ \check{\boldsymbol{y}}^i_k + \boldsymbol{D}^i_{E,k}\boldsymbol{u}_k \end{bmatrix} & -\boldsymbol{I} \end{bmatrix} \preceq 0$$

By inspection, we can see that the above matrix inequality is linear in $\boldsymbol{u}_k$, meaning it is a convex inequality constraint in $\boldsymbol{u}_k$. □

Note that if the mapping $\boldsymbol{u} \mapsto \boldsymbol{y}^i$ is discrete-time passive, it follows that $(\boldsymbol{D}^i_{E,k} + (\boldsymbol{D}^i_{E,k})^T) \succeq 0$ [38], and then Corollary 6.1 holds. Recall from Section 1.3.1 that for cases with $m = 1$ or $p = 1$, the MQCQP can be solved analytically. The below algorithm summaries the modification algorithm for MPC implementaiton:

Algorithm 1: MPC Implementation

$k = 0$
while *1* **do**
  Solve dual problem to obtain $\{\boldsymbol{u}_k^*(\boldsymbol{\lambda}_{k:k+N}^{dual}),\ \boldsymbol{q}_k^*(\boldsymbol{\lambda}_{k:k+N}^{dual})\}$
  $modify\_u = 0$
  for $i = 1$ *to* p **do**
    if $c_k^{L,i}(\boldsymbol{u}_k^*(\boldsymbol{\lambda}_{k:k+N}^{dual}),\ \boldsymbol{q}_k^*(\boldsymbol{\lambda}_{k:k+N}^{dual}), \boldsymbol{x}_k^*(\boldsymbol{\lambda}_{k:k+N}^{dual})) > 0$ **then**
      Solve the MQCQP for $\hat{\boldsymbol{u}}_k$
      $modify\_u = 1$
      Exit loop
  if $modify\_u = 0$ **then**
    $\hat{\boldsymbol{u}}_k = \boldsymbol{u}_k^*(\boldsymbol{\lambda}_{k:k+N}^{dual})$
  for $i = 1$ *to* p **do**
    if $c_k^{U,i}(\boldsymbol{u}_k^*(\boldsymbol{\lambda}_{k:k+N}^{dual}),\ \boldsymbol{q}_k^*(\boldsymbol{\lambda}_{k:k+N}^{dual}), \boldsymbol{x}_k^*(\boldsymbol{\lambda}_{k:k+N}^{dual})) > 0$ **then**
      $\hat{q}_k^i = E_k^i(\boldsymbol{u}_k^*(\boldsymbol{\lambda}_{k:k+N}^{dual}),\ \boldsymbol{q}_k^*(\boldsymbol{\lambda}_{k:k+N}^{dual}), \boldsymbol{x}_k^*(\boldsymbol{\lambda}_{k:k+N}^{dual})) - E_U^i$
    else
      $\hat{q}_k^i = q_k^{i*}(\boldsymbol{\lambda}_{k:k+N}^{dual})$
  Implement $\{\hat{\boldsymbol{u}}_k,\ \hat{\boldsymbol{q}}_k\}$
  k = k+1

Because the trajectory is adjusted from the optimal dual solution, there is no guarantee of stability. If the problem is in continuous-time, Theorem 3.1 can be used to show that the adjustment algorithm cannot destabilize the system. However, in discrete-time, the model allows for inter-time-sample energy violations as discussed in Section 3.2.4, and therefore stability is not guaranteed. Theoretically, it is possible that the modification algorithm can destabilize the system. However, we can assume that for small enough sampling times, destabilization should not be of major concern in practice. Future work will focus on stability for cases with arbitrarily large sampling times.

6.3 Example: Spherical Buoy Wave Energy Converter

This example is based off of work in [35] in collaboration with the National Renewable Energy Laboratory. WECs are devices that convert the oscillatory motion from ocean waves into electricity [20, 62]. There is increasing awareness from experts in the field of wave energy conversion that specialized control technology is vitally important to the success of wave energy power [59]. The control systems of WECs must be developed so that the technology can operate in a variety of sea states and maximize generated energy while simultaneously mitigating system damage. Although improvements to WEC mechanical and PTO systems can increase the economic feasibility of wave power, appropriate controller design has been shown to *significantly* increase the harvested energy of WECs [7, 59].

Controller design for WECs requires specialized treatment beyond well-known, standard control techniques. Because ocean waves are stochastic (i.e., they do not occur at a single frequency) and are usually modelled via a spectrum that is a function of wind velocity, the controller must accommodate for changing spectral shapes that are potentially wideband. Further, mechanical and electrical constraints need to be enforced to avoid device damage, or possible external constraints from electric grid regulators.

Controllers for WECs are sometimes designed assuming single-frequency waves [19, 21]; however, true sea states are far from narrowband phenomena, and such controllers are consequently suboptimal in realistic applications. Single-frequency WEC controllers can be extended straightforwardly to the broadband situation by implementing a dynamic feedback law equal to the complex conjugate transpose of the frequency-dependent impedance matrix of the WEC. The WEC industry refers to this technique as "complex conjugate control" [51]; however, this type of control is anticausal, cannot account for system constraints, and assumes that the PTO system can realize bidirectional power flow solutions.

A more computationally complex solution involves the execution of real-time control algorithms using MPC methods, which can account for system constraints [46]; however, two distinct complications arise when implementing MPC. First, if constraints are imposed, the associated optimization required to be solved in real time by an MPC algorithm is generally a nonconvex problem. Finding solutions for nonconvex problems is inefficient and problematic, and in most scenarios only local minimality can be assured. Second, MPC algorithms require knowledge of future disturbances, so we require a reliable wave forecasting system. Because of the interaction and propagation of waves, wave forecasting can be complex and is an active research area [1, 23].

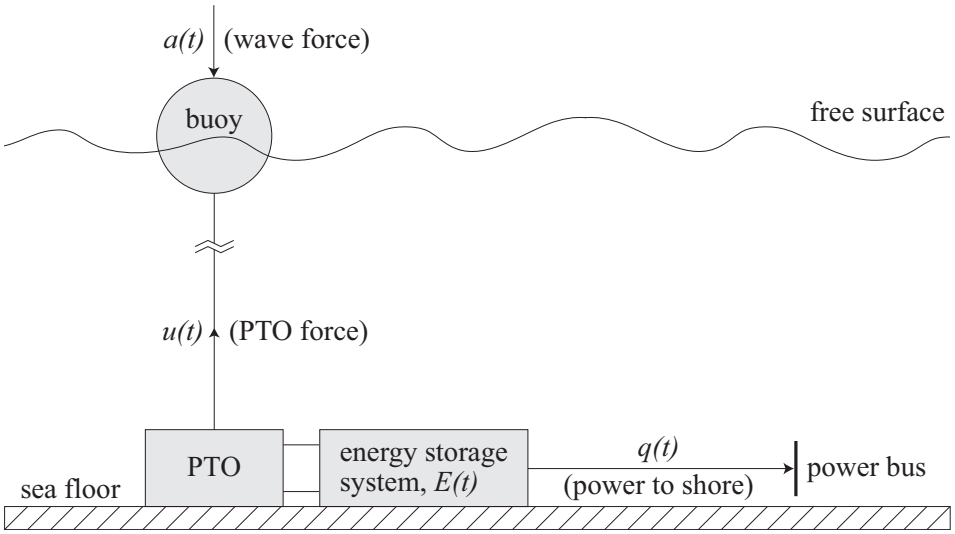

Figure 6.2: Spherical buoy wave energy converter

Many other works have used MPC techniques to control WECs. References [16, 30, 42] perform linear MPC, and [42] uses a convex relaxation of the primal cost function by implementing a sampling delay. References [70] and [58] perform nonlinear MPC while implementing displacement and generator constraints. Reference [13] minimizes tracking error and controller effort subject to constraints on displacement, velocity, and PTO. However, none of these methods have used dual optimization techniques. In this section, we implement MPC by solving the dual problem using techniques from Chapter 5, and if necessary, we modify infeasible solutions using the algorithm introduced in Section 6.2.

6.3.1 System and Disturbance Model

The WEC system considered in this study consists of a single-body sphere that is constrained to move only in the heave direction pictured in Figure 6.2. Here, we consider the case with a single buoy ($m = 1$) connected to one energy storage system ($p = 1$). The control input is the PTO force $u(t)$, the potential variable is the buoy's heaving velocity $v(t)$, and the exogenous disturbance is the force from the waves acting on the buoy. Then, the rest of the components of the model are as follows:

1. **Plant:** In this example, we use the floating spherical buoy model developed for the International Energy Agency Offshore Energy Systems Task 10 [76]. The buoy has radius $r = 5\ m$ and mass $M = 261.8 \times 10^3\ kg$. Let $G_f(j\omega)$ be the transfer function

from force to buoy velocity:

$$G_f(\omega) = \left(C_a(\omega) + j\omega \left(M + M_a(\omega) - \frac{K_s}{\omega^2} \right) \right)^{-1},$$

with added mass, $M_a(\omega)$, added damping, $C_a(\omega)$, and hydrostatic stiffness coefficient, K_s. Because of the the spherical shape of the buoy, the force due to buoyancy is nonlinear with respect to submergence depth. We approximate K_s as $dg\pi r^2$, where $d = 1000\ \frac{kg}{m^3}$ is the density of water and $g = 9.81\ \frac{m}{s^2}$ is the acceleration due to gravity. We use linear hydrodynamic theory to numerically determine the forces acting on the buoy via hydrodynamic software (such as WAMIT or ANSYS Aqwa). Let $G_a(\omega)$ be the transfer function from wave amplitude to buoy velocity: $G_a(\omega) = G_f(\omega)H_{ex}(\omega)$, where $H_{ex}(\omega)$ is the transfer function from wave amplitude to force, which is also numerically determined. This mathematical model is discretized and finite-dimensionalized to a six-state, LTI system in (4.14). An explanation of the method of discretization and finite-dimensionalization is out of the scope of this thesis; however, [47, 65, 68, 81] can be used as references.

2. **Transmission Losses:** We model the parasitic losses quadratically as a function of u_k as $\mu_k = u_k^T M_{uu} u_k$, where $M_{uu,k} = 8.5 \times 10^{-10}\ \frac{s}{kg}$.

3. **Dissipated Power From Energy Storage:** Let $q(t)$ be the power being sent from the WEC to the power grid, which we model as a power bus.

4. **Energy Storage System:** The decay of the energy in the storage system is fixed at $\gamma = 0.99$ and the lower energy storage bound at $E_L = 0\ MJ$. We consider three values for the upper energy storage limit: $E_U = \{\infty,\ 0.5,\ 0.25\}\ MJ$.

5. **Exogenous Disturbance:** In this study, we also assume perfect knowledge of future exogenous disturbances. Future studies could incorporate forecasting of future disturbances given present and past information using, for example, a Kalman filter [1, 23]. We assume the buoy sits in an ocean of infinite depth, and irregular waves excite the buoy, which can be characterized by the Bretschneider spectrum [71] as:

$$S(f) = \frac{H_s^2}{4}(1.057 f_p)^4 f^{-5} \exp\left(-\frac{5}{4}\left(\frac{f_p}{f} \right)^4 \right), \tag{6.2}$$

where frequency f is in Hz, significant wave height $H_s = 1\ m$, and peak wave period $T_p = \frac{1}{f_p} = 12\ s$.

6. **PTO Force Constraint:** In this example, we consider an additional constraint on the PTO force, $u(t)$, which is a maximum allowable force of $u_{max} = \pm 500\ kN$ (this force is of a similar magnitude used in other studies [30, 42]). Note that this constraint is a convex function of u.

6.3.2 Energy-Constrained Optimal Control Problem Formulation

Here we develop an MPC control scheme to maximize generated energy (see the energy harvesting problem in Section 4.2.2) subject to constraints on the energy storage and the maximum allowable control force, u_{max}. Let k be the current time step, and then the resultant ECOCP is:

$$
\begin{cases}
\textbf{Given:} & \boldsymbol{x}_0, E_0^1, \boldsymbol{A}, \boldsymbol{B}, \boldsymbol{C}_E^1, \boldsymbol{D}_E^1, \gamma^1, \\
& a_{k:k+N}, a_{E,k:k+N}^1, \mu_j^1(\cdot),\ \forall j \in \{k...k+N\} \\
\textbf{Minimize:} & J(u_{k:k+N}) = \sum_{j=k}^{k+N} u_j y_j^1 + \mu_j^1 \\
\textbf{Domain:} & u_{k:k+N},\ q_{k:k+N} \\
\textbf{Constraints:} & c_j^L(u_{k:k+N}, q_j^1, \boldsymbol{x}_j^\circ(u_{k:k+N}, \boldsymbol{x}_0)) \leqslant 0, \\
& c_j^U(u_{k:k+N}, q_j^1, \boldsymbol{x}_j^\circ(u_{k:k+N}, \boldsymbol{x}_0)) \leqslant 0, \\
& q_j^1 \geqslant 0, \\
& u_j^2 - u_{max}^2 \leqslant 0, \\
& \forall j \in \{k...k+N\}.
\end{cases}
$$

6.3.3 Incorporating Maximum Input Constraints

To incorporate the maximum force constraint, we need to slightly modify the theory developed in Chapter 5 to include an additional Lagrange multiplier. First, let $\lambda_j^{u_{max}}$ be the Lagrange multiplier used to enforce the maximum input constraint at the j^{th} time step, which, via the KKT conditions, is required to be nonnegative. Recall the definition of $\bar{J}$ in

(4.8). Let $\bar{J}_{u_{max}}$ be $\bar{J}$ with maximum input constraint incorporated, i.e.,

$$\bar{J}_{u_{max}} = \bar{J} + \sum_{j=k}^{k+N} \lambda_j^{u_{max}} \left(u_j^2 - u_{max}^2 \right).$$

Now, recall the formulations of the Hessian $\boldsymbol{H}(\cdot)$ in (5.5) and constant term $f(\cdot)$ in (5.7). Let $\boldsymbol{H}^{u_{max}}(\boldsymbol{\lambda}_{0:N}, \lambda_{0:N}^{u_{max}})$ and $f^{u_{max}}(\boldsymbol{\lambda}_{0:N}, \lambda_{0:N}^{u_{max}})$ be the versions that incorporate the maximum input constraint, which have the form:

$$\begin{aligned} \boldsymbol{H}_{jk}^{u_{max}}(\boldsymbol{\lambda}_{0:N}, \lambda_{0:N}^{u_{max}}) &= \boldsymbol{H}_{jk}(\boldsymbol{\lambda}_{0:N}) + \lambda_j^{u_{max}} \delta_{jk} \\ f_{jk}^{u_{max}}(\boldsymbol{\lambda}_{0:N}, \lambda_{0:N}^{u_{max}}) &= f_{jk}(\boldsymbol{\lambda}_{0:N}) - \lambda_j^{u_{max}} u_{max}^2. \end{aligned}$$

In the dual problem, we now need to optimize over the original Lagrange multipliers in addition to the new Lagrange multiplier $\lambda^{u_{max}}$. Alterations to the rest of the theory presented in Chapter 5 follow analogously.

6.3.4 Results

Let the discrete time step be $\Delta t = 0.5\ s$. The prediction horizon is one peak wave period, i.e., $N = 24$, and the MPC algorithm is run for 100 wave periods, for a total time of $T = 1200\ s$. Figures 6.3 and 6.4 show the MPC results for the energy in the storage system (E), PTO force (u), buoy displacement (w), generated power (p_T), and power sent to the grid (q).

The average generated power for the $E_U = \{0.25,\ 0.5,\ \infty\}\ MJ$ cases are 83.20 kW, 85.21 kW, and 85.34 kW, respectively. Although a WEC with $E_U = \infty$ would obviously not be designed in practice, this case gives insight into the optimal energy trajectory without the upper energy storage constraint, as well as the amount of energy storage needed to prevent upper energy bound saturation: 3.33 MJ. Note that $q = 0$ for this case because the system never runs out of energy storage.

For each time step of the MPC algorithm, the zero duality gap condition is tested by examining if each of the elements in the sequence $\Upsilon_{k:k+N}$ are uniformly positive because there is one control input ($m = 1$), so Υ_k is a scalar value. However, due to finite numerical tolerance, we assume that Theorem 5.2 is satisfied if $\Upsilon_{k:k+N} > 10^{-8}$. For the $E_U \to \infty$ and $E_U = 0.5MJ$ cases, zero duality gap is achieved at every time step. For the $E_U = 0.25MJ$ case, zero duality gap is achieved 1979 times out of the total 2400 time steps, meaning the global optimal solution is implemented in about 82% of the time steps.

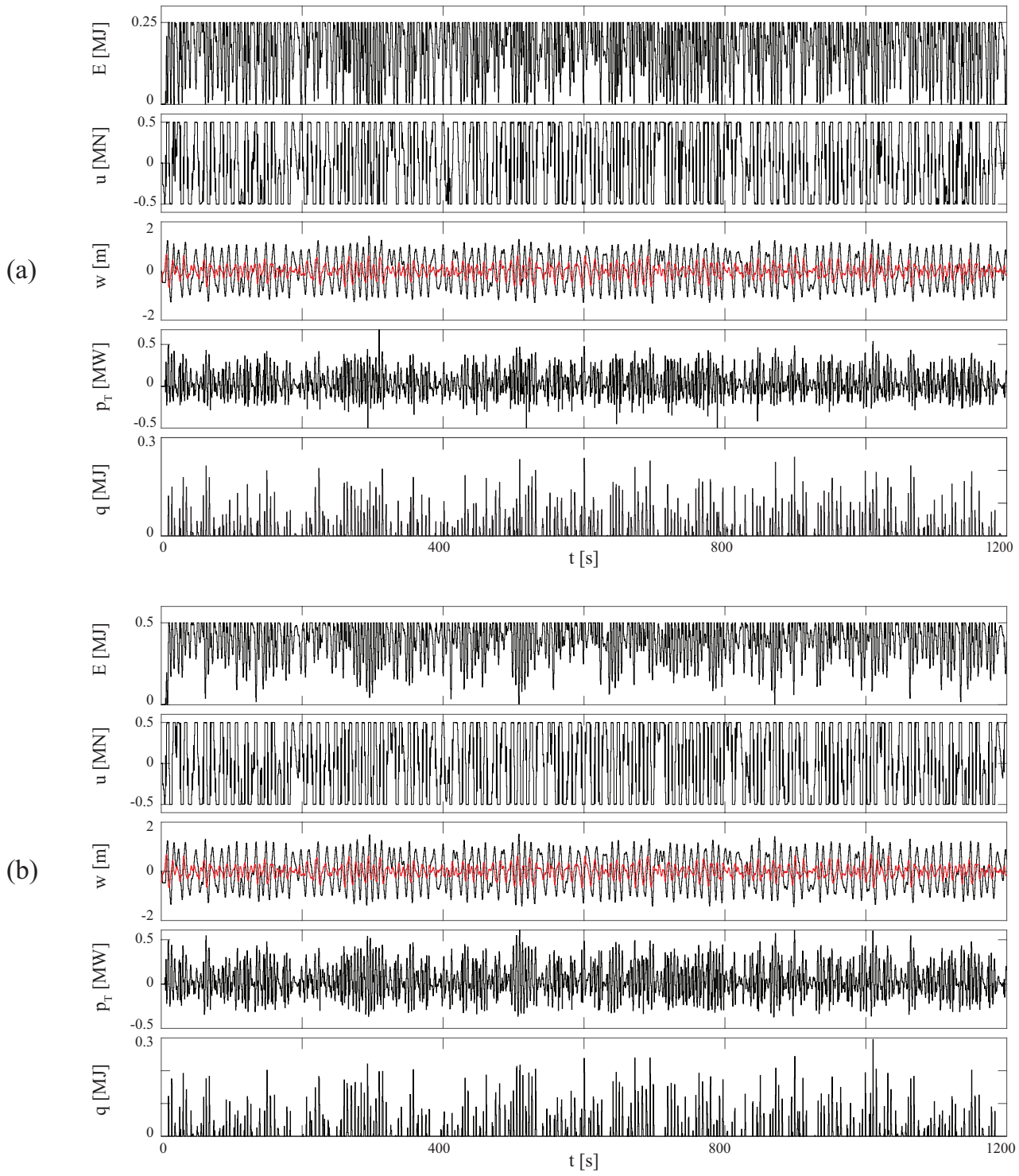

Figure 6.3: The energy in the storage system, E, PTO force, u, buoy displacement, w, generated power, p_T, energy sent to the grid, q, and the red line represents the wave elevation in meters. (a) $E_U = 0.25\ MJ$, (b) $E_U = 0.5\ MJ$.

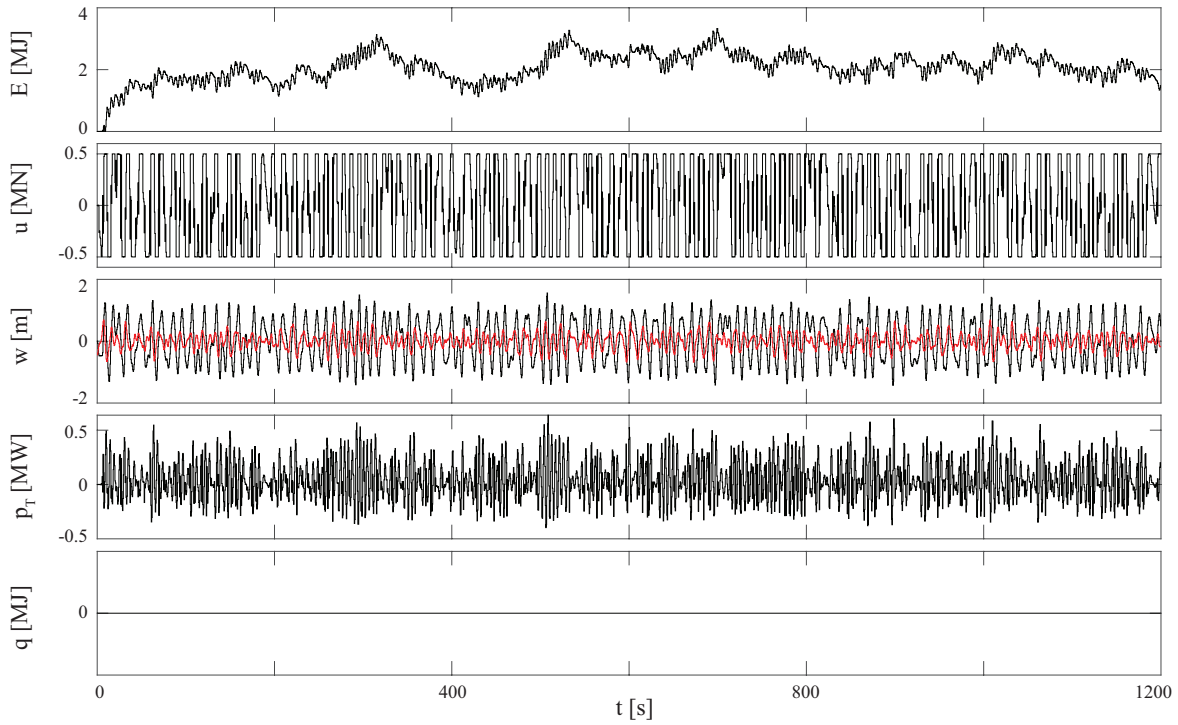

Figure 6.4: The energy in the storage system, E, PTO force, u, buoy displacement, w, generated power, p_T, energy sent to the grid, q, and the red line represents the wave elevation in meters for $E_U \to \infty$

6.4 Example: Vibration Suppression System

In this section, we present an example using an energy-harvesting active vibration suppression system. See Section 1.1 for background on vibration suppression systems in civil engineering and aerospace applications. We analyze the three systems in Figure 1.5 with one, two, and three energy storage systems. The following analysis is not meant to be representative of any particular structure, but rather demonstrate the use of the algorithm presented in Section 6.2, and is therefore performed using nondimensionalized units.

6.4.1 System and Disturbance Model

Consider the five degree-of-freedom mass-spring-damper systems pictured in Figure 1.5 with three transducers ($m = 3$) connected to one, two, or three energy storage systems ($p = \{1, 2, 3\}$). The control inputs are the transducer actions $\{u^1(t), u^2(t), u^3(t)\}$, the associated potential variables are $\{v^1(t), v^2(t), v^3(t)\}$, and the exogenous disturbance is the base acceleration $a(t)$. The rest of the components of the model are as follows:

1. **Plant:** The continuous-time dynamics evolve according to (3.1) with system states:

$$x(t) = \begin{bmatrix} z^1(t) & z^2(t) & z^3(t) & z^4(t) & z^5(t) & \dot{z}^1(t) & \dot{z}^2(t) & \dot{z}^3(t) & \dot{z}^4(t) & \dot{z}^5(t) \end{bmatrix}^T,$$

   where $z_i(t)$ is the i^{th} mass displacement, and $\dot{z}_i(t)$ is the i^{th} mass velocity. The continuous-time state space matrices are:

$$\bar{\boldsymbol{A}} = \begin{bmatrix} \boldsymbol{0} & \boldsymbol{I} \\ -\boldsymbol{M}_S^{-1}\boldsymbol{K}_S & -\boldsymbol{M}_S^{-1}\boldsymbol{C}_S \end{bmatrix}, \quad \bar{\boldsymbol{B}} = \begin{bmatrix} \boldsymbol{0} \\ \boldsymbol{U}_S \end{bmatrix}, \quad \bar{\boldsymbol{G}} = \begin{bmatrix} \boldsymbol{0} \\ \boldsymbol{E}_S \end{bmatrix}$$
$$\bar{\boldsymbol{C}} = \begin{bmatrix} \boldsymbol{0} & \boldsymbol{U}_S \end{bmatrix}, \qquad \bar{\boldsymbol{D}} = \boldsymbol{0},$$

   where $\boldsymbol{M}_S = \boldsymbol{I}_{10}$ is the mass matrix, $\boldsymbol{K}_S$ is the stiffness matrix, $\boldsymbol{C}_S$ is the damping matrix, $\boldsymbol{U}_S$ is the actuator connectivity matrix, and $\boldsymbol{E}_S$ is the disturbance matrix.

These matrices have the following forms:

$$\boldsymbol{K}_S = \begin{bmatrix} 2 & -1 & 0 & 0 & 0 \\ -1 & 2 & -1 & 0 & 0 \\ 0 & -1 & 1 & 0 & 0 \\ 0 & 0 & 0 & 2 & -1 \\ 0 & 0 & 0 & -1 & 1 \end{bmatrix}, \qquad \boldsymbol{U}_S = \begin{bmatrix} 1 & -1 & 0 \\ 0 & 1 & 0 \\ 0 & 0 & 0 \\ 0 & 0 & 1 \\ 0 & 0 & 0 \end{bmatrix}$$

$$\boldsymbol{C}_S = 0.01 \begin{bmatrix} 2 & -1 & 0 & 0 & 0 \\ -1 & 2 & -1 & 0 & 0 \\ 0 & -1 & 1 & 0 & 0 \\ 0 & 0 & 0 & 2 & -1 \\ 0 & 0 & 0 & -1 & 1 \end{bmatrix}, \qquad \boldsymbol{E}_S = \begin{bmatrix} 1 \\ 0 \\ 0 \\ 1 \\ 0 \end{bmatrix}.$$

This plant model is discretized as described in Section 3.2 with time-step $\Delta t = 0.5$.

2. **Transmission Losses:** In this example, we use the quadratic overbound of the efficiency model described in Section 3.2.3. We assume that $\eta_j = 0.9$, $\forall j \in \{1...m\}$. The design parameter is $h_{k,j} = 0.4$, $\forall j \in \{1...m\}$ and $\forall k \in \mathbb{Z}_{\geqslant 0}$, which added a reasonable level of damping to the structure, and performs well.

3. **Energy Storage Systems:** We analyze cases with $p \in \{1, 2, 3\}$, and we fix $T_S^i = 100$ for all $i \in \{1...p\}$, meaning that energy in the storage system decays about ten times slower than the dynamics of the plant. We also fix $E_L^i = 0$ for all $i \in \{1...p\}$, but vary $E_U^i \in \{\infty, 10, 1, 0.1\}$.

4. **Exogenous Disturbance:** The system is excited by a base acceleration $a(t) = \ddot{z}_g(t)$, which is characterized as i.i.d. Gaussian with zero mean and unit variance, i.e., $a \sim \mathcal{N}(0, 1)$.

6.4.2 Energy-Constrained Optimal Control Problem Formulation

Our goal is to suppress the vibration of the structures when subjected to a base acceleration $a(t)$. The Lagrangian represents the sum of the squared accelerations and is of the form:

$$L_j(\boldsymbol{u}_j, \boldsymbol{x}_j) = \begin{bmatrix} \boldsymbol{x}_j \\ \boldsymbol{u}_j \end{bmatrix}^T \begin{bmatrix} \boldsymbol{Q} & \boldsymbol{S} \\ \boldsymbol{S}^T & \boldsymbol{R} \end{bmatrix} \begin{bmatrix} \boldsymbol{x}_j \\ \boldsymbol{u}_j \end{bmatrix}, \tag{6.3}$$

with matrices:

$$\boldsymbol{Q} = \begin{bmatrix} \boldsymbol{K}_S^T \boldsymbol{K}_S & \boldsymbol{K}_S^T \boldsymbol{C}_S \\ \boldsymbol{C}_S^T \boldsymbol{K}_S & \boldsymbol{C}_S^T \boldsymbol{C}_S \end{bmatrix}, \qquad \boldsymbol{S} = \begin{bmatrix} -\boldsymbol{K}_S^T \boldsymbol{U}_S \\ -\boldsymbol{C}_S^T \boldsymbol{U}_S \end{bmatrix}, \qquad \boldsymbol{R} = \boldsymbol{U}_S^T \boldsymbol{U}_S.$$

Let k be the current time step and $p \in \{1, 2, 3\}$ be the number of energy storage units, then the associated ECOCP is:

$$\begin{cases} \textbf{Given:} & \boldsymbol{x}_0, \boldsymbol{E}_0, \boldsymbol{A}, \boldsymbol{B}, \boldsymbol{C}_E^i, \boldsymbol{D}_E^i, \gamma^i, a_j, a_{E,j}^i, \mu_j^i(\cdot), \\ & \forall j \in \{k...k+N\},\ \forall i \in \{1...p\} \\ \textbf{Minimize:} & J(\boldsymbol{u}_{k:k+N}, \boldsymbol{x}_{k:k+N}^{\circ}(\boldsymbol{u}_{k:k+N}, \boldsymbol{x}_0)) = \sum_{j=k}^{k+N} L_j(\boldsymbol{u}_j, \boldsymbol{x}_j) \\ \textbf{Domain:} & \boldsymbol{u}_{k:k+N},\ \boldsymbol{q}_{k:k+N} \\ \textbf{Constraints:} & \boldsymbol{c}_j^L(\boldsymbol{u}_{k:k+N}, \boldsymbol{q}_j, \boldsymbol{x}_j^{\circ}(\boldsymbol{u}_{k:k+N}, \boldsymbol{x}_0)) \leqslant 0, \\ & \boldsymbol{c}_j^U(\boldsymbol{u}_{k:k+N}, \boldsymbol{q}_j, \boldsymbol{x}_j^{\circ}(\boldsymbol{u}_{k:k+N}, \boldsymbol{x}_0)) \leqslant 0, \\ & \boldsymbol{q}_j \geqslant 0, \\ & \forall j \in \{k...k+N\}. \end{cases}$$

6.4.3 Results

The prediction horizon is $N = 50$, and the MPC algorithm runs for 1000 horizons. Table 6.1 summarizes the results for each considered case. Let $L_{MPC,j}$ be defined as in (6.3) after implementing the MPC control inputs at time step j, and then the sum over all 1000 time-steps is the MPC performance measure, i.e.,

$$J_{MPC} = \sum_{j=0}^{1000} L_{MPC,j}^p.$$

Column three of Table 6.1 shows the values of J_{MPC}. The fourth column of Table 6.1 indicates how many of the 1000 optimizations result in zero duality gap via the method in Section 5.4. The last column shows the number of times the modification algorithm in Section 6.2 is invoked to alter infeasible inputs from the dual relaxation. Note that all three cases satisfy Corollary 6.1, meaning that the MQCQP is convex. For the case using the system in Figure 1.5a and $E_U^1 \to \infty$, there is zero duality gap for all trajectory optimizations, but the modification algorithm is still invoked. When using numerical optimization, the algorithms

converge within numerical precision of the actual optimum. Therefore, it may be the case that optimizations with zero duality gap via Theorem 5.2 have slight feasibility violations in practice. For these situations, modifications are very small. This highlights a benefit to using Theorem 5.2 to determine strong duality versus checking the trajectory optimization for primal feasibility.

Case	E_U^1	E_U^2	E_U^3	J_{MPC}	Nonzero Duality Gap	Modifications
Figure 1.5a	∞	$\cdot$	$\cdot$	11139.6	0	1
	1	$\cdot$	$\cdot$	11184.0	0	0
	0.1	$\cdot$	$\cdot$	11369.5	24	4
	0.01	$\cdot$	$\cdot$	11465.2	104	28
Figure 1.5b	∞	∞	$\cdot$	11167.8	0	0
	1	1	$\cdot$	11196.2	0	0
	0.1	0.1	$\cdot$	11503.8	42	7
	0.01	0.01	$\cdot$	11754.5	482	239
Figure 1.5c	∞	∞	∞	11198.0	0	0
	1	1	1	11222.3	0	0
	0.1	0.1	0.1	11585.3	53	23
	0.01	0.01	0.01	12410.8	963	749

Table 6.1: Summary of vibration suppression results for the three considered systems shown in Figure 1.5 and for various values of energy storage

Figure 6.5 plots the resulting performance measure J_{MPC} for the twelve considered cases versus the amount of energy storage. For large amounts of energy storage, the three systems in Figure 1.5 perform similarly. However, for small amounts of energy storage, cases with fewer storage units perform better. This result emphasizes the advantage of connecting multiple transducers to a single storage unit: energy harvested by all of the connected transducers can then be used by any single transducer.

Figures 6.6 – 6.9 show the energy, control input, and energy dissipation trajectories for the system in Figure 1.5a with $E_U^1 = \{\infty, 1, 0.1, 0.01\}$, respectively. Figures 6.10 – 6.13 show results for the system in Figure 1.5b with two energy storage systems, and Figures 6.14 – 6.17 show results for the system in Figure 1.5c with three energy storage systems. For cases with infinite energy storage $E_U^i \to \infty$, $q^i = 0$ because the system never runs out of energy

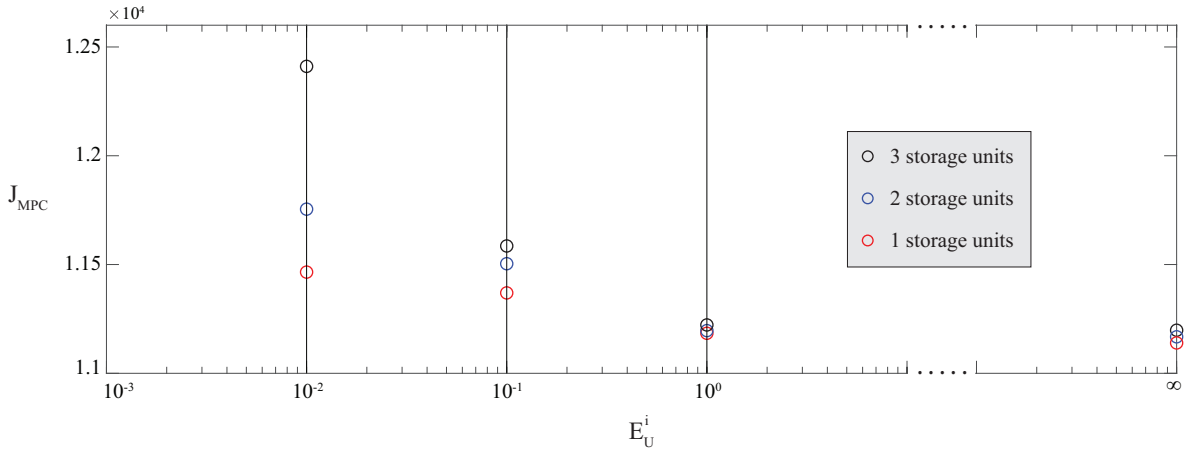

Figure 6.5: Performance measure (J_{MPC}) versus energy storage amounts (E_U^i) for all considered cases in Table 6.1, where red circles refer to results using the system in Figure 1.5a with 1 storage unit, blue circles refer to the system in Figure 1.5b with 2 storage units, and black circles refer to the system in Figure 1.5c with 3 storage units

storage, and therefore has no need to dissipate energy. However, q^i grows as the energy in the storage systems decrease. Also note that the energy trajectories for cases with $E_U^i = 0.01$ repeatedly fill and then exhaust the storage units for the entire timespan.

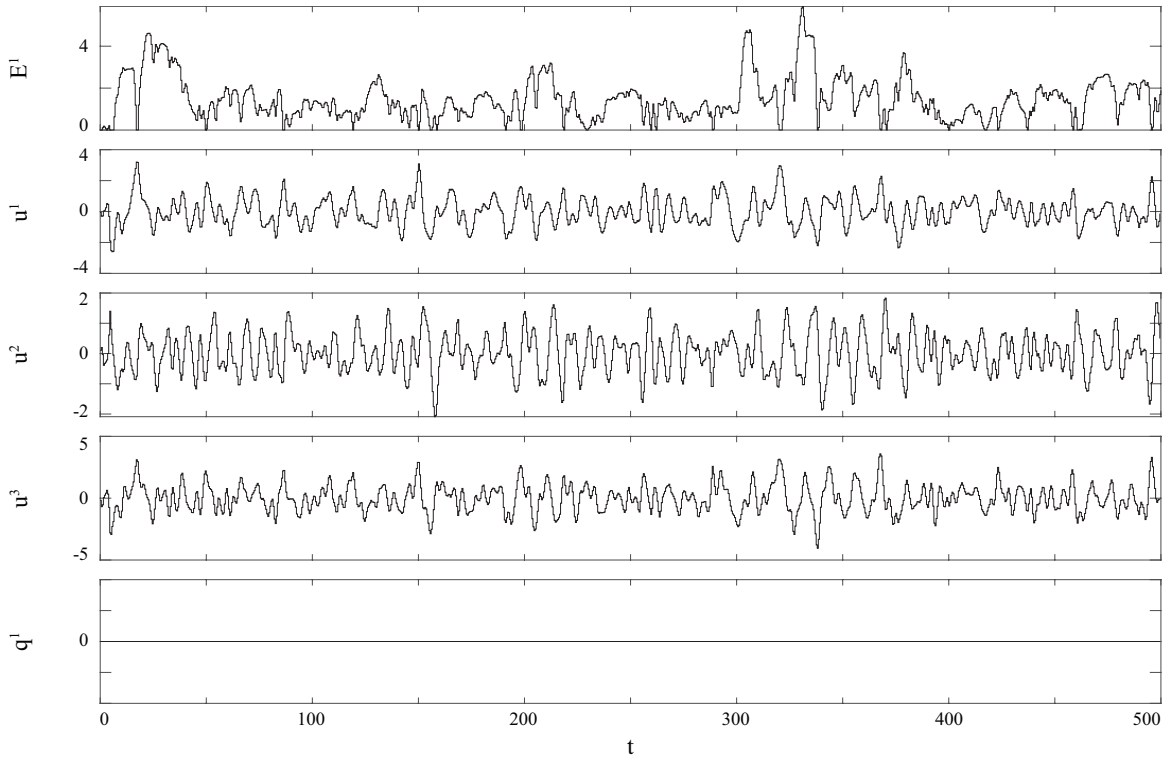

Figure 6.6: Results for Figure 1.5a with $E_U^1 \to \infty$

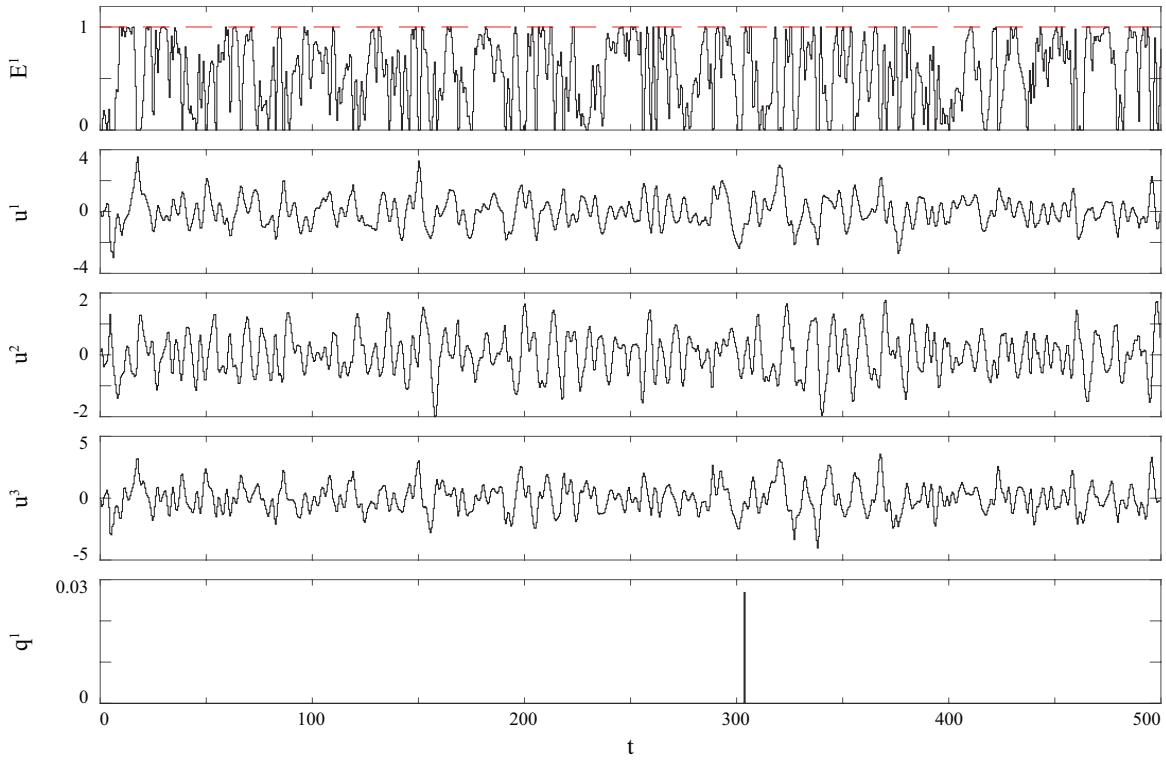

Figure 6.7: Results for Figure 1.5a with $E_U^1 = 1$

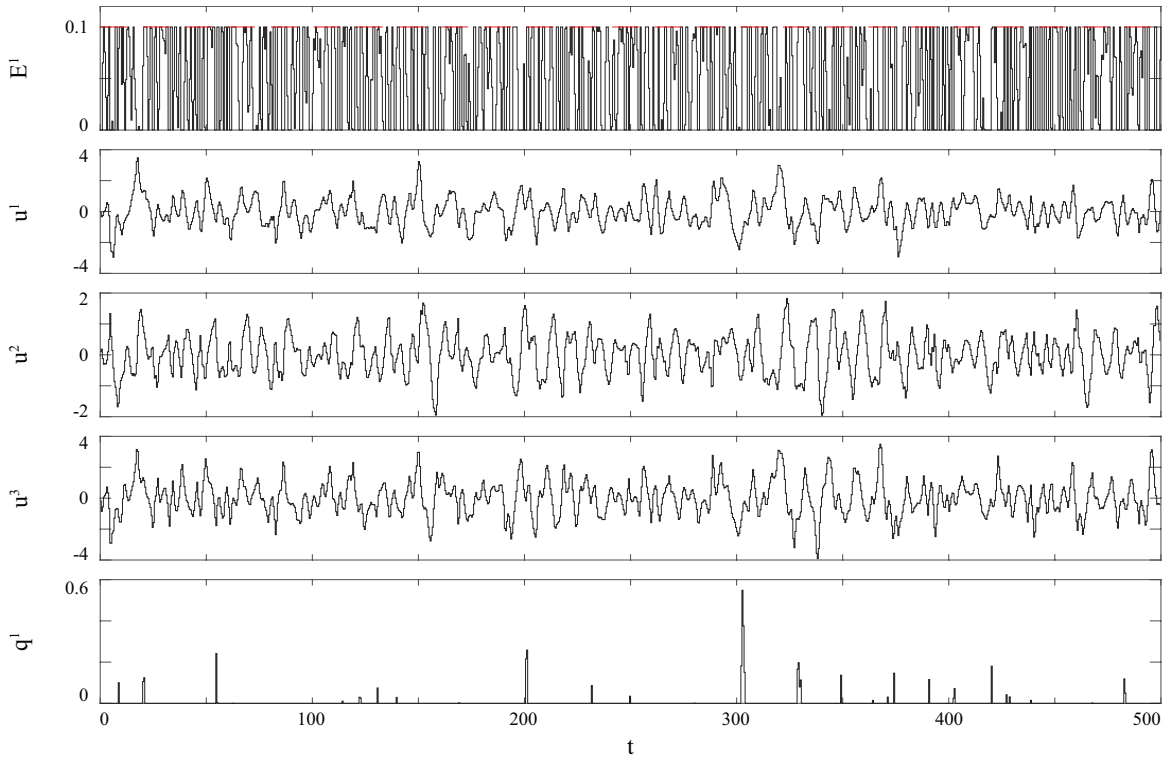

Figure 6.8: Results for Figure 1.5a with $E_U^1 = 0.1$

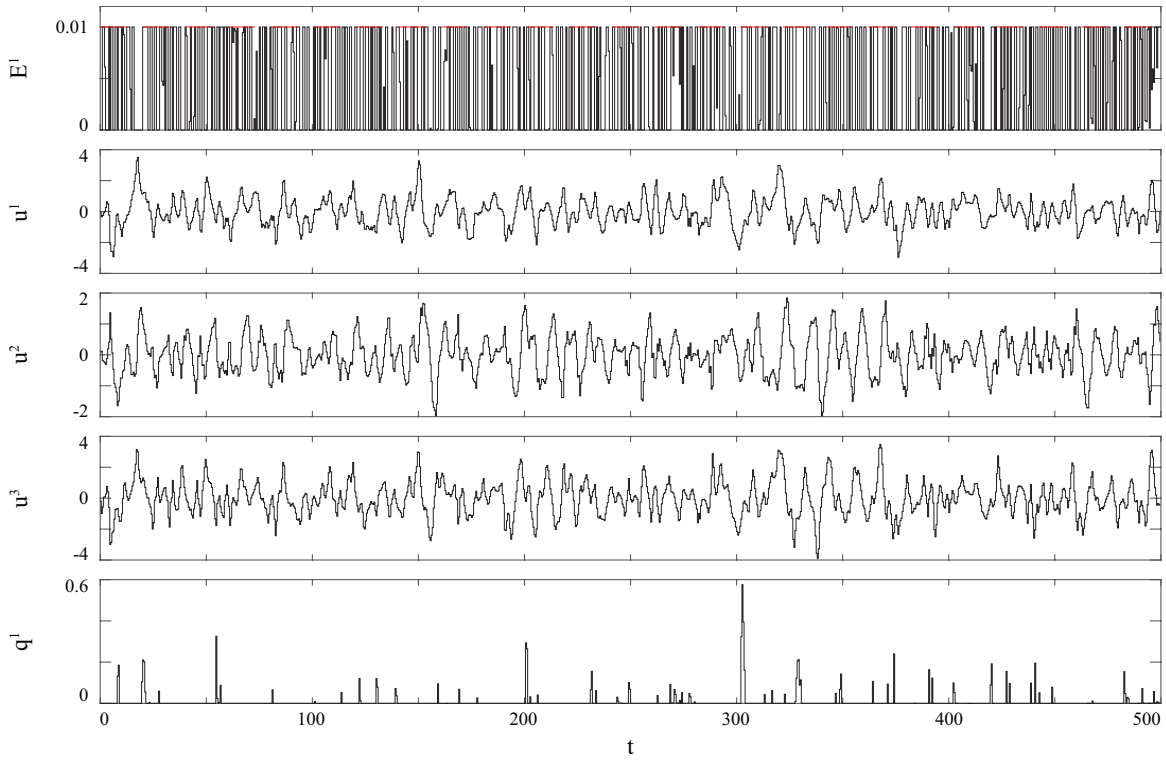

Figure 6.9: Results for Figure 1.5a with $E_U^1 = 0.01$

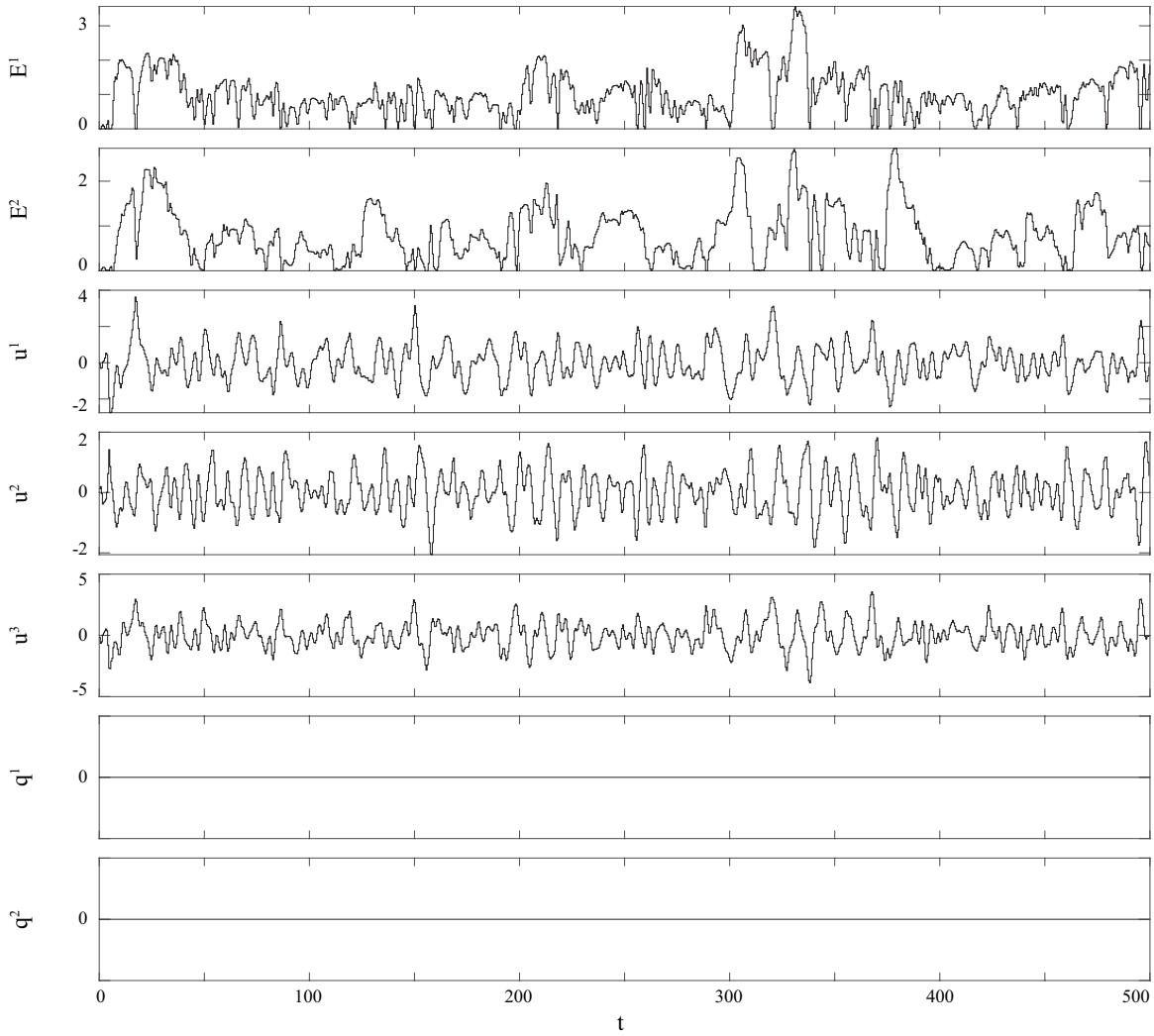

Figure 6.10: Results for Figure 1.5b with $E_U^i \to \infty$, $\forall i \in \{1, 2\}$

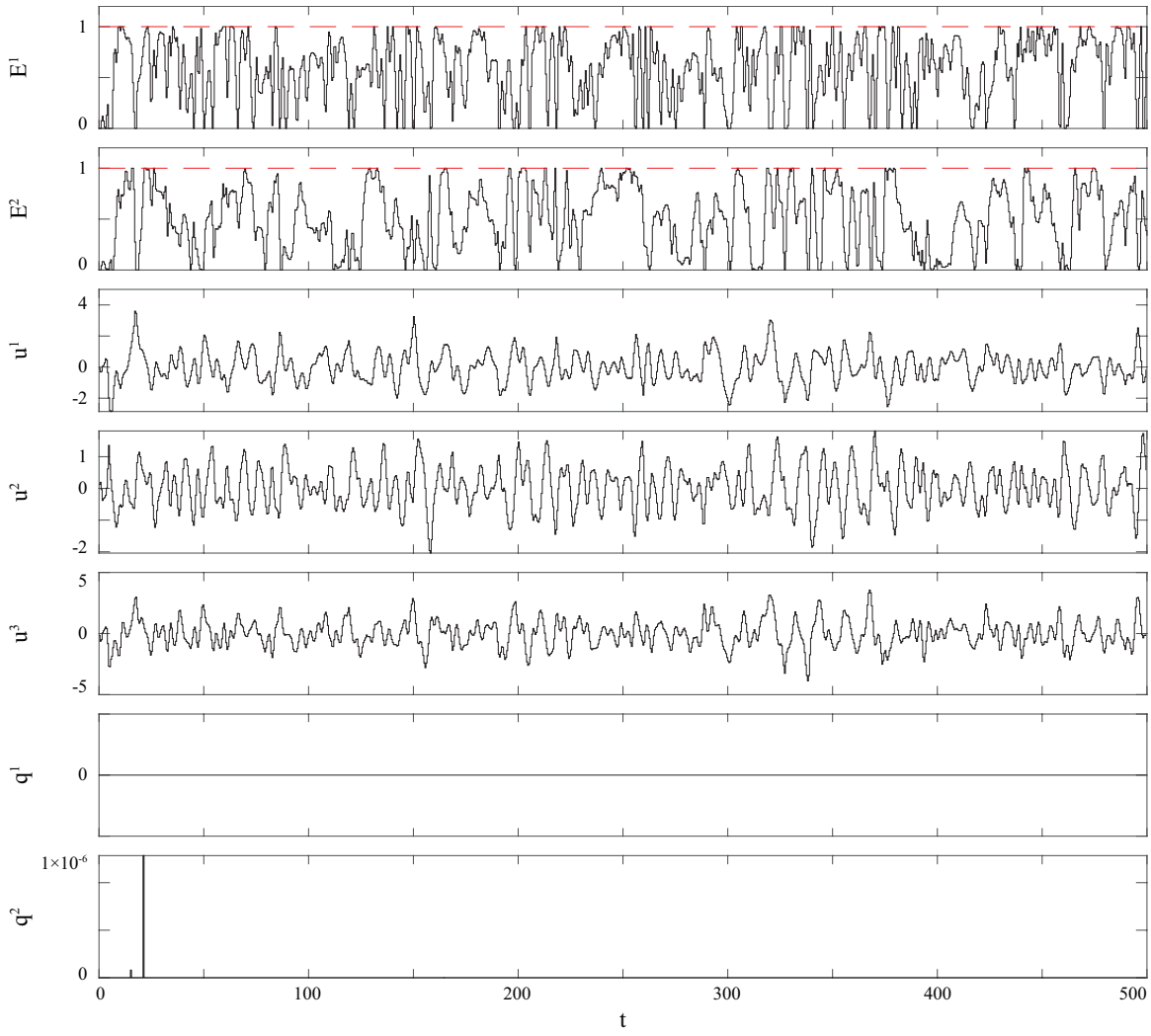

Figure 6.11: Results for Figure 1.5b with $E_U^i = 1$, $\forall i \in \{1, 2\}$

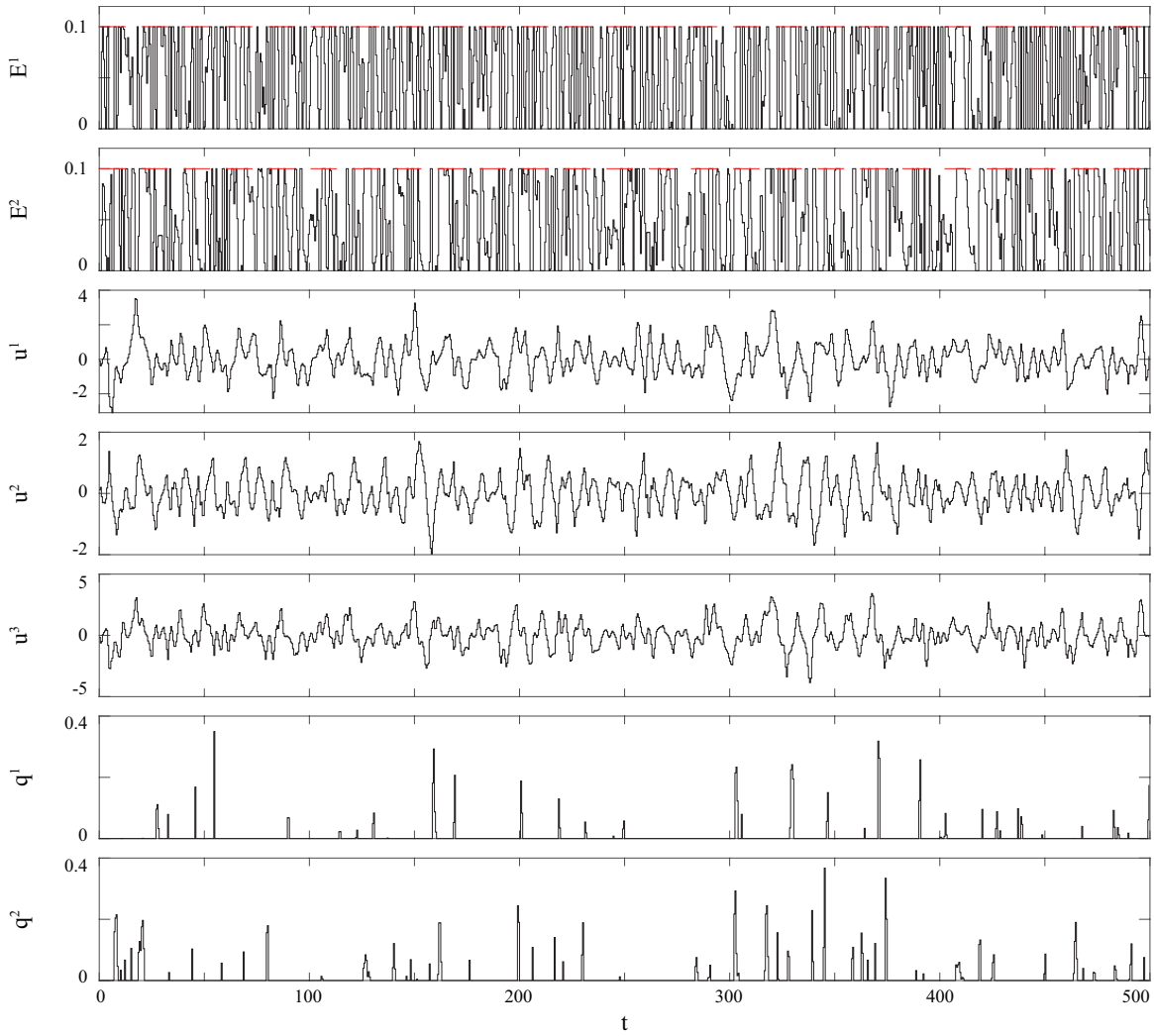

Figure 6.12: Results for Figure 1.5b with $E_U^i = 0.1$, $\forall i \in \{1, 2\}$

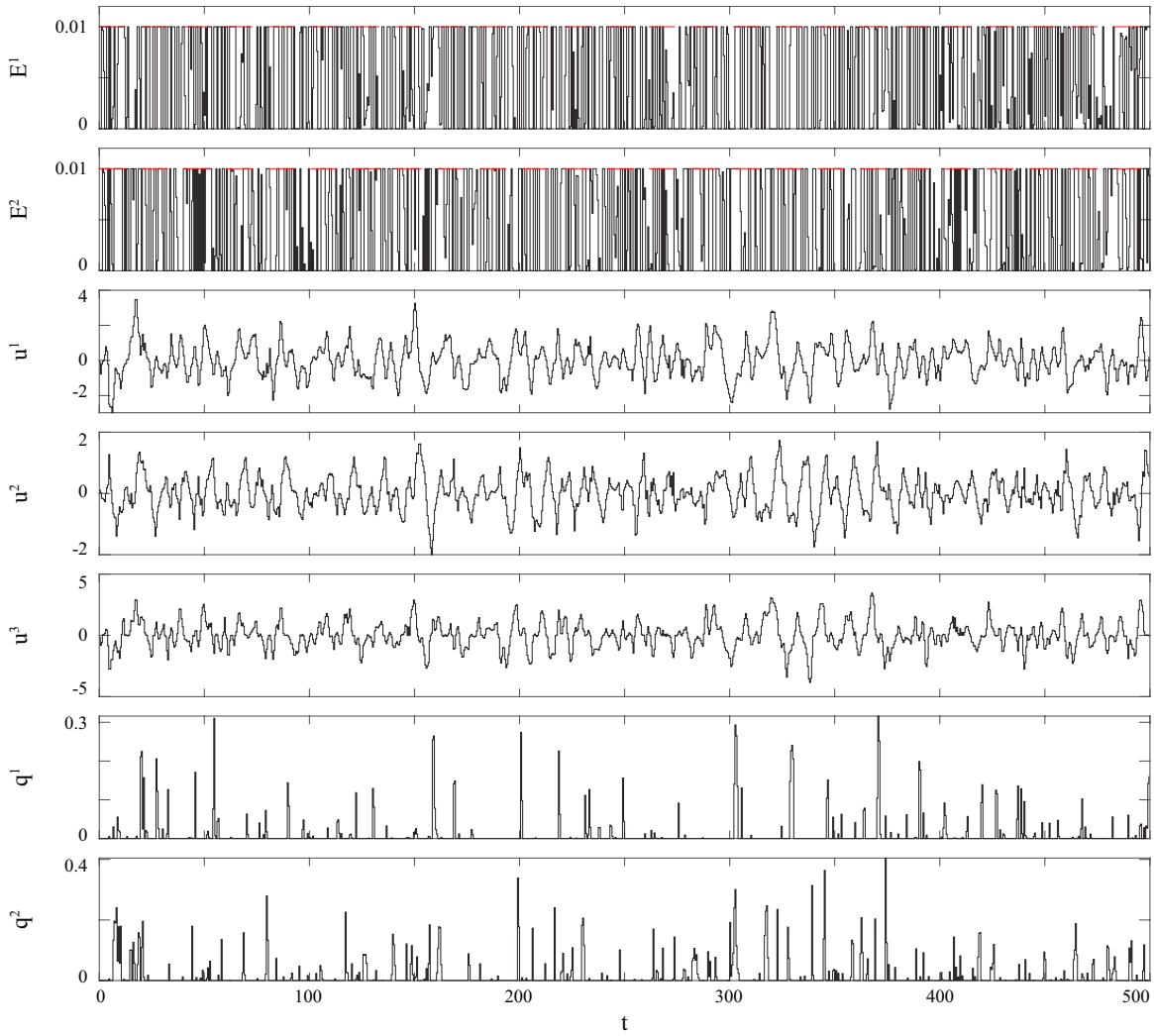

Figure 6.13: Results for Figure 1.5b with $E_U^i = 0.01$, $\forall i \in \{1, 2\}$

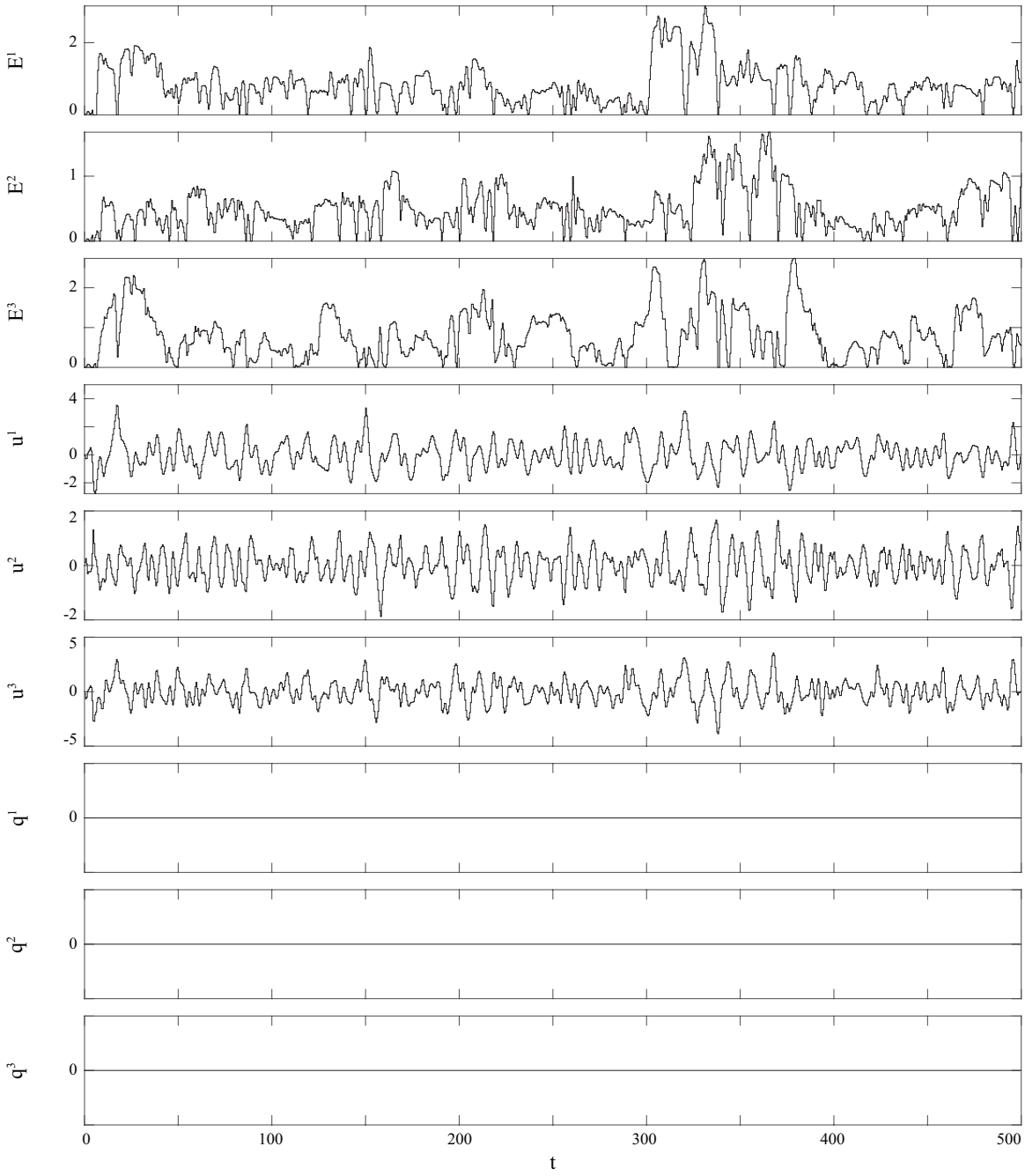

Figure 6.14: Results for Figure 1.5c with $E_U^i \to \infty$, $\forall i \in \{1, 2, 3\}$

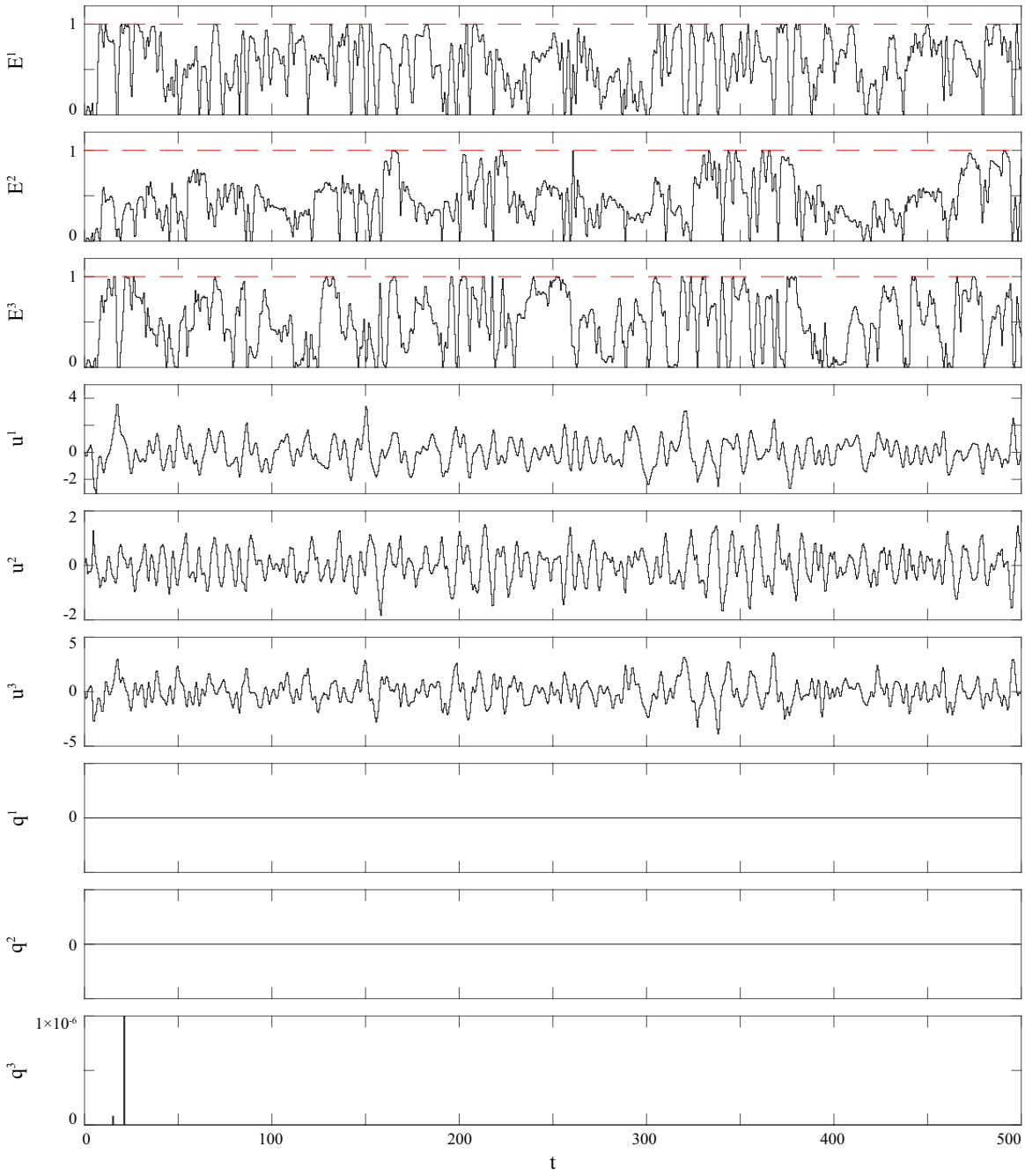

Figure 6.15: Results for Figure 1.5c with $E_U^i = 1$, $\forall i \in \{1, 2, 3\}$

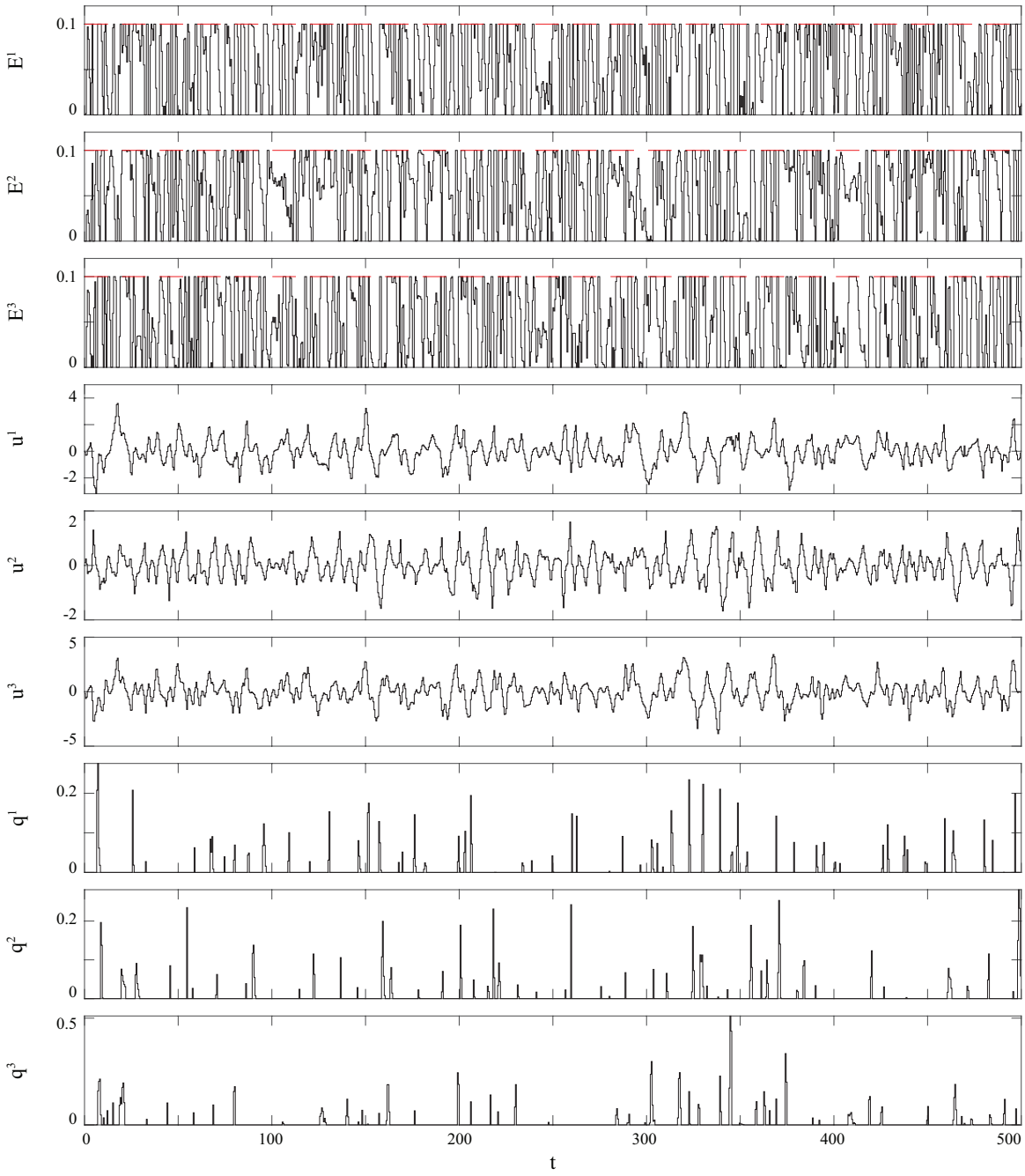

Figure 6.16: Results for Figure 1.5c with $E_U^i = 0.1$, $\forall i \in \{1, 2, 3\}$

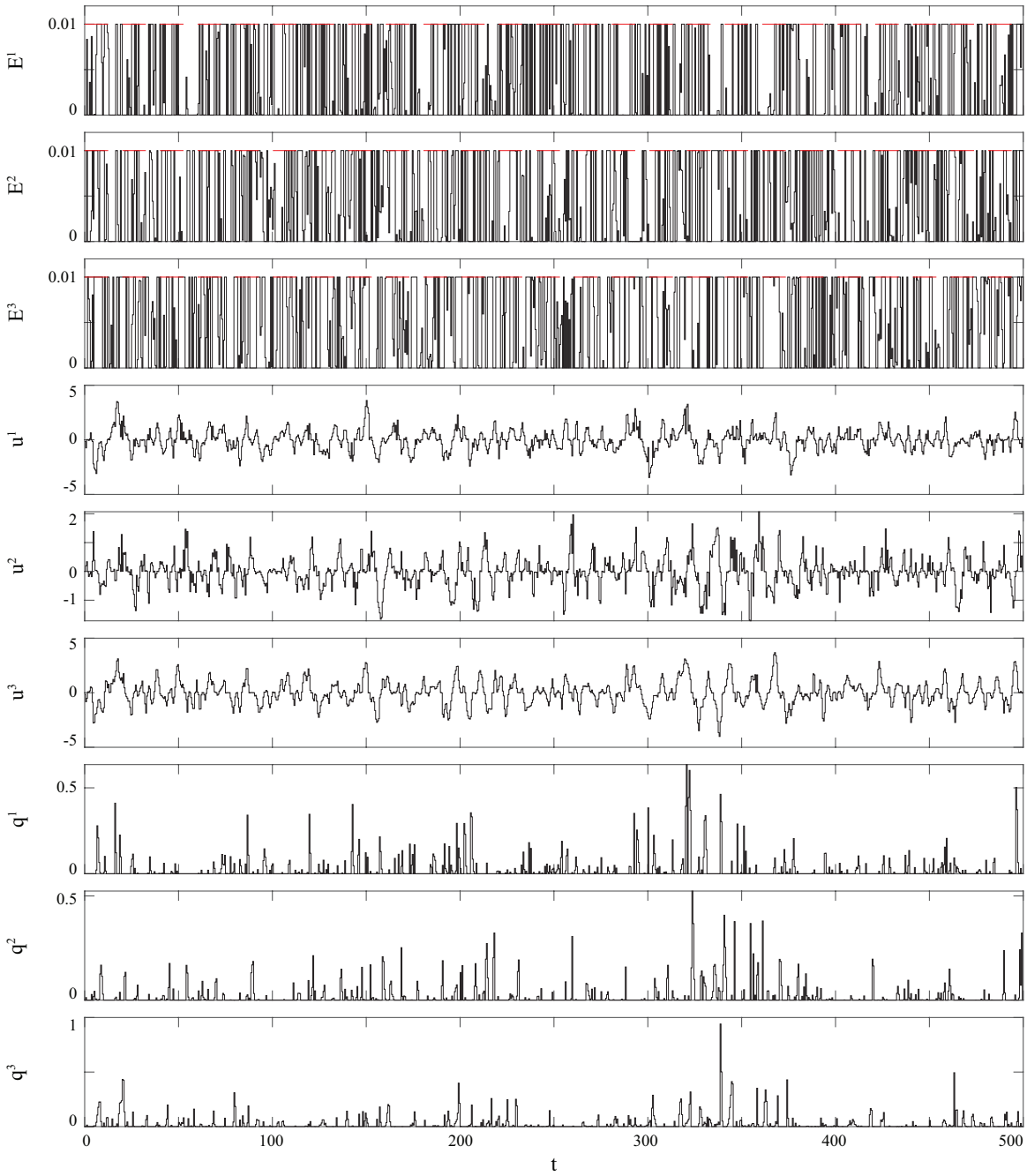

Figure 6.17: Results for Figure 1.5c with $E_U^i = 0.01$, $\forall i \in \{1, 2, 3\}$

Chapter 7

Summary of Contributions and Future Work

7.1 Summary of Contributions

The main contributions of this dissertation are as follows:

- We develop a general continuous-time model for a self-powered system, which includes the model for the energy storage subsystem that accounts for transmission losses and storage decay (see (3.2)). We derive conditions on the model parameters for problem feasibility (Lemma 3.1), and conditions for system stability (Theorem 3.1).

- We develop a discrete-time model for a general self-powered system from the continuous-time model, and address issues related to enforcing the energy storage bounds only at discrete-time points. We introduce a quadratic overbound of the efficiency loss model in Section 3.2.3, and give conditions on the discrete-time model parameters for feasibility (Lemma 3.2).

- We derive conditions for a finite quadratic performance measure (Theorem 4.1), and present the ECOCP, which accounts for the bounds on the energy storage system in (4.7).

- We show that under special conditions, the upper energy bound is a concave constraint and the lower energy bound is a convex constraint (Theorem 4.2); however, in general, these quadratic constraints are nonconvex. Then, we present conditions for the

convexity of the ECOCP (Theorem 4.3). For the case with a quadratic performance measure, the ECOCP is a nonconvex QCQP.

- We formulate the dual relaxation of the ECOCP, derive a closed-form solution for dual function (Theorem 5.1), and provide conditions for a finite dual function. Then, we show that the dual function is independent of the energy dissipation term $\boldsymbol{q}$ (Lemma 5.2).

- We present a numerical method to solve the dual relaxation and determine the Hessian and gradient of the dual function (Section 5.2.1). We also provide an alternative method using costates, which is a more computationally efficient method to solve the dual relaxation (Section 5.3).

- We derive an easy-to-check condition on the optimum dual trajectory $\boldsymbol{\lambda}^{dual}$ that guarantees zero duality gap (Theorem 5.2). We also show that for specific model parameters, there is zero duality gap for all initial conditions and exogenous disturbances via Slater's constraint qualification (Theorem 5.3).

- We present an algorithm to modify control inputs for feasibility and MPC implementation (Algorithm 1), and derive conditions for the convexity of the associated optimization, MQCQP (Corollary 6.1).

- We demonstrate Algorithm 1 using a sphere-type WEC buoy with the goal of maximizing energy generated, and on a mass-spring-damper five degree-of-freedom system with multiple energy storage systems.

7.2 Future Work

Below we present three areas in which the work presented in this thesis can be extended:

1. **Exogenous Disturbance Forecasting:** As shown in Figure 1.6, a component of the system intelligence is a disturbance forecaster, which estimates the $N+1$ exogenous disturbances $\{\hat{\boldsymbol{a}}_k \dots \hat{\boldsymbol{a}}_{k+N}\}$ to be fed into the trajectory optimization. In this thesis, we assume that the exogenous disturbances can be measured exactly. In some situations this may be a feasible assumption, for example, wave-energy converters commonly employ up-wave sensors to accurately measure incoming waves. However, in general, self-powered systems do not have the ability to accurately measure incoming future

disturbances. Therefore, future work will explore various prediction algorithms (e.g., a Kalman filter [4]).

2. **Improving Power Quality:** Reference the WEC example in Section 6.3, where Figure 6.3 shows the energy sent to the power grid q. Such poor quality power can cause frequency fluctuation or voltage deviations. However, as mentioned in Section 1.1, energy storage systems can help improve power quality. Local energy storage systems can be used to smooth out power fluctuations, store surplus energy, or provide energy during peak demand. An important extension of the WEC example in Section 6.3 is to incorporate a power smoothing algorithm that can be implemented when solving the dual problem.

   First, we introduce a new variable, $p_{grid}(t) \in \mathbb{L}^2$ to account for the power sent from the i^{th} energy storage system to the grid. Now, we modify the differential equation (3.2) to account for this new term as:

$$\frac{d}{dt}E(t) = -\tfrac{1}{T_S}E(t) - u(t)v(t) - \mu(t) - q(t) - p_{grid}(t),$$

   and then the corresponding difference equation is:

$$E_{j+1} = \gamma E_j - u_j y_j - \mu_j - q_j - \frac{p_{grid,j}}{\chi}.$$

   Now, we formulate our performance measure to maximize the power sent to the grid over a finite time horizon as:

$$J(p_{grid,k:k+N}) = -\sum_{j=k}^{k+N} p_{grid,j}.$$

   We restrict $p_{grid,j}$ to have a specific form. Figure 7.1 shows a possible structure of p_{grid}. Let $\beta \in \mathbb{Z}_{>0}$ be defined such that $\frac{N+1}{\beta} \in \mathbb{Z}_{>0}$, which is the number of time steps over which we linearly interpolate the power sent to the grid. Variables $\{\sigma_0^k, \ldots, \sigma_{\frac{N}{\beta}}^k\}$ are the power values over which we optimize to determine the trajectory of $p_{grid}(t)$. The

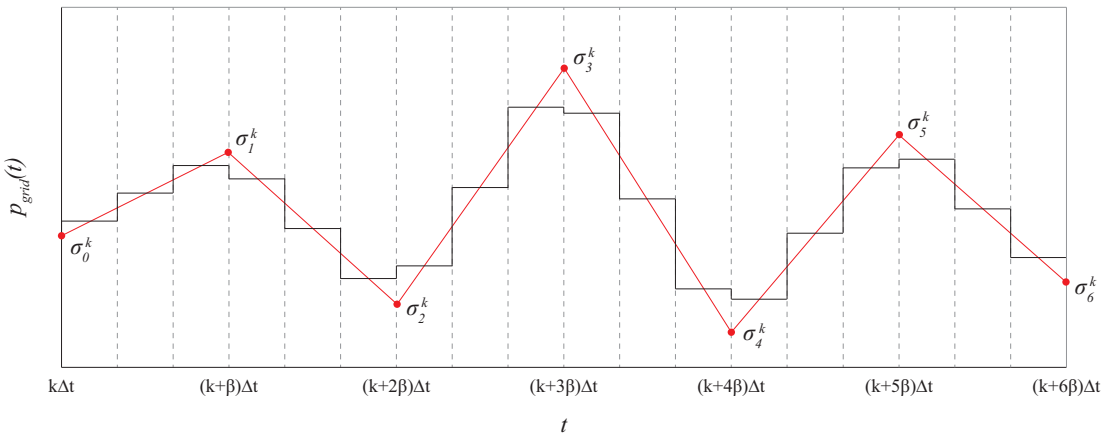

Figure 7.1: Possible structure of $p_{grid}(t)$

discrete-time power to the grid $p_{grid,j}$ is then:

$$\begin{aligned} p_{grid,j} &= \frac{(\sigma_{\alpha+1}^k - \sigma_\alpha^k)(j+\frac{1}{2})}{\beta} + \sigma_\alpha^k, \\ &\forall j \in \{k+\beta\alpha ... k+\beta(\alpha+1)-1\}, \\ &\forall \alpha \in \{0 ... \tfrac{N}{\beta}\}. \end{aligned} \tag{7.1}$$

Therefore, this method restricts the shape of $p_{grid}(t)$ without incorporating additional

Lagrange multipliers. The associated ECOCP for the WEC example in Section 6.3 is:

$$\begin{cases} \textbf{Given:} & \boldsymbol{x}_0, E_0^1, \boldsymbol{A}, \boldsymbol{B}, \boldsymbol{C}_E^1, \boldsymbol{D}_E^1, \gamma^1, \beta, \\ & a_{k:k+N}, a_{E,k:k+N}^1, \mu_j^1(\cdot),\ \forall j \in \{k...k+N\} \\ \textbf{Minimize:} & J(p_{grid,k:k+N}) = -\sum_{j=k}^{k+N} p_{grid,k} \\ \textbf{Domain:} & u_{k:k+N},\ q_{k:k+N}\ \sigma_{0:N/\beta}^k \\ \textbf{Constraints:} & c_j^L(u_{k:k+N}, q_j^1, \boldsymbol{x}_j^\circ(u_{k:k+N}, \boldsymbol{x}_0), p_{grid,j}) \leqslant 0, \\ & c_j^U(u_{k:k+N}, q_j^1, \boldsymbol{x}_j^\circ(u_{k:k+N}, \boldsymbol{x}_0), p_{grid,j}) \leqslant 0, \\ & q_j^1 \geqslant 0, \\ & u_j^2 - u_{max}^2 \leqslant 0, \\ & p_{grid,j} \text{ defined according to (7.1)} \\ & \forall j \in \{k...k+N\}. \end{cases}$$

3. **Necessary and Sufficient Conditions for Strong Duality:** In Chapter 5, we derive sufficient conditions on the optimal dual trajectory $\boldsymbol{\lambda}^d$ that guarantee zero duality gap (see Theorem 5.2). We also provide necessary and sufficient conditions for zero duality gap for all exogenous disturbances and initial conditions (see Theorem 5.3). However, these conditions are quite restrictive and require the original ECOCP to be convex (because we use Slater's constraint qualification). We would like to determine necessary and sufficient conditions for strong duality for a larger class of problems, and specifically if the optimal control problem is not guaranteed to be convex. As we discussed in Chapter 5, we know that if the dual optimum does not lie on a boundary, then the duality gap is zero. Therefore, we are investigating under what conditions we can guarantee that the dual maximum does not lie on the boundary.

4. **Loss Modeling:** Throughout this thesis we assume transmission losses are captured via the quadratic model in (3.22). In Section 3.2.3, we show how the efficiency model can be overbounded by this quadratic model. However, loss models may not be quadratic, or a quadratic overbound may not be a good estimate of the losses. Hence, we would like to be able to incorporate nonlinear loss models into the theory developed in this thesis.

Bibliography

[1] N. J. Abbas and N. Tom. "Utilization of Model Predictive Control to Balance Power Absorption Against Load Accumulation". In: *The 27th International Ocean and Polar Engineering Conference*. International Society of Offshore and Polar Engineers. 2017.

[2] H. Abou-Kandil, G. Freiling, V. Ionescu, and G. Jank. *Matrix Riccati equations in control and systems theory*. Birkhäuser, 2012.

[3] I. F. Akyildiz, W. Su, Y. Sankarasubramaniam, and E. Cayirci. "Wireless sensor networks: a survey". In: *Computer networks* 38.4 (2002), pp. 393–422.

[4] B. D. Anderson and J. B. Moore. *Optimal filtering*. Mineola, New York: Dover ed., 2005.

[5] B. D. Anderson and S. Vongpanitlerd. *Network analysis and synthesis: a modern systems theory approach*. Englewood Cliffs, New Jersey: Prentice-Hall, 1973.

[6] D. Angeli, R. Amrit, and J. B. Rawlings. "On Average Performance and Stability of Economic Model Predictive Control". In: *IEEE Transactions on Automatic Control* 57.7 (2012), pp. 1615–1626.

[7] A. Babarit and A. Clément. "Optimal latching control of a wave energy device in regular and irregular waves". In: *Applied Ocean Research* 28.2 (2006), pp. 77–91.

[8] D. P. Bertsekas. *Nonlinear programming*. 2nd ed. Belmont, Massachusetts: Athena Scientific, 1999.

[9] F. Borrelli, A. Bemporad, and M. Morari. *Predictive control for linear and hybrid systems*. Cambridge, United Kingdom: Cambridge University Press, 2017.

[10] S. Boyd and L. Vandenberghe. *Convex Optimization*. Cambridge, United Kingdom: Cambridge University Press, 2004.

[11] S. Boyd and L. Vandenberghe. "Semidefinite programming relaxations of non-convex problems in control and combinatorial optimization". In: *Communications, Computation, Control, and Signal Processing*. Springer, 1997, pp. 279–287.

[12] S. Boyd, L. El Ghaoui, E. Feron, and V. Balakrishnan. *Linear matrix inequalities in system and control theory*. Vol. 15. Siam, 1994.

[13] T. K. A. Brekken. "On Model Predictive Control for a point absorber Wave Energy Converter". In: *2011 IEEE Trondheim PowerTech*. 2011, pp. 1–8.

[14] B. Brogliato, R. Lozano, B. Maschke, and O. Egeland. *Dissipative systems analysis and control*. Vol. 2. London, United Kingdom: Springer, 2007.

[15] A. E. Bryson and Y.-C. Ho. *Applied optimal control : optimization, estimation, and control*. Waltham, Mass.: Blaisdell Publishing Company, 1969.

[16] J. Cretel, G. Lightbody, G. Thomas, and A. Lewis. "Maximisation of Energy Capture by a Wave-Energy Point Absorber using Model Predictive Control". In: *IFAC Proceedings Volumes* 44.1 (2011). 18th IFAC World Congress, pp. 3714–3721. ISSN: 1474-6670.

[17] J. Cruz. *Ocean wave energy: current status and future perspectives*. Germany: Springer Science & Business Media, 2007.

[18] S. Cui, A. J. Goldsmith, and A. Bahai. "Energy-constrained modulation optimization". In: *IEEE Transactions on Wireless Communications* 4.5 (Sept. 2005), pp. 2349–2360.

[19] D. Evans. "A theory for wave-power absorption by oscillating bodies". In: *Journal of Fluid Mechanics* 77.1 (1976), pp. 1–25.

[20] J. Falnes. "A review of wave-energy extraction". In: *Marine structures* 20.4 (2007), pp. 185–201.

[21] J. Falnes. "Radiation impedance matrix and optimum power absorption for interacting oscillators in surface waves". In: *Applied ocean research* 2.2 (1980), pp. 75–80.

[22] P. Falugi. "Model predictive control: a passive scheme". In: *IFAC Proceedings Volumes* 47.3 (2014). 19th IFAC World Congress, pp. 1017 –1022.

[23] F. Fusco and J. V. Ringwood. "Short-Term Wave Forecasting for Real-Time Control of Wave Energy Converters". In: *IEEE Transactions on Sustainable Energy* 1.2 (2010), pp. 99–106.

[24] G. Goodwin, M. M. Seron, and J. A. De Doná. *Constrained control and estimation: an optimisation approach*. Springer Science & Business Media, 2006.

[25] G. C. Goodwin and K. S. Sin. *Adaptive filtering prediction and control*. Courier Corporation, 2014.

[26] M. Green and D. J. Limebeer. *Linear robust control*. Mineloa, New York: Dover, 2012.

[27] G. Grimm, M. J. Messina, S. E. Tuna, and A. R. Teel. "Examples when nonlinear model predictive control is nonrobust". In: *Automatica* 40.10 (2004), pp. 1729–1738.

[28] J. Gripp and D. Rade. "Vibration and noise control using shunted piezoelectric transducers: A review". In: *Mechanical Systems and Signal Processing* 112 (2018), pp. 359 –383.

[29] N. W. Hagood, W. H. Chung, and A. Von Flotow. "Modelling of piezoelectric actuator dynamics for active structural control". In: *Journal of intelligent material systems and structures* 1.3 (1990), pp. 327–354.

[30] J. Hals, J. Falnes, and T. Moan. "Constrained optimal control of a heaving buoy wave-energy converter". In: *Journal of Offshore Mechanics and Arctic Engineering* 133.1 (2011), p. 011401.

[31] B. Han, S. Vassilaras, C. B. Papadias, R. Soman, M. A. Kyriakides, T. Onoufriou, R. H. Nielsen, and R. Prasad. "Harvesting energy from vibrations of the underlying structure". In: *Journal of Vibration and Control* 19.15 (2013), pp. 2255–2269.

[32] L. Hitz and B. D. O. Anderson. "Discrete positive-real functions and their application to system stability". In: *Proceedings of the Institution of Electrical Engineers* 116.1 (1969), pp. 153–155.

[33] R. A. Horn and C. R. Johnson. *Matrix analysis*. Cambridge: Cambridge University Press, 1985.

[34] G. W. Housner, L. A. Bergman, T. K. Caughey, A. G. Chassiakos, R. O. Claus, S. F. Masri, R. E. Skelton, T. Soong, B. Spencer, and J. T. Yao. "Structural control: past, present, and future". In: *Journal of engineering mechanics* 123.9 (1997), pp. 897–971.

[35] A. A. Kody and J. T. Scruggs. "Model Predictive Control of a Wave Energy Converter Using Duality Techniques". In: *Proceedings of the 2019 American Controls Conference (ACC)*. 2019.

[36] A. A. Kody and J. T. Scruggs. "Optimal self-powered control of dynamic systems: Duality techniques". In: *Proceedings of the 2018 American Controls Conference (ACC)*. 2018.

[37] A. A. Kody and J. T. Scruggs. "Optimal transmission rate for a piezoelectric energy harvesting node". In: *Proceedings of the 56th IEEE Conference on Decision and Control (CDC)*. 2017.

[38] N. Kottenstette, M. J. McCourt, M. Xia, V. Gupta, and P. J. Antsaklis. "On relationships among passivity, positive realness, and dissipativity in linear systems". In: *Automatica* 50.4 (2014), pp. 1003–1016.

[39] J. Lavaei and S. H. Low. "Zero duality gap in optimal power flow problem". In: *IEEE Transactions on Power systems* 27.1 (2011), pp. 92–107.

[40] G. Lesieutre, G. Ottman, and H. Hofmann. "Damping as a result of piezoelectric energy harvesting". In: *Journal of Sound and Vibration* 269.3–5 (2004), pp. 991–1001.

[41] F. L. Lewis, D. Vrabie, and V. L. Syrmos. *Optimal control*. John Wiley & Sons, 2012.

[42] G. Li and M. R. Belmont. "Model predictive control of sea wave energy converters – Part I: A convex approach for the case of a single device". In: *Renewable Energy* 69 (2014), pp. 453–463.

[43] Y. Liu, G. Tian, Y. Wang, J. Lin, Q. Zhang, and H. F. Hofmann. "Active piezoelectric energy harvesting: general principle and experimental demonstration". In: *Journal of Intelligent Material Systems and Structures* 20.5 (2009), pp. 575–585.

[44] Z. Luo, W. Ma, A. M. So, Y. Ye, and S. Zhang. "Semidefinite Relaxation of Quadratic Optimization Problems". In: *IEEE Signal Processing Magazine* 27.3 (2010), pp. 20–34.

[45] J. Matiko, N. Grabham, S. Beeby, and M. Tudor. "Review of the application of energy harvesting in buildings". In: *Measurement Science and Technology* 25.1 (2013), p. 012002.

[46] D. Mayne, J. Rawlings, C. Rao, and P. Scokaert. "Constrained model predictive control: Stability and optimality". In: *Automatica* 36.6 (2000), pp. 789–814.

[47] T. McKelvey, H. Akçay, and L. Ljung. "Subspace-based identification of infinite-dimensional multivariable systems from frequency-response data". In: *Automatica* 32.6 (1996), pp. 885–902.

[48] M. A. Müller, D. Angeli, and F. Allgöwer. "On Necessity and Robustness of Dissipativity in Economic Model Predictive Control". In: *IEEE Transactions on Automatic Control* 60.6 (2015), pp. 1671–1676.

[49] D. B. Murray. "Energy storage systems for wave energy converters and microgrids". PhD thesis. Cork, Ireland: University College Cork, Mar. 2013.

[50] A. Nayyar, T. Basar, D. Teneketzis, and V. Veeravalli. "Optimal Strategies for Communication and Remote Estimation With an Energy Harvesting Sensor". In: *Automatic Control, IEEE Transactions on* 58.9 (2013), pp. 2246–2260.

[51] P Nebel. "Maximizing the Efficiency of Wave-Energy Plant Using Complex-Conjugate Control". In: *Proceedings of the Institution of Mechanical Engineers, Part I: Journal of Systems and Control Engineering* 206.4 (1992), pp. 225–236.

[52] M. Nourian, A. Leong, and S. Dey. "Optimal Energy Allocation for Kalman Filtering Over Packet Dropping Links With Imperfect Acknowledgments and Energy Harvesting Constraints". In: *Automatic Control, IEEE Transactions on* 59.8 (Aug. 2014), pp. 2128–2143.

[53] W. Ongsakul and N. Petcharaks. "Unit commitment by enhanced adaptive Lagrangian relaxation". In: *IEEE Transactions on Power Systems* 19.1 (2004), pp. 620–628.

[54] O. Ozel, K. Tutuncuoglu, J. Yang, S. Ulukus, and A. Yener. "Transmission with Energy Harvesting Nodes in Fading Wireless Channels: Optimal Policies". In: *Selected Areas in Communications, IEEE Journal on* 29.8 (2011), pp. 1732–1743.

[55] P. M. Pardalos and S. A. Vavasis. "Quadratic programming with one negative eigenvalue is NP-hard". In: *Journal of Global Optimization* 1.1 (1991), pp. 15–22.

[56] J. Park and S. Boyd. "General heuristics for nonconvex quadratically constrained quadratic programming". In: *arXiv preprint arXiv:1703.07870* (2017).

[57] T. Raff, C. Ebenbauer, and P. Allgöwer. "Nonlinear Model Predictive Control: A Passivity-Based Approach". In: *Assessment and Future Directions of Nonlinear Model Predictive Control*. Ed. by R. Findeisen, F. Allgöwer, and L. T. Biegler. Berlin, Heidelberg: Springer Berlin Heidelberg, 2007, pp. 151–162.

[58] M. Richter, M. E. Magana, O. Sawodny, and T. K. A. Brekken. "Nonlinear Model Predictive Control of a Point Absorber Wave Energy Converter". In: *IEEE Transactions on Sustainable Energy* 4.1 (2013), pp. 118–126.

[59] J. V. Ringwood, G. Bacelli, and F. Fusco. "Energy-Maximizing Control of Wave-Energy Converters: The Development of Control System Technology to Optimize Their Operation". In: *IEEE Control Systems* 34.5 (2014), pp. 30–55.

[60] S. Roundy, P. K. Wright, and J. Rabaey. "A study of low level vibrations as a power source for wireless sensor nodes". In: *Computer Communications* 26.11 (2003), pp. 1131–1144.

[61] T. Sales, D. Rade, and L. de Souza. "Passive vibration control of flexible spacecraft using shunted piezoelectric transducers". In: *Aerospace Science and Technology* 29.1 (2013), pp. 403 –412.

[62] S. H. Salter. "Wave power". In: *Nature* 249.5459 (1974), pp. 720–724.

[63] J. T. Scruggs, I. L. Cassidy, and S. Behrens. "Multi-objective optimal control of vibratory energy harvesting systems". In: *Journal of Intelligent Material Systems and Structures* 23.18 (2012), pp. 2077–2093.

[64] J. Scruggs. "An optimal stochastic control theory for distributed energy harvesting networks". In: *Journal of Sound and Vibration* 320.4-5 (2009), pp. 707–725.

[65] J. Scruggs and R Nie. "Disturbance-adaptive stochastic optimal control of energy harvesters, with application to ocean wave energy conversion". In: *Annual Reviews in Control* 40 (2015), pp. 102–115.

[66] H. A. Sodano, G. Park, and D. J. Inman. "Estimation of Electric Charge Output for Piezoelectric Energy Harvesting". In: *Strain* 40.2 (2004), pp. 49–58.

[67] S. Sudevalayam and P. Kulkarni. "Energy harvesting sensor nodes: Survey and implications". In: *IEEE Communications Surveys & Tutorials* 13.3 (2011), pp. 443–461.

[68] R. Taghipour, T. Perez, and T. Moan. "Hybrid frequency–time domain models for dynamic response analysis of marine structures". In: *Ocean Engineering* 35.7 (2008), pp. 685–705.

[69] M. J. Tippett and J. Bao. "Distributed model predictive control based on dissipativity". In: *AIChE Journal* 59.3 (Mar. 2013), pp. 787–804.

[70] N. Tom and R. W. Yeung. "Nonlinear model predictive control applied to a generic ocean-wave energy extractor". In: *Journal of Offshore Mechanics and Arctic Engineering* 136.4 (2014), p. 041901.

[71] M. Tucker and E. Pitt. *Waves in Ocean Engineering*. Elsevier ocean engineering book series. Elsevier, 2001.

[72] K. Tutuncuoglu and A. Yener. "Optimum Transmission Policies for Battery Limited Energy Harvesting Nodes". In: *IEEE Transactions on Wireless Communications* 11.3 (2012), pp. 1180–1189.

[73] L. Vandenberghe and S. Boyd. "Semidefinite programming". In: *SIAM review* 38.1 (1996), pp. 49–95.

[74] S. Virmani, E. C. Adrian, K. Imhof, and S. Mukherjee. "Implementation of a Lagrangian relaxation based unit commitment problem". In: *IEEE Transactions on Power Systems* 4.4 (1989), pp. 1373–1380.

[75] Y. Wang and D. J. Inman. "A survey of control strategies for simultaneous vibration suppression and energy harvesting via piezoceramics". In: *Journal of Intelligent Material Systems and Structures* 23.18 (2012), pp. 2021–2037.

[76] F. F. Wendt, Y.-H. Yu, K. Nielsen, K. Ruehl, T. Bunnik, I. Touzon, B. W. Nam, J. S. Kim, C. E. Janson, K.-R. Jakobsen, et al. *International energy agency ocean energy systems task 10 wave energy converter modeling verification and validation*. Tech. rep. National Renewable Energy Lab.(NREL), Golden, CO (United States), 2017.

[77] Y. Yan and P. Antsaklis. "Stabilizing nonlinear model predictive control scheme based on passivity and dissipativity". In: *2016 American Control Conference (ACC)*. 2016, pp. 4476–4481.

[78] J. Yang and S. Ulukus. "Optimal Packet Scheduling in an Energy Harvesting Communication System". In: *Communications, IEEE Transactions on* 60.1 (2012), pp. 220–230.

[79] P. Youssef-Massaad, L. Zheng, and M. Medard. "Bursty transmission and glue pouring: on wireless channels with overhead costs". In: *IEEE Transactions on Wireless Communications* 7.12 (Dec. 2008), pp. 5188–5194.

[80] H. Yu, F. Zhu, M. Xia, and P. J. Antsaklis. "Robust stabilizing output feedback nonlinear model predictive control by using passivity and dissipativity". In: *2013 European Control Conference (ECC)*. 2013, pp. 2050–2055.

[81] Z Yu and J Falnes. "State-space modelling of a vertical cylinder in heave". In: *Applied Ocean Research* 17.5 (1995), pp. 265–275.

[82] M. Yuan, K. Liu, and A. Sadhu. "Simultaneous vibration suppression and energy harvesting with a non-traditional vibration absorber". In: *Journal of Intelligent Material Systems and Structures* 29.8 (2018), pp. 1748–1763.

[83] L. Zuo and W. Cui. "Dual-functional energy-harvesting and vibration control: electromagnetic resonant shunt series tuned mass dampers". In: *Journal of vibration and acoustics* 135.5 (2013), p. 051018.